The Development of Corticothalamic and Corticotectal Connections in the Murine Visual System

Eleanor Grant

Balliol College

A thesis submitted for the degree of

Doctor of Philosophy

Trinity 2014

Abstract

The Development of Corticothalamic and Corticotectal Connections in the Murine Visual System

Eleanor Grant

Balliol College

Thesis submitted for the degree of

Doctor of Philosophy

Trinity 2014

All peripheral sensory information is represented in the thalamus before being transmitted to the cortex, with the exception of olfaction. The thalamus projects to all areas of the neocortex and all neocortical areas project to the thalamus. I am interested in the development of three corticothalamic populations which are anatomically and functionally distinct; they project to different thalamic nuclei and generate different post-synaptic responses. Layer V fibres project exclusively to higher order thalamic nuclei. These projections drive thalamic neuron activity and mediate a trans-thalamic cortico-cortical relay. Layer VI and VIb fibres project to both first order and higher order thalamic nuclei. These projections modulate thalamic neuron activity and mediate feedback to the thalamus.

Using three transgenic mouse lines I demonstrate that developing corticothalamic fibres target the specific groups of thalamic nuclei to which they project in adulthood. Rbp4-Cre::tdTomato labels layer V; Ntsr1-Cre::tdTomato labels layer VI; Golli-τ-eGFP labels layer VI and VIb. By P4 layer V fibres arborise densely in higher order nuclei but do not innervate the first order nuclei at any age. In contrast, at this age VI and VIb fibres densely innervate the first order ventral posterior-medial nucleus (VPM), as well as higher order nuclei.

Layer VI and VIb fibres accumulate outside the dorsal Lateral Geniculate Nucleus (dLGN) from P2 before entering at P6. During this waiting period, retinal fibres transmit spontaneous waves of activity to the dLGN. To assess whether retinal input regulates corticothalamic circuit development I performed monocular enucleation. I demonstrate that after loss of retinal input, layer VI and VIb fibres enter the dLGN prematurely, by P2. Furthermore layer V fibres which target the retino-recipient superior colliculus also enter prematurely following enucleation. These results suggest there may be a retinal mechanism which regulates the timing of corticofugal ingrowth to joint retinal/cortical targets. The loss of retinal driver input to the dLGN also induces layer V driver fibres to aberrantly enter the first order dLGN. These results are the first to show cross-hierarchical rewiring after losing peripheral sensory input.

The role of peripheral activity in the developing nervous system is underscored by activity dependent molecular mechanisms. I therefore performed a microarray gene expression experiment to systematically analyse molecular changes in the dLGN following enucleation. The expression of numerous genes is altered following enucleation including potassium channels Kcnk9 and Kcnn3, kinase pathway mediators, Shc3 and Dgkk, and immediate early genes BDNF, Egr1 and Egr2. The majority of genes regulated by enucleation are regulated in the opposite direction over development indicating that the loss of the retinal input delays maturation of the dLGN transcriptome.

In this thesis I demonstrate that early corticothalamic development targets specific thalamic nuclei. Using the visual system as a model I demonstrate that retinal input regulates corticothalamic development and contributes to the transcriptome of thalamic nuclei.

Acknowledgements

I would firstly like to thank Professor Zoltán Molnár for giving me the opportunity to pursue this research in his laboratory. I have greatly enjoyed working in Zoltán's laboratory and have been especially grateful for his stimulating and resolutely enthusiastic supervision.

Throughout my thesis I have worked with many inspiring scientists and benefited for their great intellectual and technical expertise. I am especially grateful to Dr Anna Hoerder-Suabedissen with whom I have enjoyed many project discussions, from whom I have learnt many laboratory techniques, and who has been a great friend and coffee drinker throughout (even after the 17 hour days). Dr Wei Zhi Wang has offered me invaluable advice and support especially during tricky experiments and always provided vital reminders to check the pipette. Professor Denis Jabaudon, University of Geneva, has been an exciting and generous collaborator to work with. In addition to sharing experimental results we have had many exciting and critical discussions about my project and I was very lucky to have the chance to visit his laboratory. Dr Louise Upton very kindly taught me the intraocular injection techniques which were vital to my project, and allowed me the use the stereotaxic frame for my crucial epibatidine results. Ms Sheena Lee provided much valuable advice on how to design my microarray and methods for optimising the tissue collection in addition to performing the microarray in the OXION facility. This work would also not have been possible without the help from the BSB staff including Denise Jelfs, James Ward and Rachel Foxhall.

It is a huge credit to Zoltán that the Molnár family is filled with hard-working but lively members and I am grateful for how much fun they have made this DPhil. I thoroughly enjoyed the long chats in the office (Wei Zhi Wang, Amanda Cheung, Isabel Martinez-Garay), late night lab dancing (Melissa Bailey), sunny picnics, Halloween parties (Fernando Garcia-Moreno, Navneet Vasistha), and the lab work too.

I wouldn't have been able to accomplish any of my achievements without the immense support from my family and friends. Mum, Dad and Teeps have encouraged and supported me through 27 years of adventures, both academic and trivial, and there are many more to come and I know they will still be there cheerleading me on. James is my constant personal source of strength and has been there throughout my DPhil and even from afar made it easy to keep me going through the final experiments and writing up. I have also been lucky to surround myself with a wider family; Heather, Julie, Rhoslyn, Paul and Alex (the crucial emergency support teams), and Sarah, Dina, Helen, John and Lee (over a decade now and never surprised).

Statement of Authorship

The work presented in this thesis is my own with the following exceptions and collaborations.

Section 3.3.1.

Carbocyanine dye crystal placement in the VPM was performed in conjunction with Professor Zoltan Molnar and Ms Miriam Hillyard a final honours school medical student. Retrograde dye labelling from the VPM was attained in collaboration with Ms Miriam Hillyard. I performed experiments from E18.5- P6, she performed experiments from P2-P10 and the results from all brains were collated. The cell counts, layer proportion analysis, graphing and images for all ages were my own work.

Section 3.3.2.

The initial brains of Rbp4-Cre::tdTomato (n=9) and Nstr1-Cre::tdTomato (n=9) were perfused and fixed by Dr Dante Bortone in Professor Massimo Scanziani's laboratory.

The anti NeuN immunohistochemistry and confocal microscopy was performed in conjunction with a summer school student Ms Jacqueline Boon. The cell counts, layer proportion analysis, graphing and images were all my own work.

Figure 3.12 Tissue for panels A, C, E, G and H was processed and imaged by Dr Anna Hoerder-Suabedissen.

Section 5.3.1

The microarray tissue collection and RNA extraction was performed with additional support from Dr Anna Hoerder-Suabedissen and Dr Wei Zhi Wang.

The sample preparation and microarray was performed by Ms Sheena Lee in the OXION core facilities. The quality control and Limma microarray statistics analysis was performed by Ms Sheena Lee.

The ANOVA/t-test intercept microarray statistics analysis was performed by Professor Denis Jabaudon.

The microarray experiment comparing the dLGN at P0 and P10 including all sample preparation and statistical analysis was performed by Dr Gabrielle Pouchelon in Professor Denis Jabaudons' laboratory.

The qPCR tissue collection and RNA extraction was performed with additional support from Dr Anna Hoerder-Suabedissen and Dr Wei Zhi Wang.

Contents

Alphabetical list of abbreviations

AC	Anterior Commissure
Acan	aggrecan
Adamts3	a disintegrin-like and metallopeptidase (reprolysin type) with thrombospondin type 1 motif, 3
Adra1d	adrenergic receptor, alpha 1d
Am	Amygdala
AMPA	α-Amino-3-hydroxy-5-methyl-4-isoxazolepropionic acid
APV	2-amino-5-phosphonovalerate
BDNF	brain derived neurotrophic factor
Calb2	calbindin 2
Cau P	Caudate Putamen
Cbln2	cerebellin 2 precursor protein
CC	Corpus Callosum
Cd24a	CD24a antigen
Cer. Pe.	Cerebral Peduncle
Chrm2	cholinergic receptor, muscarinic 2, cardiac
Chst2	carbohydrate sulfotransferase 2
Col6a5	collagen, type VI, alpha 5
CP	Cortical Plate
CREB	cAMP response element binding protein
CTAs	corticothalamic axons
CTB	cholera toxin b
CTGF	Connective Tissue Growth Factor
DAG	diacyleglycerol
DG	Dentate Gyrus
Dgkg	diacylglycerol kinase, gamma
Dgkk	diacylglycerol kinase kappa
dLGN	dorsal Lateral Geniculate Nucleus
DNQX	6,7-dinitroquinoxaline-2,3-dione
DTB	diencephalon telencephalon boundary
Dusp4	dual specificity phosphatase 4
Ecm2	extracellular matrix protein 2
Efna5	ephrinA5
Egr1	early growth response 1
Egr2	early growth response 2
EPSC	excitatory post-synaptic current
EPSP	excitatory post-synaptic potential
ERK1	Extracellular signal related kinase 1
ERK2	Extracellular signal related kinase 2
Fam19a4	family with sequence similarity 19, member A4
FGF	fibroblast growth factor
Fi	Fimbria
Fos	FBJ osteosarcoma oncogene
Frem3	Fras1 related extracellular matrix protein 3
Gfra1	glial cell line derived neurotrophic factor family receptor alpha 1

Gjd2	gap junction protein, delta 2
GP	Globus Pallidus
Gpr17	G protein-coupled receptor 17
Hcrtr2	hypocretin (orexin) receptor 2
Hip	Hippocampus
Hist1h4c	histone cluster 1 h4c
Hmcn1	hemicentin 1
Hmgb2	high mobility group box 2
Hmgn5	high-mobility group nucleosome binding domain 5
HN	Habenular Nucleus
IG	Intermediate grey layer of superior colliculus
Igf1	insulin-like growth factor 1
Igf2	insulin-like growth factor 2
IPSC	inhibitory post-synaptic current
IPSP	inhibitory post-synaptic potential
IW	Intermediate white layer of superior colliculus
JNK	c-Jun N-terminal kinases
Kcnk9	potassium channel, subfamily K, member 9
Kcnn3	potassium intermediate/small conductance calcium-activated channel, subfamily N, member 3
Krtap31-2	keratin associated protein 31-2
L1	L1 cell adhesion molecule
Lce1c	late cornified envelope 1C
LP	Lateral posterior thalamic nucleus
MAPK	mitogen activated protein kinase
MD	Mediodorsal thalamic nucleus
MGN	medial geniculate nucleus
MGNd	medial geniculate nucleus- dorsal
Mir382	microRNA 382
Moxd1	monooxygenase, DBH-like 1
Mxd4	Max dimerization protein 4
Myot	myotilin
NeuN	Neuronal Nuclei
NGF	nerve growth factor
NMDA	N-methyl-d-aspartate
Ntsr1	Neurotensin Receptor 1
ON	Optic Nerve layer of superior colliculus
Osbpl3	oxysterol binding protein-like 3
Otx2	orthodenticle homologue 2 (Drosophila)
PAG	Periaquaductal Grey
Pdlim5	PDZ and LIM domain 5
PH	Posterior Hypothalamic
Plp1	proteolipid protein (myelin) 1
Po	Posterior thalamic nucleus
PSPB	pallial subpallial boundary
Ptgds	prostaglandin synthase

Ptgr1	prostaglandin reductase 1
Pvt1	plasmacytoma variant translocation 1
Rbp4	Retinol Binding Protein 4
Rmnd5a	required for meiotic nuclear division 5 homologue A
Rnf114	ring finger protein 114
Rny3	RNA, Y3 small cytoplasmic (associated with Ro protein)
SCP	Superior Cerebellar Peduncle
SG	Superficial Grey of superior colliculus
Shc3	src homology 2 domain-containing transforming protein C3
shh	sonic hedgehog
Shisa6	shisa homologue 6 (Xenopus laevis)
Siah3	seven in absentia homologue 3 (Drosophila)
Sncg	synuclein, gamma
Snord116	small nucleolar RNA, C/D box 116
Spred2	sprouty-related, EVH1 domain containing 2
Stri	Striatum
Synm	synemin, intermediate filament protein
Tac1	tachykinin 1
Tacstd2	tumor-associated calcium signal transducer 2
Taf1d	TATA box binding protein (Tbp)-associated factor, RNA polymerase I, D
TAG1	Transient Axonal Glycoprotein 1 (Contactin 2)
TCAs	thalamocortical axons
Timp4	tissue inhibitor of metalloproteinase 4
TRN	Thalamic Reticular Nucleus
TTX	tetrodotoxin
Txnip	thioredoxin interacting protein
Ucp2	uncoupling protein 2
VB	Ventrobasal thalamic nucleus (includes VPM and VPL)
VGuT1	Vesicular Glutamate Transporter 1
vLGN	ventral Lateral Geniculate Nucleus
VPL	Ventral posterior thalamic nucleus- lateral
VPM	Ventral posterior thalamic nucleus- medial
Vsnl1	visinin-like 1
ZLI	zona limitans intrathalamica

1 Introduction

Our experience of the world is mediated by sensory receptors, which transmit information about the outside world into the brain. This peripheral sensory information (all modalities except olfaction), is first transmitted to the thalamus, a midline structure, which then relays the information to the cortex for processing. This is not a one-way route, however. The cortex feeds back to the thalamus thus as a unit the cortex and thalamus dynamically moderate the transmission of information for processing. This adult sensory processing circuit is established during embryonic and postnatal development and requires the proper formation of the cortex and the thalamus, and the correct guidance of the projections which connect the two. It is the development of the connecting projections, specifically those from the cortex to the thalamus, with which I am interested. In this introduction I describe the context in which corticothalamic development occurs. I therefore introduce the cortex and thalamus, the corticothalamic and thalamocortical circuits and how these features develop. Throughout the introduction I highlight questions which are raised by the current literature and I go on to outline the aims of my thesis.

1.1. The cortex

1.1.1. The cortex

The mammalian cerebral cortex is tasked with higher cognitive functions such as sensory information processing, cognitive ability and control of behaviour. Whilst it appears as a single sheet surrounding the rest of the brain, the cortex is highly functionally organised into layers, columns and areas. Horizontal layers can be distinguished by cell density (neuronal and non-neuronal) and consist of neurons in different levels of the cortical circuit. Vertical columns span the depth of the cortex encompassing all layers and form the basis of a functional unit in the cortex. Cortical areas are large groupings of columns broadly responsible for similar cognitive, behavioural or sensory processes (Jones and Rakic, 2010; Kaas, 2012).

A cross section of the cortex reveals 6-7 layers of cells (Brodmann, 1909; von Economo

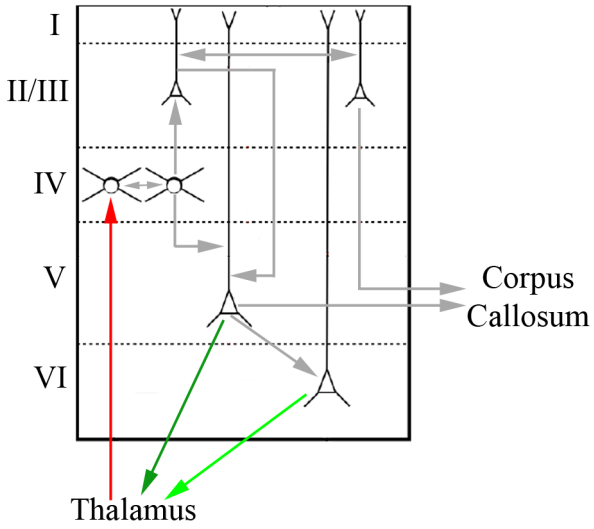

Figure 1.1. Route of information through cortical circuit. Thalamic input relaying sensory information is projected to layer IV. Layer IV neurons synapse on other layer IV neurons to amplify thalamic input, and transmits the input to layer II/III and V. Layer II/III and V project to the contralateral cortex via the corpus callosum. Layer V and VI project to the thalamus.

and Koskinas, 1925). Each layer is characterised by the cell morphology, size and density and can hence be distinguished by cellular staining methods and recently immunohistochemistry for layer specific markers (Molyneaux et al., 2007). The neurons in each layer perform specific tasks based on their afferent and efferent connections (figure 1.1) (Gilbert and Kelly, 1975; Gilbert, 1983). Thus each layer fulfils a different sub-function which contributes to the overall function of a single columnar processing unit. (Gilbert, 1983; Gilbert and Kelly, 1975; Douglas and Martin, 2004; Lubke and Feldmeyer, 2007; Thomson and Lamy, 2007; Thomson and Bannister, 2003; Gao et al., 2013). The major input to the cortex is from the thalamus, which transmits periphery related information to layer IV (figure 1.1) (Caviness and Frost, 1980). Layer IV relays this information throughout the cortex to II/III, V and VI. Layers V and VI are both cortical output layers (Sherman and Guillery, 2013). Layer V projects to the thalamus and to subcerebral targets such as the tectum and spinal cord. Layer VI projects to the thalamus. Long distance cortico-cortical connections include II/III and V which project cross-callosally. In addition to the 6 cortical layers there is layer VIb (also known as the subplate) which is a thin layer of heterogeneous neurons deep to layer VI directly above the white matter (Price et al., 1997; Hoerder-Suabedissen and Molnár, 2012; Hoerder-Suabedissen and Molnár, 2013).

Cortical layers are comprised of two types of neurons (in addition to the many non-neuronal cell types). The majority (70-80%) of cortical neurons are glutamatergic

excitatory neurons which make both local and long distance connections with neurons within and outside of the cortex (Parnavelas, 2000). The other 20% are inhibitory GABAergic neurons (Hendry et al., 1987; Sahara et al., 2012). GABAergic neurons make mainly local connections including within the layer in which they reside (Naegele and Barnstable, 1989; Markram et al., 2004).

The column is a functional organising unit of the cortex which vertically/ radially spans the 6-7 layers. The neurons across all layers in one column have been demonstrated to show the same modality and receptive field properties (Mountcastle, 1957; Mountcastle, 1997; Lubke and Feldmeyer, 2007; Feldmeyer, 2012). The structural boundaries and progenitor lineage of the cortical column are controversial (Gao et al., 2013; Rakic, 2008; Jones and Rakic, 2010). In the visual cortex for example there are functionally defined columns across all layers which are preferentially responsive to a particular orientation of visual stimuli but there is no clear anatomical definition (Hubel and Wiesel, 1968; Hubel and Wiesel, 1977; Hubel et al., 1977; Hubel and Wiesel, 1962; Hubel and Wiesel, 1963). In the somatosensory cortex there is cytoarchitectural barrel formation; the neurons in each barrel and in the same radial column as that barrel, process information from one whisker (Mountcastle, 1957; Mountcastle, 1997; Lubke and Feldmeyer, 2007; Feldmeyer, 2012). Thus functional columns are part of the radial organising principle of the cortex, the route neural signals take through the cortical layers is approximately bounded by the cortical column (Horton and Adams, 2005).

1.1.2. Development of the cortex

1.1.2.1. Cortical neurogenesis and layer development

The excitatory glutamatergic neurons and inhibitory GABAergic interneurons are generated in different proliferative zones and migrate via different routes into the cortex (Kriegstein and Noctor, 2004; Molyneaux et al., 2007).

Excitatory glutamatergic neurons are generated in a proliferative zone lining the lateral ventricles in the dorsal telencephalon/pallium; the ventricular zone (Angevine and Sidman, 1961; Noctor et al., 2004). Here the precursor cells called radial glia undergo

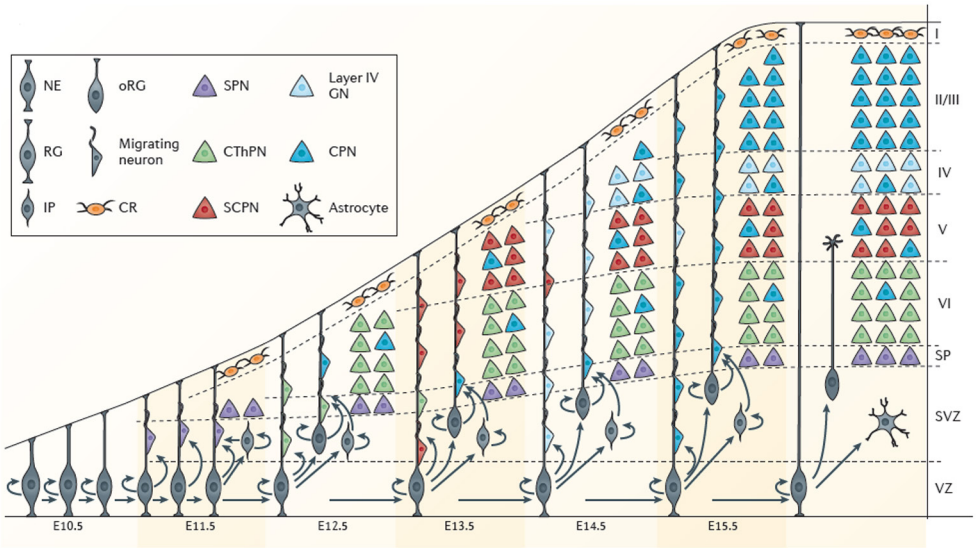

Figure 1.2. Sequential neurogenesis and radial migration. Cortical neurons are generated at the ventricular zone by radial glia from E11.5- E15.5. Layer VIb (subplate) neurons and the Cajal-Retzius cells are generated first. Successive rounds of neurogenesis generate neurons which migrate along the radial glia, past previously generated neurons to settle in layers. Each subsequent layer settles superficially to the previous layer thus the deepest layers are formed first. Abbreviations used: NE, neuroepithelial cell; RG, radial glia ; IP, intermediate progenitors; oRG, outer Radial Glia; CR, Cajal-Retzius cells; SPN, subplate neurons (layer VIb); CThPN, corticothalamic projection neurons; SCPN, subcerebral projection neurons; Layer IV GN, layer IV granular neurons; CPN, callosal projection neurons; VZ, ventricular zone; SVZ, subventricular zone; SP, subplate. Adapted from Greig et al., 2013.

asymmetric division to generate another radial glia cell and a cortical neuron (Malatesta et al., 2000; Miyata et al., 2001; Noctor et al., 2001; Noctor et al., 2002; Malatesta et al., 2003; Noctor et al., 2004; Anthony et al., 2004). In addition to their proliferative role, the radial glia also provide a scaffold along which new neurons can migrate to their position in the cortex. This is because radial glia have processes contacting both the basal surface of the ventricular zone, where neurons are generated, and the pial surface, towards which the neurons must migrate (Rakic, 1990; Misson et al., 1991; Hatanaka and Murakami, 2002; Kriegstein and Noctor, 2004).

The cortical layers are developed by the progressive addition of newly born neurons to the cortical plate. Each new layer migrates through the previously generated layers. The first neurons born migrate from the ventricular zone and generate the preplate (figure 1.2). This is then split into the marginal zone and the subplate when subsequent neurons migrate past the subplate and settle between the two layers (Marin-Padilla, 1971; Luskin and Shatz, 1985; Del Rio et al., 2000). Successively born neurons migrate radially, along the radial glia into the cortical plate settling in the layers inside out (figure 1.2)

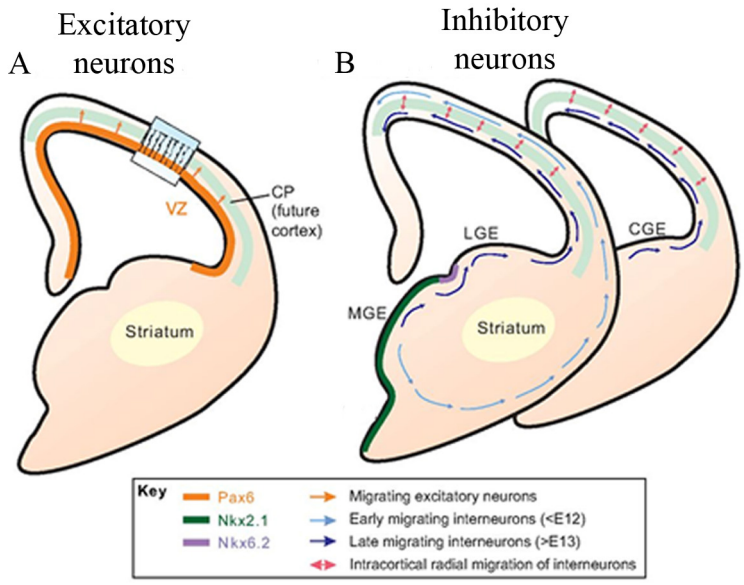

Figure 1.3. Radial and tangential migration. A. Glutamatergic neurons are generated in the ventricular zone in the pallium and migrate radially to their position. B. GABAergic neurons are generated in the ventricular zone of the subpallial ganglionic eminences and migrate tangentially into the cortex. Abbreviations used: VZ, ventricular zone; CP, cortical plate, LGE, lateral ganglionic eminence; MGE, medial ganglionic eminence; CGE, caudal ganglionic eminence. Adapted from Gao et al., 2013.

(Rakic, 1990; Misson et al., 1991; Hatanaka and Murakami, 2002; Kriegstein and Noctor, 2004). Thus neurons for the deepest layers (VI and V) are born earlier than those destined for the upper layers (II/III and IV) (Angevine and Sidman, 1961; Berry and Rogers, 1965; Luskin and Shatz, 1985; Tan and Shi, 2013). The subplate neurons which were early born and contributed to the preplate become layer VIb in the postnatal animal although many later undergo preferential cell death (Price et al., 1997).

The inhibitory GABAergic neurons are generated in a different proliferative region, the ventricular zone of the subpallium (the medial, lateral and caudal ganglionic eminences) and migrate tangentially from here into the cortex (figure 1.3) (Parnavelas, 2000; Sahara et al., 2012; Anderson et al., 1997; Kriegstein and Noctor, 2004).

1.1.2.2. Areal development

The distinct processing roles of the cortex are divided amongst areas of the brain which are functionally specified and often anatomically distinguishable (Brodmann, 1909; von Economo and Koskinas, 1925). Primary cortical areas are modality specific (visual, somatosensory, auditory) and directly receive sensory information via the thalamus (primary motor cortex receives cerebellar information). Secondary or association cortical areas are associated with the primary areas and are modality specific but do not receive direct input from the sensory relays (Brodmann, 1909; Jones and Powell, 1970). The functional specialisation of cortical areas is revealed in columnar units responsible

for processing information; barrel columns in primary somatosensory cortex (S1) (Woolsey and Van der Loos, 1970; Van der Loos and Woolsey, 1973), ocular dominance columns in primary visual cortex (V1) (Hubel and Wiesel, 1968; Hubel and Wiesel, 1962) and topographic mapping in primary cortical areas and some secondary cortical areas (Kaas, 1997). Topographic mapping is defined by areas which are adjacent in the physical world are represented by adjacent cortical areas; two adjacent barrels in S1 represent adjacent whiskers on the whisker pad, contiguous regions in V1 represent areas of the visual field which are next to one another.

How cortical areas become functionally specified during development has been of interest for some time. The role of intrinsic cues was originally formulated as the protomap model in which molecular cues in the ventricular zone dictate the future identity of the neurons generated in that particular region, and these fate determined neurons then migrate out radially to establish the areas in the cortex proper (Rakic, 1988). The protocortex or tabula rasa model on the other hand stated that post-mitotic neurons which have migrated into their cortical position are fundamentally similar across cortical areas and that the functional specialisation typical of each area arises once thalamic afferents grow into the cortex and provide modality specific input (Van der Loos and Woolsey, 1973; O'Leary, 1989).

Cortical arealisation is now thought to arise from progressive specification by the combined effect of intrinsic developmental programs of gene expression and extrinsic information from modality specific thalamic afferents. This model posits that in early development, intrinsic programs determine area specific gene expression across the cortex and then once thalamic afferents have arrived they contribute to further refinement and functional specification (Sur and Leamey, 2001; Sur and Rubenstein, 2005; Innocenti and Price, 2005; Mallamaci and Stoykova, 2006; O'Leary and Sahara, 2008).

Genes have been identified whose early expression is graded across the cortex and the loss of which disrupts normal arealisation. Morphogens are secreted ligands which

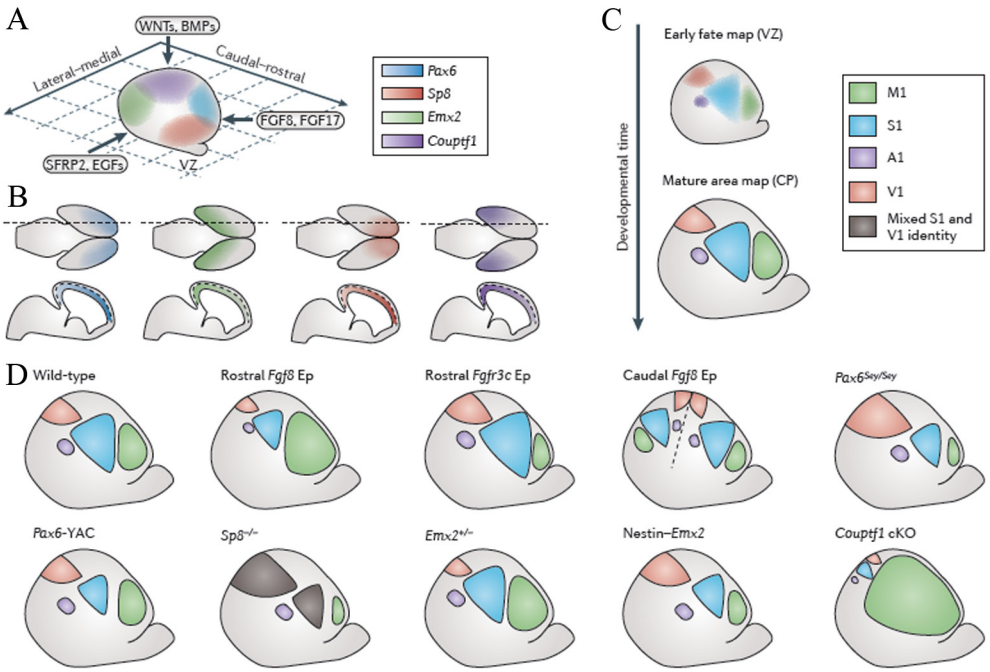

Figure 1.4. Morphogens, transcription factors and cortical arealisation. A and B. Diffusible morphogens and signalling molecules are expressed in gradients across the cortex which induce the graded expression of transcription factors such as Pax6, Sp8, Emx2 and Couptf1. C. The gradual formation of boundaries between cortical areas over development. D. Cortical area boundaries are disrupted in mutants of the graded morphogens and transcription factors. Electroporation (EP) of fibroblast growth factor 8 (Fgf8) into rostral cortex, causes expansion of rostral cortical areas. Electroporation of Fgf-receptor3 into rostral cortex causes expansion of middle cortical areas. Electroporation of Fgf8 into caudal cortex causes mirrored duplication of cortical arealisation. Pax6Sey/Sey, Pax6 'small eye' hypomorphic mutant allele causes expansion of caudal cortical areas. Pax6-YAC, overexpressing Pax6 causes contraction of somatosensory cortex. Sp8-/- causes S1 and V1 to have mixed identities. Emx2+/– causes contraction of visual cortex. Nestin-Emx2 overexpression causes contraction in rostral cortical areas. Couptf1 conditional knockout causes expansion of motor cortex. Adapted from Greig et al., 2013.

are expressed from an organising region and diffuse to a gradient. By activating intracellular signalling cascades they cause graded expression of transcription factors which direct area specific neuronal differentiation programs. Ligands include members of the Fibroblast growth factor (FGF) family (expressed from rostral and medial organiser centres), and Wnt and bone morphogenic protein (BMP) family members (expressed in the cortical hem, medial and caudal) (figure 1.4 A and B) (Mallamaci and Stoykova, 2006; O'Leary and Sahara, 2008). These morphogens cause graded expression of transcription factors including Pax6, Sp8, Emx2 and Couptf1 (figure 1.4 A and B). Gain or loss of function mutations and *in utero* manipulation of these ligands, their receptors and the downstream transcription factors cause significant disruption to cortical arealisation by expanding or contracting different cortical areas (figure 1.4 D)

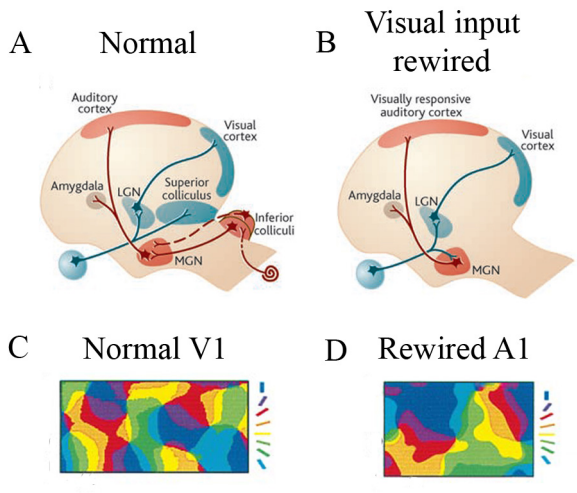

Figure 1.5. Functional rewiring of sensory circuits. A. Retinal input is transmitted to V1 via the LGN. Cochlear input is transmitted to A1 via the MGN. B. In rewired ferrets, retinal input is transmitted to both the LGN and the MGN and is therefore transmitted to both V1 and A1. C. In control animals a composite map of orientation selectivity in V1 shows orientation selective patches of neurons which organise into pinwheel formation. D. In rewired animals, A1 also shows orientation selective patches of neurons which organise into pinwheel formation. Abbreviations used: LGN, lateral geniculate nucleus; MGN, medial geniculate nucleus; V1, primary visual cortex; A1 primary auditory cortex. Adapted from Sur and Rubenstein, 2005.

(Mallamaci and Stoykova, 2006; O'Leary and Sahara, 2008; Rash and Grove, 2006; Greig et al., 2013).

Peripheral input is also important in the functional specification of cortical areas (O'Leary, 1989). Loss of sensory input can abolish normal features of specific areas and rewiring input can ascribe abnormal functional specialisation to other cortical areas. Damage to, or removal of, whiskers abolishes barrel formation and the associated dendritic rearrangements of layer VI and VIb neurons within S1 (Van der Loos and Woolsey, 1973; Piñon et al., 2009). Various properties of the visual cortex are reorganised following monocular enucleation such as ocular dominance columns (Hubel and Wiesel, 1968; Hubel and Wiesel, 1962) and the projections of the remaining eye expand to innervate regions normally innervated by the removed eye thus generating a duplicated map within V1 (Trevelyan et al., 2007). Enlarging or reducing the dLGN (size and cell number) by manipulating sonic hedgehog signalling, via a constitutively active smoothened receptor or thalamic specific knockout , causes a corresponding expansion or contraction in the size of V1 (Vue et al., 2013).

Furthermore the rerouting of sensory input from one modality, for example visual, to a cortical area normally recipient of a different modality, auditory or somatosensory, can induce that new target area to display visual properties including orientation column pinwheels and retinotopic maps (figure 1.5A, B) (Frost and Metin, 1985; Sur et al.,

1988; Metin and Frost, 1989; Roe et al., 1990; Roe et al., 1992; Angelucci et al., 1997). Although the 'auditory' neurons receiving visual input do not succeed in complete transformation, their receptive fields are less specific and have poorer responses to visual activity. None-the-less they display orientation, direction and velocity selectivity (figure 1.5 C, D) and it was later demonstrated that they can mediate visually evoked behaviour (Sur et al., 1988; Roe et al., 1990; Roe et al., 1992; Angelucci et al., 1997; von Melchner et al., 2000; Sharma et al., 2000; Frost et al., 2000). Results such as these conclusively demonstrated that the modality of thalamocortical input can elicit cortical area specialisations although it may be less fine grained without the early intrinsic molecular programs preparing the cortical areas for the appropriate inputs.

The intrinsic and extrinsic mechanisms in neural development do not act in isolation and in fact influence one another to determine neural specification. Firstly key arealisation genes may alter the targeting of thalamic inputs. Emx2 is expressed in a high caudal to low rostral gradient (figure 1.4 B) (Mallamaci et al., 1998). Emx2 mutant mice demonstrate drastically reduced visual cortex (figure 1.4 D). The thalamus is unaffected by the mutation however thalamocortical input from the VPM expands to innervate caudal areas of cortex normally innervated by the dLGN (Bishop et al., 2000; Mallamaci et al., 2000). Thus early organiser gene expression contributes to thalamic afferent ingrowth, which can then contribute to further transcriptional and functional specification of cortical areas.

Secondly the effect of peripheral input on cortical arealisation and functional specification is underscored by downstream molecular mechanisms; disrupting peripheral input alters gene expression within the cortex. Genetically ablating thalamic input to primary cortical areas abolishes gene expression boundaries that distinguish primary and association cortex. RORβ, cadherin8, m2AChR and SMI-32 are normally restricted to primary cortex areas such as V1; Igfbp4, Igfbp5 and Lmo4 are restricted to association cortex including association visual areas. These genes become diffusely expressed across primary and association cortex when thalamic axons are abolished

(Chou et al., 2013; Vue et al., 2013).

Recently the advent of microarray gene expression analysis has enabled research into how the peripheral input is translated into molecular cascades that could determine areal development. For example thalamic input to the primary somatosensory cortex (S1) from the posterior thalamic nucleus (which normally projects to the secondary somatosensory cortex (S2)) can specify S2 gene expression in the S1 neurons (Pouchelon et al., 2014b).

Thus cortical arealisation and functional specification is determined by the combination of and interaction between intrinsic genetic programs and extrinsic input driven mechanisms which intersect during early cortical circuit generation.

1.2. The thalamus

1.2.1. The thalamus

The thalamus, a diencephalic structure, straddles the midline with mirrored nuclei in each hemisphere. In the mammalian brain peripheral sensory information is transmitted to the thalamus before being relayed from the thalamus to the neocortex. All peripheral sensory information is represented in the thalamus with the exception of olfaction (which is represented indirectly via pyriform cortex projection to mediodorsal thalamic nucleus) (Jones, 1985).

The thalamus is comprised of numerous nuclei each of which for the purposes of this thesis will be considered as a structural and functional entity (figure 1.6). The reality is more complex as thalamic nuclei contain at least two types of relay cells which may be integrated into parallel processing pathways (Jones, 2001; Sherman and Guillery, 2006). Core relay cells (which are parvalbumin positive in primate) are present in most thalamic nuclei and project to layer IV of primary cortex (Jones, 2001). There are also the calbindin positive matrix relay cells. These are present in all thalamic nuclei (although much reduced in the nuclei which also contain core relay cells) and send diffuse projections to the superficial layers (I-III) throughout the cortex (Jones, 2001).

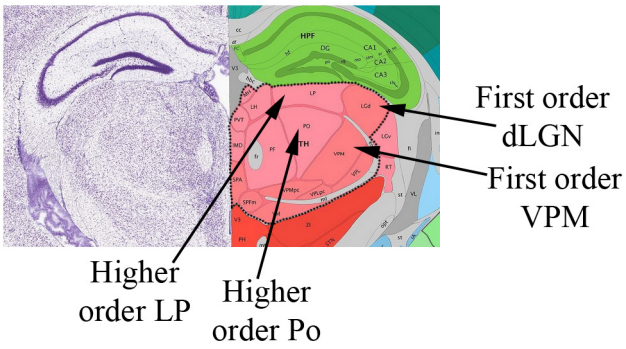

Figure 1.6. Coronal section of the thalamus showing first order and higher order thalamic nuclei. Thalamus outlined by black dots. First order thalamic nuclei are shaded darker pink and at this coronal level include the dLGN (LGd) and VPM. Higher order thalamic nuclei are shaded lighter pink and at this coronal level include the LP and Po. LGv and RT are pre-thalamic structures. Important abbreviations: dLGN/ LGd, dorsal Lateral Geniculate Nucleus; VPM, ventral posterior-medial nucleus; Po, posterior thalamic nucleus; LP, lateral posterior nucleus; LGv, ventral Lateral Geniculate Nucleus (vLGN); RT, thalamic reticular nucleus (TRN). Adapted from Allen Institute for Brain Science. Allen Mouse Brain Atlas [Internet]. Available from: http://mouse.brain-map.org/

These matrix relay cells may provide modulator input from the thalamus to the cortex rather than driver inputs (more detail on this distinction is considered in section 1.3.1.1) (Viaene et al., 2011a; Viaene et al., 2011b; Viaene et al., 2011c). The core thalamic relay cells are present in most thalamic nuclei and it is their function and integration into the cortex which is of interest in this thesis. Consequently future use of 'thalamic relay cells' refers to core thalamic relay cells.

The nuclei of the thalamus can be divided into two orders. The first order nuclei are modality specific and receive input from subcortical afferents (figure 1.7 A). Retinal ganglion cells project directly from the retina to the dorsal Lateral Geniculate Nucleus (dLGN) which is the first order thalamic nucleus integrated into the visual system (Le Gros Clark, 1932). Somatosensory information is relayed via the trigeminal ganglion to the thalamic ventral posterior nucleus (medial) (VPM), auditory information is relayed via the cochlear nucleus and inferior colliculus to the medial geniculate nucleus (MGN) (Le Gros Clark, 1932). The core thalamic relay cells in these first order nuclei transmit the modality specific information to the corresponding cortical area; the dLGN projects to V1, VPM projects to S1, MGN projects to the primary auditory cortex (A1) (Le Gros Clark, 1932; Sherman and Guillery, 1996; Guillery and Sherman, 2002).

The second order of thalamic nucleus is the higher order nucleus. These also show modality specificity however they do not receive direct input from subcortical sensory structures. Instead they receive input from the cortex and thus provide a trans-thalamic route for cortico-cortical information (figure 1.7 A) (Sherman and Guillery, 1996; Guillery and Sherman, 2002). The nature of different inputs to the higher order thalamic nuclei will be discussed in more detail in section 1.3.1.4.

The thalamic nuclei also exhibit functional specialisations. They have cytoarchitectural specialisations such as the barreloid formation in the VPM (each barreloid corresponding to one whisker on the whisker pad, and projecting to one barrel in S1) (Van Der Loos, 1976; Durham and Woolsey, 1984). The thalamic nuclei are also topographically mapped (Udin and Fawcett, 1988; Hohl-Abrahao and Creutzfeldt, 1991; Adams et al., 1997; Kaas, 1997).

1.2.2. The development of the thalamus

1.2.2.1. Thalamic development

The thalamus develops in the diencephalon, its rostral extent limited by the sonic hedgehog expressing zona limitans intrathalamica (ZLI), its caudal extent limited by the pretectum (Price et al., 2012). Excitatory glutamatergic thalamic neurons are generated in the proliferative ventricular zones which line both sides of the third ventricle. The thalamic ventricular zone has distinct progenitor zones; progenitors expressing different combinations of Gbx2, Olig3, Sox2, Ngn1 and Ngn2 generate glutamatergic thalamic neurons (Jones and Rubenstein, 2004; Vue et al., 2007; Price et al., 2012). Post-mitotic neurons migrate from the ventricular zone outwards to the nascent thalamic mantle zone which leads to the progressive generation of the specific thalamic nuclei.

In the mouse the majority of glutamatergic thalamic neurons are generated between E11 and E13 (Angevine, 1970). Neurons destined for lateral/caudal/ventral nuclei arise earlier than those contributing to medial/rostral/dorsal nuclei (Angevine, 1970; McAllister and Das, 1977; Altman and Bayer, 1979; Altman and Bayer, 1989).

In primates local GABAergic neurons integrate into all thalamic nuclei however in

rodents GABAergic interneurons are only present in the dLGN (Arcelli et al., 1997). The GABAergic neurons are generated in a prethalamus ventricular zone and migrate into the thalamus sometime after the glutamatergic neurons have differentiated (Jones, 2002a; Golding et al., 2013).

The thalamic reticular nucleus (TRN) is in fact a prethalamic structure and is developed from the Mash1 and Dlx positive prethalamus ventricular zone which predominantly generates GABAergic neurons (Jones, 2002a; Hayes et al., 2003; Jones and Rubenstein, 2004; Vue et al., 2007).

1.2.2.2. Thalamic nuclei specification

Like the arealisation of the cortex, the specification of nuclei in the thalamus involves both intrinsic genetic programs and peripheral input. Genetic programs determining any individual thalamic nucleus have yet to be elucidated, however families of molecules have been identified which are differentially and combinatorially expressed in the thalamus and which have been proposed to organise the nascent thalamic mantle into distinct aggregates of cells. The precise combination of transcription factor expression in a group of neurons may contribute to their nuclear identity (Price et al., 2012).

Several transcription factors are differentially expressed in the developing thalamic nuclei (Nakagawa and O'Leary, 2001; Vue et al., 2009; Suzuki-Hirano et al., 2011). At E16.5 Lhx2, Lhx9, Gbx2 and Ngn2 are expressed in the MGN but only Lhx9 and Ngn2 are expressed in the dLGN and VPM. As early as E14.5 these transcription factors distinguish between these thalamic nuclei. The putative border between the dLGN and the LP is not visible by histological techniques such as Nissl but can be seen by Gbx2 *in situ* hybridisation (Nakagawa and O'Leary, 2001). These transcription factors may be downstream of signalling molecules such as FGF8 and Shh which are expressed in gradients. Knockout of Shh in the thalamus abolishes normal RORα patterning and causes Gbx2 expression in presumptive first order thalamic nuclei (Vue et al., 2009). FGF8 over expression close to the ZLI causes a caudal shift of the VPM, antagonising FGF8 activity causes a rostral shift of VPM (Kataoka and Shimogori, 2008).

Nuclear receptors RORα and RORβ differentiate between first and higher order thalamic nuclei. At E17.5 RORα is expressed exclusively in first order nuclei the dLGN, VPM and MGN whereas RORβ is expressed more widely; VPM, MGN, Po, the medial dorsal nucleus (MD) and the central medial (CM) nucleus (Nakagawa and O'Leary, 2003). Other first order nuclei specific genes include p57Kip2, a cyclin-dependent kinase inhibitor and SERT, a serotonin transporter (Lebrand et al., 1998; Yuge et al., 2011).

Transcription factors and nuclear receptors contribute to nuclear specification of the thalamus via the action of genes that they regulate the transcription of. Downstream genes which directly contribute to the nuclear specification are less well known however there are some candidates.

Eph tyrosine kinase receptors and their ligands, ephrins, are well known guidance molecules. Due to their repulsive interactions they have also been suggested to play a role in cellular aggregation. EphA4 and A7 are expressed throughout the thalamic nuclei and EphA8 is expressed in the dLGN, LP and Po but is distinctly absent from the VPM (Yuge et al., 2011; Price et al., 2012; Lehigh et al., 2013). Ligand ephrinA5 is expressed in the VPM, the dLGN, the LP and Po (Lehigh et al., 2013; Yuge et al., 2011). Cells expressing EphA7 aggregate separately from cells expressing ephrinA5, and EphA7 knockout causes the thalamus to have less clearly defined nuclei (Lehigh et al., 2013).

To date genes which distinguish between groups of thalamic nuclei tend to differentiate between the first order- sensory input receiving nuclei and the higher order nuclei. A microarray gene expression analysis was recently used to compare gene expression in the first order VPM, dLGN and higher order Po at early postnatal stages, P0, P3, P10 (Pouchelon et al., 2014a). These results demonstrate that the thalamic nuclei have distinct gene expression patterns and that higher order nuclei cluster together and first order nuclei cluster together (Pouchelon et al., 2014a).

There is significant progress in understanding genetic mechanisms of developmental specification however genetic programs which specify a particular nucleus have not

yet been identified. As in the cortex, genetic programs are not the sole determinants of thalamic nuclei; peripheral sensory input has also been demonstrated to contribute to the molecular specification of thalamic nuclei.

Somatosensory input to the whisker field in the VPM can be removed by infraorbital nerve transection. By using microarray gene expression experiments Pouchelon and colleagues showed that the VPM which lacks input from the infraorbital nerve has a gene expression profile which is more similar to the Po (Pouchelon et al., 2014a). The Po is the higher order somatosensory thalamic nucleus. Thus these results suggest that the sensory input contributes to the transcriptional identity of the nucleus to which it projects. Furthermore the input may contribute to the specialisation of first order nuclei gene expression, and serve to distinguish them from higher order nuclei.

Furthermore rerouting of peripheral input from one first order nucleus to another has demonstrated that peripheral input can determine modality specific first order gene expression. Retinal input can be induced to project to the MGN (the auditory thalamic nucleus, figure 1.5 B) instead of the dLGN in young ferrets by removing the cochlear and inferior colliculus (Roe et al., 1993; Angelucci et al., 1997; Angelucci et al., 1998; Frost et al., 2000). A microarray analysis comparing the control MGN, control dLGN and rewired MGN demonstrated that the rewired MGN began expressing genes which were normally expressed in the dLGN (Horng et al., 2009).

Such results confirm that peripheral input contributes to the developmental gene expression of specific first order thalamic nuclei. However the role of peripheral input on the early development of various first order thalamic nuclei has not been extensively studied for example the role of retinal input on gene expression in the developing dLGN has not been addressed.

1.3. The adult corticothalamic circuit

1.3.1. Corticothalamic circuit

I have introduced the development of the cortex, responsible for processing and higher

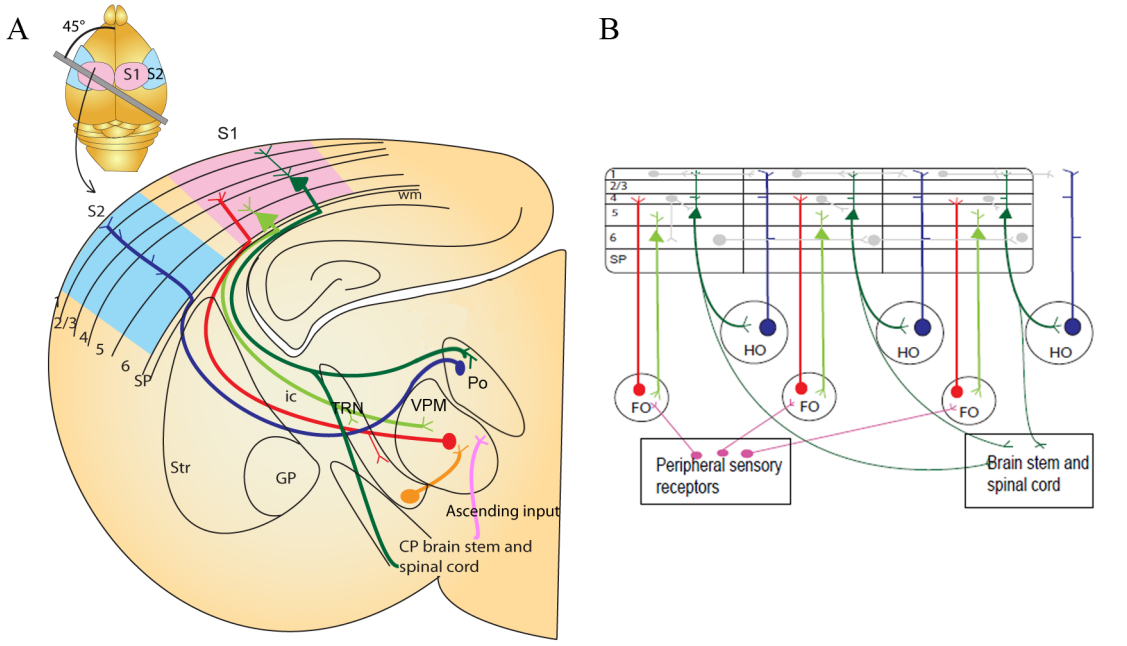

Figure 1.7. The adult corticothalamic circuit. A. Coronal schematic demonstrating the connections between the cortex and thalamus using the somatosensory system (idealised section). The first order VPM thalamic nucleus receives somatosensory peripheral input (pink). The VPM projects axons (red) to layer IV of the S1 (light pink). Layer VI 'modulator' neurons (light green) in S1 project back to the VPM. Layer V neurons (dark green) in S1 project to sub-cerebral structures, and to the higher order posterior thalamic nucleus (Po). The higher order Po projects (dark blue) to an area of cortex that is different from the one it received input from (S2; light blue). This projection pattern generates an open loop. B. Schematic of the possible functional circuits generated by this reoccurring open loop connectivity. Sensory information is relayed through the first order thalamic nucleus to the cortex (red). The cortical area then projects from layer VI reciprocally to the first order nucleus (light green). Each area is also non-reciprocally connected to a higher order thalamic nucleus via layer V (dark green). Higher order nuclei project to association cortex (blue). Direct cortico-cortical connections are also depicted between cortical layers and cortical areas (pale grey). CP, cerebral peduncle; FO, first order thalamic nuclei; GP, globus pallidus; HO, higher order thalamic nuclei; ic, internal capsule; TRN, reticular thalamic nuclei; SP, subplate; Str, striatum; S1, primary somatosensory cortex; S2, secondary association somatosensory cortex; Po, posterior thalamic nuclei; VPM, ventral posterior- medial thalamic nucleus; wm, white matter. Adapted from Grant et al., 2012.

cognitive abilities, and the thalamus which receives input from the sensory periphery and relays it to the cortex via thalamocortical projections. However, the thalamus is not a mere relay station, transmitting unchanged sensory information to the cortex. Instead the thalamus and cortex combined form an integrated processing unit that regulates the transmission of peripheral data for cortical processing (Sherman and Guillery, 1998). As part of this unit, all neocortical areas send projections back to the thalamus, via corticothalamic projection neurons (Caviness and Frost, 1980).

The corticothalamic circuit consists of three populations of cortical neurons and two orders of thalamic nuclei (figure 1.7). The flow of information through the thalamus is categorised into two orders of relays (first order and higher order). Different thalamic

nuclei and different cortical layers contribute to each ‘order’. The thalamic nuclei can be considered first order and higher order based on which relay they most significantly contribute to.

The cortical component of the circuit consists of glutamatergic projection neurons in layers IV, V and VI. As discussed previously the neurons in each layer have distinct functions which can be most simply categorised by their connections. Layer IV neurons receive input from the thalamic afferents and project to layer II/III, V and IV. Layer V and VI neurons project either sub-cortically, to structures such as the thalamus and the spinal cord (corticofugal projections- V and VI), or across the corpus callosum (cortico-cortical projections- V) (Douglas and Martin, 2004; Molyneaux et al., 2007).

1.3.1.1. Driver and modulator input

Numerous classes of functionally distinct neuronal inputs have been characterised in the nervous system. For the purposes of this thesis I will distinguish between two classes of synaptic inputs, drivers and modulators, which have different effects on the post-synaptic cell.

Driver (class I) inputs transmit messages; they define the fundamental activity and receptive field properties of the post-synaptic neuron (Sherman and Guillery, 1996; Sherman and Guillery, 1998; Sherman and Guillery, 2006). Modulator (class II) inputs modify the way in which messages are transmitted, altering the effectiveness of the driver without altering the fundamental characteristics of the message (Sherman and Guillery, 1996; Sherman and Guillery, 1998; Sherman and Guillery, 2006). Modulators can include inhibitory, GABAergic interneurons. However, for the most part our interest is in the glutamatergic modulators which arise from the cortex. The table below discusses the distinctions between driver and modulator inputs to the core thalamic relay neurons.

	Driver properties	Modulator properties (excitatory)	Modulator properties (inhibitory)
Populations	Subcortical sensory input (e.g. retinal ganglion cells), Layer V from the cortex	Layer VI from the cortex	GABAergic neurons in thalamic reticular nucleus (TRN), GABAergic interneurons within thalamic nuclei
Receptive field properties	Determines receptive field properties in thalamic relay neurons	Does not determine receptive field properties in thalamic relay neurons	Does not determine receptive field properties in thalamic relay neurons
Receptors	Ionotropic only	Metabotropic only	TRN: metabotropic, no data for interneurons
EPSPs	Large	Small EPSPs	TRN: small IPSPs, no data for interneurons
Terminals	Large terminals on proximal dendrites, multiple contacts	Small terminals on distal dendrites, single contacts	Small terminals, TRN: distal, interneurons: proximal. Both single contacts
Convergence on target	Little	Much	-
Neurotransmitter	Glutamatergic	Glutamatergic	GABAergic
Synapse features	Paired pulse inhibition	Paired pulse facilitation	-
Branch innervation	Other sub-telencephalic targets	Thalamus only	Thalamus only
Targets in corticothalamic circuit	Thalamus, doesn't target TRN	Thalamus and TRN	TRN: thalamus and TRN, interneurons: thalamus

Table 1.1. Key characteristics of driver and modulator inputs to the core thalamic relay cells. Abbreviations used: TRN, thalamic reticular nucleus; EPSP, excitatory post-synaptic potential; IPSP, inhibitory post-synaptic potential. Based on a table in Sherman and Guillery 2006, Chapter 7 Drivers and Modulators (Sherman and Guillery, 2006).

There are other presumed modulator inputs to the thalamus. These include cholinergic, noradrenergic and serotonergic inputs from the brainstem, however they are sparse, less well characterised and it is not known how they contribute to the corticothalamic circuit (Sherman and Guillery, 1998; Sherman and Guillery, 2006). Thus for simplicity these

are not considered in further detail here.

Thalamic relay neurons may also split into driver and modulator classes; the core relay cells provide driver input to layer IV of the cortex and are the main focus of this thesis, the matrix relay cells may provide modulatory input to the cortex via their diffuse projections (Wimmer et al., 2010; Viaene et al., 2011a).

1.3.1.2. The first order thalamocortical relay

The first order thalamic relay is most easily defined as it is concerned with the transmission of sensory information via modality specific thalamic nuclei to the corresponding cortical area (figure 1.7).

First order thalamic nuclei include the dorsal Lateral Geniculate Nucleus (dLGN), ventral posterior-medial nucleus (VPM) and the ventral portion of the medial geniculate nucleus (MGN). These nuclei contain core thalamic relay cells that receive driver input from their respective subcortical sensory sources. The optic nerve is the primary driver to dLGN relay neurons (Valverde, 1968; Godement et al., 1980; Reichova and Sherman, 2004). Medial lemniscal fibres from the trigeminal ganglion transmit somatosensory information to the VPM (Ralston III, 1969; Smith, 1973). The inferior colliculus projects auditory information to the MGN (Jones and Rockel, 1971; Lee and Sherman, 2010).

These thalamic relay cells then project to the corresponding primary cortex based on sensory modality. The dLGN projects to layer IV of the primary visual cortex (V1) (Frost and Caviness, 1980; Crandall and Caviness, 1984; Sherman and Guillery, 2006). The VPM projects to layer IV of the primary somatosensory cortex (S1) (figure 1.7A) (White, 1978; Frost and Caviness, 1980; Crandall and Caviness, 1984; Keller et al., 1985). The thalamic projections largely target cortical neurons situated in layer IV, but almost all cortical layers receive some thalamic input (Frost and Caviness, 1980).

1.3.1.3. Layer VI cortical input to the first order thalamic nuclei

Cortical innervation of thalamic nuclei depends on the laminar identity of the cortical

neurons (figure1.7).

Layer VI corticothalamic neurons provide modulator input to all thalamic nuclei; first order and higher order (Jones and Powell, 1968; Diamond et al., 1969; Gilbert and Kelly, 1975; Abramson and Chalupa, 1985; Hoogland et al., 1987; Conley and Raczkowski, 1990; Lozsádi et al., 1996; Sherman and Guillery, 1998; Olsen et al., 2012). The layer VI axons from a primary cortical area project to the first order thalamic nucleus from which it receives input, continuing modality specificity; from V1 they project to dLGN (Guillery, 1967; Olsen et al., 2012), from S1 to VPM (figure 1.7A) (Hoogland et al., 1987; Jones and Powell, 1968; Reichova and Sherman, 2004), and from auditory cortex (A1) to medial geniculate nucleus (MGN) (Diamond et al., 1969). Layer VI input to higher order nuclei is also modality specific; layer VI in V1 projects both to the dLGN and the LP (the higher order visual thalamic nucleus) (Olsen et al., 2012; Sherman and Guillery, 2013).

Synapses from layer VI fibres largely outnumber synapses from the sensory input to the first order thalamic nuclei (Mitrofanis and Guillery, 1993). Approximately 5% of synapses onto relay cells in the dLGN originate from retinal neurons (Van Horn et al., 2000; Bickford et al., 2010) whereas layer VI axons contribute 40-50% of synapses this is similar in the VPM (Liu et al., 1995; Guillery, 1969; Wilson et al., 1984).

Layer VI corticothalamic inputs display clear modulator properties. They terminate in small but numerous glutamatergic synapses on the distal dendrites of thalamic relay cells and facilitate relay neuron activity by generating small excitatory post-synaptic potentials/ currents (EPSP/Cs) which have an NMDA, AMPA and mGluR1 component and demonstrate paired-pulse facilitation (Rouiller and Welker, 2000; Guillery, 1995; Jones, 2002b; Sherman and Guillery, 1998; Reichova and Sherman, 2004; Lam and Sherman, 2010).

In addition to direct excitatory modulation of thalamic relay cell activity, layer VI axons also generate indirect (disynaptic) inhibitory modulation of thalamic relay

neuron activity. Layer VI collaterals innervate the GABAergic thalamic reticular nucleus (TRN) which projects to the thalamus, thus generating an inhibitory feed-forward circuit (Hoogland et al., 1987; Lozsádi et al., 1996; Jones, 2002b; Lam and Sherman, 2010; Olsen et al., 2012). Activation of layer VI in S1 by uncaging glutamate or channel rhodopsin causes a biphasic EPSC/IPSC (inhibitory post-synaptic current) response in the VPM (Lam and Sherman, 2010; Cruikshank et al., 2010). The initial short latency (monosynaptic) EPSC is followed by a longer latency IPSC via layer VI activation of the TRN neurons which inhibit the VPM relay neurons (Lam and Sherman, 2010). This indirect cortical inhibition of thalamic relay cell activity alters cortical activity downstream. Channel rhodopsin activation of layer VI in V1 causes a rapid but reversible reduction of dLGN neuron activity (via the TRN) in response to visual input and subsequently reduces the firing of cortical neurons in all layers of V1 (Olsen et al., 2012). Silencing layer VI modulation of the dLGN by stimulating parvalbumin positive GABAergic cortical interneurons facilitated dLGN neuron activity (Olsen et al., 2012).

Thus layer VI corticothalamic inputs modulate first order thalamic relay cell activity by two mechanisms, one excitatory which is monosynaptic and the other inhibitory via the TRN (Guillery, 1995; Jones, 2002b). The ability of the layer VI corticothalamic projections to have two distinct effects on the thalamic relay cells via these two separate pathways is thought to be based in the capacity of the relay neurons to operate in different functional modes depending on membrane potential (Jones, 2002b). Layer V fibres on the other hand provide only driver input to thalamic relay neurons (Sherman and Guillery, 1998; Jones, 2002b).

1.3.1.4. The higher order thalamocortical relay and layer V input

Higher order thalamic nuclei receive their driver input from layer V of the cortex and project to other cortical areas (figure 1.7A). This cortical driver input in part distinguishes them from the first order nuclei whose driver input arises from the sensory afferents (Reichova and Sherman, 2004).

The higher order relay provides a trans-thalamic pathway for cortico-cortical

information which is distinct from direct cortico-cortical connections and can be between primary cortical areas and higher/ association cortical areas or between two association cortical areas (figure 1.7 A and B) (Jones, 2002b; Guillery and Sherman, 2002).

Corticothalamic fibres arising from layer V have a more restricted thalamic projection pattern targeting only higher order thalamic nuclei (unlike layer VI which targets first order and higher order nuclei). Layer V corticothalamic fibres are branches of layer V corticotectal and corticospinal neurons (Deschênes et al., 1994; Sherman and Guillery, 2002; Groh et al., 2008; Reichova and Sherman, 2004). These higher order nuclei are associated with sensory systems despite lacking direct driver input from the sensory periphery and appear to be involved in behaviours that collate input across several modalities.

The lateral posterior nucleus (LP) receives driver input from layer V of V1 (Deschênes et al., 1994; Bourassa and Deschenes, 1995; Li et al., 2003b; Olsen et al., 2012) and projects to numerous association visual cortex areas (Kamishina et al., 2009; Guillery and Sherman, 2002; Sherman and Guillery, 2002) in addition to the medial prefrontal cortex (Sukekawa, 1988), the posterior parietal cortex (Reep et al., 1994) and the medial agranular cortex (Reep and Corwin, 1999). These projections have been suggested to mediate a variety of behaviours such as directed attention and visuo-motor integration (Sukekawa, 1988; Kamishina et al., 2009; Reep et al., 1994; Reep and Corwin, 1999).

The posterior thalamic nucleus (Po) receives driver input from layer V of S1 (Diamond et al., 1992; Bourassa et al., 1995; Reichova and Sherman, 2004; Theyel et al., 2010). The Po then projects to S2 (Wimmer et al., 2010; Viaene et al., 2011a) as well as S1 and primary and secondary motor cortex (M1 and M2 respectively) (Ohno et al., 2012; Kichula and Huntley, 2008). This trans-thalamic cortico-cortical pathway via the Po can robustly drive S2 (Theyel et al., 2010).

As these circuits relay information from one cortical area to numerous different

cortical areas this trans-thalamic relay forms an open loop circuit (figure 1.7 B) which allows the integration of information processing across several cortical areas and the synchronisation of cortical and thalamic cell populations (Jones, 2001; Jones, 2002b; Sherman and Guillery, 2002; Guillery and Sherman, 2002).

1.3.1.5. First order/ higher order nuclei and relays

In this thesis I define first order and higher order nuclei as nuclei which are mainly concerned with the first order or higher order relay of information. The definitions of these nuclei and relays are likely to be refined over time especially with evidence that some nuclei may have both first order and higher order neurons within them. The higher order pulvinar in the cat receives some input from the superior colliculus (Kelly et al., 2003) and Po neurons can receive inputs from the trigeminal ganglion in addition to layer V (Groh et al., 2013). These results demonstrate that some neurons in higher order nuclei receive 'first order' subcortical input. Thus as our knowledge of the thalamic relays deepen we may prefer to refer to first order and higher order relays, rather than nuclei, as the cells from both relays may reside in the same nucleus. Furthermore we may eventually identify neurons on which first order and higher order relays converge which may contribute to sensory processing. Despite these evolving definitions, for the purposes of this thesis the distinction between first order and higher order thalamic nuclei is useful.

1.3.1.6. The thalamic reticular nucleus

A third important component of the corticothalamic circuit is that of the thalamic reticular nucleus (TRN) (figure 1.7) which is in fact a derivative of the prethalamus (not the thalamus which has concerned us thus far). The TRN is a nucleus of GABAergic reticular neurons that provide inhibitory input to the thalamic relay cells (45% of synapses onto thalamic relay cells) (Jones, 2002b; Guillery and Sherman, 2002). Immediately after birth GABAergic IPSCs are recorded in mouse thalamic relay cells in response to reticular neuron activity. This inhibitory innervation increases over early postnatal weeks and adult properties are established by P9 (Warren et al., 1997; Evrard and Ropert, 2009).

Collaterals from both corticothalamic (VI and VIb) and thalamocortical axons synapse onto the GABAergic neurons residing in the thalamic reticular nucleus (TRN) (Molnár and Cordery, 1999; Mitrofanis and Baker, 1993; Molnár et al., 1998a; Jones, 2002b). Thus, reticular neurons are situated in the middle of an inhibitory feedback loop from the thalamus, and an inhibitory feed-forward loop from cortex to thalamus both of which modulate the activity of thalamic relay cells (figure 1.7) (Jones, 2002b; Cruikshank et al., 2010; Lam and Sherman, 2010; Olsen et al., 2012). Layer V does not project to the TRN (Hoogland et al., 1987; Rouiller and Welker, 2000).

1.4. The development of the corticothalamic circuit

1.4.1. The development of the corticothalamic circuit

1.4.1.1. The route and timing of the developing corticothalamic projections

The temporal progress of corticofugal fibres en route to specific thalamic nuclei has been described in some detail in various species, here I will describe the timing mostly in mice and occasionally in rat. Post-mitotic cortical neurons migrate into the nascent preplate around embryonic day (E) 10. Before reaching the cortical plate, the migrating neurons begin to extend neurites (Noctor et al., 2004; Bicknese et al., 1994; Lickiss et al., 2012). This extension becomes directed, laterally, medially, rostrally or caudally, depending on transcription factor expression. Ctip2 is highly expressed in laterally projecting corticofugals; conversely Satb2 is highly expressed in callosal projections (Fishell and Hanashima, 2008; Molyneaux et al., 2007). Corticofugal fibres project ventro-laterally, through the intermediate zone deep to the cortex, reaching the pallial-subpallial boundary (PSPB) from E13 and E15.5 (figure 1.8) (Jacobs et al., 2007; Auladell et al., 2000; Erzurumlu and Jhaveri, 1992). Fibres from lateral cortical areas arrive first and accumulate until dorsal fibres arrive (De Carlos and O'Leary, 1992; Molnár and Cordery, 1999). Here the fibres reorient ventro-medially and at E15.5 cross the PSPB to enter the internal capsule (Richards et al., 1997). After traversing the internal capsule the axons arrive at and cross the diencephalic-telencephalic boundary (DTB) and reach the TRN at E16. Here there is a second pause in corticofugal fibre front progression until E17.5 (Molnár and Cordery, 1999). Then the corticothalamic

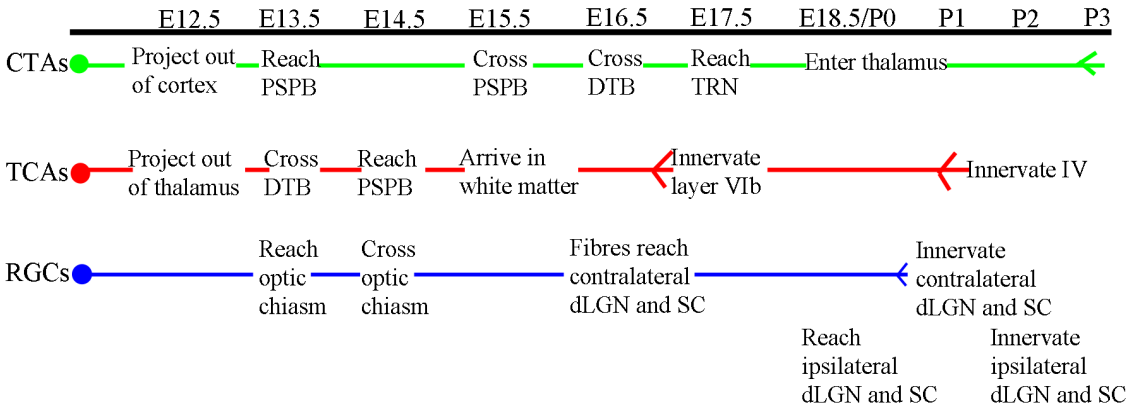

Figure 1.8. Timeline of corticothalamic and thalamocortical fibre progression. Cortical fibres reach the PSPB by E13.5. They cross the PSPB at E15.5, and cross the DTB and E16.5 to reach the TRN by E17.5. At E18.5 cortical fibres start to enter the thalamus. Thalamic fibres project out of the thalamus at E12.5. They reach the PSPB by E14.5. At E15.5 they reach the white matter deep to the cortical plate. At E17.5 they innervate the deepest cortical layer (layer VIb/ the subplate). They innervate their final target in layer IV by P2. Retinal ganglion cell axons which cross the midline reach the optic chiasm by E13.5. They cross the chiasm at E14.5 and reach the contralateral dLGN and SC by E16.5. Fibres which do not cross the midline reach the ipsilateral dLGN and SC by E18.5. Abbreviations used: CTAs, corticothalamic axons; TCAs, thalamocortical axons; RGCs, retinal ganglion cells; PSPB, pallial subpallial boundary; DTB, diencephalon telencephalon boundary; dLGN, dorsal Lateral Geniculate Nucleus; SC, superior colliculus.

axons alter orientation once more to invade the thalamus, a process that takes several days with most thalamic nuclei being innervated postnatally in rats, mice and hamsters (Molnár and Cordery, 1999; Jacobs et al., 2007; Miller et al., 1993).

The three corticothalamic populations grow towards the thalamus with distinct temporal patterns. However, which cortical layer reaches the thalamus first is contested. Subplate (VIb) neurons are well placed to pioneer the course whilst the distance is smaller and provide structural guidance to layer V and VI axons. In support of this hypothesis, in several species the first axons to reach the lateral internal capsule do so before the cortical plate cells become post-mitotic therefore indicating that the projections arise from the earlier-born subplate cells (McConnell et al., 1989; McConnell et al., 1994; Molnár et al., 1998a; Molnár et al., 1998b; Molnár and Blakemore, 1995; De Carlos and O'Leary, 1992; Jacobs et al., 2007). In cats the ablation of subplate cells with timed kainic acid administration leads corticothalamic axons to fail to connect with appropriate thalamic nuclei (McConnell et al., 1994).

However, these results do not confirm in which order the subplate, layer VI and layer

V fibres invade the thalamus and retrograde tracing studies are not conclusive. In hamsters retrograde carbocyanine dye tracing showed that limited numbers of layer VI and subplate axons arrive first and are back-labelled by thalamic DiI crystal placement on postnatal day 0 (P0). This is quickly followed at P3 by the extensive ingrowth of layer V axons (Miller et al., 1993). However cholera toxin-B tracing in ferrets and cats revealed different temporal patterns, demonstrating instead that layer V axons arrive in the thalamus several days before deeper layers (Clascá et al., 1995).

Thus the exact timing of each cortical layer's arrival is currently unresolved and may differ in different species.

1.4.1.2. The development of reciprocal thalamocortical projections

The reciprocal thalamocortical projections develop at much the same time as the corticothalamic pathway. Their development is temporally coincident and overlaps geographically; the fibres traverse the same structures and it has been suggested they may even extend within the same fibre compartments (Erzurumlu and Jhaveri, 1992; Molnár et al., 1998a; Molnár et al., 1998b). This has led to suggestions that the fibres of each projection may use fibres of the opposite population to aid their guidance (Molnár et al., 1998a; Molnár et al., 1998b).

In the mouse post-mitotic thalamic neurons are generated between E10 and E13 (Angevine, 1970). As early as E12.5 thalamocortical axons have exited the thalamus extending ventro-laterally until at E13 they reorient sharply away from the hypothalamus to cross the DTB to enter the subpallial telencephalon (figure 1.8) (Braisted et al., 1999; Erzurumlu and Jhaveri, 1992). At E14 the thalamocortical fibres reach the PSPB in the mouse (Bicknese et al., 1994), E15 in the rat (De Carlos and O'Leary, 1992), where the fibres reorient again to begin projecting into the cortex. By E15 in the mouse the thalamocortical fibres arrive in the white matter underneath the cortex (Bicknese et al., 1994; Catalano et al., 1991; Erzurumlu and Jhaveri, 1992). Here they wait for several days before beginning to invade the cortical plate at E17 (mouse) (rat; E18) (Catalano et al., 1991; Lund and Mustari, 1977). At this age the

thalamocortical axons have made functional connections with the subplate although this is not their final projection target. By P0 the fibres extend through layers V and VI of the cortex (Auladell et al., 2000) and by P2 they innervate their target neurons in layer IV (López-Bendito and Molnar, 2003; Garel and Rubenstein, 2004; Lund and Mustari, 1977).

1.4.1.3. Waiting periods in thalamocortical and corticothalamic development

Thalamocortical fibres reach the cortex and remain in the deeper layer VIb for several days before invading the cortical plate and innervating their target layer IV (López-Bendito and Molnar, 2003; Molnár et al., 2003a; Lund and Mustari, 1977). The waiting period is several weeks in carnivores and primates, compared to a day in rodents (Rakic, 1976; Rakic, 1977; Shatz and Luskin, 1986; Auladell et al., 2000). During the waiting period, thalamocortical fibres integrate into a transient circuit with the subplate/VIb neurons (Kostovic and Rakic, 1980; Allendoerfer and Shatz, 1994; Kanold and Luhmann, 2010). At this stage thalamocortical activation elicits responses in layer IV neurons however the latency suggests it is disynaptic and therefore via VIb until several days later when thalamocortical fibres activate IV directly and indirectly via layer VIb (Friauf and Shatz, 1991; Higashi et al., 2002; Molnár et al., 2003b; Zhao et al., 2009). This transient feed-forward excitatory innervation via VIb is proposed to strengthen the synapses between the thalamic axons and the layer IV neurons in the developing cortical plate (Kanold et al., 2003; Kanold and Luhmann, 2010; Zhao et al., 2009). Furthermore this circuit regulates the maturation of cortical inhibition in layer IV of areas targeted by thalamic afferents (Kanold and Shatz, 2006), the development of ocular dominance and orientation columns in visual cortex (Ghosh et al., 1990; Ghosh and Shatz, 1994; Kanold et al., 2003; Kanold and Shatz, 2006), and barrel organisation in somatosensory cortex (Tolner et al., 2012). The thalamocortical fibres also undergo rearrangements deep to the cortical plate which are vital for the transformation of topographic representations between the thalamus and the cortex (Connolly and Van Essen, 1984; Nelson and LeVay, 1985; Grant et al., 2012).

Waiting periods (in temporal order of fibre progression) have also been described for the corticothalamic projections. In several species corticofugal fibres undergo a waiting period at the pallial subpallial boundary (PSPB) for a day before progressing into the subpallium (McConnell et al., 1989; McConnell et al., 1994; Clascá et al., 1995; Molnár et al., 1998a; Auladell et al., 2000; Jacobs et al., 2007). This waiting period is important for the appropriate guidance of the corticothalamic fibres across the PSPB and may be due to a reliance of corticothalamic and thalamocortical fibres on each other the cross the PSPB (Deck et al., 2013). This waiting period is mediated by the transient repulsion of PlexinD1 expressing corticothalamic axons from the Semaphorin3E expressing subpallium. When these guidance cues are knocked-out, the corticothalamic fibres no longer wait at the PSPB and enter the subpallium via a ventral route and thus fail to navigate to the thalamus (Deck et al., 2013).

A second corticothalamic waiting period occurs at the TRN (Molnár and Cordery, 1999). This waiting period may serve two functions which mimic those of the thalamocortical waiting period at the subplate despite differences in the adult circuitry. Corticothalamic fibres innervate TRN neurons earlier than other thalamic structures (Mitrofanis and Guillery, 1993; Grant et al., 2012). Thus the TRN may be the site of an early transient circuit between the cortex and the thalamus (although the role and properties of such a circuit have not been established). Furthermore the corticothalamic fibres rearrange at the TRN which may be important for appropriate map formation, as for thalamocortical fibres at the subplate (Lozsádi et al., 1996; Adams et al., 1997).

A final waiting period of the visual corticothalamic fibres has been described outside the dLGN in the cat, rhesus monkey and mouse (Shatz and Rakic, 1981; Anker, 1977; Grant et al., 2012). However the role this final waiting period serves has yet to be elucidated.

1.5. The visual system

1.5.1. The visual system and its development in mouse

To study corticothalamic development I focus on the visual system of the mouse, which I introduce here.

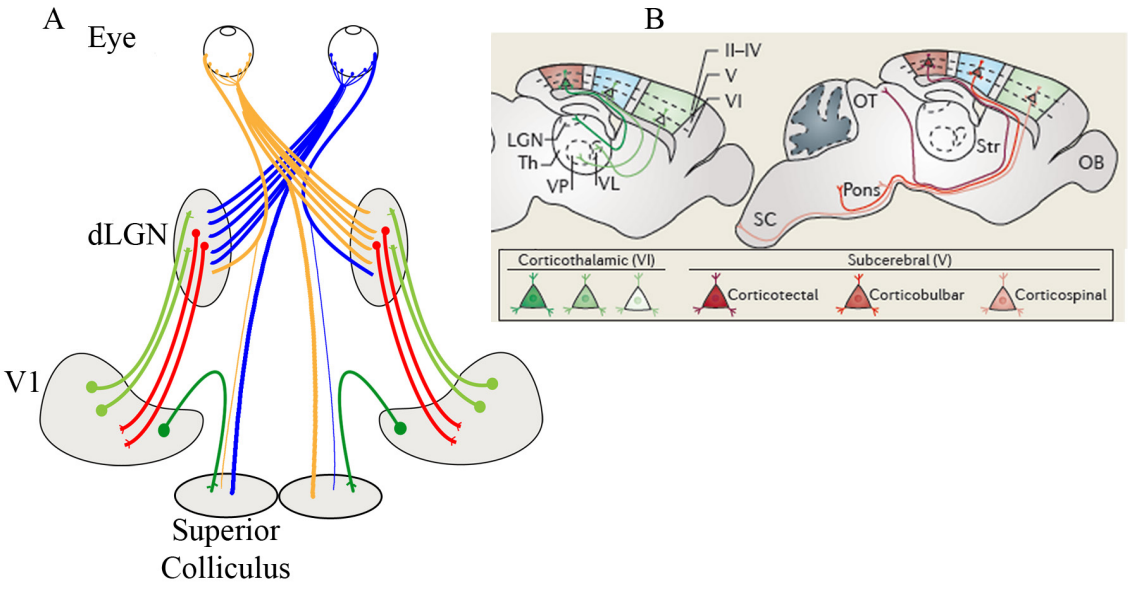

Figure 1.9. The visual system. A. Horizontal schematic of the important projections in the visual system. Retinal fibres project across the optic chiasm to the contralateral dLGN and superior colliculus (blue and orange fibres). In the mouse only a small proportion project to the dLGN ipsilateral to the eye and superior colliculus. Thalamocortical fibres project from the dLGN to V1 (red fibres). Layer VI cortico-thalamic fibres project to the dLGN (light green fibres). Layer V corticofugal fibres project to the superior colliculus (dark green fibres). B. Sagittal section of the corticofugal projections in the visual system. Layer VI (6) and VIb (SP) projects to the thalamus. Layer V (5) projects to the tectum. Abbreviations used: dLGN, dorsal lateral geniculate nucleus; V1, primary visual cortex. B: adapted from Greig et al., 2013.

1.5.1.1. The retinogeniculate and retinocollicular pathway

Visual information is transmitted from the retina to the dLGN via the retinogeniculate pathway. The retinal ganglion cells (RGCs) project out of the retina through the optic nerve, to the optic chiasm where they cross the midline. The RGCs then, via the optic tract, project to the dLGN where they terminate on thalamic relay cells (figure 1.9). RGCs also project past the dLGN to the superior colliculus (figure 1.9) where they densely innervate the superficial layer.

Mice have limited binocular vision as 85- 90% of retinal projections project to the contralateral dLGN (figure 1.10C) (Valverde, 1968; Godement et al., 1980; Jaubert-Miazza et al., 2005) unlike other species. The crossed pathway arise from the nasal retina and the uncrossed projections arise from the temporal retina (Godement et al., 1987). Throughout this thesis I use the terms contralateral and ipsilateral with reference to the eyes. Thus the majority of retinal input from one eye crosses the midline and projects to the contralateral dLGN; the dLGN ipsilateral to that eye receives only minor retinal input from it. The contralateral and ipsilateral projections initially overlap but are

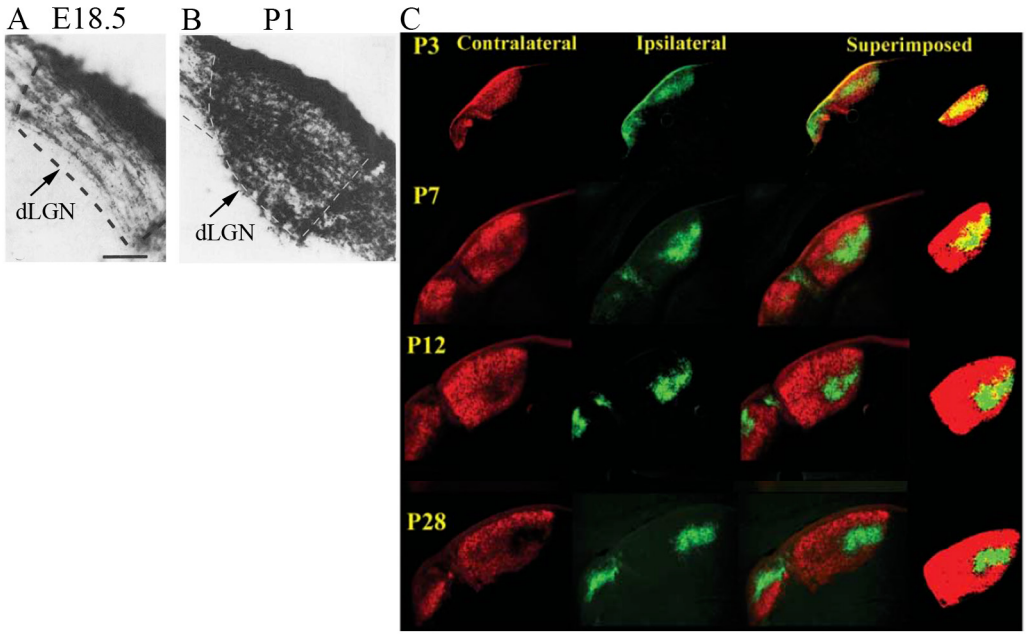

Figure 1.10. Retinal fibre ingrowth to the dLGN in the mouse. A. At E18.5 retinal ganglion fibres have entered the contralateral dLGN and are most dense in a thick band at the dorsal/lateral edge of the nucleus. B. At P1 the retinal ganglion fibres densely innervate the whole contralateral dLGN. C. Cholera toxin B injections into each eye demonstrate the contralateral and ipsilateral projections from the eye to the dLGN from P3 to P28. The contralateral fibres (red) provide the major input to the dLGN, ipsilateral (green) projections form a minor input in a dorsal/medial patch. Over development there is progressive segregation of the projections from each eye. Abbreviations used: dLGN, dorsal lateral geniculate nucleus. A and B; adapted from (Godement et al., 1984), C; adapted from Jaubert-Miazza et al., 2005.

segregated over development to form the adult arrangement (figure 1.10 C) (Valverde, 1968; Godement et al., 1980; Jaubert-Miazza et al., 2005).

In mice RCG axons reach the optic chiasm by E13.5, crossing it by E14 and reaching the contralateral dLGN by E18 (figure 1.8, 1.10 A) (Godement et al., 1984). The fibres initially project along the dorsal/lateral edge of the dLGN before densely invading the dLGN, from dorsal/lateral to medial, at P0 (figure 1.10 A, B) (Godement et al., 1984). Fibres from the uncrossed eye reach the lateral edge of the ipsilateral dLGN at P0 and enter by P3 (Godement et al., 1984; Godement et al., 1987). The proportion of ipsilateral and contralateral projecting fibres is likely determined by genetic programs including guidance cues at the optic chiasm and transcription programs determining the competence to respond to such factors. Foxg1 expression may suppress ipsilateral projection fate in retinal ganglion cells by down-regulating expression of guidance cue receptors such as Ephb1 (Tian et al., 2008).

Initially fibres from the ipsilateral and contralateral eye are not segregated and dLGN neurons can be innervated by RGCs from both eyes. Eye specific segregation begins by P4; crossed fibres reduce innervation in the presumptive ipsilateral region and by P8 there is eye specific segregation of the retinal fibres with the clear ipsilateral region in the rostro/medial dLGN (figure 1.10C) (Godement et al., 1984; Chen and Regehr, 2000; Jaubert-Miazza et al., 2005; Ziburkus and Guido, 2006; Guido, 2008). By two weeks after birth dLGN neurons are innervated by only one eye and by one to three RGCs (Godement et al., 1984; Chen and Regehr, 2000; Jaubert-Miazza et al., 2005; Ziburkus and Guido, 2006; Guido, 2008).

Retinal fibres also project to the midbrain structure the superior colliculus which they innervate by E16 (figure 1.8, 1.9) (Godement et al., 1984). The retinal fibres innervate the superficial grey layer of the contralateral superior colliculus (Drager and Hubel, 1975; Lund, 1965; Godement et al., 1984; Godement et al., 1980; Ackman et al., 2012). In the superior colliculus, as in the dLGN, retinal fibres initially project diffusely and then refine to their adult terminal patterns. This refinement involves both molecular and activity dependent mechanisms (Upton et al., 1999; Upton et al., 2002; O'Leary and McLaughlin, 2005).

1.5.1.2. The geniculocortical pathway

As discussed in section 1.3.1, the geniculocortical projections transmit the visual information from the dLGN to V1 synapsing primarily on layer IV pyramidal cortical neurons (Frost and Caviness, 1980) and eliciting large glutamatergic EPSPs (Stratford et al., 1996; Lee and Sherman, 2008). Their development follows much the same temporal and physical pattern as that of other thalamocortical axons (Lund and Mustari, 1977; Kageyama and Robertson, 1993).

1.5.1.3. The corticogeniculate and corticocollicular pathway

Corticothalamic projections from layer VI in V1 provide modulator input to the thalamic relay cells of the dLGN. Layer VI fibres are visible densely arborising in the dLGN after injecting primary visual cortex with a stop floxed-tdTomato virus in the

layer VI cre mouse Ntsr1-cre (Olsen et al., 2012). As discussed previously, synapses from this corticogeniculate projection outnumber synapses from retinal ganglion cells. These layer VI corticogeniculate fibres reach the thalamus by P0 however they are not seen to enter the dLGN until P6 (Grant et al., 2012; Jacobs et al., 2007; Seabrook et al., 2013). How this corticothalamic waiting period immediately outside the dLGN is regulated and what purpose it serves is as yet unknown.

Because of the first order nature of the dLGN, layer V corticothalamic fibres do not project to the dLGN. The visual cortex layer V fibres do, however, project to subcortical components of the visual circuit; the superficial grey layer of the superior colliculus in the tectum. The corticotectal fibres reached the superior colliculus by P1/P2 (figure 1.8) (De Carlos and O'Leary, 1992; Clascá et al., 1995) however their exact timing of entry to the superficial grey layer is not clearly established.

Both the dLGN and the superior colliculus receive input from both the retina and the cortex. In both systems retinal fibres enter and innervate the dLGN and superior colliculus substantially earlier than cortical fibres do. Whether retinal fibres regulate corticofugal ingrowth to these two structures has not been assessed.

1.5.2. Early activity in the visual system

In the mouse the eyes do not open until 12 days after birth thus the early retinal projections to the dLGN and superior colliculus do not transmit visually evoked activity. However, prior to eye opening there are spontaneous retinal waves which propagate across the retina (O'Leary and McLaughlin, 2005; Maccione et al., 2014).

There are three classes of spontaneous retinal waves. During early embryonic gestation the spontaneous waves of calcium transients are mediated by gap junctions (Bansal et al., 2000; Syed et al., 2004a; Syed et al., 2004b). Later in embryogenesis and the first two postnatal weeks the second class of spontaneous waves propagate across the retina (represented in figure 1.11) which are cholinergic (Meister et al., 1991; Wong et al., 1993; Feller et al., 1996; Penn et al., 1998; Bansal et al., 2000; Syed et al., 2004a;

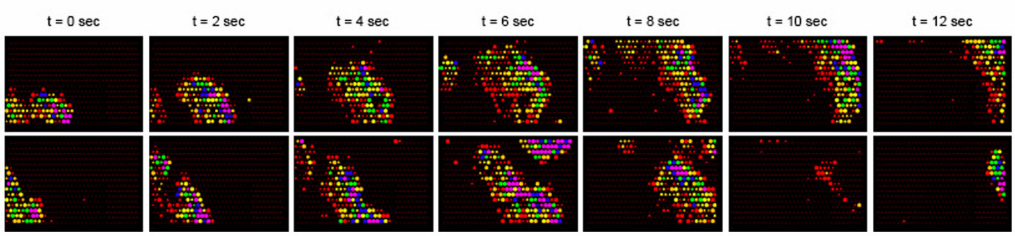

Figure 1.11. Retinal waves. Multielectrode recording time series of spontaneous waves of activity propagating across the retina. Adapted from http://mcd.ucsc.edu/faculty/feldheim.html

Syed et al., 2004b; Ackman et al., 2012; Maccione et al., 2014). From P10 in the mouse glutamate signalling drives a third class of retinal waves (Bansal et al., 2000; Syed et al., 2004b; Maccione et al., 2014).

This spontaneous retinal activity is transmitted throughout the visual system. The RGCs convey the spontaneous waves to the dLGN and to the superior colliculus, from the dLGN they are transmitted to the visual cortex (Mooney et al., 1996; Weliky and Katz, 1999; Ackman et al., 2012). This spontaneous activity is crucial for the eye specific segregation of retinogeniculate projections and retinogeniculate synapse remodelling (Penn et al., 1998; Hooks and Chen, 2006; Rebsam et al., 2009; Rebsam et al., 2012). Furthermore this activity contributes to the refinement of retinotopic mapping in the central visual system after coarse topography is established using gradients of guidance molecules such as ephrins (O'Leary and McLaughlin, 2005; Rashid et al., 2005; Torii and Levitt, 2005; Feldheim and O'Leary, 2010).

In addition to retinogeniculate development, spontaneous retinal activity is likely to play a role in other features of visual system development including the emergent cortical activity and intra-cortical circuits (Sur and Leamey, 2001). The early blockade of spontaneous retinal activity permanently disrupts cortical ocular dominance columns and increases receptive field size in the visual cortex (Huberman et al., 2006). Despite the propagation of spontaneous retinal waves throughout the visual system, it is currently unknown whether spontaneous retinal activity is important for the development of corticothalamic circuitry.

1.6. The somatosensory system

Whilst focussing on the visual system for the majority of this thesis there is a brief section on the ingrowth of corticothalamic fibres to the VPM. As such here follows a brief introduction to the somatosensory system that mainly collates information which has been introduced previously.

Somatosensory information from peripheral sensory nerves, including those in the whisker pad of rodents, are transmitted to the ipsilateral trigeminal ganglion in the brain stem (Le Gros Clark, 1932). Medial lemniscal fibres from the trigeminal ganglion then cross the midline and transmit somatosensory information to the VPM thalamic nucleus (Ralston III, 1969; Smith, 1973; Erzurumlu and Gaspar, 2012). Layer VI corticothalamic fibres from S1 provide modulatory innervation to the VPM (Hoogland et al., 1987; Jones and Powell, 1968; Reichova and Sherman, 2004; Lam and Sherman, 2010; Cruikshank et al., 2010).

1.7. The interplay between genetics and neuronal activity in the development of the nervous system

1.7.1. Neuronal activity and development

Many features of the nervous system including arealisation, axon guidance and projection refinements require both genetic programs and neural activity for proper development (Katz and Shatz, 1996; Rubenstein and Rakic, 1999; Sur and Leamey, 2001; Sur and Rubenstein, 2005; Abe, 2008; O'Leary and Sahara, 2008; McCoy et al., 2009; Tropea et al., 2009; Ben-Ari and Spitzer, 2010; Yamamoto and López-Bendito, 2012). The extent to which each mechanism contributes to developing a mature nervous system is an interesting topic of debate. This extensive topic is beyond the scope of this introduction however here I discuss some of the important features of neuronal activity in corticothalamic/ thalamocortical development and how neuronal activity could regulate molecular effectors.

1.7.1.1. The role of neuronal activity in thalamocortical target selection

In section 1.1.2, I discuss how early corticothalamic development relies on arealisation

genes and thalamocortical activity instructing functional specialisation. However activity may also guide thalamic fibres to target the correct cortical area.

Abolishing cortical activity *in vivo*, or *in vitro* using tetrodotoxin (TTX), or glutamate receptor antagonists APV (NMDA receptors) or DNQX (AMPA and kainate receptors) or increasing neuronal activity with potassium causes thalamocortical fibres to overshoot layer IV and reduces the extent of arborisation in layer IV (Herrmann and Shatz, 1995; Anderson and Price, 2002; Uesaka et al., 2007). Furthermore TTX infusion can cause dLGN thalamocortical fibres to aberrantly target other cortical areas (Catalano and Shatz, 1998). Whether the effect is cell autonomous or not is unclear as these manipulations disrupt neuronal activity in both the thalamic and the cortical neurons.

Despite the role of glutamate receptors, knocking-out synaptic fusion core complex protein Snap25, which abolishes calcium dependent evoked synaptic release, does not disrupt thalamocortical fibre arborisation (Washbourne et al., 2002; Molnár et al., 2002; Blakey et al., 2012).

How neuronal activity regulates the guidance and branching of thalamic axons in early development is still under investigation. One potential mechanism is neuronal activity dependent calcium signalling via molecules such as calcium/calmodulin-dependent protein kinase II (CaMKII) in the growth cone (Zou and Cline, 1996; Hayano and Yamamoto, 2008; Yamamoto and López-Bendito, 2012)). Intracellular calcium transients can regulate growth cone extension (Gomez and Spitzer, 1999; Gomez et al., 1995). Such calcium transients can be modulated by interactions between guidance molecules such as netrin-1 (Hong et al., 2000), which is expressed in the subpallium along the corticothalamic and thalamocortical route (Métin et al., 1997; Braisted et al., 2000), and L1 which is expressed on thalamocortical fibres (Fukuda et al., 1997; Gomez et al., 2001; Yamamoto and López-Bendito, 2012). Furthermore modulating intracellular calcium spiking can alter thalamocortical axon outgrowth in culture (E. Mire, C. Messera and G. López-Bendito, unpublished data; Yamamoto and López-Bendito 2012).

1.7.1.2. The role of spontaneous and peripheral activity in circuit refinement

In the visual system both spontaneous (section 1.5.2) and visually evoked retinal activity are important for refinement and functional specification of the central visual system.

The blockade of class II cholinergic spontaneous retinal waves disrupts eye specific segregation in the dLGN (Penn et al., 1998; Bansal et al., 2000; Pfeiffenberger et al., 2005; Pfeiffenberger et al., 2006; Hooks and Chen, 2006; Rebsam et al., 2009; Rebsam et al., 2012), alters the development ocular dominance columns and increases the size of binocular receptive fields in V1 (Huberman et al., 2006; Huberman, 2007). After eye specific segregation is established, visually evoked activity is crucial for maintaining the refined projection of retinal fibres on the dLGN neurons (Hooks and Chen, 2006).

Spontaneous retinal activity is also crucial for the refinement of the early coarsely mapped retinal projections to become the fine grained retinotopic map present in adult animals (O'Leary and McLaughlin, 2005; Pfeiffenberger et al., 2005; Pfeiffenberger et al., 2006; Huberman et al., 2008; Nicol et al., 2007). The blockade of neuronal activity in the cortex by TTX disrupted the topography of dLGN thalamocortical fibres within V1 (Catalano and Shatz, 1998).Furthermore here activity and molecular guidance mechanisms appear to overlap: cAMP oscillations in retinogeniculate neurons in response to spontaneous retinal waves are crucial for the proper guidance and topographic mapping mediated by ephrinA5 repulsion (Nicol et al., 2007).

1.7.1.3. The role of peripheral activity in target specialisation

As discussed in more detail in sections 1.1.2. and 1.2.2, peripheral activity is crucial for the functional specification of cortical areas and thalamic nuclei. The loss of peripheral input by eyelid suture, removing one or both eyes, or transecting the infraorbital nerve disrupts cortical circuitry development (Hubel and Wiesel, 1962; Hubel and Wiesel, 1968; Van der Loos and Woolsey, 1973; Kaas, 1997; Sur and Leamey, 2001; Sur and Rubenstein, 2005). Cortical functional specification is neuronal activity dependent; the loss of glutamatergic signalling via NMDA receptors prevents the normal refinement of

afferents into whisker related patterns in somatosensory cortex (Lee et al., 2005a; Lee et al., 2005b).

Thus peripheral input is important to establish the appropriate cortical circuits. This feature may underlie the ability for cross-modal cortical plasticity following the loss of a particular peripheral input, thus enabling other sensory modalities to utilise available cortical areas. Bilateral enucleation (removal of both eyes) enables thalamocortical fibres from the VPM, MGN, motor ventrolateral nucleus and limbic/hippocampal anterior dorsal and anterior ventral thalamic nuclei to invade and innervate the visual cortex (Karlen et al., 2006; Chabot et al., 2007; Chabot et al., 2008; Charbonneau et al., 2012).

In addition to rewiring in the cortex, the thalamic nuclei can also be rewired. The loss of whisker input by infraorbital nerve transection causes the recruitment of other somatosensory lemniscal driver input to the relay neurons normally targeted by infraorbital nerve inputs (Takeuchi et al., 2012). As discussed earlier in the introduction the rewiring of retinal inputs to the MGN causes visual processing within the auditory system (Angelucci et al., 1997; Angelucci et al., 1998; Frost et al., 2000; Roe et al., 1993).

Thus neuronal activity, both spontaneous and periphery driven, plays a crucial role in the proper development of the nervous system, including the thalamic/ cortical systems with which this thesis is primarily concerned.

1.7.1.4. Activity dependent gene expression in response to peripheral input

The downstream mechanisms by which neural activity regulates circuit and system development is harder to discern however research has begun to identify the intersection between activity and molecular effectors by identifying genes which are regulated by peripheral input dependent neuronal activity.

Various families of genes have been classed as regulated by peripheral input including the prototypical activity regulated genes; immediate early genes such as Fos, Egr1

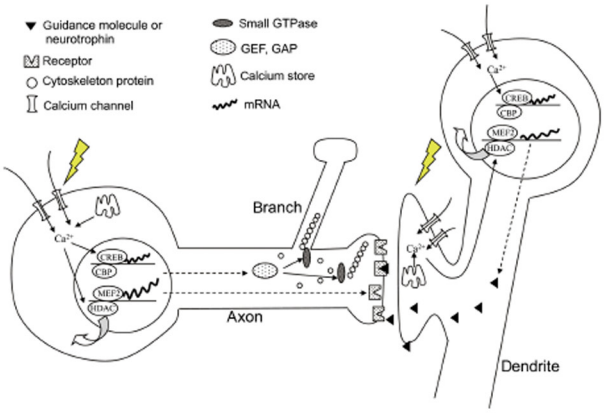

Figure 1.12. Activity dependent changes in gene expression. Neuronal activation can alter gene expression via several pathways. Increased intracellular calcium in the post-synaptic cell in response to glutamatergic synaptic transmission can activate protein kinase pathways which activate transcription factor pathways particularly CREB mediated transcription. Adapted from Yamamoto and López-Bendito, 2012.

and 2; genes involved in axon guidance such as ephrins and Robo1; neurotrophins, especially BDNF and its associated TrkB receptors; genes which contribute to synaptic plasticity such as neurotransmitter receptors AMPA and NMDA; and genes which signal via the known activity dependent CREB transcription factor family (figure 1.12) (Bozzi et al., 1995; Schoups et al., 1995; Kaczmarek et al., 1999; Majdan and Shatz, 2006; Abe, 2008; Cheng et al., 2008; McCoy et al., 2009; Tropea et al., 2009; Bracken and Turrigiano, 2009; Dye et al., 2012; Yamamoto and López-Bendito, 2012; Kind et al., 2013; Brooks et al., 2013).

Sequences in the promoters of several genes have been identified which are activity regulated such as CRE (cAMP response elements) and the calcium responsive sequence 1. Both are in the promoter sequence of BDNF, which is established to have activity dependent regulation (Shieh et al., 1998; Tao et al., 1998; Tao et al., 2002). Intracellular calcium signalling can regulate CREB mediated transcription and epigenetic transcriptional regulation of genes such as guidance cues and neurotrophins (figure 1.12) (Yamamoto and López-Bendito, 2012).

Other genes have been identified by their highly dynamic developmental expression profile over periods such as the ocular dominance critical period (Lyckman et al., 2008; Yang et al., 2009; Maeda et al., 2013). However, whether the expression of

these genes is regulated by intrinsic programs of gene changes or peripheral activity cannot be resolved merely by analysing developmental expression. It is likely that both mechanisms regulate different genes to different extents; indeed monocular deprivation reverses almost all gene changes over the critical period (Lyckman et al., 2008).

Furthermore the precise nature and modality of input driven neuronal activity can regulate gene expression. Rewiring retinal inputs to the MGN caused the rewired MGN to express genes which are normally expressed in the dLGN such as transcription factor Zic4, and down-regulate MGN genes such as transcription factor Foxp2 (Horng et al., 2009). These results demonstrate that gene expression in specific nuclei of the thalamus can be regulated by the specific inputs those thalamic nuclei receive. However there is still a lot to learn about how peripheral inputs regulate gene expression in specific thalamic nuclei during early development.

1.8. Aims of this thesis

In this introduction I have discussed the nature, function and development of connections between the cortex and the thalamus. Several questions are raised by this introduction. Firstly, what order do corticothalamic fibres enter the thalamus in, and how are they patterned with regards to the first order and higher order thalamic nuclei? Secondly, what role does peripheral input play in the regulation of corticofugal fibre entry to the thalamus and subcortical targets; does retinal input regulate the timing of corticothalamic fibre ingrowth to the dLGN and the superior colliculus? Finally does peripheral input to the thalamic nuclei contribute to gene expression in thalamic relay neurons; does retinal input regulate gene expression in the dLGN?

To answer these questions I have studied the development of the connections from the cortex, layer V, VI and VIb, to the thalamus. I use the visual system of the mouse as my primary model as it is easy to manipulate and has clear anatomical features which can be assessed. I use reporter gene expressing lines to monitor selective corticofugal projection populations. My work is focussed on the mechanisms regulating ingrowth of corticothalamic fibres from layers V,VI and VIb to the dLGN and the cellular and

molecular maturation of the dLGN during this period.

1.8.1. Aims of chapter 3: Are developing corticothalamic fibres patterned with regards to the first order and higher order thalamic nuclei?

As I state in the introduction to corticothalamic development, the broad temporal pattern by which corticothalamic fibres progress towards and enter the thalamus has been established in several species. However the exact order in which the three corticothalamic fibre populations from layers V, VI and VIb reach and enter the thalamus has not been established due to the difficulties with selectively labelling these populations with the available tracing methods. Furthermore the exact pattern of the fibres in the thalamus (the thalamic nuclei each population of fibres specifically project to) is also intractable using most axon tracing methods. In my first chapter I endeavour to clarify the timing and the exact nuclear specific pattern by which the three corticothalamic populations enter the thalamus.

To do this I take advantage of the recent development of a variety of transgenic mouse lines that allow us to label the three corticothalamic subpopulations selectively. I use the Rbp4-Cre mouse, which expresses Cre in layer V projection neurons. Crossed with a tdTomato Cre reporter line this experiment allows me to precisely characterise the ingrowth of layer V fibres to the thalamic nuclei. I use the Ntsr1-Cre mouse, which expresses Cre in layer VI projection neurons, crossed with a tdTomato reporter line to characterise the precise ingrowth of layer VI fibres to the thalamus. Finally I use the Golli-τ-eGFP mouse which expresses GFP in layer VIb (and layer VI) corticothalamic projection neurons (Jacobs et al., 2007) to characterise the ingrowth of VIb and VI fibres into the thalamus. In the adult the different corticothalamic populations target complementary sets of thalamic nuclei; layer V targets only higher order and layer VI and VIb target first and higher order. My research will establish whether this selective pattern is present from the earliest cortical ingrowth to the thalamus.

I also demonstrate that the timing of corticothalamic ingrowth to different thalamic nuclei is highly regulated. Specifically layer VI and VIb fibres accumulate outside of

the dLGN before entering several days after birth. This is unusual as the VI and VIb corticothalamic fibres enter other ventral/lateral thalamic nuclei such as the VPM early.

1.8.2. Aims of chapter 4: does retinal input regulate the timing of corticofugal ingrowth to targets?

The timing of the layer VI and VIb fibres accumulation outside of the dLGN prior to ingrowth is highly coincident with the postnatal period in which retinal fibres are transmitting spontaneous retinal waves to the dLGN. As such I hypothesise that retinal input is important in the guidance of layer VI and VIb corticothalamic fibres into the dLGN.

To answer this question I perform two different visual deprivation paradigms on Golli-τ-eGFP pups and Ntsr1-Cre::tdTomato pups. I firstly perform monocular enucleation in which I surgically remove one eye on the day of birth. I then use epibatidine (a potent cholinergic agonist which causes receptor desensitisation (Penn et al., 1998; Rebsam et al., 2009)) to pharmacologically abolish the cholinergic spontaneous retinal waves which propagate across the retina in the first postnatal weeks. I then assess the ingrowth of VI and VIb corticothalamic fibres to the dLGN following these manipulations.

The loss of retinal input caused by monocular enucleation deprives the dLGN thalamic relay neurons of their driver input. The layer VI and VIb inputs to the dLGN are modulatory and may be unlikely to overtake driving of the thalamic relay neurons after enucleation. I then assess whether the layer V fibres, which normally drive thalamic relay neurons in the higher order nuclei, are induced to aberrantly enter the dLGN following enucleation, thus restoring some driver input to the dLGN. To do this I perform monocular enucleation on the Rbp4-Cre::tdTomato mouse and assess layer V patterning in the control and enucleated dLGN. This experiment enables us to probe whether cross-hierarchical rewiring can occur by testing whether layer V fibres (which normally innervate exclusively higher order nuclei) will innervate the first order dLGN following the loss of retinal driver input.

I further go on to assess whether the loss of retinal input alters cortical ingrowth to

another structure which receives input from both the retina and the cortex; the superior colliculus. The superior colliculus receives input from layer V and I perform monocular enucleation on the Rbp4-Cre::tdTomato mouse and assess layer V patterning in the control and enucleated superior colliculus.

1.8.3. Aims of chapter 5: Does retinal input regulate gene expression in the dLGN?

In this introduction I discuss the importance of peripheral activity on the functional specialisation of cortical areas and thalamic nuclei. The focus of many experiments has now shifted to address the molecular cues that are directed by peripheral input, and how these molecules underlie the maturing functional specialisations in response to modality specific input. It has not yet been systematically assessed what molecular cues in the dLGN are regulated by retinal input. As such in this chapter I perform monocular enucleation and using a microarray based gene expression analysis to assess the transcriptome of the control dLGN compared to the dLGN which lacks retinal input. This chapter answers the question of genes in the dLGN which are regulated by retinal input and also suggests how dLGN maturation in the first postnatal week of the mouse requires retinal input.

1.8.4. Aims of chapter 6

After each experimental chapter I provide a specific discussion regarding the implications and predictions of that particular chapter. In Chapter 6 I shall provide a general discussion addressing the role of the corticothalamic waiting period outside the dLGN, cross-hierarchical rewiring in the corticothalamic system and how peripheral input may contribute to the specification of the hierarchical identity of thalamic nuclei (first order and higher order) and how this process is reflected in their transcriptome and connectivity. I shall also speculate on future research directions.

2 General Methods

This general methods chapter describes the methods that are relevant for all experimental chapters. Each experimental chapter contains the relevant methods described in detail.

2.1. Experimental animals

All experiments were approved by local ethical review committee and conducted in accordance with personal and project licenses in accordance with the Animals (Scientific Procedures) Act, 1986 (ASPA).

C57/BL6 wild type (WT), Golli-τ-eGFP, Rbp4-Cre, Ntsr1-Cre, Ai14-R26-tdTomato, and Lpar1-eGFP mice were maintained on a standard diet and light cycle in accordance with ASPA and were mated in the Biomedical Sciences Building Colony, Oxford University, UK.

Whilst setting up the Rbp4-Cre and Ntsr1-Cre colonies in Oxford, paraformaldehyde (PFA) fixed Rbp4-cre::Ai14-R26-tdTomato and Ntsr1-cre::Ai14-R26-tdTomato brains were received from the Scanziani Laboratory, University of California, San Diego (USA).

For microarray and qPCR experiments timed mated pregnant female C57/BL6 were obtained from Charles River (UK).

Strain name	Genotype	Description	Mated with	Source
C57/BL6	Wild type	Wild type	C57/BL6	Charles River
Golli-τ-eGFP	Homozygous eGFP expression under Golli-τ promoter of Myelin Basic Protein Promoter complex	eGFP expression in VIb and VI neurons and neurites (Jacobs et al., 2007)	Golli-τ-eGFP	Erin Jacobs

Ntsr1-Cre Tg(Ntsr1-cre) GN220Gsat/ Mmucd	Heterozygous cre expression under Ntsr1-promoter.	Expresses cre in layer VI neurons and neurites. When mated with tdTomato reporter line layer VI neurons are labelled (Olsen et al., 2012).	Ai14-R26R -tdTomato	Mutant Mouse Regional Resources Centre, (MMRRC) UCSD
Rbp4-Cre Tg(Rbp4-cre) KL100Gsat/ Mmucd	Heterozygous cre expression under Rbp4-promoter.	Expresses cre in layer V neurons and neurites. When mated with tdTomato reporter line layer V neurons are labelled.	Ai14-R26R -tdTomato	MMRRC, UCSD
Ai14-R26R -tdTomato Ai14-R26-tdTomato (B6;129S6-Gt(ROSA) 26Sor$^{tm14(CAG-tdTomato)Hze}$/J)	Homozygous lox-p flanked stop cassette prior to tdTomato.	Cre reporter line: tdTomato is expressed in cells expressing Cre following Cre mediated recombination (Madisen et al., 2010).	Ntsr1-Cre Rbp4-Cre	MMRRC, UCSD locally from Paul Riley laboratory
Lpar1-eGFP Tg(Lpar1-EGFP) GX193Gsat (GENSAT)	eGFP on Y chromosome	eGFP expression in layer VIb neurons. Only males are transgenic, NIHS females were used for breeding.	NIHS females	Lpar1-eGFP: MMRRC, UCSD. NIHS: Harlan, UK.

Table 1.1. Animal lines used for experiments in this thesis.

2.2. Genotyping

Animals for genotyping were ear clipped at weaning.

2.2.4.1. Cre genotyping

DNA extraction: Ear clip submerged in 280µl tissue lysis buffer with 2.8µl proteinase-K over night at 55°C (tissue lysis buffer solution in 'Frequently used solutions' table 1.5). Proteinase-K is denatured at 99°C for 10 minutes. Crude extract is centrifuged for 10 minutes.

Polymerase chain reaction (PCR): 0.5µl of extract is added to 1x PCR mix. NEB One-Taq Quick Load buffer including taq enzyme was used (M0486S, NEB, Hertfordshire, UK). Primers from Sigma Aldrich (Gillingham, UK), sequences in table 1.3, annealing

temperature 54°C.

PCR mix	1x
NEB One-Taq buffer	12.5µl
Cre Forward primer	1.0
Cre Reverse primer	1.0
DNA extract	0.5
nH_20	10

Table 1.2.PCR mix used for Cre genotyping per reaction

Cre Forward primer	5' TGGAAAATGCTTCTCTCCGT
Cre Reverse primer	5' CATCGCTCGACCAGTTTAGT

Table 1.3. Cre forward and reverse primers

Step		Temperature	Time
Initial denaturation		94°C	60s
40 cycles	Denaturation	94°C	15s
	Annealing	54°C	15s
	Lengthening	72°C	30s
Hold		10°C	-

Table 1.4. Cycling conditions for Cre PCR.

2.3. Tissue collection

2.3.4.1. Embryonic tissue collection

Timed pregnant dams were killed by cervical dislocation and embryos were removed by caesarean section. Brains (E16-E18) were dissected out and post-fixed in 4% paraformaldehyde (TAAB, Reading, UK) (PFA) in 0.1M Phosphate Buffered Saline (PBS)(pH=7.4) at 4°C for 24 hours.

2.3.4.2. Postnatal fixed tissue collection

P0-P10 mice were anaesthetised with an intraperitoneal injection of pentobarbitone (150mg/kg, Pentoject, Animal Care Ltd, UK) and transcardially perfused with 0.1M PBS. Alternatively animals were killed by cervical dislocation. P10- adult following perfusion with 0.1M PBS, animals were perfused with 4%PFA in 0.1M PBS. In all cases brains were dissected out and fixed in 4% PFA for 24 hours at 4°C. Brains were stored

at 4°C in 0.1M PBS with 0.05% sodium azide (Sigma, Gillingham, UK) (PBSA).

2.3.4.3. Postnatal fresh tissue collection

P6 pups were killed by cervical dislocation. Brains were immediately dissected out in RNase free conditions and processed or transferred to appropriate storage for microarray or qPCR experiments. More details in chapter 5.

2.4. Image acquisition

Fluorescent microscope images were taken using a Leica DMR fluorescence microscope with DC500 camera and Leica Firecam software (Leica Microsystems, Milton Keynes, UK). Confocal images were taken using a Zeiss LSM 710 confocal microscope (Carl Zeiss Microimaging, Germany). Fluorescent dissecting microscope images were taken using a Leica MZFLIII. Images were compiled and analysed using Adobe Photoshop CS5 (Adobe Systems Inc., CA, USA) and ImageJ (Image Analysis in Java (Schneider et al., 2012)).

2.5. Statistics

Cell quantification analysis was performed using paired t-test in GraphPadPrism (GraphPad Software, CA, USA). Fibre ingrowth to dLGN was analysed by paired t-test in GraphPadPrism. Microarray analysis was performed using GeneSpring GX 12.6.1 (Agilent Technologies, Germany) and Partek (Partek Inc., MO, USA). qPCR results were analysed using paired t-test in Excel (Microsoft, WA, USA). Graphics were generated using GraphPadPrism.

2.6. Frequently used solutions

0.5M Phosphate Buffer (PB), pH7.4	72.1g $Na_2HPO_4.2H_2O$ 14.8g $NaH_2PO_4.2H_2O$ 1L RO H_2O
0.1M Phosphate Buffered Saline (PBS) pH7.4	200ml PB 0.9g NaCL 800ml RO H_20
0.05% Phosphate Buffered Sodium Azide (PBSA)	0.05mg sodium azide 1L PBS
5µg/mL DAPI	50µl DAPI 50ml 0.1M PBS

RNase free PBS 1M Stock	80g NaCl 2g KCl 14.4gNa_2HPO_4 (anhydrous) 2.4g KH_2HPO_4 1L double autoclaved nanoH_2O
0.1M working RNase free PBS	100ml 1M stock PBS 900ml double autoclaved nanoH_2O.
Artificial Cerebro-Spinal Fluid (aCSF) Stock I per litre	2.94g $CaCl_2$.2H2O 4.93g $MgSO_4$.7H2O 2.24g KCl 73.70g NaCl 1.95g, $H_2NaPO_4.2H_2O$ 1L DEPC nH_20
aCSF Stock II per litre	$NaHCO_3$ 20.16 1L DEPC nH_20.
Fresh aCSF	100ml stock I 110ml stock II 890ml DEPC nH_2O 1.8g glucose.
Tissue Lysis Buffer	100mM Tris-Cl (pH 8.5) 5mM EDTA (pH 8.0) 200mM NaCl 0.2% (w/v) SDS

Table 1.5. Table detailing frequently used solutions.

3 Cortical layer specific ingrowth to the thalamus and superior colliculus

3.1. Introduction

Corticothalamic axons arising from layer V and VI are active in functionally distinct corticothalamic circuitry; they innervate different (though overlapping) sets of thalamic nuclei, and provide different classes of synaptic input (Guillery, 1995; Rouiller et al., 1998; Sherman and Guillery, 2002; Grant et al., 2012; Sherman and Guillery, 1998). Layer V corticothalamic fibres provide driver (class I) input to higher order nuclei (including the lateral posterior (LP) and the posterior thalamic nucleus (Po)). Layer VI corticothalamic fibres provide modulator (class II) input to all thalamic nuclei including first order nuclei ventral posterior-medial (VPM) and dorsal Lateral Geniculate Nucleus (dLGN) and higher order nuclei (LP and Po) (Sherman and Guillery, 1996; Guillery and Sherman, 2002).

Given these differences in both projection pattern and type of input, the different corticothalamic subpopulations are likely to use different mechanisms for guidance to the thalamus and it is therefore important to regard these populations separately when studying their development. However, due to difficulties distinguishing these two subpopulations by conventional tracing techniques, research into their development has often grouped them together (Lozsádi et al., 1996; Adams et al., 1997; Molnár and Cordery, 1999; Jones et al., 2002; Hevner et al., 2002; Grant et al., 2012). Early attempts to distinguish the development of these axon populations have demonstrated that each population invades the thalamus at different times (introduction 1.4) (McConnell et al., 1989; De Carlos and O'Leary, 1992; Miller et al., 1993; Clascá et al., 1995; Molnár et al., 1998a). However, the exact pattern, which layer arrives and invades earliest, is contested with evidence suggesting that each of layer V, VI and VIb arrive at the thalamus first.

One hypothesis is that the early born subplate (VIb) neurons pioneer the corticothalamic route whilst the distances in the brain are small (Allendoerfer and Shatz, 1994). In

support of this hypothesis, there are several species in which the first axons to reach the lateral internal capsule do so before cortical plate neurons are post-mitotic thus indicating that the projections arise from the earlier-born subplate cells (McConnell et al., 1989; McConnell et al., 1994; Auladell et al., 2000; Molnár et al., 1998b; Molnár and Blakemore, 1995; Jacobs et al., 2007; De Carlos and O'Leary, 1992). Furthermore within the internal capsule, the growth cones of the early subplate projections are more complex and exploratory than the layer V and VI projections (Kim et al., 1991). Additionally, in cats, ablation of subplate cells with timed kainic acid administration can disrupt corticothalamic targeting of the appropriate thalamic nuclei (McConnell et al., 1994).

These results, however, do not directly confirm the temporal order in which layer VIb, VI and V fibres invade the thalamus. In cats and hamsters a limited number of layer VI and VIb axons are the first to be back-labelled from thalamic DiI placements (Miller et al., 1993; McConnell et al., 1989). This is quickly followed by substantial ingrowth from layer V, which is later supplanted by layer VI (Miller et al., 1993). However similar tracing experiments using DiI and cholera toxin B (CTB) in ferrets indicated that early retrograde labelling of subplate cells by DiI maybe due to transneuronal spread of the DiI. The CTB results demonstrated instead that layer V axons arrive in the thalamus up to 10 days before VI and VIb (E40 compared to E50) (Clascá et al., 1995). Thus the exact timing of each cortical layer's arrival to the thalamus is currently unresolved and may differ in different species.

Furthermore the spatial pattern of the corticothalamic fibres as they invade the thalamus has not been resolved. This is because retrograde tracing from the thalamus obscures the cortical fibre patterns and anterograde tracing from the cortex also labels thalamocortical projection neurons. Early attempts show precise patterned ingrowth to specific nuclei. Anterograde tracing from the putative primary visual cortex in embryonic rhesus monkey demonstrated a waiting period extending several weeks before the corticothalamic projections invaded the dLGN (Shatz and Rakic, 1981).

Since much of the research on this development was first performed, the advancement in molecular techniques has produced transgenic mouse lines which can now aid us to resolve the specific details of corticothalamic ingrowth (e.g. The Gensat Project, International Mouse Mutagenesis Consortium). Three recently developed transgenic mouse lines can be used to selectively label the three corticothalamic subpopulations. These lines are the Rbp4-Cre mouse line which expresses Cre-recombinase in layer V cortical neurons (Gong et al., 2007; Gong et al., 2003), the Ntsr1-Cre mouse line expresses Cre-recombinase in layer VI cortical neurons (Olsen et al., 2012) and the Golli-τ-eGFP mouse expresses eGFP in layer VI and VIb cells and neurites (Jacobs et al., 2007).

3.1.1. Aims of chapter 3

Despite continued interest the exact timing and pattern of layer specific corticothalamic ingrowth to the first order and higher order thalamic nuclei has not be fully elucidated. This is due to inherent difficulties using conventional tracing techniques to exclusively label one subpopulation of corticothalamic fibres without labelling the other corticothalamic populations or ingrowing thalamic projections. However a revolution in mouse genetic techniques has allowed for the generation of transgenic lines to specifically label the distinct corticothalamic subpopulations. In this chapter I aim to address two questions using these lines.

1) Firstly I will study the temporal pattern of ingrowth of layer V, VI and VIb corticothalamic fibres of the mouse.
    a) I use carbocyanine dye tracing from the VPM to retrogradely label corticothalamic neurons in the primary somatosensory cortex at E18.5, P2, P4, P6, and P10.
2) Secondly I will characterise the spatial patterns of the different corticothalamic subpopulations as they develop within the thalamus.
    a) To do this I use three transgenic mouse lines, Rbp4-Cre::tdTomato, Ntsr1-

Cre::tdTomato and Golli-τ-eGFP which label the layer V, VI and VI/VIb corticothalamic projection subpopulations, respectively.

i) I first characterise the cellular tdTomato expression in the Rbp4-Cre::tdTomato and Ntsr1-Cre::tdTomato mice.

ii) I then analyse the layer specific pattern of ingrowth of the cortical fibres to distinct thalamic nuclei including the first order dLGN and VPM and the higher order LP and Po at P2, P6 and P10.

iii) I also characterise ingrowth of layer V corticofugal fibres to the superficial grey layer of the superior colliculus.

3.2. Methods

Animal husbandry, tissue collection and image acquisition as described in general methods chapter 2; section 2.1.

3.2.1. Retrograde DiI labelling of cortical neurons from the thalamus- to determine layer specific ingrowth to the thalamus over early postnatal development

To analyse the order in which corticothalamic fibres reach the thalamus I placed carbocyanine dyes in the VPM and assessed retrograde cell labelling in the presumptive somatosensory cortex.

Using Leica dissection microscope (MZFL III), stainless steel wires were used to place small crystals of DiI (1,1'-dioctadecyl-3,3,3',3'-tetramethylindocarbocyanine perchlorate) or DiA (4-(4-[dihexadecylamino]styryl)-N-methylpiridinium iodide) (Invitrogen, Paisley, UK) in the VPM of C57/Bl6 wild-type mice. Brains were incubated in PBSA at 37°C to allow dye diffusion (Molnár et al., 1998a). Brains were embedded in 5% agarose (Bioline, London, UK) in 0.1M PBS, and sectioned coronally on a Leica VT1000S vibrating microtome. Sections were counterstained with 5µg/mL DAPI (4',6-diamidino-2-phenylindole, dilactate), (Invitrogen, D3571) for 5 minutes. Sections were cover-slipped in 0.1M PBS and sealed with nail varnish. Dye crystal placement

was confirmed in the VPM by fluorescent microscope analysis. Brains with non VPM placements were excluded from analysis.

Age	n	Dye	Incubation time at 37°C	Section thickness
E18.5	5	DiI	3 weeks	100µm
P2	3	DiI	4 weeks	50µm
P4	3	DiI	4 weeks	50µm
P6	2	DiI	6 weeks	50µm
P10	4	DiA	6 weeks	50µm

Table 3.1. Numbers of brains with crystal placement in the VPM, including carbocyanine dye used. Details including incubation times and section thickness. One litter was used per age and different litters were used for each age.

Cell density was quantified on sections in which barrel cortex, or presumptive barrel cortex was present (figure 3.1 A). Back-labelled cells were counted in a grid 100µm wide by the depth of the cortical layer in µm (figure 3.1 B). The depth of layer V and VI was identified using DAPI. Cells were quantified in as many full quantification grids as fit per image. Numbers were collated to give a number per brain. Firstly raw numbers were compared, secondly the cell counts were normalised for the area of the layers by comparing the density of back-labelled cells in each layer as described below.

1. Counting area was defined as: *100µm * depth of the cortical layer in µm*

2. The total cell count for each layer was normalised for the area of the layers by

$$\textit{Density of back-labelled cells in layer } x = \frac{\textit{total cells counted in layer } x}{\textit{total counting area of layer } x}$$

This was repeated for layer V and for layer VI.

To compare the density of back-labelled cells in layer V and layer VI directly, a ratio was calculated. The ratio of the density of back-labelled cells in layer V to layer VI was calculated by:

1. $$\textit{Ratio of density} = \frac{\textit{density of back-labelled cells in layer V}}{\textit{density of back-labelled cells in layer VI}}$$

In order to analyse these results by exact crystal placement the VPM was divided into three regions, dorsolateral, middle and ventromedial (figure 3.2).

3.2.2. Immunohistochemistry

In order to characterise the cortical expression of Cre in the Rbp4-Cre::tdTomato and Ntsr1-Cre::tdTomato brains, I performed immunohistochemistry for pan neuronal

marker NeuN and known subplate markers CTGF and Complexin3 (Hoerder-Suabedissen et al., 2009). In order to assess the maturity of layer V corticotectal fibres in the superior colliculus I performed immunohistochemistry for mature corticofugal synapse marker VGluT1.

For free floating fluorescent immunohistochemistry brains were embedded in 4% agarose (Bioline, London, UK) and sectioned coronally to 50µm. Sections were stored at 4°C in PBSA. Sections were blocked for 2 hours at room temperature with 0.1% Triton-X100 (BDH, Poole, UK) and 2% normal donkey serum (Sigma Aldrich, Gillingham, UK) in 0.1M PBS. The only exception was CTGF for which a blocking solution of 1% Triton-X100, 2% donkey serum was used. Sections were incubated

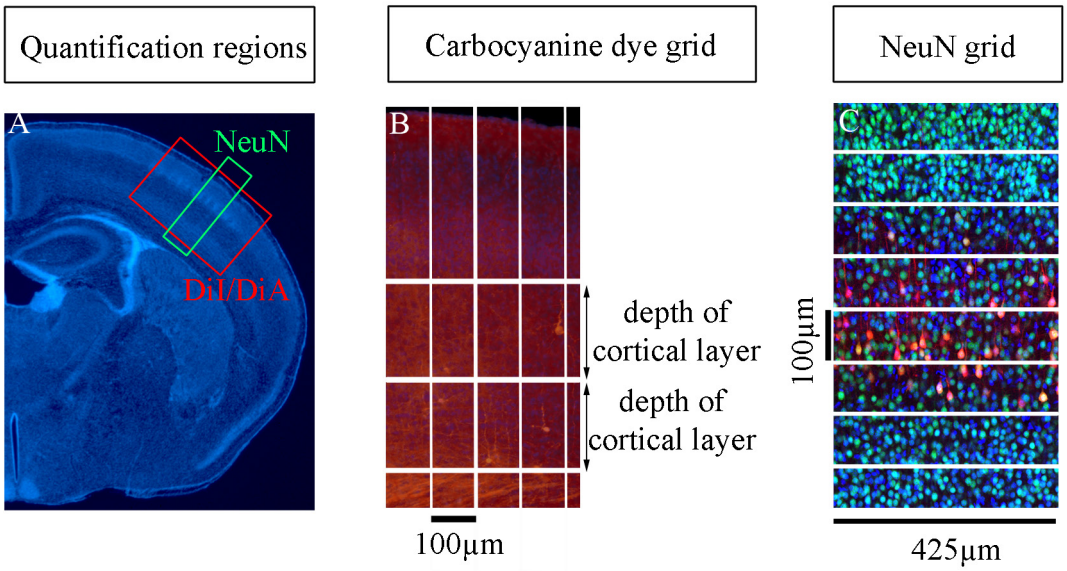

Figure 3.1. Example of cell quantification grids. A. Area of cortex used for quantification. Red box denotes area used for carbocyanine dye quantification. Green box denotes area used for NeuN, Rbp4-Cre::tdTomato and Ntsr1-Cre::tdTomato quantification. B. 100µm wide grid, over-laid on fluorescent microscope images used to quantify cells in the cortex which are back-labelled by VPM carbocyanine dye placements. C. Grid over-laid on confocal microscope images use to quantify NeuN and Rbp4-Cre::tdTomato and Ntsr1-Cre::tdTomato expression.

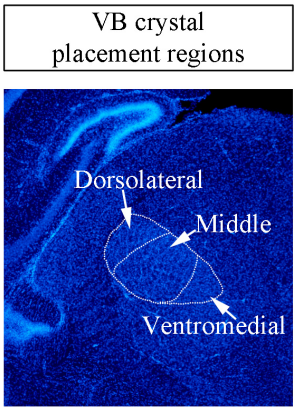

Figure 3.2. Schematic showing how areas of the VPM were categorised for exact carbocyanine dye placement. Three areas were defined; dorsolateral VPM, middle VPM and ventromedial VPM.

with primary antibody in blocking solution at 4°C overnight. Sections were incubated with secondary antibody in blocking solution for 2 hours at room temperature. If a biotinylated secondary antibody was used sections were then incubated with a streptavidin conjugated fluorophore for 1 hour at room temperature. Sections were counterstained with DAPI as above. Details of antibody combinations in table 3.2.

Strains	Primary antibodies	Secondary antibodies	Block
Rbp4-Cre::tdTomato Ntsr1-Cre::tdTomato	Mouse anti-NeuN 1:1000 (Chemicon, MAB377)	Donkey anti-mouse AlexaFluor488 1:500 (Invitrogen, A21202)	0.1% Triton-X100 2% donkey serum 0.1M PBS
Rbp4-Cre::tdTomato Ntsr1-Cre::tdTomato	Goat anti-CTGF 1:500 (sc-14939, Santa Cruz)	Donkey anti-goat AlexaFluor488 1:500 (Invitrogen, A11055)	1% Triton-X100 2% donkey serum 0.1M PBS
Rbp4-Cre::tdTomato Ntsr1-Cre::tdTomato	Rabbit anti-Complexin3 1:1000 (122301, Synaptic Systems)	Donkey anti-rabbit AlexaFluor488 1:500 (Invitrogen, A21206)	0.1% Triton-X100 2% donkey serum 0.1M PBS
Rbp4-Cre::tdTomato	Guinea-pig anti VGluT1 1:5000 (Chemicon, AB5905)	Donkey anti-guinea-pig biotinylated 1:100 (Jackson Immuno Research, Newmarket, UK, 706-065-148). Streptavidin AlexaFluor488 1:500 (Invitrogen, S32354).	0.1% Triton-X100 2% donkey serum 0.1M PBS

Table 3.2. Combinations of primary and secondary antibodies for immunohistochemistry experiments.

3.2.3. Quantification of tdTomato positive NeuN cells in Rbp4-Cre::tdTomato and Ntsr1-Cre::tdTomato brains

In order to characterise Ntsr1-Cre::tdTomato and Rbp4-Cre::tdTomato expression I performed immunohistochemistry against pan neuronal marker NeuN at P10 and quantified the number of NeuN cells which expressed tdTomato. Initial litters were from the Scanziani laboratory at the University of California, San Diego (USA) until the colony was established at Oxford. Immunohistochemistry against pan-neuronal marker NeuN was performed as described.

Confocal images were taken 425µm wide and spanning the cortex from pia to white matter using 20x objective. Two brains, three sections from somatosensory cortex per brain, were used for quantification. Sections were alternate sections, 100µm apart. The 425µm width of the confocal image was used to define the width of the bins for quantification (region shown in figure 3.1A). A z-stack of three z-planes was taken, each 3.8µm apart, and quantification was performed on the middle z-plane. Cell labelling which was brightest in the middle z-plane was counted, any labelling which was brighter in either of the external z-planes was discounted. A grid with bins 100µm thick was placed over the cortex (figure 3.1 C). Only bins over layer V (for Rbp4-Cre) or VI (for Ntsr1-Cre) were quantified from. The density of neurons labelled with tdTomato was determined by counting the number of NeuN positive neurons also expressing the reporter tdTomato. The number of non-neuronal cells labelled by each Cre within the specific layer was also established by counting the number of tdTomato positive cells which did not express NeuN. The numbers for each section per brain were averaged to make a number for the whole brain.

Genotype	n	Litter	Slices/ brain	NeuN cells counted	tdTomato cells counted	Cells expressing both counted
Ntsr1-Cre::tdTomato	2	1	3	1812	882	656
Rbp4-Cre::tdTomato	2	1	3	834	153	118

Table 3.3. Number of brains used for quantifying tdTomato expression in two Cre lines and number of cells quantified for each genotype.

3.2.4. Anterior-posterior analysis of fluorescent fibre ingrowth to dLGN on para-sagittal sections

In order to characterise the precise pattern of ingrowth of Golli-τ-eGFP layer VI and VIb fibres and Ntsr1-Cre::tdTomato layer VI fibres to the dLGN, I analysed fibre ingrowth from the anterior pole of the dLGN to the posterior edge of the dLGN on parasagittal sections.

P6 Golli-τ-eGFP, P8 Golli-τ-eGFP and P6 Ntsr1Cre::tdTomato brains were cut to 50 µm parasagittal sections and counterstained with DAPI. Fluorescent microscope images of the dLGN were taken with a 10x objective. Images were fluorescence intensity

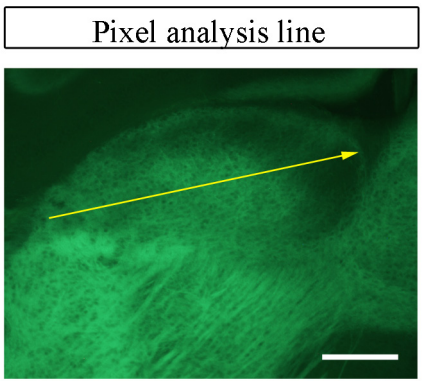

Figure 3.3. Example of line drawn across dLGN for pixel analysis. A line was drawn from the anterior most pole of the dLGN (beginning of arrow) to the posterior most edge (arrow head). Pixel intensity along this line was analysed.

standardised in ImageJ using the ventral hippocampus. Two images were used per brain. A line was drawn from the anterior tip of the dLGN to the posterior edge of the dLGN (figure 3.3). The Plot Profile tool was used to measure the intensity of the pixels beneath the line. The pixel intensity values were averaged and normalised for each brain and the values for the brains were plotted to show the change in pixel intensities along the anterior to posterior axis of the dLGN.

Age and genotype	n	Number of litters
P6 Golli-τ-eGFP	2	1
P8 Golli-τ-eGFP	3	1
P6 Ntsr1-Cre::tdTomato	2	1

Table 3.4. Number of brains used for sagittal images of fibre ingrowth to the dLGN, one hemisphere used per brain. Different litters were used for the two ages of Golli-τ-eGFP.

3.3. Results

3.3.1. Retrograde carbocyanine dye labelling of cortical neurons projecting to the thalamus

3.3.1.1. Back-labelled cells in the cortex from VPM carbocyanine dye placements

Carbocyanine dyes diffuse retrogradely and anterogradely along cell membranes thus labelling the axons of neurons which pass through a crystal placement site (Godement et al., 1987; Honig and Hume, 1989). To determine the laminar origin of the first corticothalamic projections that reach thalamus, I placed crystals of carbocyanine dye into the ventral posterior-medial nucleus (VPM) and observed the laminar distribution of the back-labelled projection neurons in putative primary somatosensory cortex.

DiI or DiA was placed into the VPM, at five developmental time points E18.5, P2, P4, P6 (DiI) and P10 (DiA). The VPM was chosen because it is the first thalamic

nucleus which developing corticothalamic fibres encounter due to its lateral and ventral position. As such back-labelling from the VPM should represent the earliest pattern of development for corticothalamic fibres.

By E18.5 post-mitotic neurons forming cortical layers V, VI and VIb have completed their migration whilst the upper layers are still migrating. At E18.5 sparse back-labelled neurons were visible in layers V, VI and VIb (figure 3.4). Thus a few projections from all three corticothalamic subpopulations have reached the thalamus. By P2 back-labelled cells in the cortex are more numerous indicating more fibres have reached the VPM. At P2 layer V contains the majority of back-labelled cells however some back-labelled cells are still present in layer VI and VIb. At P4 all three layers contain back-labelled projection neurons; however by now layer VI is most densely back-labelled. At P6 and P10 layer VI is more densely labelled than layer V however there are clear cells in all three layers; V, VI and VIb.

Throughout the period of study (E18.5-P10) layer VIb projection neurons were consistently, though sparsely, labelled (table 3.5). This confirms that VIb neurons project to VPM from late embryonic stages continuing through early postnatal development.

Age	n	Raw number of cells counted				Average cells per brain			
		Total	V	VI	VIb	Total	V	VI	VIb
E18.5	5	190	54	105	31	38	10.8	21	6.2
P2	3	690	471	196	23	230	157	65.33	7.67
P4	3	147	46	92	9	49	15.3	30.67	3
P6	2	382	57	316	9	191	28.5	158	4.5
P10	4	968	113	811	44	242	28.25	202.75	11

Table 3.5. Numbers of hemispheres with DiI/DiA placement in the VPM for each age. Number of cells counted within layers V, VI and VIb from 3-6 coronal sections through the putative primary somatosensory cortex. One litter was used per age and different litters were used for each age.

Quantification of back-labelled soma in layer V and VI confirmed that the layer with the greatest back-labelling of cells switches between layer V and VI over the first 10 postnatal days. The total number of cells back-labelled in layer V and VI were quantified (table 3.5). These counts were compared raw (figure 3.5 A and B) and normalised by layer area by comparing the ratio of the density of back-labelled cells in

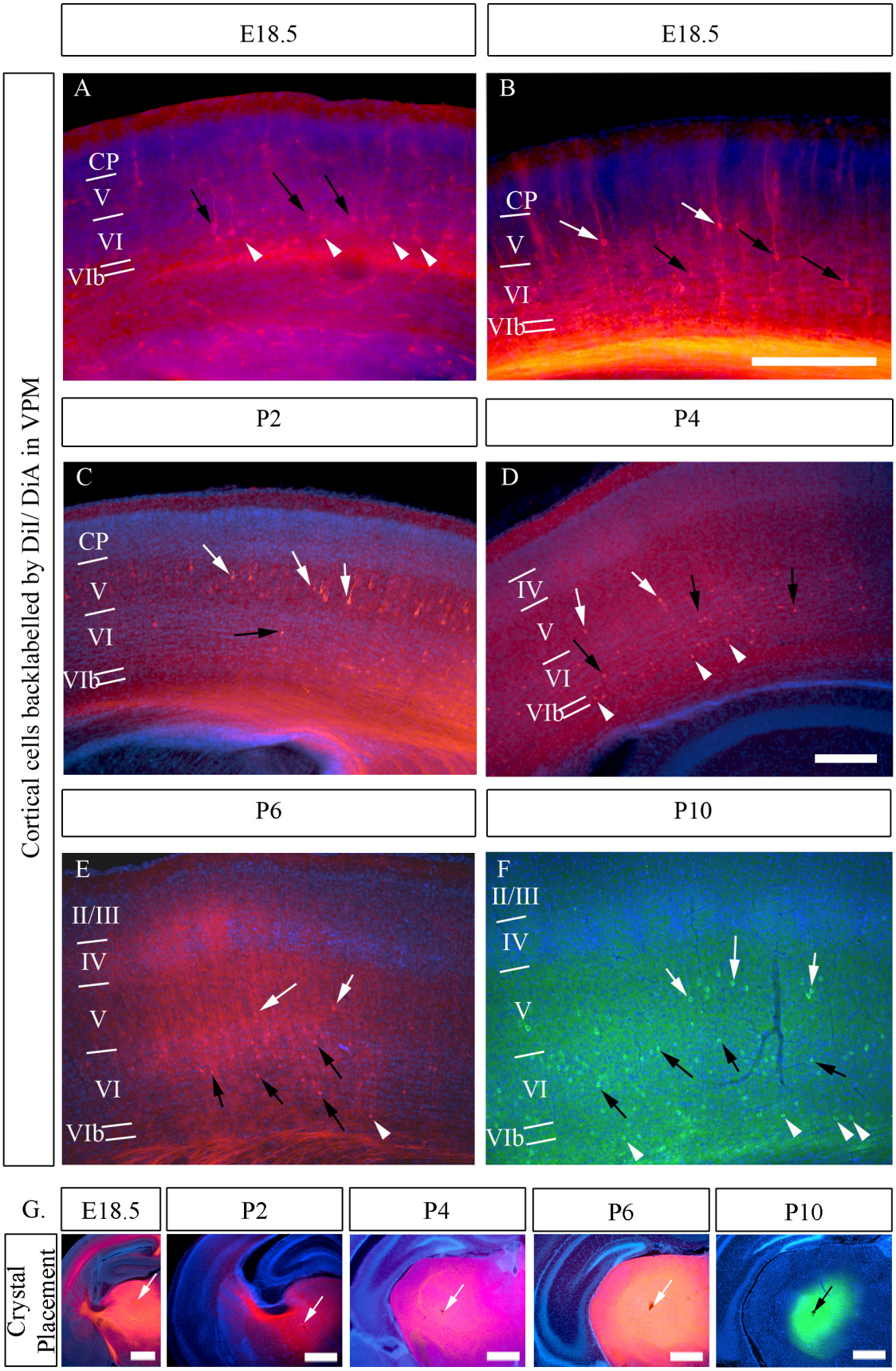
E18.5
E18.5
A
CP
V
VI
VIb
B
CP
V
VI
VIb
P2
P4
C
CP
V
VI
VIb
D
IV
V
VI
VIb
P6
P10
E
II/III
IV
V
VI
VIb
F
II/III
IV
V
VI
VIb
Cortical cells backlabelled by DiI/ DiA in VPM
G.
E18.5
P2
P4
P6
P10
Crystal Placement

Figure 3.4. Cortical neurons in layers V, VI and VIb of presumptive somatosensory cortex are back-labelled from carbocyanine dye crystals placed in the VPM from E18.5-P10. A and B. At E18.5 sparse neurons back-labelled by DiI placed in the VPM are visible in layer VIb (white arrow heads), layer VI (black arrows) and V (white arrows). C. By P2 more back-labelled neurons are in layer V than in layer VI and VIb. D. By P4 there are more back-labelled neurons in layer VI than layer V. E. This pattern is sustained at P6. F. At P10 there are back-labelled neurons present in layer V, VI and VIb from DiA placed in the VPM. More neurons are back-labelled within layer VI than layer V. No back-labelled neurons are visible in the upper cortical layers at any age. G. Representative examples of crystal placement sites within the VPM at E18.5, P2, P4, P6 and P10. Abbreviations used: CP, cortical plate; VPM, Ventrobasal Nucleus. Scale bars = 100µm (A-B), 200µm (C-F), 500µm (G).

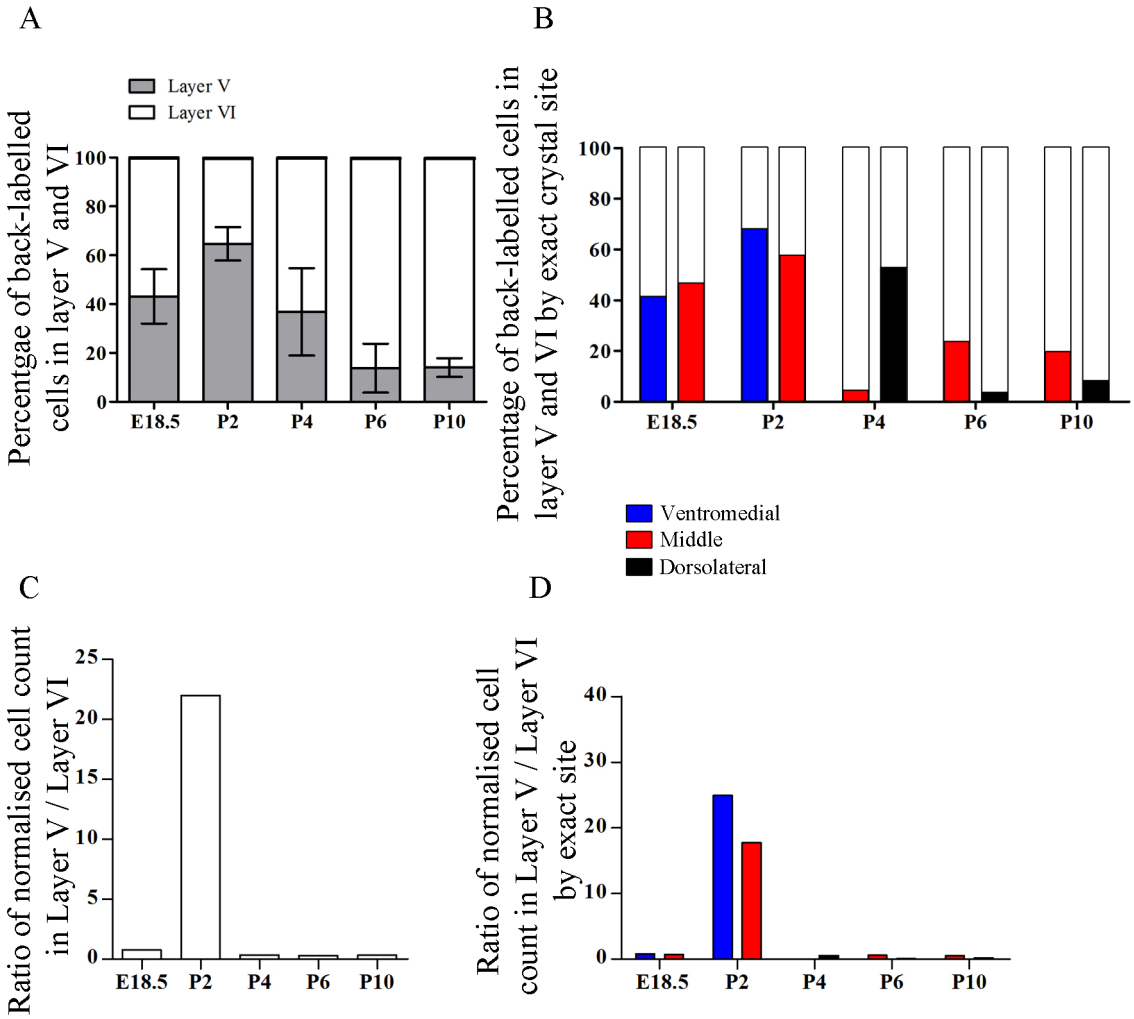

Figure 3.5. Comparison of cells back-labelled in layer V and VI in putative somatosensory cortex from carbocyanine dye crystal placement in the VPM from E18.5 to P10. A. Proportion of the raw number of back-labelled cells residing in layer V and VI following carbocyanine dye placements in VPM at different time point. At E18.5 cells are similarly back-labelled in both layers. By P2 substantially more of the back-labelled cells are within layer V compared to layer VI. From P4 onwards the majority of cells reside in layer VI compared to layer V. B. Results split by the exact site of the crystal placement within the VPM. C. Ratio of the density of layer V back-labelling to layer VI back-labelling. D. Ratio of layer V back-labelling to layer VI back-labelling divided by exact dye placement. The Values given are mean ± SEM.

layer V or layer VI was compared (figure 3.5 C and D). I used the ratio of the density of back-labelling in layer V compared to density of back-labelling in layer VI in order to account for the difference in area of layer V and layer VI, which may skew results, and to account differential changes in layer area over development. Proportional quantification for layer VIb cells was not performed because the scarcity of cells could lead to unrepresentative results.

At E18.5 slightly more back-labelled cells were in layer VI (table 3.5 and figure 3.5 A). At E18.5 there was large variability between brains (see table 3.6 for mean±s.d.). This variability may be because E18.5 may be a transition stage. As the ratio of densities shows the same trend it is unlikely, but not impossible, that different sized DiI crystal could produce such variability. Although all crystal placement sites were verified, it is possible that some produced a more extensive halo with a larger sphere of uptake. By P2 the majority of back-labelled cells were within layer V. The proportion reverses again by P4 so that the majority of back-labelled cells were in layer VI (figure 3.5 A). From P4 through P6 to P10 the relative proportions do not change; layer VI is more densely back-labelled than layer V. Cell counts at P4, P6 and P10 also showed large variability between brains (see table 3.6 for percentage of cells in each layer, mean±s.d.). A potential cause of this variability is discussed in the next section.

Age	Percentage of cells in layer V mean ± s.d.	Percentage of cells in layer VI mean ± s.d.
E18.5	43.2 ± 24.9	56.9 ± 24.9
P2	64.7 ± 11.79	35.3 ± 11.79
P4	36.9 ± 30.92	63.2 ± 30.92
P6	13.8	86.2
P10	14.1 ± 7.655	86 ± 7.655

Table 3.6. Percentage of total back-labelled cells which are in each layer.

3.3.1.2. Cortical back-labelling by analysing the data according to the position of carbocyanine dye crystal within VPM

To determine if the site of the carbocyanine dye crystal within the VPM affected back-labelling in the cortex, the results were divided into three groups based on exact crystal placement site; dorsolateral, middle and ventromedial VPM (figure 3.2). The results

demonstrate that the laminar distribution of cortical back-labelling is broadly similar from different sites in the VPM although there are important differences.

At E18.5 and P2 carbocyanine crystal placements were categorised as ventromedial and middle VPM (no dorsolateral VPM placements were seen at these ages). At E18.5 and P2 the proportion of back-labelled cells was very similar for crystals in both placements (figure 3.5. B and D). Regardless of placement at E18.5 slightly more cells were in layer VI than layer V. By P2 a majority of back-labelled cells were in layer V with both placements. At P4, P6 and P10 crystals were categorised into middle and dorsolateral VPM. There were differences between back-labelling from middle and dorsolateral placements at these ages (figure 3.5.B and D). At P4 layer VI is more densely labelled by middle sites than dorsolateral sites. At P6 and P10 layer VI is more densely labelled by dorsolateral sites than middle sites (figure 3.5.B and D). Due to the shift between P4 and P6 we cannot discern a clear trend in the difference between middle and dorsolateral VPM. Dorsolateral crystal placements at E18.5 and P2 may have helped to elucidate a pattern however no crystals were categorised in the dorsolateral VPM at E18.5 or P2. No crystals were categorised as ventromedial at P4, P6 or P10 so we cannot comment on ingrowth to this region of the VPM at these ages.

These results show there may be a difference between corticothalamic ingrowth to the middle VPM and dorsolateral VPM as there are differences in the V:VI back-labelled cells from these sites at P4, P6 and P10. Despite the differences between back-labelled cells from middle and dorsolateral sites the relationship between layer V and VI is the same; more back-labelled cells are apparent in layer VI compared to layer V. This variability between dorsolateral and middle placements may explain the variability at those ages for the combined VPM results (table 3.6).

My results contribute to the patterns of layer specific ingrowth to the literature as assessed by carbocyanine dye tracing and are most similar to those described in hamsters and cats (Miller et al., 1993; McConnell et al., 1989).

3.3.2. Novel transgenic lines which selectively label layer V, VI and

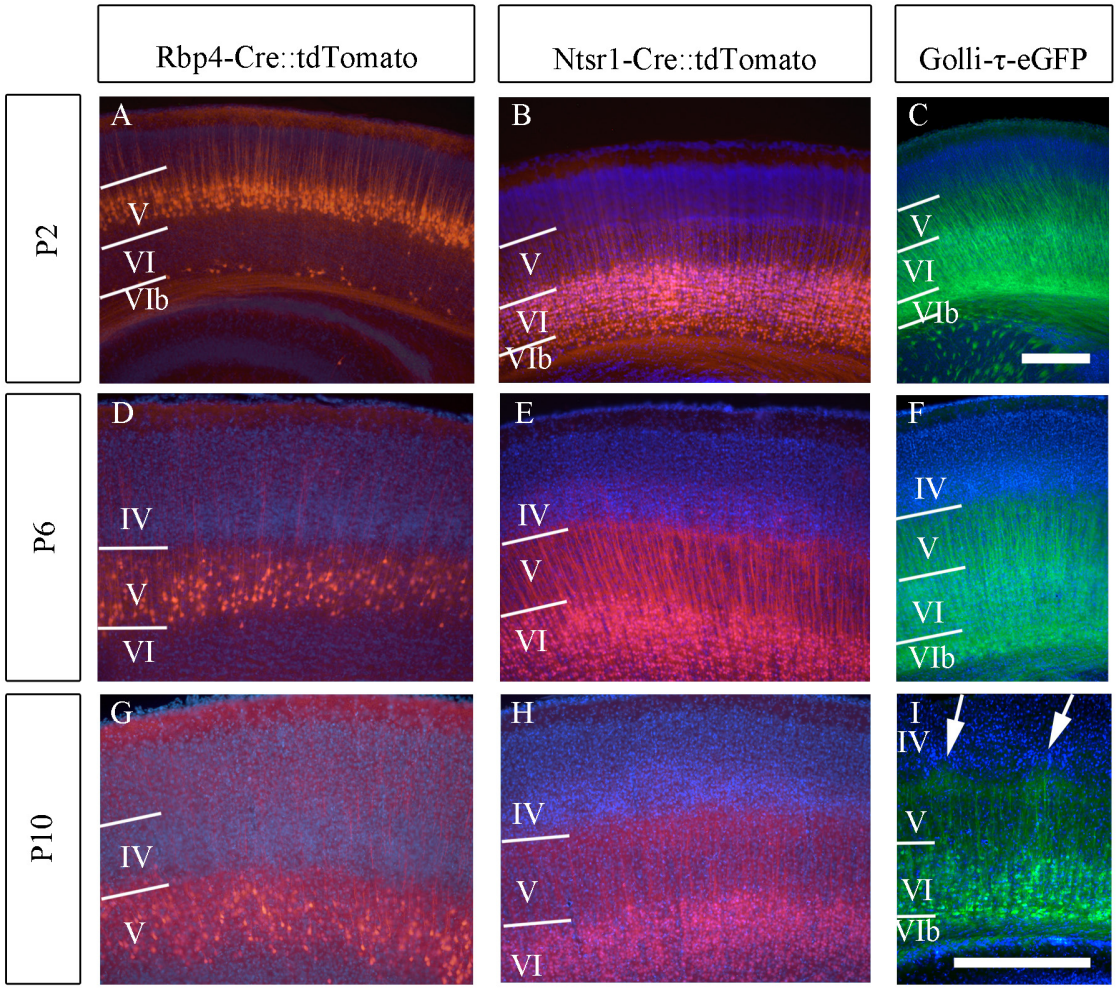

Figure 3.6. Cortical expression of fluorescent label in layer V (Rbp4-Cre::tdTomato), layer VI (Ntsr1-Cre::tdTomato) and layer VI and VIb (Golli-τ-eGFP). Three different transgenic mouse lines Rbp4-Cre::tdTomato, Ntsr1-Cre::tdTomato and Golli-τ-eGFP express fluorescent proteins which label cell bodies and neurites of three corticothalamic neuron populations. Rbp4-Cre::t-dTomato labels layer V. Ntsr1-Cre::tdTomato labels layer VI. Golli-τ-eGFP labels layer VI and VIb. A. At P2 Rbp4-Cre::tdTomato labels the cell body, dendrites and axons of layer V projection neurons. Their apical dendrites extend through the cortical plate to the marginal zone and are tufted. tdTomato positive axons run in the white matter tracts below layer VIb. Sparse layer VIb neurons are also labelled. B. At P2 Ntsr1-Cre::tdTomato densely labels the cell body, dendrites and axons of layer VI projection neurons. The apical dendrites extend to the marginal zone and axons exit the cortex via the white matter tracts which are tdTomato positive. Sparse cells in layer VIb are also labelled. C. At P2 Golli-τ-eGFP labels layer VI and VIb. eGFP positive dendrites are visible projecting into the upper cortical layers. eGFP positive axons run in the white matter tracts below layer VIb of the cortex. D- F. P6 labelling of all three lines. At P6 the distinctive barrel patterning of the primary somatosensory cortex is apparent however the labelled cortical neurons do not show a barrel related pattern. G. At P10 the layer V Rbp4-Cre::tdTomato fibres do not reorient to a barrel pattern. H. At P10 the layer VI Ntrs1-Cre::tdTomato fibres do not reorient to a barrel pattern. J. At P10 the Golli-τ-eGFP dendrites from layer VI and VIb neurons have rearranged to project into the septa of the barrels (white arrows). Scale bars= 250μm (A-H, I).

VIb cortical neurons and neurites

I selected three recently developed transgenic mouse lines which can be used to label the three corticothalamic subpopulations separately. Using these lines I was able to visualise the layer-specific ingrowth to thalamic nuclei by layer V, VI and VIb. The Rbp4-Cre mouse line expresses Cre-recombinase in layer V cortical neurons (GENSAT; Gong et al., 2007; Gong et al., 2003; Gerfen et al., 2013). The Ntsr1-Cre mouse line expresses Cre-recombinase in layer VI cortical neurons (GENSAT; Gerfen et al., 2013; Olsen et al., 2012). Both lines were crossed with a STOP floxed tdTomato reporter line which has *loxP*-flanked STOP cassette preventing transcription of CAG driven fluorescent protein tdTomato (Madisen et al., 2010). When either Cre line is bred with the STOP floxed tdTomato line the STOP cassette is excised in any cells which express Cre thus enabling transcription of tdTomato and labelling the cells and their neurites. The Golli-τ-eGFP mouse expresses eGFP in layer VI and VIb cells and neurites (Jacobs et al., 2007). Summarily: Rbp4-Cre::tdTomato, Ntsr1-Cre::tdTomato and Golli-τ-eGFP label layer V, VI, and VI and VIb respectively (figure 3.6).

3.3.2.1. Characterising Rbp4-Cre::tdTomato cells in layer V and Ntsr1-Cre::tdTomato cells in layer VI

At P2 tdTomato expression is clearly visible in layer V of the Rbp4-Cre::tdTomato mouse and layer VI of the Ntsr1-Cre::tdTomato mouse indicating that Cre mediated recombination of the STOP floxed cassette has occurred before P2 (figure 3.6, 3.7 A and B).

By P2 Rbp4-Cre::tdTomato labels the cell body, dendrites and axons of layer V pyramidal neurons. The tdTomato positive neurons are positioned in both upper (Va) and lower (Vb) layer V (figure 3.7A). The apical dendrites of the tdTomato layer V neurons extend through the cortical plate into the marginal zone and have a tufted appearance. Initially all layer V projection neurons have tufted apical dendrites (Koester and O'Leary, 1992) and as such tdTomato positive cells could be both type I (corticospinal, corticothalamic and corticotectal projecting) and type II (cross-callosal and corticostriatal projecting) layer V neurons. tdTomato positive axons from the layer

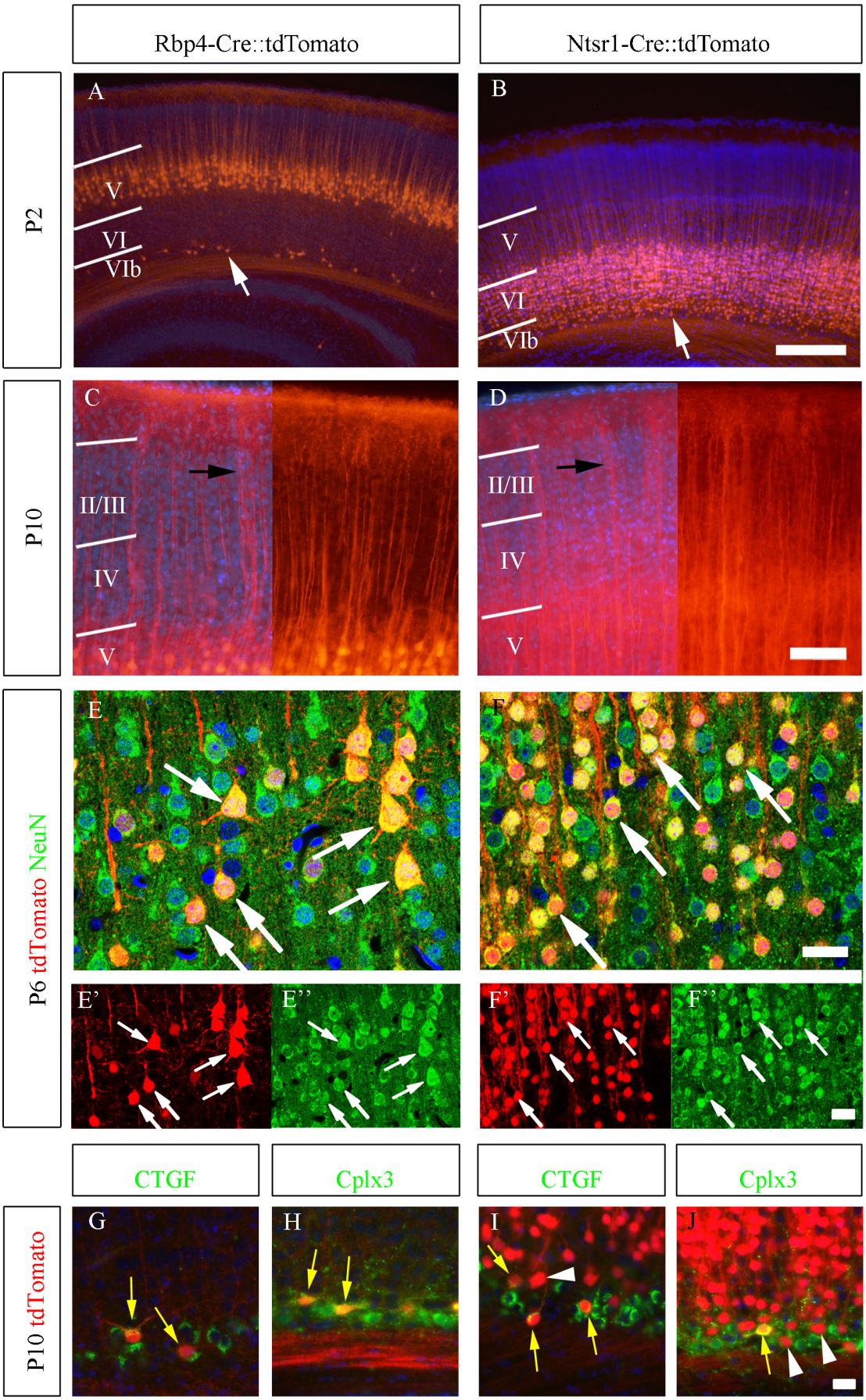
Rbp4-Cre::tdTomato
Ntsr1-Cre::tdTomato
P2
A
V
VI
VIb
B
V
VI
VIb
P10
C
II/III
IV
V
D
II/III
IV
V
P6 tdTomato NeuN
E
F
E'
E''
F'
F''
CTGF
Cplx3
CTGF
Cplx3
P10 tdTomato
G
H
I
J

Figure 3.7. Cortical expression of tdTomato reporter in Rbp4-Cre::tdTomato and Ntsr1-Cre::tdTomato. Rbp4-Cre and Ntsr1-Cre express Cre recombinase in layer V and VI respectively. A. At P2 Rbp4-Cre::tdTomato labels the cell body, dendrites and axons of layer V projection neurons. Their apical dendrites extend into the cortical plate and marginal zone and are tufted. tdTomato positive axons run in the white matter tracts below layer VIb of the cortex. Sparse layer VIb neurons are also labelled (white arrow). B. At P2 Ntsr1-Cre::tdTomato densely labels the cell body, dendrites and axons of layer VI projection neurons. The apical dendrites extend into cortical plate and marginal zone and axons also exit the cortex via the white matter tracts which are tdTomato positive. Sparse cells in layer VIb are also labelled (white arrow). C. At P10 the apical dendrites (black arrow) of the Rbp4-Cre::tdTomato neurons extend to layer I and maintain tufted morphology. D. By P10 Ntsr1-Cre::tdTomato apical dendrites (black arrow) still project to the marginal zone. In addition to fibres reaching the marginal zone there is dense fibre labelling in layer V. E and F. Anti-NeuN immunohistochemistry demonstrates that Rbp4-Cre::tdTomato and Ntsr1-Cre::tdTomato positive neurons are NeuN positive (white arrows). Rbp4-Cre::tdTomato positive neurons residing in layer VIb are CTGF (G.) and Complexin3 (H.) positive (yellow arrows) but Rbp4-Cre::tdTomato is not present in all CTGF expressing or Complexin3 expressing cells in layer VIb. Ntsr1-Cre::tdTomato positive cells in layer VIb do express CTGF (I.) and Complexin3 (J.) (yellow arrows) however not all tdTomato expressing cells within layer VIb express CTGF or Complexin3 (white arrow heads). Scale bars= 250μm (A, B), 100μm (C, D) and 25μm (E-F, E'- F", G-J).

V pyramidal cells run in a fibre tract in the white matter deep to layer VIb. Sparse tdTomato positive cells are also present in layer VIb (figure 3.7 A). At P10 the apical dendrites of the Rbp4-Cre::tdTomato neurons are still visible within layer I and maintain a tufted morphology (figure 3.7 C). The tdTomato labelling is too dense to enable reconstruction of single cell somatodendritic morphology, however the maintenance of a tufted morphology at P10 suggests that type I layer V neurons are labelled by the Rbp4-Cre::tdTomato. Type I layer V neurons maintain their tufted morphology into adulthood compared to type II, which remodel their apical dendrite to terminate in layer IV by P7 (Koester and O'Leary, 1992).

By P2 Ntsr1-Cre::tdTomato densely labels the cell body, dendrites and axons of layer VI pyramidal neurons (figure 3.7 B). The tdTomato positive apical dendrites extend to the marginal zone and tdTomato positive axons exit the cortex via the white matter tracts. Some tdTomato cells were also present in layer VIb (figure 3.7 B). At P10 the apical dendrites still project to the layer I (figure 3.7 D). In addition to fibres reaching layer I, there is dense fibre labelling within upper layer V suggesting that these layer VI fibres arborise in both layer I and layer V. This is consistent with previous descriptions of layer VI pyramidal neurons labelled by Ntsr1-Cre which used biocytin back-filled neurons to show that Ntsr1-Cre labels two morphologically distinct populations of layer VI neurons based on their apical dendrites (Olsen et al., 2012; Bortone et al., 2014). The majority

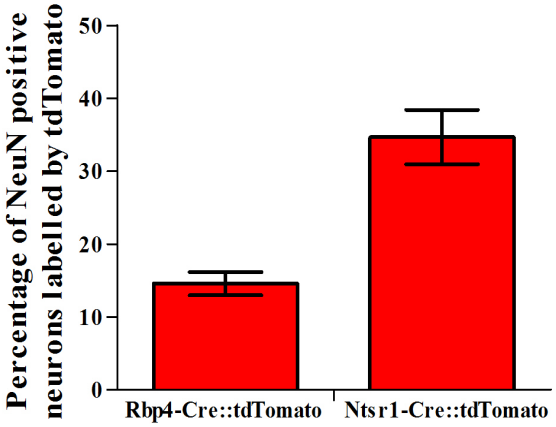

Figure 3.8. Percentage of NeuN positive neurons which express tdTomato in layer V of the Rbp4-Cre::tdTomato line and layer VI of the Ntsr1-Cre::tdTomato line at P10. Quantification of immunohistochemistry against mature neuronal marker NeuN on Rbp4-Cre::tdTomato and Ntsr1-Cre::tdTomato somatosensory cortex at P10 showing the percentage of NeuN positive neurons which express the tdTomato reporter. Rbp4-Cre::tdTomato was expressed in 15% of NeuN positive neurons in layer V. Ntsr1-Cre::tdTomato was expressed in 35% of NeuN positive neurons in layer VI. Two animals, three sections per animal, were quantified from; total of 3681 cells were counted. Values given are mean ± SEM.

of Ntsr1-Cre cells (68%) had apical dendrites that reached layer I, the remaining 32% had apical dendrites within layer IV and upper layer V (Olsen et al., 2012). The Ntsr1-Cre::tdTomato fibres visible in layer V may, in fact, be axons innervating layer V (Kim et al., 2014).

Immunohistochemistry against mature neuronal marker NeuN was used to quantify the number of neurons (NeuN positive cells) labelled by tdTomato in the relevant layer of each Cre line. Rbp4-Cre::tdTomato and Ntsr1-Cre::tdTomato positive neurons expressed NeuN (white arrows figure 3.7 E and F respectively). Some tdTomato cells were classified as NeuN negative. This might be because of two reasons. NeuN may not be expressed in all cortical neurons at P10, or the bright cytoplasmic tdTomato may be in a different focal plane from the NeuN positive nucleus. I chose to only quantify from the middle z-plane to ensure the most reliable quantification.

At P10, Rbp4-Cre::tdTomato was expressed in 15% of NeuN positive neurons in layer V (14.54±3.9, mean±s.d.; figure 3.8). At P10, Ntsr1-Cre::tdTomato was expressed in 35% of NeuN positive neurons in layer VI (34.66±9.137, mean±s.d.; figure 3.8). Previous work characterising Ntsr1-Cre cells has shown that 65% of NeuN positive neurons in layer VI were tdTomato positive (Olsen et al., 2012). The disparity between our results may arise from a difference in age of mouse or cortical area, Olsen and

colleagues performed quantification on adult mice in V1 whereas my results were performed at P10 in S1. Another possibility is that the strength of NeuN signal was stronger in our immunohistochemistry thus leading to over representation of NeuN positive cells. The brains I performed NeuN immunohistochemistry on were over a year old I therefore used a stronger than normal concentration of anti-NeuN primary antibody, which could more cells were visible within the optical confocal slice plane. Indeed NeuN positive cells were less dense in the immunohistochemistry images from Olsen et al 2012 compared to mine.

3.3.2.2. Characterising Rbp4-Cre::tdTomato and Ntsr1-Cre::tdTomato cells in layer VIb

To characterise the Rbp4-Cre::tdTomato and Ntsr1-Cre::tdTomato cells in layer VIb immunohistochemistry against known VIb markers CTGF and Complexin3 (Hoerder-Suabedissen et al., 2009) was performed.

Rbp4-Cre::tdTomato cells residing in layer VIb expressed CTGF and Complexin3 (yellow arrows, figure 3.7 G- H). All Rbp4-Cre::tdTomato cells imaged (29 cells) also expressed the layer VIb marker that had been labelled (149 marker expressing cells imaged). Whether the scattered Rbp4-Cre::tdTomato cells in layer VIb express both CTGF and Complexin3 concurrently cannot be assessed as double immunohistochemistry was not performed. This pattern of expression suggests the small subpopulation of layer VIb cells labelled by Rbp4-Cre::tdTomato could fit within a CTGF/Complexin3 double positive subpopulation of layer VIb neurons (Hoerder-Suabedissen and Molnár, 2013) . Rbp4-Cre::tdTomato did not label all CTGF expressing or Complexin3 expressing cells in layer VIb.

Ntsr1-Cre::tdTomato positive cells in layer VIb express CTGF and Complexin3 (yellow arrows figure 3.7). However, not all Ntsr1-Cre::tdTomato expressing cells within layer VIb co-express CTGF or Complexin3 (white arrow heads figure3.7 I-J). These tdTomato positive, CTGF/Complexin3 negative cells reside within the VIb marker positive band below layer VI. This indicates they are indeed layer VIb cells rather

than layer VI cells mistaken for residing within VIb. Whether the population of Ntsr1-Cre::tdTomato positive cells which express one of CTGF and Complexin3 also express the other is unknown as double immunohistochemistry was not performed.

The characterisation of the sparse Rbp4-Cre::tdTomato and Ntsr1-Cre::tdTomato cells in layer VIb is qualitative as immunohistochemistry was performed on only one brain for each genotype. Therefore any strong conclusions may be spurious. Despite this these results suggest Rbp4-Cre::tdTomato and Ntsr1-Cre::tdTomato label a small population of layer VIb neurons.

3.3.2.3. Characterising non-cortical Cre expression in the Rbp4-Cre::tdTomato and Ntsr1-Cre::tdTomato mouse lines

In addition to labelling selective cortical populations there was some Cre induced tdTomato cellular labelling in non-cortical structures (figure3.9 and table 3.7).

Non cortical cellular expression	Rbp4-Cre::tdTomato	Ntsr1-Cre::tdTomato
Hippocampus	Granular cell layer of dentate gyrus	Sparse cells
Thalamus	Mediodorsal thalamic nucleus, posterior thalamic nucleus, sparse cells in dLGN	Ventral posterior-medial thalamic nucleus, sparse cells in vLGN
Amygdala	Amygdala	-
Hypothalamus	Regions of anterior hypothalamus and posterior hypothalamic nucleus	Ventral hypothalamus
Midbrain	Superior colliculus	Periaquaductal grey
Cerebellum	Lobules of cerebellum	Deep cerebellar nucleus

Table3.7. Table summarising the non-cortical cellular expression of tdTomato in Rbp4-Cre::tdTomato and Ntsr1-Cre::tdTomato brains at P6.

In Rbp4-Cre::tdTomato, dense tdTomato cells were visible is the dentate gyrus of the hippocampal formation. The labelled cells displayed granule cell morphology; cell bodies in the granular cell layer, dense dendrite arborisation in the molecular layer and axons projecting out of the dentate gyrus through the hilus (figure 3.9A). A cluster of cells were labelled in the amygdala (figure 3.9 E).

Rbp4-Cre::tdTomato positive cells were seen in several thalamic nuclei (figure 3.9 B-D). Sparse cells were present in the mediodorsal thalamic nucleus. There were also

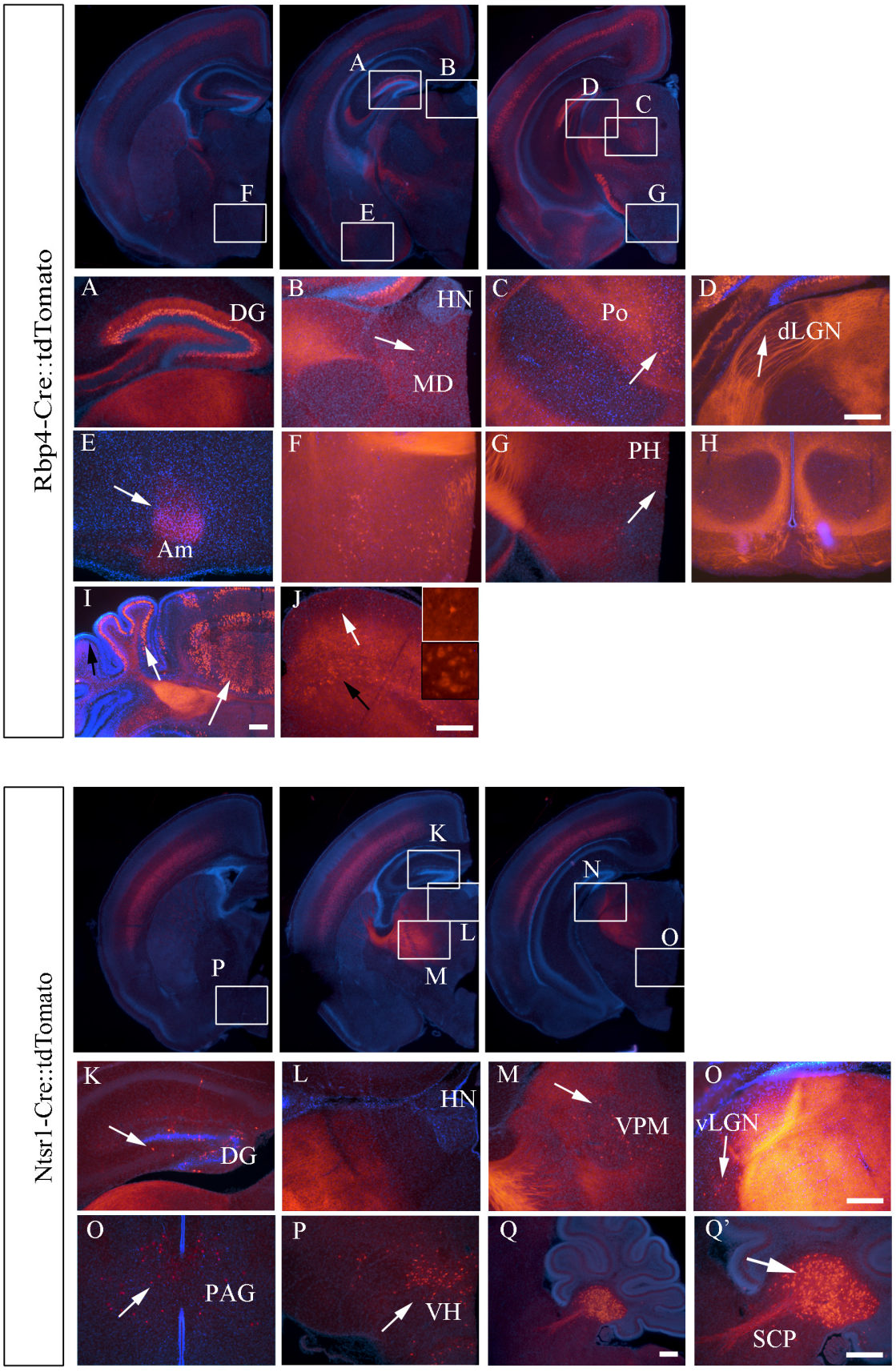
Rbp4-Cre::tdTomato
A
B
C
D
E
F
G
DG
HN
MD
Po
dLGN
Am
PH
H
I
J
Ntsr1-Cre::tdTomato
K
L
M
N
O
P
DG
HN
VPM
vLGN
PAG
VH
Q
Q'
SCP

Figure 3.9. Characterisation of non-cortical Cre recombinase induced tdTomato expression in P6 Rbp4-Cre::tdTomato and Ntsr1-Cre::tdTomato brains. A. Dense Rbp4-Cre induced tdTomato cells are visible is the dentate gyrus (DG) of the hippocampus. Sparse Rbp4-Cre::tdTomato positive cells were visible in thalamic nuclei; B. mediodorsal thalamic nucleus (MD), C. posterior thalamic nucleus (Po), and D. very sparse cells in the dLGN . E. A cluster of cells were labelled in the amygdala (Am). F. Scattered cells can be seen in several regions in the anterior hypothalamus and the posterior hypothalamic nucleus (PH) (G and H.). I. There was dense labelling of cells in the granular layer of the lobules of the cerebellum. J. Scattered cells were visible in the superior colliculus. K. Ntsr1-Cre::tdTomato positive cells were sparse in the hippocampus, not restricted to a particular sub-region or cell layer. L. Cells are present in the VPM (M.) and the vLGN (N.). Ntsr1-Cre::tdTomato cells are visible in the periaqueductal grey (PAG) of the midbrain (O.) and the ventral hypothalamus (VH) (P.). Q and Q' Sagittal sections showed a dense bundle of cells in the deep cerebellar nuclei (white arrow Q') with clear fibres projecting out through the superior cerebellar peduncle (SCP). Abbreviations used: DG, dentate gyrus; HN, habenular nucleus; MD, mediodorsal thalamic nucleus; Po, posterior thalamic nucleus; dLGN, dorsal Lateral Geniculate Nucleus, Am, amygdala; PH, posterior hypothalamic nucleus; VPM,ventrobasal thalamic nucleus; vLGN, ventral Lateral Geniculate Nucleus; PAG, periaqueductal grey; SCP, superior cerebellar peduncle. Scale bars= 250μm (A-H, I, J, K-P, Q, Q').

very sparse cells in the dLGN (figure 3.9 D). Numerous cells were labelled in the Po. These cells are unlikely to account for the fibres extending between cortex and thalamus because they do not appear to have long-range axons and they are not numerous enough to account for the strength of fibre labelling. Despite this it cannot be ruled out. Rbp4-Cre::tdTomato positive cells could be seen in several regions in the anterior hypothalamus and the posterior hypothalamic nucleus (figure 3.9 F, G).

Occasional Rbp4-Cre::tdTomato cells were present in midbrain in the superficial grey layer of the superior colliculus (figure 3.9 J). In the hind brain there was dense labelling of GABAergic Purkinje cells of the cerebellum (figure 3.9 I). Interestingly not all lobules are labelled (figure 3.9 I) suggesting Cre expression differs between lobules. There were Rbp4-Cre::tdTomato positive axons visible projecting through the internal granular layer and into the cerebellar white matter to exit the cerebellar cortex. Purkinje cells project out of the cerebellar cortex and synapse on cells in the deep cerebellar nuclei (De Camilli et al., 1984). The characteristic Purkinje cell dense dendritic trees, which arborise in the molecular layer, are not yet visible.

In the Ntsr1-Cre::tdTomato brains, very sparse labelled cells were visible in the hippocampus but were not associated with a particular structure (figure 3.9 K). In the diencephalon Ntrs1-Cre::tdTomato cells were visible within the VPM and the vLGN (figure 3.9 M, O). These cells were sparse and had short projections suggesting

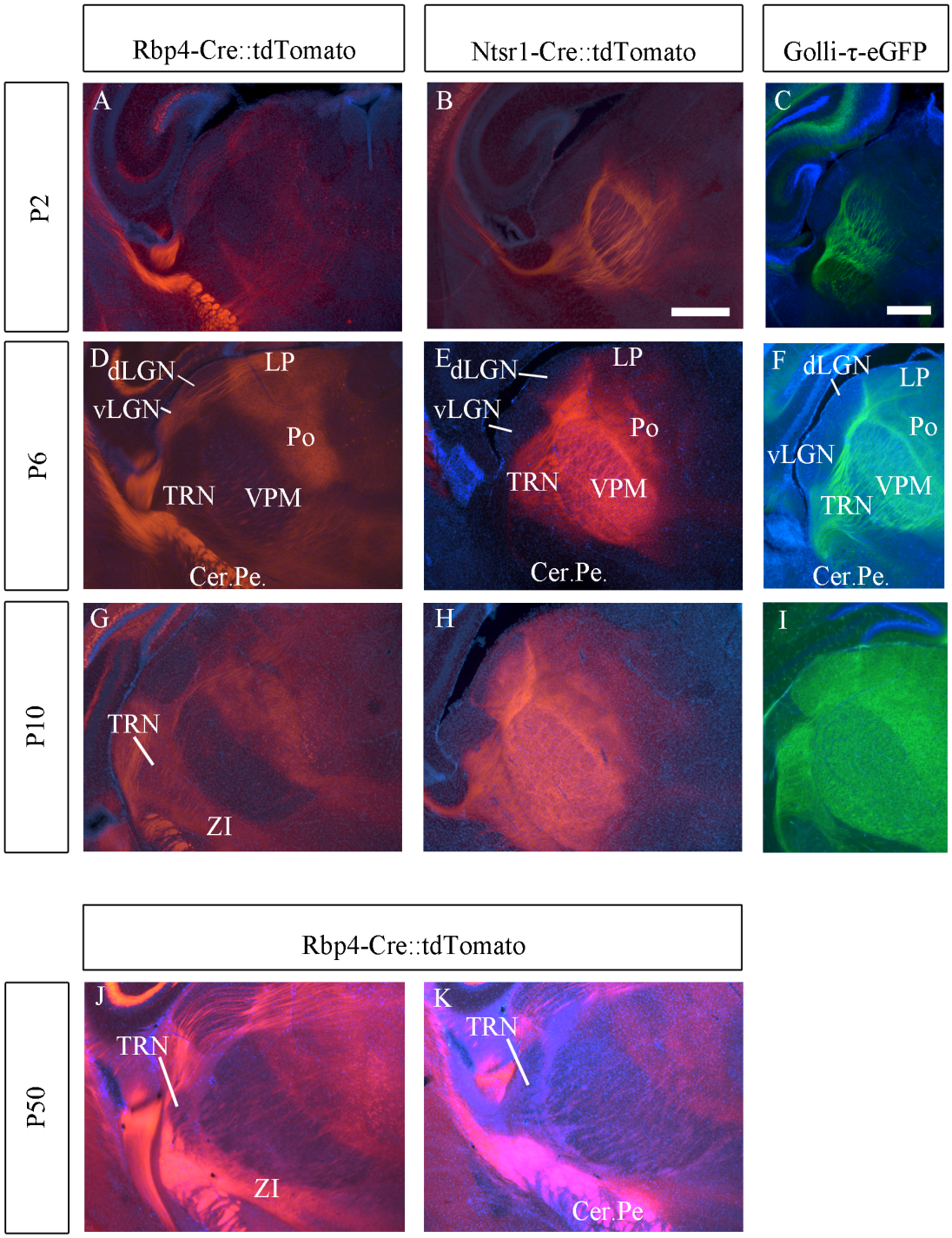

Figure 3.10. Specific corticothalamic projections from layer V (Rbp4-Cre::tdTomato), VI (Ntsr1-Cre::tdTomato), and VI and VIb (Golli-τ-eGFP) over development.
Layer V, VI and VIb fibres innervate the thalamus with specific projection patterns. A. At P2 tdTomato positive fibres arising from layer V have entered the thalamus and ¬project through the vLGN, dLGN and VPM to reach more medial thalamic nuclei including the posterior thalamic nucleus (Po) and the lateral posterior nucleus (LP). Layer V fibres do not innervate the thalamic reticular nucleus (TRN). Layer V corticospinal projections are visible in the cerebral peduncle (CerPe). B. At P2 Ntsr1-Cre::tdTomato positive layer VI fibres were visible in the TRN, VPM and Po but not the LP. No fibres are present in the dLGN but a band of tdTomato positive fibres lines the ventral border of the dLGN. Fibres are absent from the cerebral peduncle. C. At P2 Golli-τ-eGFP positive layer VI and VIb fibres innervate the TRN and VPM. Fibres have not reached the dLGN or the LP. At this stage Rbp4-Cre::tdTomato fibres are complementary to the Ntsr1-Cre::tdTomato positive and Golli-τ-eGFP positive fibres. D. By P6 Rbp4-Cre::tdTomato positive

layer V fibres have arbourised densely within the vLGN, the Po and the LP. The fibres do not innervate the TRN, dLGN or VPM instead coursing through these structures to the more medial nuclei. The cerebral peduncle is strongly labelled. E. By P6 layer VI Ntrs1-Cre::tdTomato fibres densely innervate the TRN, the VPM and the Po and have reached the LP but are not densely arborising within it. A dense band of fibres is present at the lateral, ventral and medial border of the dLGN and fibres have started to enter the dLGN. F. By P6 eGFP positive fibres densely innervate the TRN, the VPM, Po and LP. A clear band of eGFP positive fibres is visible on the ventral and medial border of the dLGN. The Rbp4-Cre::tdTomato fibres are still mostly complementary to the Ntsr1-Cre::tdTomato positive and Golli-τ-eGFP positive fibres however all three populations project to the higher order LP and Po. G. By P10 there is dense innervation of the LP, the Po and the vLGN by Rbp4-Cre::tdTomato layer V fibres. Fewer fibres go through the dLGN and VPM instead projecting to more medial nuclei via a path between them. The cerebral peduncle remains densely labelled. There is also dense labelling visible within the Zona Inserta (ZI). H. By P10 the layer VI Ntsr1-Cre::tdTomato fibres within the dorsal VPM are arranged in a barreloid pattern. Fibres have innervated over half of the dLGN but do not yet reach the dorsal most edge. The LP and Po are densely innervated. The TRN remains densely innervated. I. By P10 eGFP positive VI and VIb fibres densely innervate the whole dLGN, VPM (with a barreloid pattern), LP, Po and TRN. J and K. P50 Rbp4-Cre::tdTomatol layer V fibres do not innervate TRN but innervate ZI. Abbreviations used: dLGN, dorsal Lateral Geniculate Nucleus; vLGN, ventral Lateral Geniculate Nucleus; LP, lateral posterior thalamic nucleus; Po, posterior thalamic nucleus; VPM, ventral posterior-medial thalamic nucleus; TRN, thalamic reticular nucleus; Cer. Pe., cerebral peduncle; ZI, zona inserta. Scale bars= 500μm (A-K., scale bar in B refers to all panels except scale bar in C refers to F and I).

these cells are not responsible for the dense fibres projecting between the cortex and the thalamus. Cells were also present in the ventral hypothalamus (figure 3.9 P). In midbrain structures sparse Ntsr1-Cre::tdTomato cells were visible in the periaqueductal grey. In sagittal sections of the hind brain a dense bundle of Ntsr1-Cre::tdTomato cells is visible in the deep cerebellar nuclei which project to the thalamus and cerebral cortex (Asanuma et al., 1983; Dum and Strick, 2003). Ntsr1-Cre::tdTomato positive fibres project out of the dentate nucleus through the superior cerebellar peduncle (figure 3.9 Q, Q').

My analysis of the cortical and extra-cortical expression of tdTomato confirmed that, despite sparse extra-cortical labelling, Rbp4-Cre::tdTomato and the Ntsr1-Cre::tdTomato lines are suitable for studying layer V and layer VI corticothalamic projections. The Golli-τ-eGFP is suitable for layer VIb and some VI projections (Jacobs et al., 2007).

3.3.2.4. Corticothalamic development in three transgenic lines labelling layer V, layer VI and layer VI and VIb neurons

After selecting three models (Rbp4-Cre::tdTomato, Ntsr1-Cre::tdTomato, Golli-τ-eGFP) I analysed the development of the three populations of cortical fibres into the thalamus in the first two postnatal weeks (figure 3.10). My results show that the ingrowth of

layer V fibres (Rbp4-Cre::tdTomato) and layer VI/VIb fibres to the thalamic nuclei are complementary (Ntsr1-Cre::tdTomato, Golli-τ-eGFP).

At P2 layer V tdTomato corticothalamic fibres have reached the thalamus and project through the lateral/ventral nuclei such as the dLGN and VPM to reach more medial, higher order nuclei including the lateral posterior nucleus (LP) and the posterior nucleus (Po) (figure 3.10 A). The density of fluorescence from the fibres suggests they pass through the dLGN and VPM without arborising. They also do not arborise in the TRN which concurs with previous literature (Hoogland et al., 1987; Rouiller et al., 1998; Kakei et al., 2001). The fluorescence in the Po is denser suggesting the fibres are arborising here. This early P2 fibre pattern within the thalamus replicates the adult fibre pattern of layer V fibres which project to higher order thalamic nuclei (such as the Po) but not first order thalamic nuclei (such as the dLGN and VPM) (Abramson and Chalupa, 1985; Conley and Raczkowski, 1990; Guillery, 1995; Sherman and Guillery, 1998).

In Rbp4-Cre::tdTomato brains the cortico-subcerebral (including corticospinal) layer V projections are also labelled and can be seen in thick bundles running in the cerebral peduncle (figure 3.10 A, D, G) towards the brainstem and spinal cord. Whether the layer V fibres which innervate the thalamus are collaterals of the corticospinal neurons is currently unresolved (Deschênes et al., 1994; Oswald et al., 2013).

At P2 in the layer VI line (Ntsr1-Cre::tdTomato) and the layer VI and VIb line (Golli-τ-eGFP) the pattern of fluorescent fibres is complementary to the layer V fibres in the Rbp4-Cre::tdTomato brains. At P2 Ntsr1-Cre::tdTomato positive layer VI fibres have reached the thalamus and densely label the TRN (figure 3.10 B). These collateral branches of layer VI corticothalamic fibres densely innervate the GABAergic reticular neurons in the adult mouse (Hoogland et al., 1987; Lozsádi et al., 1996; Jones, 2002b) providing inhibitory feedback to the thalamus. Dense Ntsr1-Cre::tdTomato fibres were visible projecting throughout the first order VPM and the higher order Po. Layer VI fibres project to both first order and higher order thalamic nuclei (Gilbert and Kelly,

1975; Abramson and Chalupa, 1985; Conley and Raczkowski, 1990; Diamond et al., 1969; Hoogland et al., 1987; Lozsádi et al., 1996; Guillery, 1967; Jones and Powell, 1968). No fibres were visible entering the first order dLGN but a band of tdTomato positive fibres projects along its ventral border. Fibres were absent from the cerebral peduncle (figure 3.10 B).

At P2 the Golli-τ-eGFP positive layer VI and VIb fibres display a very similar pattern to the Ntsr1-Cre fibres and densely label the TRN (figure 3.10 C). By P2, the fibres have entered the VPM although the layer VI and VIb eGFP fibres are less advanced than the layer VI Ntsr1-Cre::tdTomato fibres (figure 3.10 B and C). The VI and VIb eGFP fibres have not progressed to the far edge of the VPM and have not reached the Po unlike the Ntsr1-Cre fibres. Golli-τ-eGFP VI and VIb fibres were visible at the ventral edge of the dLGN but unlike the Ntsr1-Cre::tdTomato fibres they have not reached the dorsal/ medial edge of the dLGN.

As such at P2 the layer V Rbp4-Cre fibres are projecting through first order dLGN and VPM, and innervate the higher order LP and Po. The Layer VI (Ntsr1-Cre) and Layer VI and VIb (Golli-τ-eGFP) fibres project to both first order (VMP) and higher order (Po) nuclei but the Ntsr1-Cre fibres are more advanced.

By P6 Rbp4-Cre::tdTomato layer V fibres have arborised densely within the vLGN, the LP and the Po (figure 3.10 D). The layer V fibres do not innervate the TRN, dLGN or VPM merely coursing through these structures. The cerebral peduncle is strongly labelled by the cortico-subcerebral fibres.

By P6 layer VI Ntsr1-Cre::tdTomato fibres densely innervate the TRN, the VPM and the Po (figure 3.10 E). Fibres had reached the LP but do not appear to be densely arborised within it. A strong band of fibres is clear at the lateral, ventral and dorsal border of the dLGN and tdTomato fibres had started to enter the dLGN from the ventral/medial edge. The Golli-τ-eGFP positive fibres densely innervate the TRN, the VPM and the Po (figure 3.10 F). A clear band of eGFP positive fibres is visible at the ventral and dorsal

border of the dLGN although they have not begun entering the nucleus, unlike the Ntsr1-Cre layer VI fibres.

By P10 in the Rbp4-Cre::tdTomato brains there was dense layer V innervation of the LP, Po and vLGN. Fewer fibres go through the dLGN and VPM instead coursing between them. The cerebral peduncle remains densely labelled.

By P10 the layer VI Ntsr1-Cre::tdTomato fibres within the dorsal VPM have rearranged to a barreloid pattern with stronger labelling at the septa of the barreloids (figure 3.10 H). Fibres have innervated the majority of the dLGN, filling the ventral/medial half although they do not yet project to the furthest lateral/ dorsal edge. The TRN is densely innervated by collateral branches of the layer VI fibres. The LP and Po are densely innervated. The vLGN does not have fibres projecting to it.

By P10 Golli-τ-eGFP positive VI and VIb fibres densely innervate the whole dLGN, the VPM (with a barreloid pattern), the LP and Po (figure 3.10 I). The dynamic rearrangement to a barreloid pattern of these eGFP positive fibres (and the Ntsr1-Cre::tdTomato layer VI fibres) in the VPM mimics the barrel pattern which cortical Golli-τ-eGFP fibres, presumed dendrites, rearrange to in the cortex (Piñon et al., 2009).

Thus layer VI and VIb (labelled by Ntsr1-Cre::tdTomato and Golli-τ-eGFP) both produce collaterals which innervate the TRN. The layer V Rbp4-Cre::tdTomato line is well suited to address whether layer V sends collaterals to the TRN as a considerable number of layer V fibres are labelled but there is no contamination by labelling of other corticothalamic fibres. These results demonstrate that from P2- P10, layer V fibres do not innervate the TRN although they do innervate the zona inserta (ZI) (figure 3.10 G). At P50 layer V corticothalamic fibres still innervate the ZI but do not innervate the TRN (figure 3.10 J, K). As such my results on the Rbp4-tdTomato convincingly demonstrate that layer V projection neurons do not innervate the TRN. This concurs with previous research which demonstrate that layer V does not innervate the TRN (Hoogland et al., 1987; Rouiller et al., 1998; Rouiller and Welker, 2000; Kakei et al., 2001)

	Cer. Pe.	TRN	vLGN	dLGN	VPM	LP	Po
Rbp4-Cre::tdTomato	+	-	+	-	-	+	+
Ntsr1-Cre::tdTomato	-	+	-	+	+	+	+
Golli-τ-eGFP	-	+	-	+	+	+	+

Table 3.8. Table summarising fluorescent fibre innervation of cerebral peduncle, the TRN and different thalamic nuclei. Though Rbp4-Cre::tdTomato positive fibres run through the TRN, dLGN and VPM they do not appear to arbourise here and as such are classified negative (-). These patterns are complementary apart from the higher order Po which all three corticothalamic populations project to. Abbreviations used: Cer.Pe., cerebral peduncle; TRN, thalamic reticular nucleus; vLGN, ventral Lateral Geniculate Nucleus; dLGN, dorsal Lateral Geniculate Nucleus; VPM, ventral posterior-medial thalamic nucleus; LP, lateral posterior thalamic nucleus; Po, posterior thalamic nucleus.

3.3.2.5. Characterising cortico-subcerebral and cortico-cortical projections in the Rbp4-Cre::tdTomato, Ntsr1-Cre::tdTomato and Golli-τ-eGFP mouse lines

Fibres from each transgenic line also demonstrate specific patterning through the striatum and to the contralateral cortex (figure 3.11). Corticothalamic/ cortico-subcerebral Rbp4-Cre::tdTomato fibres cross the caudate putamen in a narrow dorsal

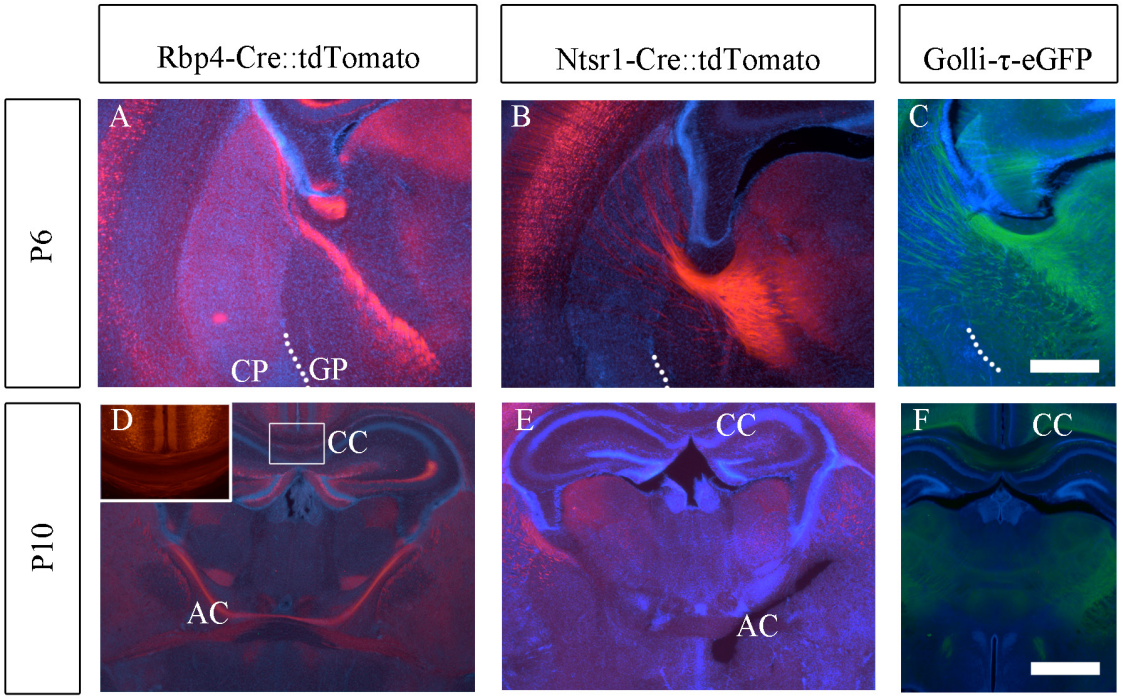

Figure 3.11. Subcortical and inter-hemispheric projection patterns from layer V (Rbp4-Cre::tdTomato), VI (Ntsr1-Cre::tdTomato) and VI and VIb (Golli-τ-eGFP). A. Layer V Rbp4-Cre::tdTomato fibres project through the caudate putamen of the striatum and narrow to project through the corridor before widening at the cerebral peduncle. Many fibres continue in the cerebral peduncle. Some fibres turn dorsally to enter the thalamus. There is also dense labelling of the caudate putamen. Ntsr1-Cre::tdTomato layer VI (B.) and Golli-τ-eGFP VI and VIb (C.) neurons project through the caudate putamen and narrow to project through the globus pallidus before reorienting to project dorsally into the TRN and thalamus. Dotted line represents boundary between caudate putamen and globus pallidus. D. Rbp4-Cre::tdTomato also labels layer V cortico-cortical projection neurons whose fibres cross the corpus callosum (CC) and the anterior commissure (AC). E. Ntsr1-Cre::tdTomato does not label fibres in the corpus callosum or anterior commissure. F. Golli-τ-eGFP also labels cross-callosal intracortical fibres. Abbreviations used: CP, caudate putamen; GP, globus pallidus; AC, anterior commissure; CC, corpus callosum. Scale bars= 500μm (A-C), 250μm (D-F).

band and thick bundles of fibres continue into the cerebral peduncle with other fibres turning dorsally from the cerebral peduncle to cross the TRN and enter the thalamus (figure 3.11 A). The narrow dorsal projection path of the layer V corticothalamic/ cortico-subcerebral layer V fibres contradicts previous work suggesting the cortico-subcerebral fibres project along a more ventral route to the cerebral peduncle compared to corticothalamic fibres (Deck et al., 2013). Rbp4-Cre::tdTomato also labels layer V corticostriatal (type II) neurons because the caudate putamen has denser red fluorescence that surrounding structures suggesting fibre arborisation here.

The layer VI fibres labelled by Ntsr1-Cre::tdTomato fan out to cross the caudate putamen (figure 3.11 B). Many fibres then join together in a thick bundle at the dorsal tip of the globus pallidus and project through the permissive corridor through which thalamocortical fibres can pass to the cortex (López-Bendito et al., 2006). Several smaller strands of Ntsr1-Cre fibres are visible projecting through the globus pallidus. The VI and VIb corticothalamic fibres labelled by Golli-τ-eGFP also project through the caudate putamen in a fanned out manner, many continue in this fanned out way through the globus pallidus and others make a thick bundle at the dorsal end of the globus pallidus (figure 3.11 C). These results suggest that the globus pallidus is not repulsive to corticothalamic fibres in the way it is to thalamocortical fibres (López-Bendito et al., 2006). This agrees with previous results showing corticothalamic fibres can traverse the globus pallidus (Deck et al., 2013).

Rbp4-Cre::tdTomato also labels layer V cortico-cortical projection neurons whose axons can be seen crossing the corpus callosum (CC) and the anterior commissure (AC) (figure 3.11 D). The presence of cross-callosal fibres in addition to corticofugal fibres suggests that Rbp4-Cre is expressed by both morphologically and electro-physiologically distinct layer V populations; type I and II. Type I project cortico-sub-cerebrally and corticothalamically, have tufted morphology, reside in layer Vb and fire in bursts. Type II project cross-callosally and cortico-striatally, remodel to a non-tufted morphology over development, reside in layer Va and have a non-bursting physiology

(Koester and O'Leary, 1992; Molnár and Cheung, 2006; Hattox and Nelson, 2007). That Rbp4-Cre::tdTomato labelling displays characteristics of both populations of projection neurons within layer V accounts for cells residing throughout layer V rather than clustering in either Va or Vb.

Ntsr1-Cre::tdTomato layer VI does not label fibres in the corpus callosum or anterior commissure (figure 3.11 E). Golli-τ-eGFP labels cross-callosal cortico-cortical fibres (figure 3.11 F) which may belong to the few layer V fibres which are labelled in the Golli-τ-eGFP line (Jacobs et al., 2007) or layer VI or VIb fibres which project to the contralateral hemisphere (Arimatsu et al., 1999a; Arimatsu et al., 1999b; Arimatsu and Ishida, 2002; Grant et al., 2012).

These results demonstrate that the three corticothalamic subpopulations have distinct but overlapping temporal and spatial patterns of ingrowth to the thalamus with layer VI and VIb projecting to first and higher order nuclei and layer V projecting only to higher order nuclei.

3.3.2.6. Development of layer VIb, VI and V corticothalamic fibres into the dLGN in the Golli-τ-eGFP, Ntsr1-Cre::tdTomato and Rbp4-Cre::tdTomato mouse

In the Golli-τ-eGFP mouse, eGFP positive VI and VIb fibres have reached the thalamus and entered the VPM from P2 (figure 3.12 A). Despite this, instead of entering the dLGN, which is immediately adjacent to the VPM, the eGFP positive fibres accumulate along the ventral border of the dLGN. At P4 fibres have accumulated at the ventral and medial borders of the dLGN (figure 3.12 B). At P6 some eGFP positive fibres begin to enter the ventral most part of the dLGN in anterior coronal sections (posterior sections remain mainly empty) (figure 3.12 C). At P8 eGFP positive fibres have progressed through the ventral half of the dLGN and by P10 the fibres have reached the dorsal/ lateral edge although they are still not as dense here as in more ventral regions of the dLGN (figure 3.12 D, E). At P12 there is only a lateral corner of the dLGN that is not filled with eGFP fibres (figure 3.12 F). By P14 fibres have fully entered the whole dLGN (figure 3.12 G). Mice do not have a laminar dLGN, in contrast to carnivores

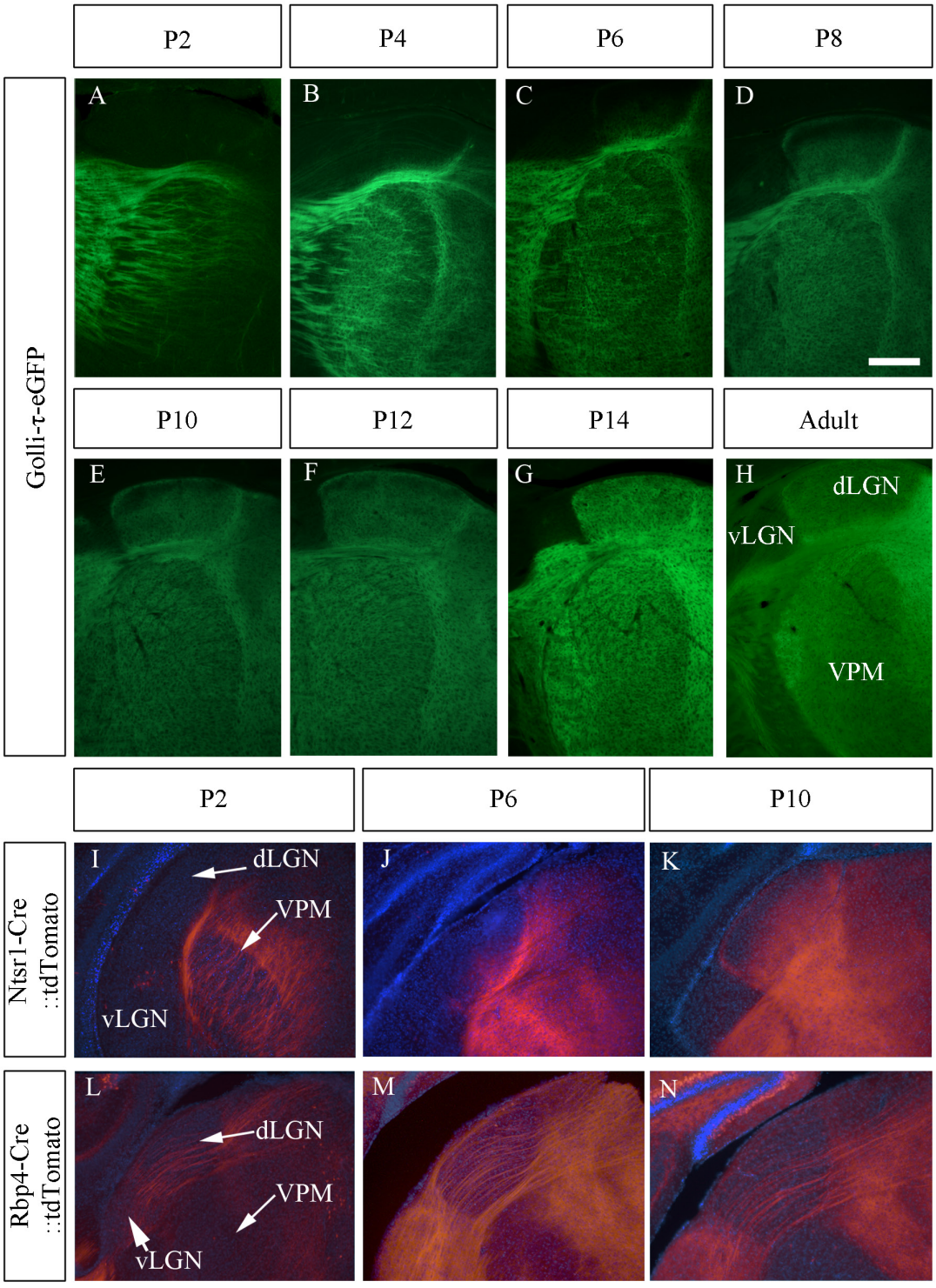

Figure 3.12. Development of layer VI, VIb and V corticothalamic fibres into the dLGN in the Golli-τ-eGFP, Ntsr1-Cre::tdTomato and Rbp4-Cre::tdTomato mice. A. eGFP positive VI and VIb fibres enter the VPM from P2 but accumulate along the ventral border of the dLGN through P4 (B.) until P6 (C.). D- G. Fibres project further into the dLGN from the ventral edge until P14 when fibres have fully entered the dLGN. I. Layer VI fibres labelled by Ntsr1-Cre::tdTomato begin accumulating at the ventral border of the dLGN by P2 and enter the dLGN by P6 (J.). By P10 fibres have progressed through the dLGN but have not yet filled it (K.). L. Layer V corticothalamic fibres labelled by Rbp4-Cre::tdTomato project through the dLGN by P2 and do not arbourise within it. M. By P6 these fibres are still present and two bundles are visible projecting along the dorso-lateral edge of the dLGN and the ventro-medial edge of the dLGN. N. By P10 fibres are still present running through the dLGN. Scale bars= 250μm (A-N).

and primates (Sherman and Guillery, 2006). Instead there is a patch in the dorsomedial corner of the dLGN which ipsilateral retinal projections synapse in, that accounts for 5-10% of the dLGN (Godement et al., 1984; Seabrook et al., 2013). There is no visible patterning of the eGFP positive VI and VIb corticothalamic fibres in or around this patch.

Layer VI fibres labelled by Ntsr1-Cre::tdTomato begin accumulating at the ventral border of the dLGN by P2 which is earlier than the eGFP positive layer VI and VIb fibres (figure 3.12 I). These Ntsr1-Cre layer VI fibres are visible entering the ventral dLGN by P6 (figure 3.12 J). This is slightly advanced compared to the eGFP positive VI and VIb fibres labelled by Golli-τ-eGFP. At P10 fibres have progressed through the dLGN but have not yet reached the dorsal edge- at this stage their progress is similar to that of the Golli-τ-eGFP positive VI and VIb fibres (figure 3.12 K). As discussed previously layer V corticothalamic fibres labelled by Rbp4-Cre::tdTomato project through the dLGN by P2 however they remain in thick fascicles and do not arborise within it (figure 3.12 L). By P6 these fibres are still present extending through the dLGN. At this age there are two thicker bundles which are visible projecting along the dorso-lateral edge and the ventro-medial edge of the dLGN (figure 3.12 M). By P10 fibres are still visible passing through the dLGN to more medial targets. No fibres are visible branching off to arborise in the dLGN (figure 3.12 N). These results directly demonstrate a waiting period of VI and VIb fibres outside the dLGN.

3.3.2.7. Anterior to posterior ingrowth of VI and VIb corticothalamic fibres to the dLGN in a sagittal section of the brain

Coronal sections showed that anterior sections of the dLGN were more filled by Golli-τ-eGFP or Nstr1-Cre::tdTomato positive fibres than posterior sections (data not shown). I therefore studied sagittal sections of the dLGN. These results showed that Golli-τ-eGFP positive VI and VIb fibres enter the dLGN from the ventral anterior-most pole first. At P6 eGFP positive fibres have entered the anterior half of the dLGN at the ventral edge and are directed towards the posterior/ dorsal corner of the nucleus (figure 3.13 A- A''). This projection pattern can be characterised by analysis of the pixel intensity along a

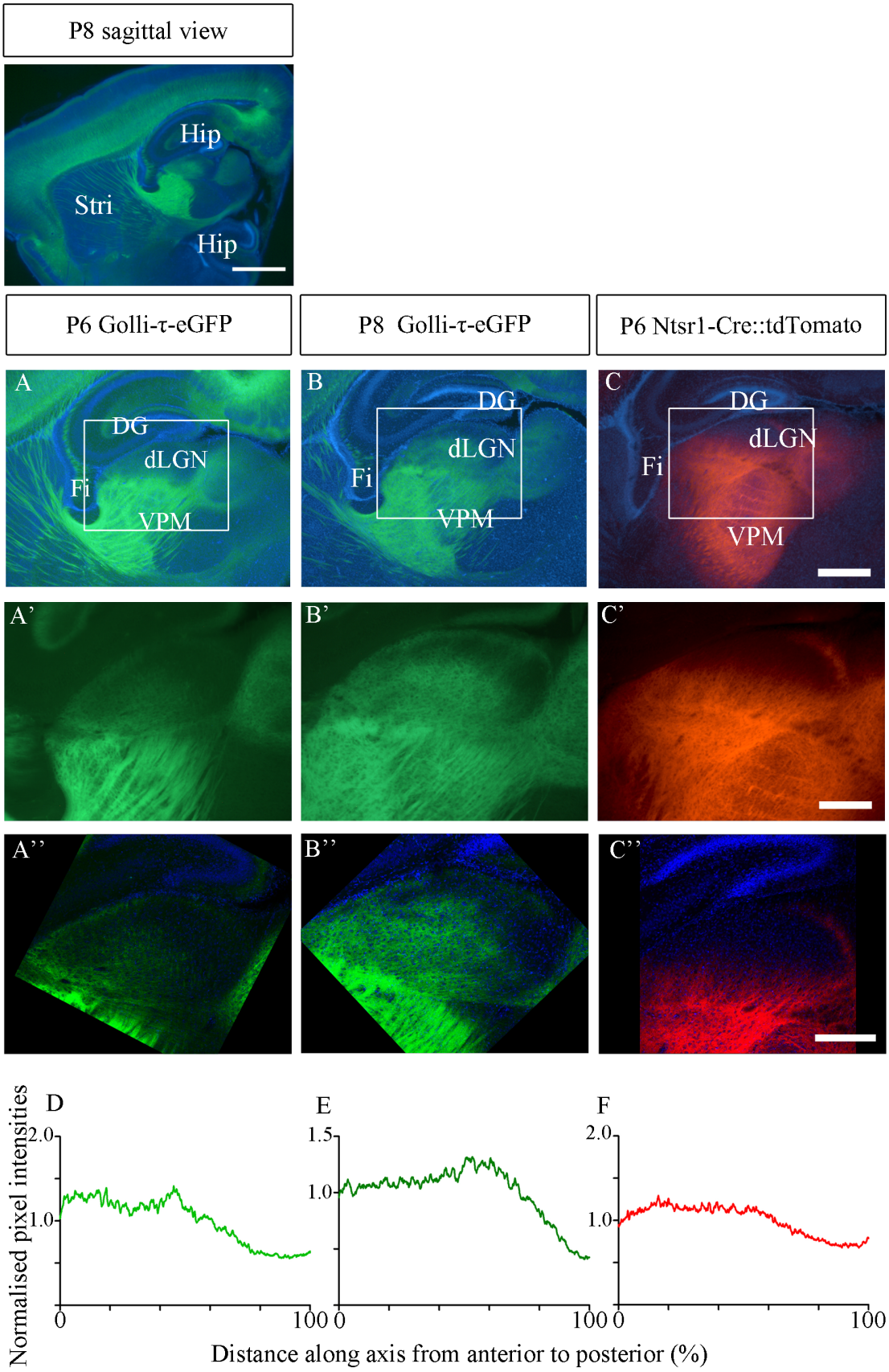
P8 sagittal view
Hip
Stri
Hip
P6 Golli-τ-eGFP
P8 Golli-τ-eGFP
P6 Ntsr1-Cre::tdTomato
A
DG
dLGN
Fi
VPM
B
DG
dLGN
Fi
VPM
C
DG
dLGN
Fi
VPM
A'
B'
C'
A''
B''
C''
D
E
F
Normalised pixel intensities
2.0
1.0
0
100
1.5
Distance along axis from anterior to posterior (%)

Figure 3.13. Parasagittal view demonstrates anterior to posterior ingrowth of corticothalamic fibres from layer VI and VIb to the dLGN. Golli-τ-eGFP positive layer VI and VIb fibres enter the dLGN from the ventral anterior-most pole. Sagittal section includes olfactory bulb and dorsal and ventral hippocampus. A - C. Parasagittal view of thalamus; white box denotes region of higher magnification images. A'- C'. At P6 eGFP positive fibres have entered the anterior half of the dLGN. By P8 the fibres have extended more caudally. The layer VI fibres labelled by Ntsr1-Cre::tdTomato enter from the ventral border of the dLGN and progress dorsally and posteriorly from there, by P6 fibres have reached the ventral portion of the nucleus. A"-C". Higher resolution confocal microscope image. E - G. Graphs showing the normalised intensity of pixels along line drawn from the anterior tip to the posterior end of dLGN. E. At P6 in the Golli-τ-eGFP mouse the pixel intensity values show the highest intensity of fluorescence from eGFP positive fibres is in the anterior 50% of the dLGN. F. By P8 the highest intensity of fluorescence from eGFP positive fibres is in the anterior ~70% of the dGN. G. In the Ntsr1-Cre::tdTomato mouse the highest intensity of tdTomato fluorescence is in the anterior part of the dLGN however there is not such a difference along the whole dLGN because fibres enter more from the ventral edge. Abbreviations used: Hip, hippocampus; Stri, striatum; DG, dentate gyrus; Fi, fimbria, dLGN, dorsal Lateral Geniculate Nucleus; VPM, ventrobasal nucleus. Scale bars= 1mm (top left sagittal schematic), 500μm (A, B, and C.), 250μm (A', B', and C'.), 100μm (A", B", and C".).

line drawn from the anterior pole to the posterior edge of the dLGN (figure 3.13 D). At P6 the fluorescence was highest in the anterior 50% of the dLGN and decreased over the next 30% and plateaued at the lowest intensity (least fluorescent fibres) for the final 20% of the dLGN (figure 3.13A). By P8 the eGFP fibres have reached a more posterior region but still do not reach the posterior most edge of the dLGN (figure 3.13 B-B''). The highest pixel intensity in the anterior 70% of the dLGN with a sharp decline in intensity in the posterior 30% of the dLGN (figure 3.13E).

The layer VI fibres labelled by Ntsr1-Cre::tdTomato have a distinct pattern from the Golli-τ-eGFP fibres in the sagittal section. The Ntsr1-Cre layer VI fibres enter from the ventral border of the dLGN (figure 3.13 C-C''). From the ventral edge the Ntsr1-Cre fibres progress dorsally and posteriorly from there. At P6 Ntsr1-Cre layer VI fibres have extended in through the ventral portion to the middle of the dLGN. Though they are denser in the anterior pole the Ntsr1-Cre::tdTomato positive layer VI fibres have a more ventral to dorsal pattern of ingrowth compared with the anterior to posterior ingrowth of the Golli-τ-eGFP layer VI and VIb fibres. This is also shown by the pixel analysis where the anterior to posterior profile of the intensities is flatter with a smaller decrease in intensity from anterior to posterior (figure 3.13F).

There are also differences in the patterning of the labelled fibres within the VPM. At P6 in sagittal sections of the Ntsr1-Cre::tdTomato line, barreloid patterning of the fibres is

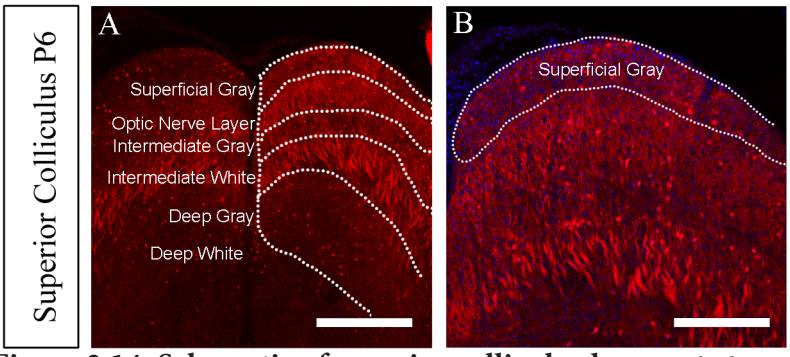

Figure 3.14. Schematic of superior colliculus layers. The layered structure of the superior colliculus includes the superficial grey layer, the optic nerve layer, the intermediate grey layer, the intermediate white layer, the deep grey layer and the deep white layer. Scale bars= 200μm (left) and 100μm (right).

already visible in the VPM (figure 3.13 C-C'). This patterning is not yet visible in the Golli-τ-eGFP line although they do show barreloid patterning later in development.

The distinctive ingrowth to the dLGN and fibre patterns in the VPM in the sagittal plane, along with the slightly different timings of ingrowth in the coronal plane suggest that Ntsr1-Cre::tdTomato and Golli-τ-eGFP label subtly different but overlapping layer VI projection neuron populations. Whilst Golli-τ-eGFP also labels VIb fibres this in itself is unlikely to explain such different patterns of ingrowth. This is because the Golli-τ-eGFP fibres appear to lag behind the Ntsr1-Cre fibres as they innervate the thalamus, if the difference were just due to the additional labelling of VIb one would not expect to see delayed fibre progression as the layer VI fibres would be expected to still grow at the same rate.

One possible explanation is that the two transgenic lines label overlapping but unique layer VI corticothalamic populations that have subtly distinct projections to the thalamus. A second option is that layer VI is made up of morphologically distinct populations which are independently labelled by Ntsr1-Cre and Golli-τ-eGFP. Scanziani and colleagues showed that Nstr1-Cre labels ~65% of layer VI neurons and that the remaining 35% are morphologically distinct from those which are labelled (Olsen et al., 2012). Quantification of the Golli-τ-eGFP mouse shows that 45% of layer VI cells are eGFP positive (Jacobs et al., 2007). The Ntsr1-Cre negative population of layer VI neurons and the eGFP positive population of layer VI neurons may overlap. Whilst Olsen et al characterise the dendrites of the Ntsr1-Cre positive and Cre negative neurons

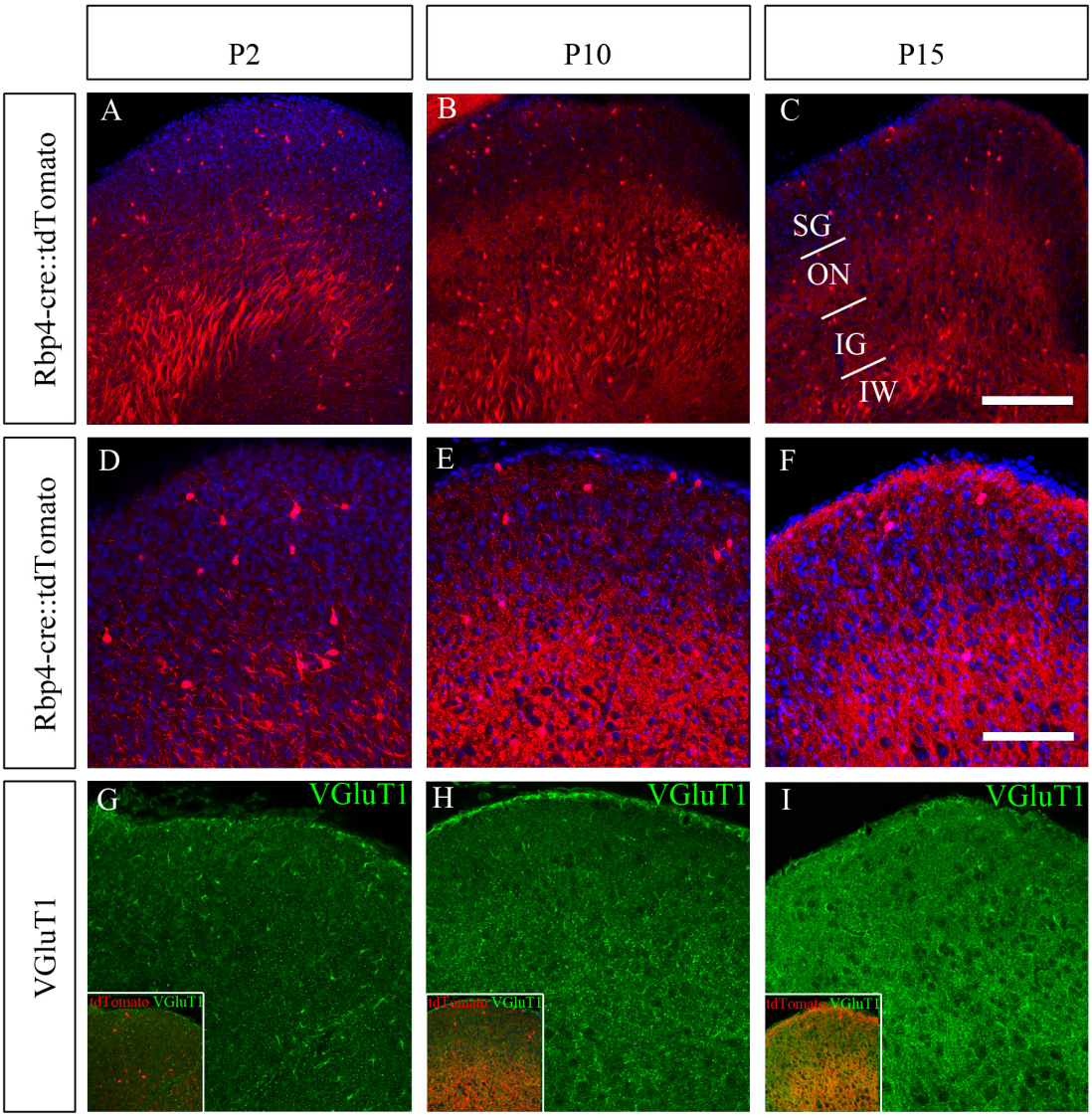

Figure 3.15. Rbp4-Cre::tdTomato positive layer V fibre ingrowth to the superior colliculus and maturation of VGluT1 positive synapses over development. A-F. At P2 layer V fibres run in thick bundles in the intermediate white and have reached the optic nerve layer of the superior colliculus. The fibres have not reached the dorsal border of the optic nerve layer and have not yet entered the superficial grey layer. By P10 the Rbp4-Cre::tdTomato positive fibres more densely innervate the optic nerve layer and have reached the superficial grey layer. G. At P2 mature cortical synapse marker VGluT1 immunohistochemistry shows little staining indicating the cortico-collicular synapses are not functionally mature. VGluT1 staining is visible by P10 (H.) and becomes much denser by P15 (I.). Abbreviations used: SG, superficial grey; ON, optic nerve layer; IG, intermediate grey layer; IW, intermediate white layer. Scale bars= 100µm (A-C), 50µm (D-I).

they did not characterise their axons so we do not know if the Cre negative neurons also project to the thalamus.

These two possibilities could be explored by breeding the Ntsr1-Cre line with Golli-τ-eGFP and performing immunohistochemistry for Cre thus labelling both populations and enabling quantification of the overlap.

3.3.2.8. Layer V Rbp4-Cre::tdTomato fibre projection to the superior colliculus over development

Layer V fibres have been demonstrated to project to the superior colliculus in several species arriving E17.5- E18.5 (De Carlos and O'Leary, 1992; Clascá et al., 1995). Therefore I characterised the development of layer V fibres labelled by tdTomato in the Rbp4-Cre mouse into the superior colliculus which is a layered structure in the midbrain (figure 3.14).

By P2 tdTomato positive layer V fibres have reached the superior colliculus (figure 3.15 A). The tdTomato positive fibres run in thick bundles in the intermediate white layer and have reached the optic nerve layer. At this age they have not yet entered the retino-recipient superficial grey layer (figure 3.15 D). By P10 dense tdTomato positive fibres are visible in the superficial grey layer of the superior colliculus (figure 3.15 B, E). By P15 this innervation is even denser (figure 3.15 C, F). There are some cell bodies in the Rbp4-Cre::tdTomato superior colliculus, therefore a fraction of the labelling might have originated from these cells, rather than the dominant layer V corticofugal projections.

In order to assess the maturity of the cortico-collicular fibres in the superficial grey I performed immunohistochemistry for VGluT1 (figure 3.15 G- I). VGluT1 is a marker for mature cortical synapses (Nakamura et al., 2005; Wilson et al., 2005). The results showed that at P2 there is very little VGluT1 staining in the superior colliculus suggesting any layer V fibres present are not synaptically mature (figure 3.15 G). By P15 the VGluT1 staining is denser suggesting the layer V synapses are functionally mature (figure 3.15 I).

3.4. Discussion

In this chapter I have characterised the specific and unique ingrowth patterns of distinct corticothalamic and cortico-collicular populations from layers V, VI and VIb to specific thalamic nuclei.

3.4.1. Laminar specific retrograde labelling in the cortex from the VPM

I first used retrograde carbocyanine dye tracing from the VPM to study the laminar specific timing of corticothalamic fibres innervating the thalamus. At the earliest age studied (E18.5) very few cells are back-labelled thus few projections have reached the VPM. This could indicate that the cells back-labelled at E18.5 are pioneers; navigating the route and entering the thalamus early whilst the brain is smaller and acting as guidance for later corticothalamic axons. All three layers have some cells back-labelled from the VPM at this age suggesting that all three subpopulations may have neurons which act as pioneers. To fully establish whether different fibre populations pioneer each segment of the route one would need to trace from various points along the route including the internal capsule and TRN. Previous research suggests that VIb projections pioneer the route from cortex to the internal capsule but VI and VIb projections catch up as fibres accumulate close to the thalamus (McConnell et al., 1989; Kim et al., 1991; De Carlos and O'Leary, 1992; McConnell et al., 1994; Molnár et al., 1998a).

My retrograde tracing shows that layer VIb cells can be back-labelled from thalamic DiI crystal placement as early as E18.5 confirming previous results (Molnár and Cordery, 1999). Although sparse, back-labelled cells in VIb are present at all ages studied up to P10. This is despite previous findings which suggest that layer VIb neurons have mainly died off by this age (Allendoerfer and Shatz, 1994; Price et al., 1997). At P2 my results show that a substantial majority of back-labelled cells reside within layer V. Then from P4-P10 the majority of cells back-labelled from the VPM are in layer VI.

My results in the mouse suggest there are three waves of ingrowth of corticothalamic fibres to the thalamus. Initially there is sparse ingrowth from all three layers; this is followed by a wave of layer V ingrowth and a later wave of layer VI ingrowth. This pattern is similar to previous results in the hamster and rat; initially a very small population of VI and VIb cells are back-labelled before there is a large increase in layer V labelling until finally VI is strongly labelled (Miller et al., 1993; Molnár and Cordery, 1999). My results are thus subtly distinct from those in ferrets in which there is extensive layer V ingrowth prior to the remaining layer VI and VIb projection entering

the thalamus (Clascá et al., 1995) or those in which the earliest fibres to project to the thalamus are exclusively from layer VIb (McConnell et al., 1989; De Carlos and O'Leary, 1992; Auladell et al., 2000).

Carbocyanine dye labelling and other retrograde tracing methods have been used extensively however the precise order and pattern of corticothalamic entry and growth towards the thalamus remained contested within the literature. My results provide evidence in favour of three waves of corticothalamic ingrowth however this model does not unify previous results thus confirming the need for more sensitive methods to properly characterise this ingrowth by cortical subpopulation and target thalamic nucleus. I therefore chose to use three novel transgenic mouse lines to selectively label the cell bodies and neurites of the three corticothalamic subpopulations.

3.4.2. Ingrowth of layer V, VI and VIb, specifically labelled by fluorescent proteins

I have used these recently developed transgenic lines to clarify the distinctive patterns of ingrowth of projections from layer V, VI and VIb to thalamic nuclei. Not only can we distinguish the patterning of layer V corticothalamic fibres from layer VI/VIb fibres but we can also distinguish subtly different corticothalamic projection populations within layer VI and VI/VIb. These distinct patterns of ingrowth were previously difficult to resolve because of the inherent difficulties with dye tracing techniques. These difficulties arise from several characteristics of the tracers used. Firstly many tracers are propagated along axons in both a retrograde and anterograde direction thus meaning any tracers placed in the thalamus or cortex would label all fibres from both populations (Honig and Hume, 1989; Godement et al., 1987). Secondly tracers placed within the cortex label all cells and therefore cannot distinguish between the three layers (V, VI and VIb). These transgenic lines are selective to the corticothalamic subpopulations and label their cells and fibres thus allowing a detailed description of the different

populations and their ingrowth to the thalamus. Indeed the accuracy of labelling in these transgenic lines allowed me to speculate as to the source of the variation in the tracing literature.

Firstly my results from Rbp4-Cre, Ntsr1-Cre and Golli-τ-eGFP reveal that developing fibres from layer V, VI and VIb innervate different thalamic nuclei. As early as P2, layer V fibres exclusively target higher order thalamic nuclei; merely coursing through the more lateral first order nuclei. Layer VI and VIb fibres on the other hand innervate both, entering the lateral first order nuclei early and the higher order nuclei only a couple of days later.

This distinct ingrowth pattern may explain the variability in retrograde tracing experiments. Retrograde tracers placed in a nucleus which has different ingrowth from the different layers (for example the VPM) would be taken up differently between the two populations. Layer VI fibres are visibly denser in the VPM than layer V fibres and therefore more layer VI fibres are likely to take up tracer. As such layer VI fibres may be over-estimated in studies with the tracer placed in the VPM such as mine. In addition to genuine differences between species studied, the effect of the density of fibres within the nuclei labelled from could contribute to the variability within the literature.

Secondly my results show uniform ingrowth within the VPM; specifically no population innervates one part of the VPM more densely than another. However, my carbocyanine dye retrograde tracing results showed variable back-labelling from different regions of the VPM; layer VI fibres were proportionally more labelled from the dorsolateral VPM. Given the uniform ingrowth of the fluorescent protein labelled fibres it is unclear how the difference in back-labelling of cortical cells between the middle and dorsolateral VPM arose. Dorsolateral regions of the VPM are very close to the external medullary laminar where VI and VIb fibres accumulate before entering the dLGN. Thus crystals of carbocyanine dyes in this dorsolateral region of VPM may therefore also label these layer VI fibres.

Cortical layer specific ingrowth to the thalamus and superior colliculus

My results also show that the layer V corticotectal fibres which innervate superior colliculus are also labelled in the Rbp4-Cre::tdTomato line. My results demonstrate that the layer V fibres reach the superficial grey early (in concurrence with previous results (De Carlos and O'Leary, 1992; Clascá et al., 1995)) however the fibres continue to increase in density in the second postnatal week.

3.4.2.1. Implications from selective labelling of the three corticothalamic populations

My study is one of the first to demonstrate that these complementary patterns of ingrowth are present as early as P2 when the different populations of corticothalamic fibres first reach the thalamus. This early patterning suggests that intrinsic guidance mechanisms within the thalamic nuclei may be specified early. For example defining first and higher order specific expression of guidance cues would direct V, VI and VIb fibres to the appropriate order of thalamic nuclei. The different corticothalamic subpopulations may also be differently responsive to the guidance mechanisms. So far cues determining the guidance of corticothalamic fibres to the different thalamic nuclei have not been elucidated but recent work has distinguished molecular characteristics of specific thalamic nuclei some of which may contribute to such guidance (Brooks et al., 2013; Pouchelon et al., 2014a).

In this regard my results demonstrate the importance of recognising the difference between corticothalamic subpopulations. These subpopulations are likely to undergo different guidance mechanisms en route to the thalamus and perhaps different synaptic plasticity and refinement mechanisms (Mitrofanis and Baker, 1993; Grant et al., 2012; Deck et al., 2013). These lines which distinguish the different corticothalamic populations will aid future research to distinguish between mechanisms which are relevant for all three populations and mechanisms which only impact on an individual population.

One question these transgenic mouse lines have not been able to address is the temporal pattern of the three distinct populations from exiting the cortex, traversing the internal

capsule, to arriving at the thalamus. The Golli-τ-eGFP is suitable for embryonic tracing of the VI and VIb fibres through the internal capsule (Jacobs et al., 2007). However, Rbp4-Cre::tdTomato and Ntsr1-Cre::tdTomato cannot be used for very early embryonic labelling as Cre mediated recombination does not robustly label either population of neurons and fibres by E16.5/ E17.5. Therefore the majority of the corticothalamic progression towards the thalamus has occurred before the labelling can be used to visualise the layer specific axons.

3.4.2.2. Innervation of the TRN by corticothalamic subpopulations

In addition to differential guidance cues there may be distinct cues which control the formation of collateral branches.

Ntsr1-Cre::tdTomato and Golli-τ-eGFP confirmed the presence of previously well documented collaterals from layer VI innervating the TRN. Previous research suggests that layer V does not innervate the TRN (Hoogland et al., 1987; Rouiller et al., 1998; Rouiller and Welker, 2000; Kakei et al., 2001). However this work was based on single cell reconstruction (Rouiller et al., 1998; Kakei et al., 2001) or tracing which labelled both layer V and VI fibres (Hoogland et al., 1987) and as such may have been unable to resolve layer V fibres within the TRN. Furthermore, despite the results from tracing experiments, research in the macaque has shown two distinct bouton types synapsing on the same TRN axon one of which has layer V characteristics (Zikopoulos and Barbas, 2006). The Rbp4-Cre::tdTomato mouse labels more fibres than single cell labelling and is selective for layer V unlike early tracing methods and as such is more sensitive to detect layer V collateral projections to the TRN. My results demonstrate dense layer V fibres in the zona inserta but not in TRN. As such my results convincingly demonstrate that layer V projection neurons do not have collateral branches innervating the TRN.

3.4.2.3. Cortical area specific labelling

Due to the expression of tdTomato in all Cre expressing cells when Ntsr1-Cre is crossed with the Ai14 tdTomato line, our results cannot distinguish which cortical areas project to which thalamic nuclei. However, injection of an AAV floxed tdTomato reporter into

specific cortical areas can be used to show this detail (Olsen et al., 2012). AAV floxed tdTomato injection into primary visual cortex labels only V1 corticothalamic Ntsr1-Cre neurons. These neurons were demonstrated to densely innervate dLGN and LP but did not project to Po, VPM or vLGN (Olsen et al., 2012). The Ntsr1-Cre::tdTomato positive fibres densely innervating the other thalamic nuclei in our transgenic cross must come from other cortical areas.

3.4.2.4. Temporal regulation of ingrowth to the dLGN

My analysis of the layer VI line (Ntsr1-Cre::tdTomato), and the VI/VIb line (Golli-τ-eGFP), demonstrate layer VI corticothalamic fibres delay before entering the dLGN, also previously published (Jacobs et al., 2007; Grant et al., 2012; Seabrook et al., 2013). The fibres arrive at the border of the dLGN two days after birth but accumulate outside the dLGN for several days before growing into it between P6 and P8. A similar delay has been previously described in foetal rhesus monkey using anterograde tracing from the cortex to the dLGN (Shatz and Rakic, 1981). In this paper Shatz and Rakic compare the delay of the corticogeniculate ingrowth to the dLGN to the waiting period that geniculocortical axons undergo within the layer VIb (the subplate) of the cortex prior to growing into the cortex. Whilst this highly regulated timed ingrowth of VI and VIb corticothalamic fibres to the dLGN is developing, the retinal ganglion cell axons have innervated the dLGN and are propagating spontaneous activity to the dLGN (Godement et al., 1984; Mooney et al., 1996; Weliky and Katz, 1999). The ingrowth of the corticothalamic fibres from ventral to dorsal dLGN is opposite of retinal ganglion cell ingrowth which densely innervates the dorsal edge before projecting ventrally (Godement et al., 1984; Seabrook et al., 2013).

3.4.2.5. Conclusion

In this chapter I have described the precise pattern of development of three distinct corticothalamic populations from layer V, VI and VIb to specific thalamic nuclei. The use of novel transgenic mouse lines to perform these experiments has enabled me to answer questions regarding the development and layer specific innervation of various nuclei of the thalamus which have been of interest for some time but were not

resolvable until now. In addition to nucleus specific ingrowth I have also demonstrated that there is specific temporal regulation of the layer VI and VIb corticothalamic fibres to the dLGN.

4 The role of retinal input on corticofugal development

4.1. Introduction

Layer VI and VIb corticothalamic input enters the dLGN over the first 10 postnatal days in the mouse (chapter 3 and (Grant et al., 2012; Jacobs et al., 2007; Seabrook et al., 2013)). I have shown that both the Golli-τ-eGFP labelled VI and VIb fibres and the Ntsr1-Cre::tdTomato labelled VI fibres do not begin growing into the dLGN until P4 filling the dLGN by P14 (chapter 3 and (Grant et al., 2012; Jacobs et al., 2007; Seabrook et al., 2013)). Before growing into the dLGN, the layer VI and VIb fibres accumulate outside the dLGN for several days (P2-P6). This delay to their ingrowth suggests the development of corticothalamic innervation of the dLGN is specifically temporally regulated.

The retinal ganglion cell fibres which provide driver input to the dLGN enter by E18.5 and functionally innervate the dLGN by P2 (Godement et al., 1984; Ackman et al., 2012), several days prior to the ingrowth of layer VI and VIb corticogeniculate fibres. The superior colliculus also receives input from both the retina and the cortex (layer V specifically) (De Carlos and O'Leary, 1992; Clascá et al., 1995). The retinal fibres reach the superior colliculus by E16.5 and have mature functional synapses by P3, before the layer V corticothalamic fibres enter the superficial grey layer of the superior colliculus (Godement et al., 1984; Ackman et al., 2012).

This early retinal innervation of the dLGN and superior colliculus is prior to visually evoked activity because the eyes do not open until 12 days after birth. Despite the lack of visually evoked activity during this period, there are cholinergic spontaneous waves of activity which propagate across the retina (Galli and Maffei, 1988; Meister et al., 1991; Wong et al., 1993; Feller et al., 1996; Penn et al., 1998; Bansal et al., 2000; Ackman et al., 2012). These waves of activity are transmitted throughout the visual system to the dLGN, from where they are transmitted to the visual cortex, and to the superior colliculus (Mooney et al., 1996; Weliky and Katz, 1999; Ackman et al., 2012).

These spontaneous waves provide early peripheral input which is well established to play an important role in the developing circuits of the nervous system, including the thalamocortical circuits (Sur and Leamey, 2001; Yamamoto and López-Bendito, 2012).

Given the coincidence of the propagation of spontaneous retinal activity to the dLGN by retinal ganglion cells and the highly temporally regulated ingrowth of layer VI and VIb fibres to the dLGN, I chose to investigate whether retinal input to the dLGN was involved in regulating corticothalamic ingrowth from layer VI and VIb by manipulating retinal input by removing one eye or abolishing spontaneous waves using epibatidine injections.

Retinal input drives the spiking activity of dLGN relay neurons therefore the loss of retinal input represents the loss of the main driver input to the dLGN. Layer VI and VIb input to the dLGN is only modulatory, whereas layer V, which normally innervates exclusively higher order thalamic nuclei, provides driver input to thalamic relay cells (Sherman and Guillery, 1998; Rouiller and Welker, 2000; Reichova and Sherman, 2004). Given that monocular enucleation deprives the dLGN neurons of driver input I then investigated whether enucleation could lead to layer V fibres rewiring to innervate the first order dLGN.

As retinal waves are also propagated to the superior colliculus I analysed whether monocular enucleation affects ingrowth of layer V corticothalamic fibres to the superior colliculus.

4.1.1. Aims of chapter 4

1. Test whether retinal input to the dLGN regulates layer VI and VIb fibre ingrowth to the dLGN.

    a. I first use monocular enucleation on the Golli-τ-eGFP line and analyse the ingrowth of the layer VI and VIb fibres into the dLGN.

    b. Next, to target retinal activity specifically I use intraocular injections of cholinergic agonist epibatidine which disrupts spontaneous retinal

activity input to the dLGN without removing the retinal axons (Penn et al., 1998; Rebsam et al., 2009; Sun et al., 2008; Rebsam et al., 2012; Ackman et al., 2012).

c. I then perform monocular enucleation on the Ntsr1-Cre::tdTomato line to analyse the effect on ingrowth of the layer VI fibres into the dLGN.

d. I will also test whether Golli-τ-eGFP VI and VIb fibre ingrowth to the visual sector of the TRN is affected after monocular enucleation.

2. Assess the impact that loss of driver input to the dLGN has on layer V corticothalamic fibres which normally project to higher order thalamic nuclei only

    a. Using monocular enucleation on the Rbp4-Cre::tdTomato line, I will assess whether layer V fibre patterning within the thalamus is affected over development. This includes looking at whether there is aberrant ingrowth of layer V fibres to the dLGN and whether layer V fibre patterning within the LP and Po is affected.

3. Assess the role retinal input has on the ingrowth of layer V corticotectal fibres which innervate the superficial grey layer of the superior colliculus.

    a. Following monocular enucleation I will assess the ingrowth of layer V fibres to the superficial grey layer of the superior colliculus.

4.2. Methods

Animal husbandry, tissue collection and image acquisition as described in general methods chapter 2.

In order to refer to distinct regions of the dLGN I define some anatomical reference terminology for simplicity. The use of the terms dorsal, ventral, medial and lateral refer to positions in the dLGN as shown in figure 4.1 A.

4.2.1. Monocular enucleation- surgical removal of the left eye

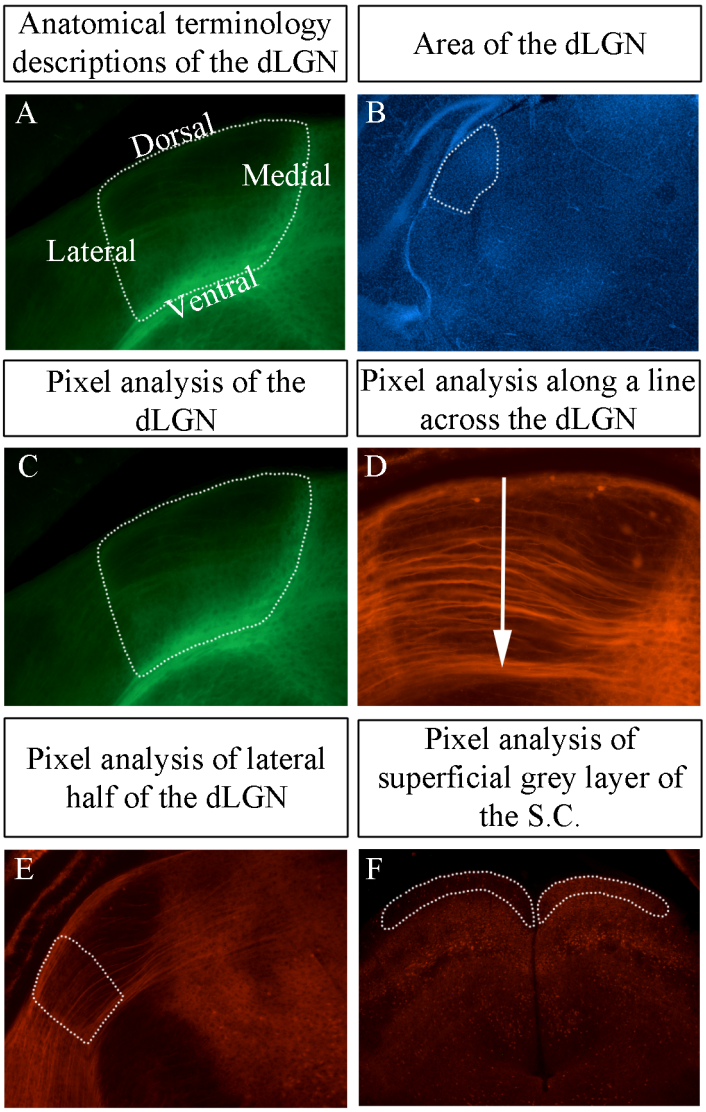

Figure 4.1. Outlines used for a¬nalysis of the dLGN. A. Anatomical terminology used to describe the regions of the dLGN throughout chapter. B. Outline of the dLGN guided by DAPI counterstain for area analysis on 5x images. C. The dLGN outline for pixel analysis in Golli-τ-eGFP and Ntsr1-Cre::t-dTomato using 20x objective. D. Line drawn across the dLGN from the dorsal edge of the dLGN (start of arrow) to the ventral edge (end of arrow) using 20x objective. E. Outline of lateral half of dLGN for pixel analysis in Rbp4-Cre::tdTomato using 5x objective. F. Outline of the superficial grey layer of the superior colliculus for pixel analysis in the Rbp4-Cre::tdTomato using 5x objective.

In order to assess the role retinal input plays in the developing corticothalamic circuit I performed monocular enucleation and then assessed the ingrowth of layer VI and VIb (Golli-τ-eGFP), VI (Ntsr1-Cre::tdTomato) and V (Rbp4-Cre::tdTomato) fibres to the dLGN and superior colliculus.

P0 mouse pups were anaesthetised by hypothermia on ice for 2-3 minutes until unresponsive to pressure on the rear paw. A 5mm stab microsurgical-knife was used to make a small incision in the skin over the left eye, the incision was opened slightly

using forceps. Sharp forceps were used to separate the eye from surrounding tissue and behind the eye the optic nerve was pinched off with the forceps. The entire left eye including lens, retina and retinal pigmented epithelium, was removed through the incision by forceps.

After surgery animals were warmed in a temperature controlled incubator until pink and moving normally before all pups were returned to the home cage. Animals were killed at P2, P4, P6, P8 and P10 by administration of pentobarbital and transcardial perfusion with 0.1M PBS. Brains were dissected out and post-fixed overnight in 4% PFA. Brains were stored in 0.05% PBSA. Brains were set in 4% agarose and sectioned coronally to 50µm on the vibrating microtome before analysis.

Strain	Condition	Age	n	Litters
Golli-τ-eGFP	Monocular Enucleation on P0	P2	3	1
Golli-τ-eGFP	Monocular Enucleation on P0	P4	6	2
Golli-τ-eGFP	Monocular Enucleation on P0	P6	6	2
Golli-τ-eGFP	Monocular Enucleation on P0	P8	4	1
Golli-τ-eGFP	Monocular Enucleation on P0	P10	5	1
Ntrs1-Cre::tdTomato	Monocular Enucleation on P0	P4	3	1
Ntrs1-Cre::tdTomato	Monocular Enucleation on P0	P6	4	1
Ntrs1-Cre::tdTomato	Monocular Enucleation on P0	P8	1	1
Rbp4-Cre::tdTomato	Monocular Enucleation on P0	P4	3	2
Rbp4-Cre::tdTomato	Monocular Enucleation on P0	P6	4	1
Rbp4-Cre::tdTomato	Monocular Enucleation on P0	P8	3	1

Table 4.1. Number of animals for each monocular enucleation experiment. Note different litters were used for each age apart from P4 Rbp4-Cre::tdTomato included one pup from the same litter as the P8 Rbp4-Cre::tdTomato brains.

4.2.2. Intraocular injections of epibatidine or sterile physiological saline

To distinguish the role of retinal activity from retinal axon presence in the target tissue I performed intraocular injection of cholinergic agonist epibatidine or sterile physiological saline and then assessed the ingrowth of Golli-τ-eGFP layer VI and VIb corticothalamic fibres into the dLGN.

1mM epibatidine (epibatidine dihydrocholoride hydrate, Sigma Aldrich, E1145; dissolved in sterile physiological saline) was injected daily from P0 to P5. 0.5µl was injected at P0, increasing by 0.1µl per day until 1µl at P5. Pups were anaesthetised

using hypothermia as above and kept ice cold for the duration of surgery. A small incision over the anterior half of the left eye was made using a 5mm stab microsurgical-knife and using a platinum wire a small hole was made in the sclera in the anterior quarter of the eye, avoiding the lens. Using a stereotaxic frame, a10µl Hamilton Syringe (Hamilton Company USA, Nevada, USA) filled with epibatidine was guided through the hole into the vitreous humour. The epibatidine was injected steadily over 60 seconds to prevent mechanical disruption of the retina or eye. The syringe was removed and the eyelid was gently pressed closed using sterile cotton-buds. The injection procedure was repeated daily until P5. To reduce damage the eye was reopened at the line of the first cut and the syringe was inserted through the same hole in the sclera which could be identified because of a hole in the retinal pigmented epithelium. Control litters were injected with sterile physiological saline using identical procedure.

After surgery animals were warmed until pink and moving normally before being returned to the home cage. Animals were killed at P6 by cervical dislocation. Brains were dissected out and post-fixed overnight in 4%PFA. Brains were set in 4% agarose and sectioned coronally at 50µm on the vibrating microtome before analysis.

Experiment	Age	n	Number of litters
Epibatidine injection	P6	7	3
Sham injections	P6	8	3

Table 4.2. Number of animals used for each intraocular injection experiment. Note different litters were used for the epibatidine injections and the sham sterile physiological saline injections.

4.2.3. dLGN area analysis after peripheral manipulation

The area of the dLGN was outlined and measured in ImageJ. Analysis was done blind to experimental condition. Minimum 3 images were measured per hemisphere and images were well-matched for anterior/posterior position. The following border criteria were used: the lateral border of the dLGN is defined by the reduced DAPI cell density between dLGN and vLGN. The ventral border is defined by a band of reduced cell density between the dLGN and VPM. The medial border was defined as the curved reduction in cell density between the dLGN and the LP. The dorsal border was defined as the edge between the dLGN tissue and the lateral ventricle (for representative outline see figure 4.1 B). The areas for several images of one hemisphere were averaged to

generate an area for the dLGN in that hemisphere. A paired t-test using GraphPadPrism was used to compare the area of the control dLGN and the dLGN receiving input from the manipulated eye. In all graphs *= significant at p=0.05, **= significant at p=0.005, ***= significant at p<0.0005.

4.2.4. Proportional pixel analysis: quantification of fluorescent fibre ingrowth to the dLGN following retinal manipulation

The ingrowth of fluorescent fibres to the dLGN was quantified by analysing the intensity profiles of pixels within the dLGN. Anti-GFP immunohistochemistry was performed on all Golli-τ-eGFP sections to amplify the eGFP signal (see section 4.2.9 for immunohistochemistry details).

The dLGN contralateral to the manipulated (removed/ injected) eye was compared to the dLGN ipsilateral to the manipulated eye of the same brain (as an intra-animal control). Analysis was done blind to experimental condition. To quantify the fluorescent fibre ingrowth to the dLGN, I developed a method of measuring the intensity profiles of the pixels within the dLGN. This analysis was based on previous methods in the literature (Rebsam et al., 2009).

A minimum of three sections were analysed per hemisphere per brain. Images were standardised for intensity using fluorescence within the VPM to normalise between the two conditions. The intensity of GFP/ tdTomato fluorescence was measured along a 100µm line in the VPM. Using the ImageJ linear brightness/contrast adjustment tool the brightness of the image was adjusted to standardise the fluorescence intensity within the VPM thus ensuring standard fluorescence intensity across all images. Images were then converted to grey scale. In Adobe Photoshop the dLGN was selected using the following criteria (see figure 4.1 C for representative outline). The lateral border of the dLGN defined by the clear ‘intralaminar’ GFP or tdTomato bundle between dLGN and vLGN, the ventral border was the thick GFP/tdTomato positive bundle between the dLGN and VPM, the medial border was defined as the curved GFP/tdTomato bundle between the dLGN and the Po and the dorsal border was defined as the edge between

the dLGN tissue and the lateral ventricle. In the ventral border the line selection tool was drawn through the mid-point of the GFP/tdTomato bundle which is accumulating at the ventral border of the dLGN (figure 4.1C).

The pixel intensity data was captured using the Record Measurements tool in Adobe Photoshop, and exported to Excel. This tool records the grey scale intensity value of every pixel thus quantifying the number of pixels at every grey scale intensity value from 0-255. Using this data the frequency of pixels above the threshold was calculated for every intensity threshold (0-255). To normalise for the area of the dLGN, this data was divided by the total number of pixels in the dLGN area. This generates a proportional value; the proportion of pixels within the dLGN which are above any grey scale intensity threshold. The data from the images were averaged to generate the intensity values for that hemisphere.

Statistical comparisons were performed at every 10th intensity threshold (10- 120) for the thresholds above which the proportion of pixels drops from 1 and below which the proportion of pixels is above 0. Statistical comparisons were performed in GraphPadPrism. Statistical comparisons were performed on all thresholds displayed with error bars on the graphs. For each experiment a bar graph was produced comparing the intensity values at one threshold. The threshold value for bar chart comparison at each age was chosen to be within the first third to the first half of the curve after the proportion of pixels begins to drop from 1. This was to demonstrate the difference between the dLGN and takes into account differing fluorescent intensities at different ages.

4.2.5. Pixel intensity analysis along a line from the dorsal to ventral edge of the dLGN of the Rbp4cre::tdTomato after monocular enucleation

In order to characterise the patterning of Rbp4-Cre::tdTomato layer V fibres within the dLGN the intensity value of pixels on a line drawn from the dorsal edge to the ventral edge was assessed. Images were standardised for intensity as above.

A 300µm line was drawn from the dorsal edge of the dLGN to the ventral edge, perpendicular to the dorsal edge (figure 4.1D). The plot profile tool in ImageJ was used to record the intensity value of pixels every 0.5µm along this line. The pixel intensity values were plotted.

Strain	Experiment	Age	n	Litters
Rbp4-Cre::tdTomato	Monocular Enucleation on P0	P4	3	2
Rbp4-Cre::tdTomato	Monocular Enucleation on P0	P6	4	1
Rbp4-Cre::tdTomato	Monocular Enucleation on P0	P8	3	1

Table 4.3. Number of Rbp4-Cre::tdTomato positive brains used for this experiment at each age. Note these are the same brains used for analysis referred to in section 4.2.6 and 4.2.7.

4.2.6. Proportional pixel analysis: quantification of fluorescent fibre ingrowth to the lateral half of the dLGN following monocular enucleation

In the Rbp4-Cre::tdTomato mouse, proportional pixel analysis was performed in the lateral corner of the dLGN. The process was as described above in section 4.2.4 with the following adjustment: the lateral dLGN was outlined as shown in figure 4.1E. The dorsal, lateral and ventral edge of the dLGN were defined as above. To outline just the lateral half of the dLGN, the 'medial' outline was done halfway between the lateral edge of the nucleus and the medial edge of the nucleus.

Strain	Experiment	Age	n	Litters
Rbp4-Cre::tdTomato	Monocular Enucleation on P0	P4	3	2
Rbp4-Cre::tdTomato	Monocular Enucleation on P0	P6	4	1
Rbp4-Cre::tdTomato	Monocular Enucleation on P0	P8	3	1

Table 4.4. Number of Rbp4-Cre::tdTomato positive brains used for this experiment at each age. Note these are the same brains used for analysis referred to in section 4.2.5 and 4.2.7.

4.2.7. Proportional pixel analysis: quantification of fluorescent fibre ingrowth to the superficial grey layer of the superior colliculus following monocular enucleation

In order to test whether layer V corticothalamic fibre ingrowth to the superior colliculus was affected by monocular enucleation, the ingrowth of Rbp4-Cre::tdTomato fluorescent fibres to the superficial grey layer of the superior colliculus was analysed. The superficial grey layer contralateral to the removed eye was compared to the superficial grey layer ipsilateral to the removed eye, the latter being the intra-animal

control. The analysis was done blind to experimental condition. To quantify the fluorescent fibre ingrowth to the superficial grey layer the same method as described above was used with the following alterations.

Using a 100 μ m line in the periaqueductal grey, pixel intensity was adjusted in ImageJ as described above. Images were then converted to grey scale. In Adobe Photoshop the superficial grey layer was selected using the following criteria (see figure 4.1 F for representative outline). The ventral border of the superficial grey was the border between the superficial grey layer and the optic nerve layer as assessed by the density of tdTomato positive fibres (which are in thicker bundles in the optic nerve layer). The dorsal edge of the superior colliculus was used as the dorsal border of the superficial grey layer. The medial edge of the superior colliculus was used as the medial edge of the superficial grey layer. At the lateral edge the superficial grey layer tapers off and as such as much of the superficial grey layer was included before tapering off (figure 4.1F).

Strain	Experiment	Age	n	Litters
Rbp4-Cre::tdTomato	Monocular Enucleation on P0	P4	3	2
Rbp4-Cre::tdTomato	Monocular Enucleation on P0	P6	4	1
Rbp4-Cre::tdTomato	Monocular Enucleation on P0	P8	3	1

Table 4.5. Number of Rbp4-Cre::tdTomato positive brains used for this experiment at each age. Note these are the same brains used for analysis referred to in section 4.2.5 and 4.2.6.

4.2.8. Carbocyanine dye tracing to determine cortical origin of layer VI/VIb fibres entering the dLGN prematurely after monocular enucleation

In order to determine from which cortical area the prematurely-entering eGFP derive, I performed retrograde carbocyanine dye tracing from the control and enucleated dLGN. Small crystals of DiI were placed in the control and enucleated dLGN following monocular enucleation at P0. The brains were incubated in 0.05% PBSA at 37°C for 5 weeks. Only brains where the DiI was placed in the dLGN were subsequently analysed. Due to scarcity of correctly placed DiI crystals one brain from the Lpar1-eGFP line aged P7 was included in the analysis. All other brains were from the Golli-τ-eGFP line aged P6 (table 4.6). Brains were embedded in 5% agarose and sectioned coronally to 50µm on a vibrating microtome. Sections were counterstained with 5µg/mL DAPI for 5

minutes.

The extent of retrograde labelling in layer VI and VIb of the whole cortex was analysed by comparing presence of back-labelled layer VI and VIb neurons in primary and secondary sensory cortical areas throughout the anterior-posterior extent of the cortex. Cortical areas were identified by reference to the Franklin and Paxinos Mouse Brain Atlas (Frankin and Paxinos, 1996). Ipsilateral (to the removed eye) cortex and contralateral (to the removed eye) cortex were compared in each cortical area.

Strain	Age	Experimental condition	n	Litters
Golli-τ-eGFP	P6	Enucleated (contralateral) dLGN	4	2
Golli-τ-eGFP	P6	Control (ipsilateral) dLGN	2	2
Lpar1-eGFP	P7	Control (ipsilateral) dLGN	1	1

Table 4.6. Number of brains used for retrograde DiI tracing from the dLGN.

4.2.9. Immunohistochemistry

To amplify the eGFP signal in the Golli-τ-eGFP mouse, anti-GFP immunohistochemistry was performed as below. To assess the impact of monocular enucleation on the presence of aggrecan protein in the dLGN and superior colliculus, anti-aggrecan immunohistochemistry was performed (Table 4.7).

For free floating fluorescent immunohistochemistry brains were embedded in 4% agarose and sectioned coronally to 50µm. Sections were stored at 4°C in PBSA. Sections were blocked for 2 hours at room temperature. Sections were incubated with primary antibody in blocking solution overnight at 4°C. Sections were incubated with secondary antibody in blocking solution for 2 hours at room temperature. Sections were counterstained with DAPI as above. Details of antibody combinations and block in table 4.7.

Strains	Primary antibodies	Secondary antibodies	Block
Golli-τ-eGFP	Rabbit anti-GFP 1:500 (Invitrogen, A11122)	Donkey anti-rabbit AlexaFluor488 1:500 (Invitrogen, A21206)	0.1% Triton-X100 (BDH, Poole, UK) 2% donkey serum (Sigma Aldrich, Gillingham, UK) 0.1M PBS
Rbp4-Cre:: tdTomato Ntsr1-Cre:: tdTomato	Mouse anti-Chondroitin Sulfate Proteoglycan Antibody, Core Protein Epitope, 1:2500 (Chemicon, MAB1581). Specific for aggrecan (Matthews et al., 2002; Brooks et al., 2013)	Donkey anti-mouse AlexaFluor488 1:500 (Invitrogen, A21202)	0.1% Triton-X100 2% donkey serum 0.1M PBS

Table 4.7. Antibody combinations and block conditions used for anti-GFP and anti-aggrecan immunohistochemistry.

4.3. Results

Retinal fibres enter the dLGN and establish mature connections some time before the cortical fibres enter the dLGN (figure 1.8 and 1.10 in introduction) (Godement et al., 1984; Jaubert-Miazza et al., 2005; Jacobs et al., 2007; Grant et al., 2012; Ackman et al., 2012; Seabrook et al., 2013). Prior to corticothalamic fibres entering, the retinal ganglion cells transmit spontaneous retinal activity to the dLGN (Mooney et al., 1996; Weliky and Katz, 1999; Ackman et al., 2012). Given the coincidence of early spontaneous retinal waves and the highly regulated ingrowth of the corticothalamic subpopulations to their target thalamic nuclei, I decided to test whether retinal input to the dLGN was important for this regulated ingrowth of corticothalamic fibres. I performed two sets of experiments, one performing monocular enucleation, and one abolishing spontaneous retinal waves. In both groups I studied the ingrowth of layer specific cortico-thalamic projections from layers V, VI and VIb, using the transgenic lines characterised in chapter 3.

4.3.1. Early peripheral manipulation alters corticothalamic ingrowth

I performed monocular enucleation at birth and studied the ingrowth of the corticothalamic fibres over the first 10 postnatal days. Monocular enucleation has been used extensively to study the role of retinal input in numerous aspects of cortical and

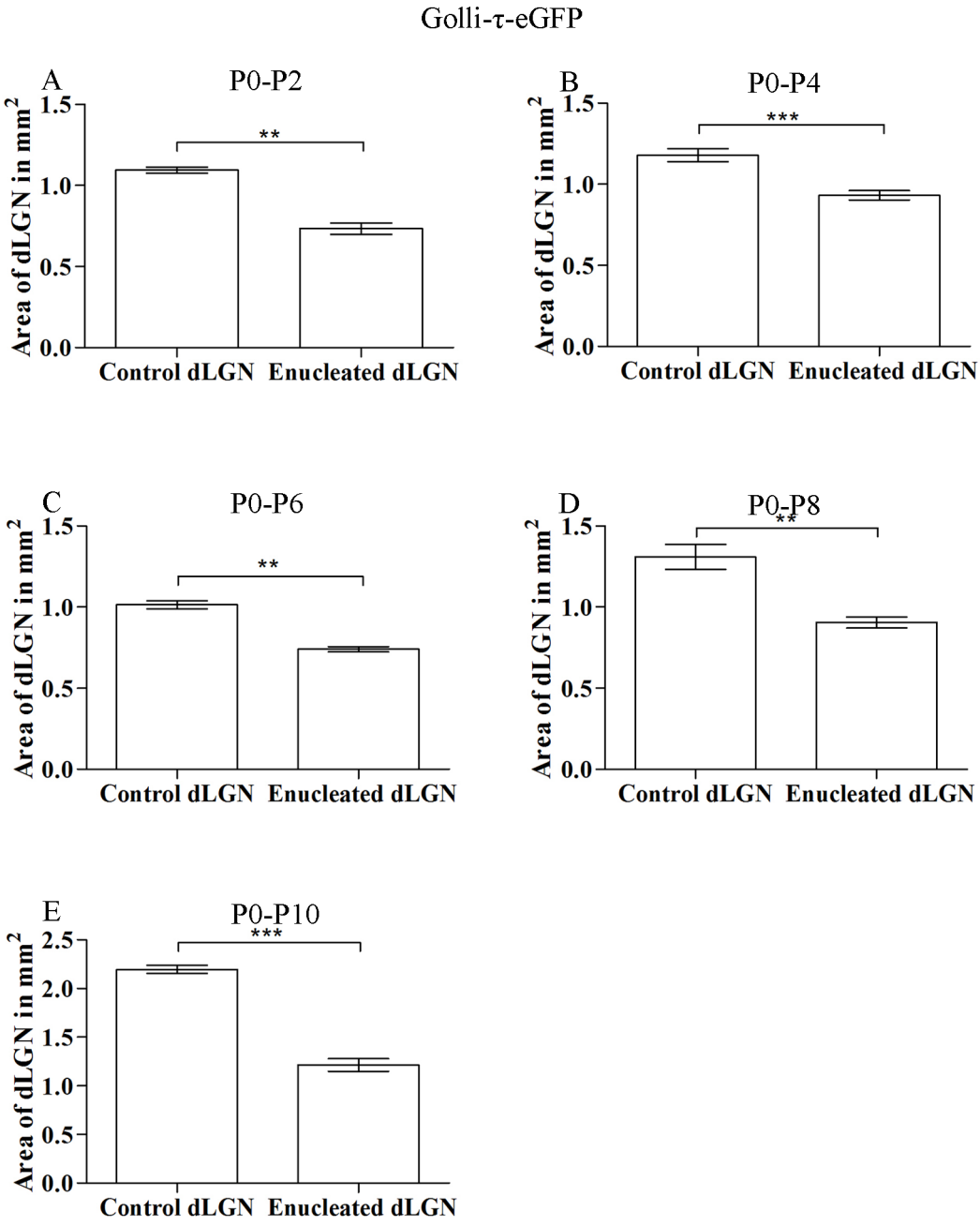

Figure 4.2. Graphs of area of control and enucleated dLGN (mm2) on coronal slices in the Golli-τ-eGFP line. A-E. The area in mm2 of the dLGN in coronal sections is reduced in the hemisphere contralateral to the removed eye (referred to as the enucleated dLGN) in the Golli-τ-eGFP line at P2, P4, P6, P8 and P10. Values shown are mean and standard error. Results based on 3 animals at P2, 6 animals at P4 and P6, 4 animals at P8 and 5 animals at P10.

visual system development (Toldi et al., 1996; Golding et al., 2013; Brooks et al., 2013; Seabrook et al., 2013).

In mice 85-95% of retinal input crosses the midline at the optic chiasm and projects to the contralateral dLGN (Valverde, 1968; Godement et al., 1980; Jaubert-Miazza et al., 2005). As such the hemisphere contralateral to the removed eye only receives retinal input from the ipsilateral fibres (from the eye which is not removed). Throughout this chapter the hemisphere contralateral to the removed eye will be referred to as the 'enucleated' hemisphere, including the 'enucleated thalamus', the 'enucleated dLGN' and the 'enucleated superior colliculus'.

4.3.1.1. Visual deprivation by monocular enucleation causes a reduction in size of the dLGN in the Golli-τ-eGFP

The volume of the dLGN is reduced after the loss of retinal input from one eye (Cullen and Kaiserman-Abramof, 1976; Godement et al., 1980; Heumann and Rabinowicz, 1980; Hada et al., 1999). I followed the time-course of this reduction by measuring the area of the dLGN in coronal DAPI stained sections.

My results showed that after monocular enucleation in the Golli-τ-eGFP mouse, the coronal area of the dLGN was significantly reduced (Figure 4.2, Table 4.8). As early as P2 the enucleated dLGN was significantly smaller compared to the control dLGN (figure 4.2 A). This remains the case at P4, P6, P8 and P10 (figure 4.2 and table 4.8). The reduction in the area of the enucleated dLGN is consistent with results showing a reduction in cell number within the dLGN (Heumann and Rabinowicz, 1980).

Despite this relative reduction in the size, the enucleated dLGN continues to grow over the first 10 postnatal days. From P2 to P10 the area of the control dLGN doubled from 1.095mm^2 to 2.196mm^2, whereas the enucleated dLGN grows at a slightly reduced rate (0.7342mm^2 at P2 to 1.215mm^2 at P10). Unexpectedly the area of the dLGN slightly decreases between P4 and P6 however this may be due to developmental variability between the litters. Between P8 and P10 there is a jump in the area of both the control and the enucleated dLGN. This could be due to the large increase in neuronal volume

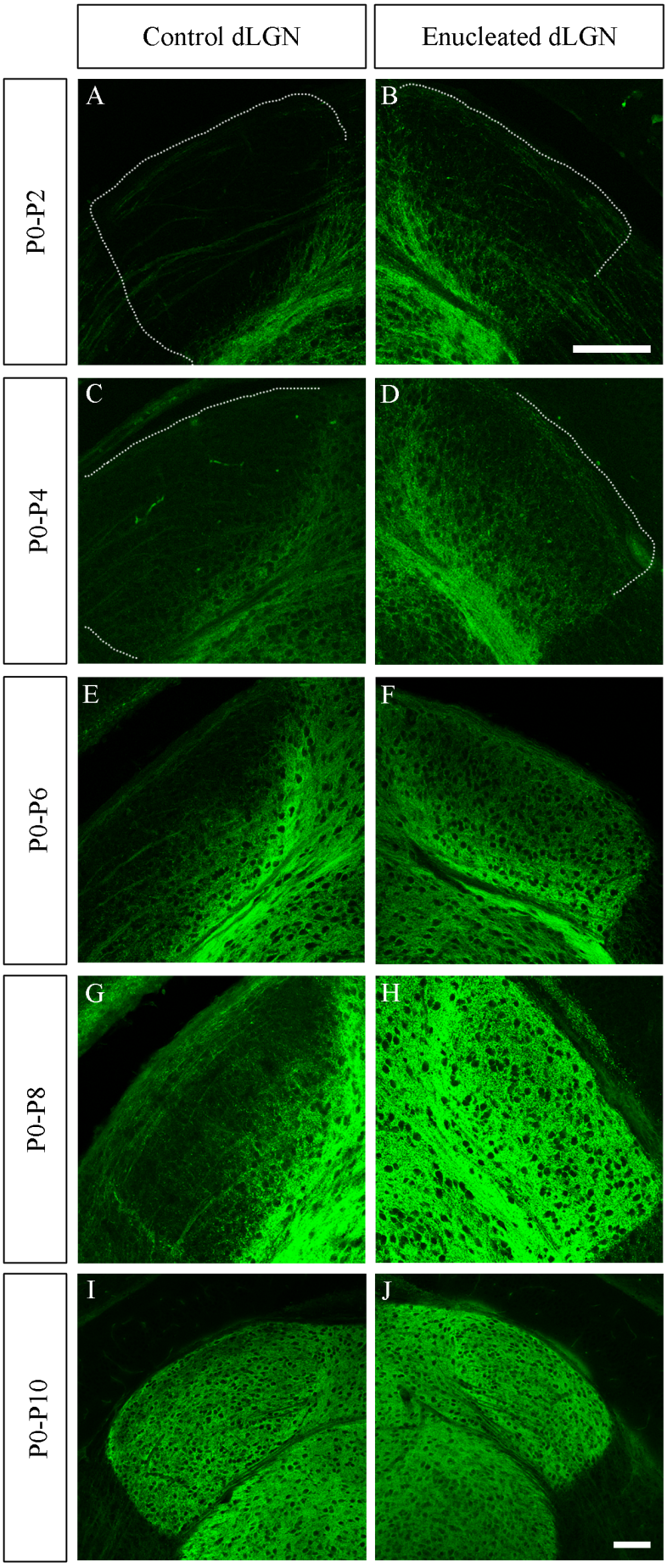
Control dLGN
Enucleated dLGN
P0-P2
P0-P4
P0-P6
P0-P8
P0-P10
A
B
C
D
E
F
G
H
I
J

Figure 4.3. Ingrowth of Golli-τ-eGFP layer VI and VIb fibres into the control and enucleated dLGN over development. A. At P2 eGFP positive fibres have reached the ventral boarder of the control dLGN. B. The eGFP fibres have begun to enter the dLGN from the ventral edge. C. By P4 eGFP fibres have not entered the control dLGN. D. Fibres have extended more dorsally in the enucleated dLGN. E. At P6 eGFP positive VI and VIb fibres have begun to enter the control dLGN from the ventral edge. F. In the enucleated dLGN the eGFP fibres have extended throughout the ventral-dorsal extent of the nucleus, they are denser in the ventral part than the dorsal part. G. At P8 in the control dLGN the fibres were in the ventral part of the nucleus whilst the fibres are densely arborised and evenly distributed in the enucleated dLGN (H.). I. By P10 eGFP fibres have extended to the dorsal edge of the control dLGN however they are most dense in the ventral part. J. At P10 the fibres are evenly distributed within the enucleated dLGN. A-D white dots outline dLGN. Scale bars= 50μm (A-H, I-J).

that occurs at this age (Heumann and Rabinowicz, 1980).

	Area of control dLGN in mm^2 ± s.d.	Area of enucleated dLGN in mm^2 ± s.d.	p	n
P2	1.095 ± 0.03204	0.7342 ± 0.06000	0.0041	3
P4	1.179 ± 0.09664	0.9316 ± 0.07085	0.0003	6
P6	1.015 ± 0.05616	0.7400 ± 0.03643	0.0013	6
P8	1.310 ± 0.1550	0.9052 ± 0.06824	0.0014	4
P10	2.196 ± 0.09352	1.215 ± 0.1469	0.0002	5

Table 4.8. Table showing the mean area of control and enucleated dLGN of the Golli-τ-eGFP mouse on coronal sections in mm^2 ± s.d. A one tailed, paired t-test comparing control dLGN with enucleated dLGN at each age shows that the area of the dLGN was significantly different between control dLGN and enucleated dLGN at all ages, p value shown.

4.3.1.2. Monocular enucleation causes premature ingrowth of Golli-τ-eGFP positive layer VI and VIb fibres into the dLGN.

Monocular enucleation was performed at P0 thus depriving the enucleated dLGN of its main retinal driver input. The ingrowth of layer VI and VIb eGFP positive corticothalamic fibres, which provide modulator input to the dLGN, was assessed at P2, P4, P6, P8 and P10. Throughout this chapter the regions of the dLGN are described using dorsal, ventral, medial and lateral as shown in methods figure 4.1 A.

My results showed that following enucleation, eGFP positive VI and VIb corticothalamic fibres enter the dLGN prematurely (figure 4.3).

At P2 eGFP fibres are present at the ventral border of the control dLGN, no fibres can be seen turning to enter the dLGN (figure 4.4 C). In the enucleated hemisphere however, eGFP positive fibres are visible along the ventral and medial border of the dLGN and fibres have branched off from the ventral band and turned to enter the enucleated dLGN (figure 4.4 D). The premature ingrowth of the eGFP positive VI and VIb corticothalamic

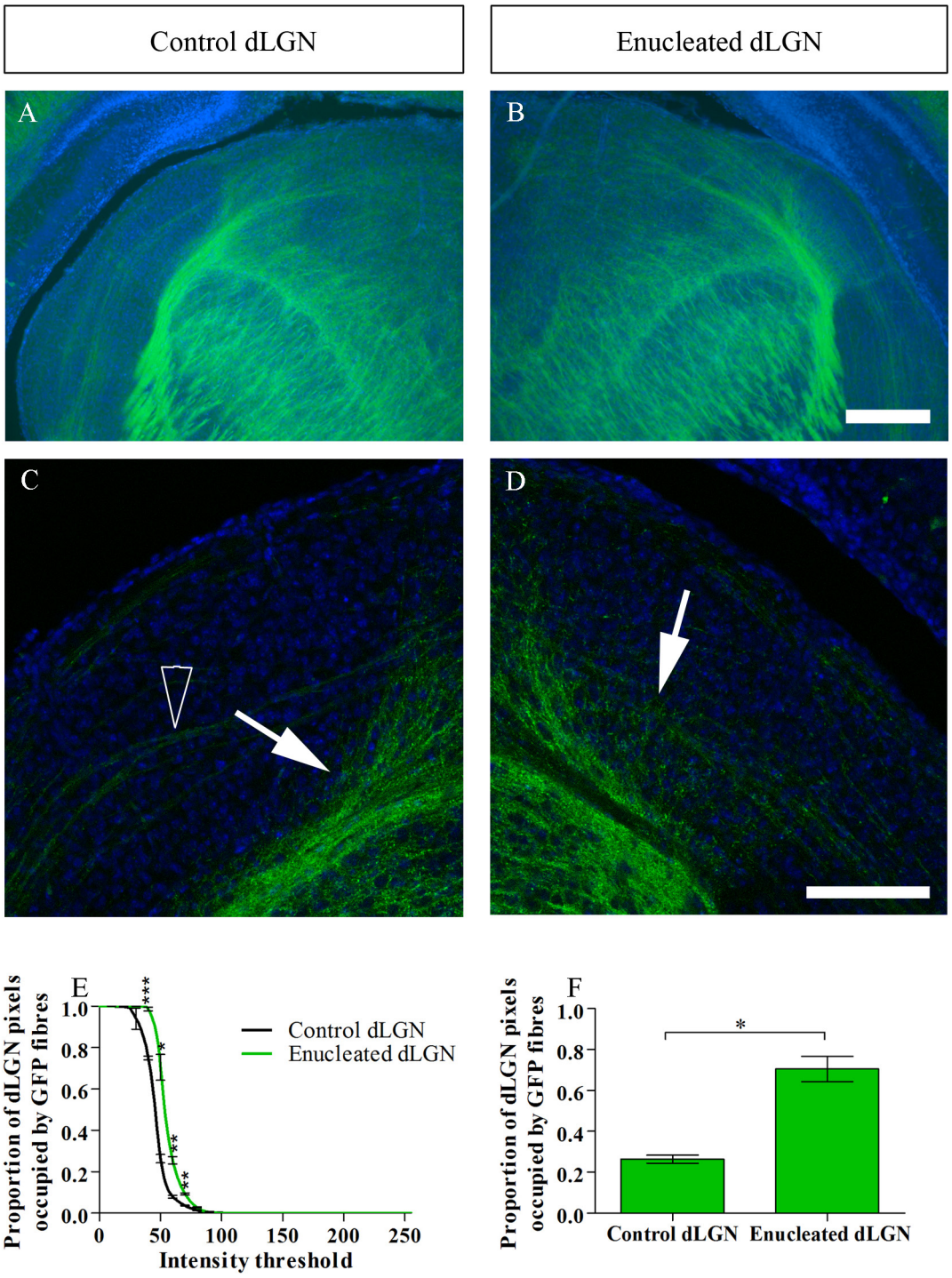

Figure 4.4. Ingrowth of Golli-τ-eGFP layer VI and VIb fibres into the control and enucleated dLGN at P2. A and B. At P2 the eGFP positive fibres grow into the thalamus in both the control and enucleated hemisphere. C. eGFP positive fibres have reached the ventral boarder of the control dLGN (white arrow) but have not entered. There are also eGFP positive fibres which cross the dLGN (hollow arrow head). D. The eGFP fibres have begun to enter the nucleus from the ventral edge (white arrow). E. The proportion of pixels in the dLGN with an intensity value over the intensity threshold for all 255 grey scale intensity values. F. The proportion of pixels which are above intensity threshold 50. Results based on 3 animals. Values shown on graphs are mean and standard error. Scale bars= 250µm (A, B), 50µm (C, D).

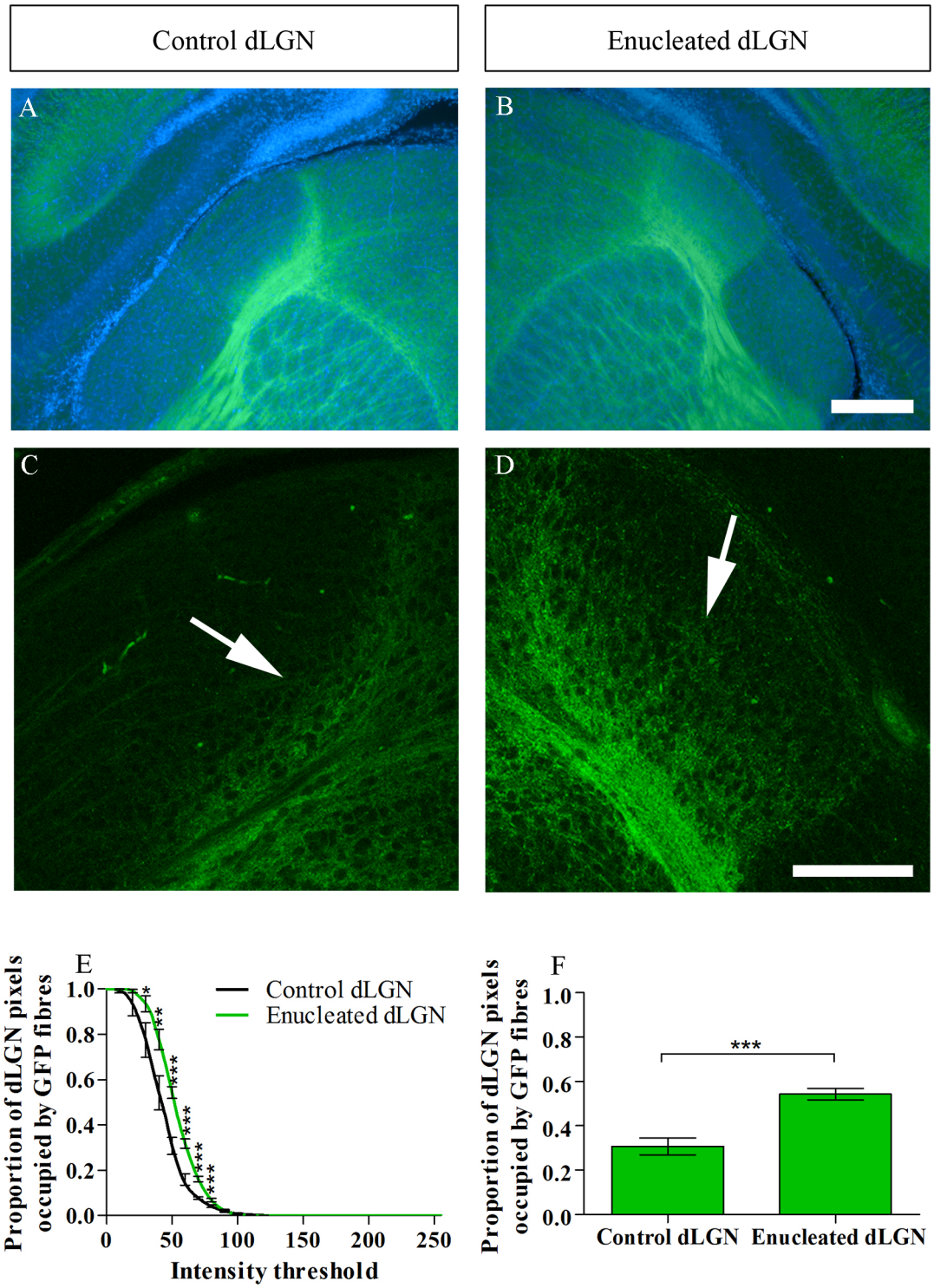

Figure 4.5. Ingrowth of Golli-τ-eGFP layer VI and VIb fibres into the control and enucleated dLGN at P4. A and B. At P4 in both the control and the enucleated thalamus, eGFP positive fibres show signs of early rearrangements to a barreloid patterning in the VPM. The eGFP positive fibres grow into the Po and LP thalamic nuclei. C. At the dLGN eGFP positive fibres make a thick band at the ventral boarder of the control dLGN (white arrow). D. The eGFP fibres have entered the enucleated dLGN from the ventral edge and extend as far as the middle of the dLGN (white arrow). E. The proportion of pixels in the dLGN with an intensity value over the intensity threshold for all 255 grey scale intensity values. F. The proportion of pixels which are above intensity threshold 50. Results based on 6 animals. Values shown on graphs are mean and standard error. Scale bars= 250μm (A, B), 50μm (C, D).

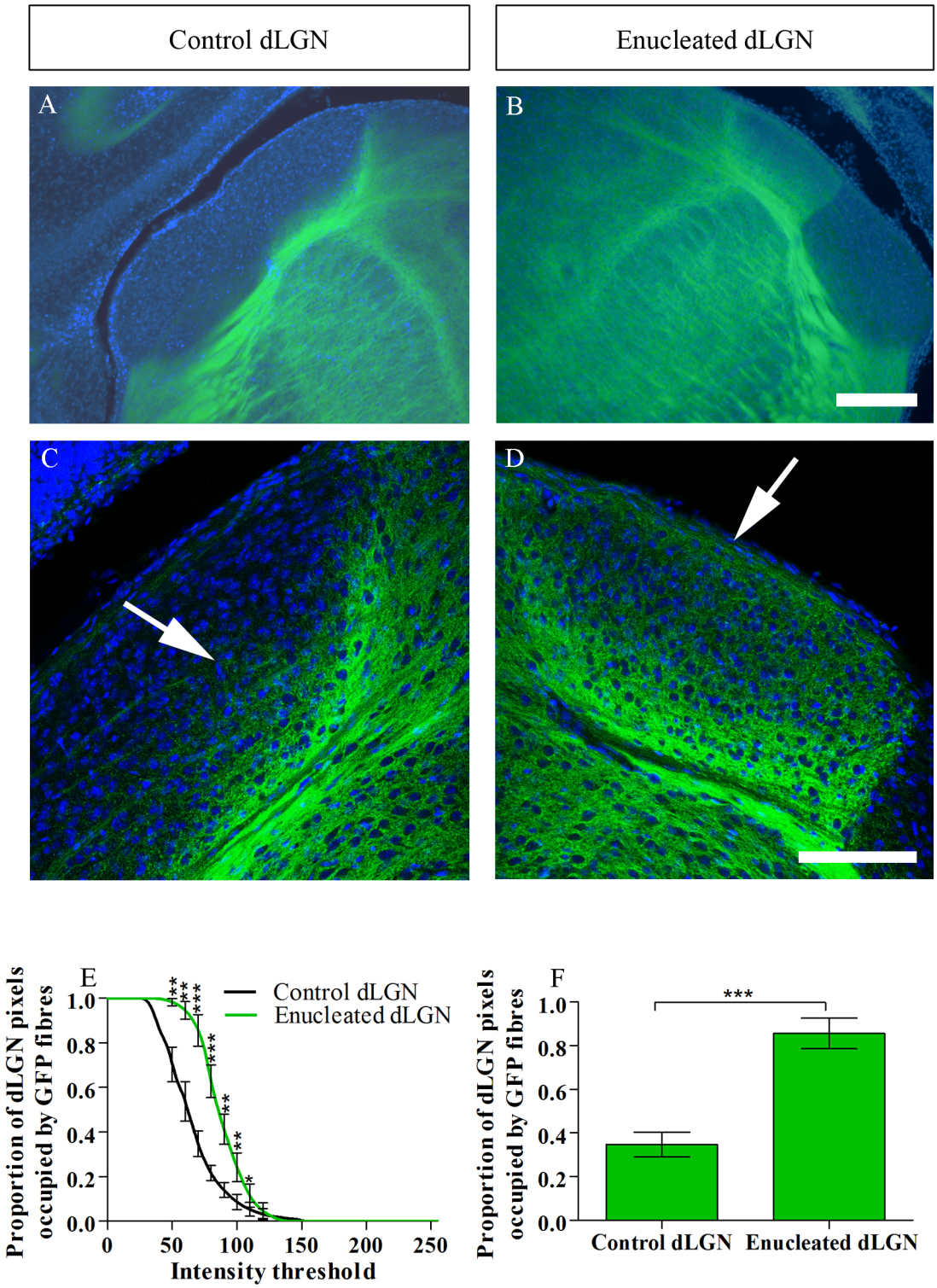

Figure 4.6. Ingrowth of Golli-τ-eGFP layer VI and VIb fibres into the control and enucleated dLGN at P6. A and B. At P6 the characteristic barreloid patterning of the eGFP positive fibres is visible in the VPM in both hemispheres. eGFP positive fibres are visible innervating both the LP and Po. The enucleated dLGN is visibly smaller than the control dLGN. C. At the dLGN eGFP positive fibres have entered the ventral edge of the control dLGN (white arrow). D. The eGFP fibres have extended to the dorsal edge of the dLGN (white arrow). The fibres are densely arbourising in the ventral half of the enucleated dLGN and are less dense in the dorsal half of the enucleated dLGN. E. The proportion of pixels in the dLGN with an intensity value over the intensity threshold for all 255 grey scale intensity values. F. The proportion of pixels which are above intensity threshold 70. Results based on 6 animals. Values shown on graphs are mean and standard error. Scale bars= 250μm (A, B), 50μm (C, D).

fibres into the enucleated dLGN was quantified by comparing pixel intensities (high intensity provided by the presence of GFP+ fibres) within the dLGN. The control and the enucleated dLGN were outlined and the grey scale intensity values of the pixels in the area of the dLGN was analysed. This was graphed as the proportion of pixels in the dLGN which are over the intensity threshold for all 255 grey scale intensity thresholds (figure 4.4 E). This analysis demonstrated that there are a higher proportion of pixels which have an intensity value above a given threshold in the enucleated dLGN compared to the control dLGN (graph E figure 4.4). A higher proportion of pixels above a given intensity threshold represents the fluorescent fibres occupying more of the area of the dLGN. From now on I will refer to this as having a higher proportion of bright pixels.

At P2 the control dLGN is still mainly devoid of eGFP fibres (figure 4.4C) and most pixels are of a similar, low, intensity. This is represented in the graph as a steep (sigmoid) curve (figure 4.4 E). In the enucleate dLGN, eGFP fibres have begun to enter the ventral most edge (figure 4.4D). This is represented by the sigmoid curve being shifted to the right (figure 4.4 E). Once fibres enter the dLGN, the variance of the pixel intensities increases, this is graphically represented as a less steep curve. At P2 the enucleated dLGN has a significantly higher proportion of bright pixels than the control dLGN (figure 4.4 E, F).

Statistical comparisons were performed and significant differences were found between the enucleated and control dLGN at P2, P4, P6, P8 and P10 (table 4.9). The difference is greatest at P6. These results are summarized across development for one intensity threshold value (table 4.9 and figure 4.3).

In the Golli-τ-eGFP mouse occasional eGFP positive fibres can be seen crossing the dLGN in a manner similar to the layer V Rbp4-Cre::tdTomato fibres (for example hollow arrow head in figure 4.4 C). The Golli-τ-eGFP line has been demonstrated to label some, sparse, layer V neurons (Jacobs et al., 2007) which these fibres may come from.

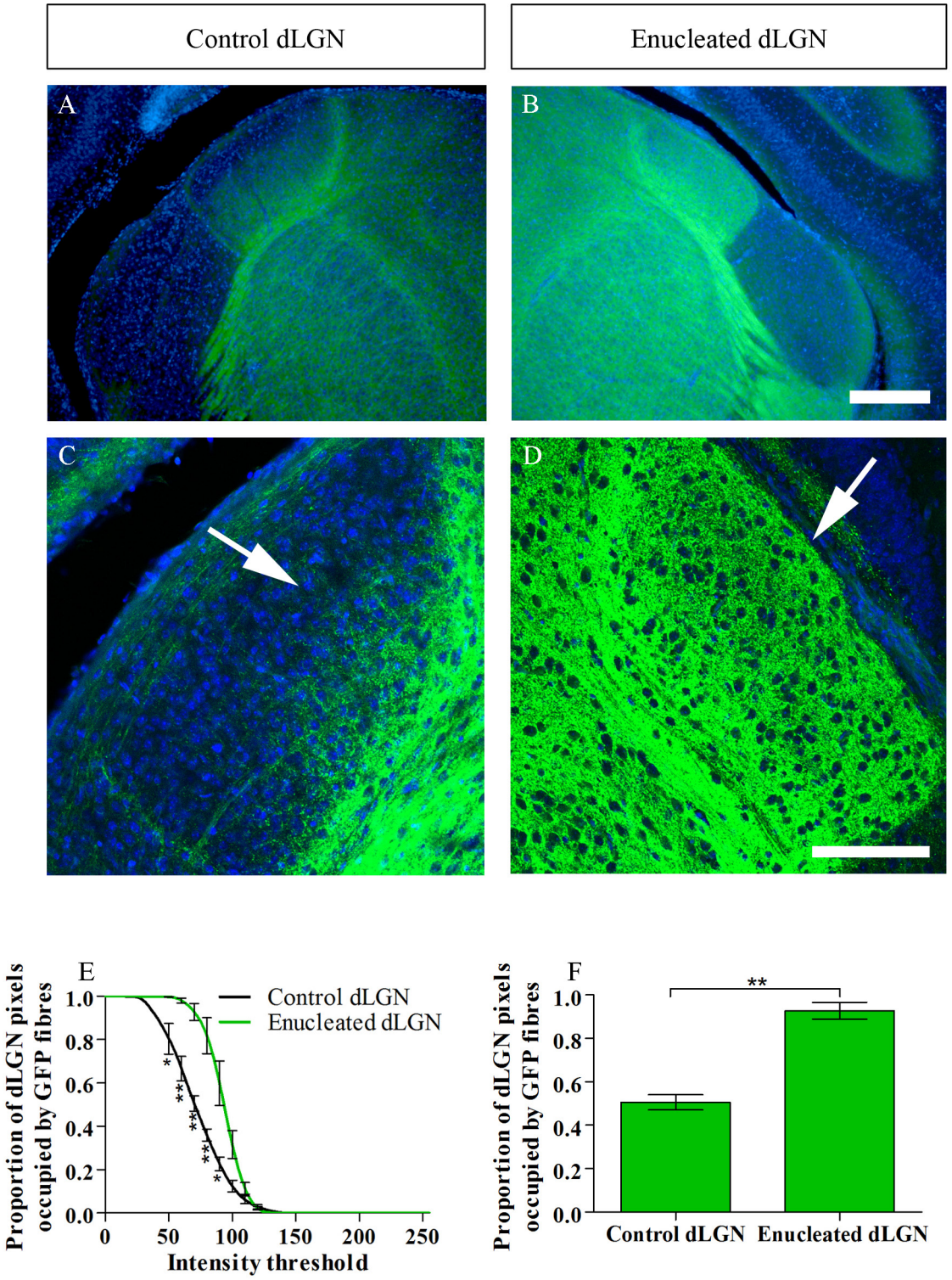

Figure 4.7. Ingrowth of Golli-τ-eGFP layer VI and VIb fibres into the control and enucleated dLGN at P8. A and B. At P8 the eGFP positive fibres are patterned with the characteristic barreloid patterning in the VPM. The fibres grow into the LP and Po thalamic nuclei. The enucleated dLGN is visibly smaller than the control dLGN. C. At P8 the dLGN eGFP positive fibres have entered the ventral part of the control dLGN. D. The VI and VIb fibres have filled the enucleated dLGN nucleus (white arrow). The eGFP fibres are evenly distributed in the nucleus and densely arbourising throughout. E. The proportion of pixels in the dLGN with an intensity value over the intensity threshold for all 255 grey scale intensity values. F. The proportion of pixels which are above intensity threshold 70. Results based on 4 animals. Values shown on graphs are mean and standard error. Scale bars= 250µm (A, B), 50µm (C, D).

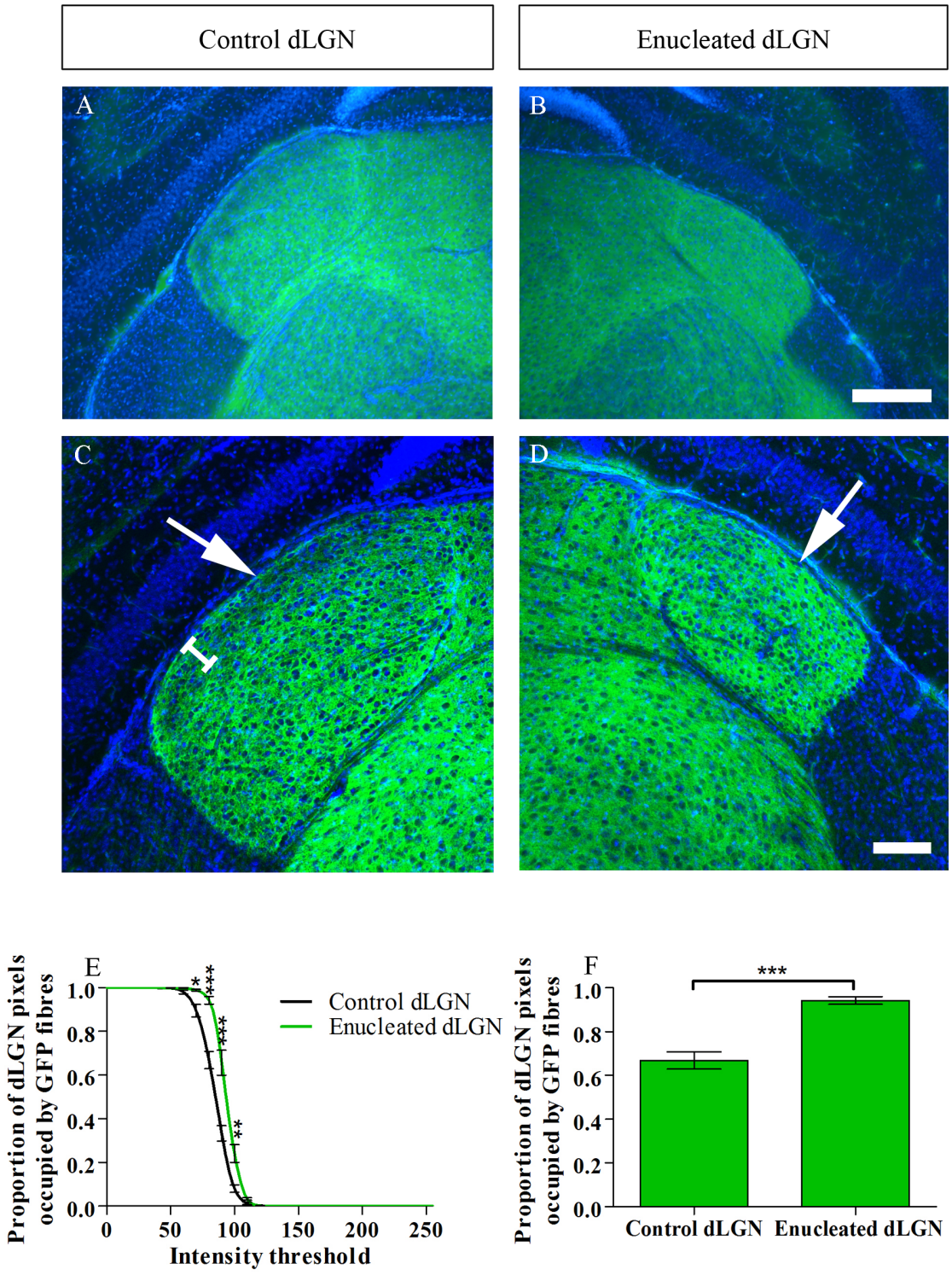

Figure 4.8. Ingrowth of Golli-τ-eGFP layer VI and VIb fibres into the control and enucleated dLGN at P10. A and B. At P10 the eGFP, VI and VIb fibres display barreloid patterning in the VPM. C. eGFP positive fibres have extended throughout the control dLGN (white arrow). The fibres are densely arbourising the ventral portion but are less dense in the dorsal most part (white bracket). D. eGFP positive VI and VIb fibres are evenly distributed throughout the enucleated dLGN. E. The proportion of pixels in the dLGN with an intensity value over the intensity threshold for all 255 grey scale intensity values. F. The proportion of pixels which are above intensity threshold 80. Results based on 5 animals. Values shown on graphs are mean and standard error. Scale bars= 250μm (A, B), 50μm (C, D).

	Intensity threshold used for bar graph	Proportion of pixels above intensity threshold in control dLGN± s.d.	Proportion of pixels above intensity threshold in enucleated dLGN± s.d.	p	n
P2	50	0.2639 ± 0.03547	0.7050 ± 0.1083	0.0144	3
P4	50	0.3071 ± 0.09320	0.5423 ± 0.06308	< 0.0001	6
P6	70	0.3475 ± 0.1374	0.8564 ± 0.1726	0.0003	6
P8	70	0.5055 ± 0.07082	0.9276 ± 0.07811	0.0026	4
P10	80	0.6687 ± 0.08803	0.9423 ± 0.03868	0.0002	5

Table 4.9. Table showing the intensity threshold values chosen for the bar graphs and the proportion of pixels in the area of the dLGN which are above that intensity threshold at each age for the Golli-τ-eGFP. Values shown are mean ± standard deviation (s.d.). The p value of a one-tailed, paired t-test comparing control and enucleated dLGN is given for each age.

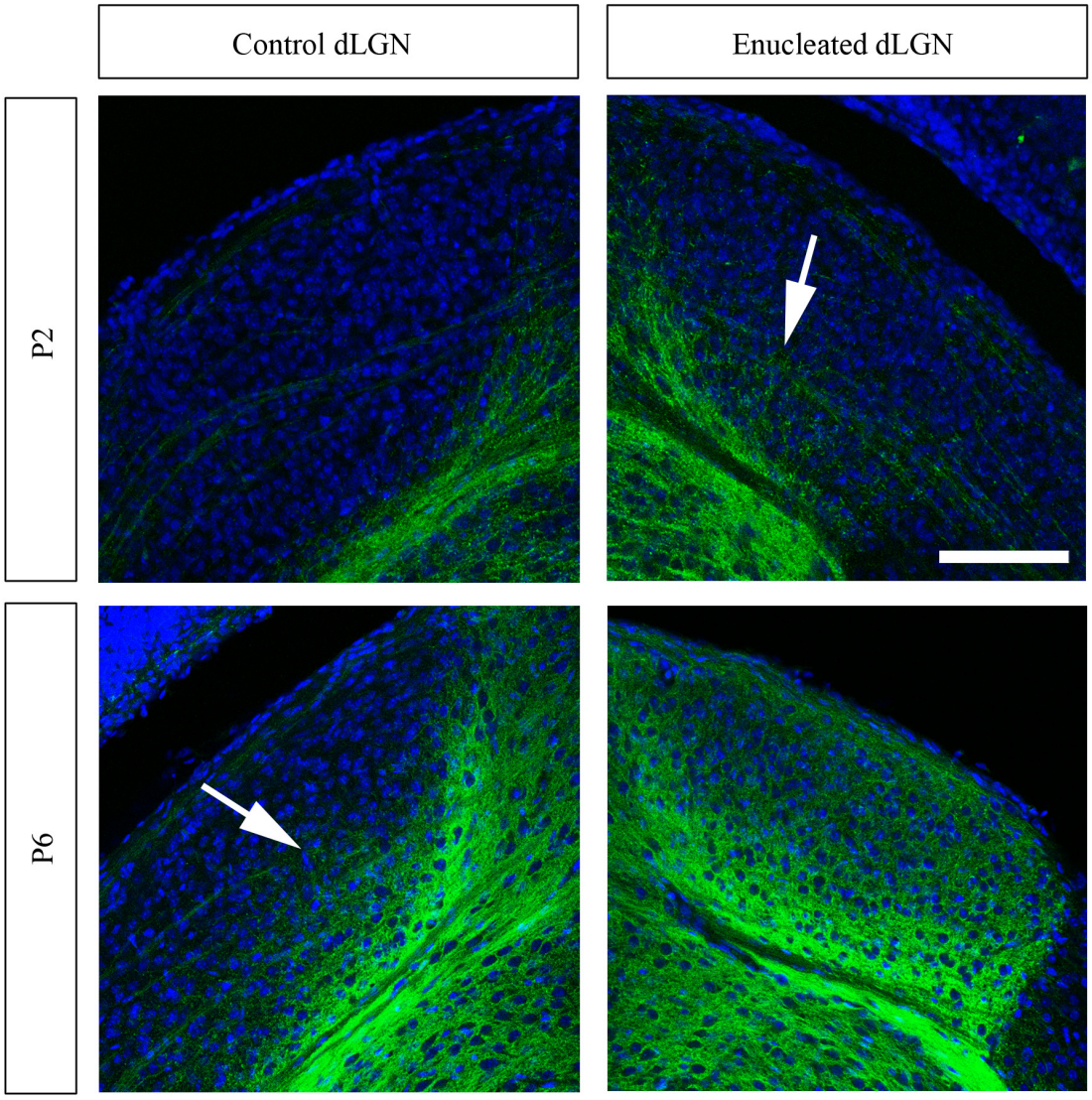

Figure 4.9. Golli-τ-eGFP layer VI and VIb fibres ingrowth to control and enucleated dLGN at P2 and P6. At P2 eGFP fibres accumulate at the boarder of the control dLGN. The eGFP positive fibres have begun to enter the enucleated dLGN at P2 without accumulating. At P6 in the control dLGN fibres begin entering the dLGN after accumulating since P2. By P6 fibres have filled the entire dLGN on the enucleated side. Scale bar= 50μm.

By P4, fibres have extended past the midpoint into the enucleated dLGN (figure 4.5 D) where as they remain in the ventral band accumulating outside the control dLGN. There are proportionally more bright pixels in the enucleated dLGN compared to the control dLGN (graph E and F, figure 4.5). This is more significant at P4 than at P2. The curve of the graph is shallower than at P2; there is more variability in the pixels intensities as more fibres have entered into the nucleus.

At P6 eGFP fibres have extended throughout the ventral-dorsal extent of the enucleated dLGN and are denser in the ventral part than the dorsal part (figure 4.6 D). The fibres appear to be arbourising; the fibres are patterned densely around cells and there are no thick bundles. In the control hemisphere eGFP fibres have begun to enter the dLGN (figure 4.6 C). There is substantially and significantly more bright pixels in the enucleated dLGN (figure 4.6 E, F). There is also a difference in the steepness of the curve between control and enucleated dLGN. The curve is steeper in the enucleated dLGN because it is entirely filled with fluorescing fibres, whereas the curve of the control dLGN is shallower because it is only partially filled with fibres.

At P8 in the control dLGN eGFP fibres are still in the ventral region of the nucleus (figure 4.7 C) whereas in the enucleated dLGN the fibres are evenly distributed throughout (figure 4.7D). There are still significantly more bright pixels in the enucleated dLGN (graph E, F, figure 4.7).

By P10, layer VI and VIb eGFP fibres are densely patterned within the enucleated dLGN (figure 4.8). The eGFP fibres have extended throughout the control dLGN however they are less dense in a band at the dorsal most edge of the nucleus (figure 4.8 C). At P10 there is still a significant difference between the fluorescent intensity of the pixels in the dLGN however it is less pronounced than at earlier ages (figure 4.8 E, F). The curves for both the control and the enucleated dLGN are steep because of the dense eGFP positive fibres.

These results show that layer VI and VIb fibres enter the enucleated dLGN as much as

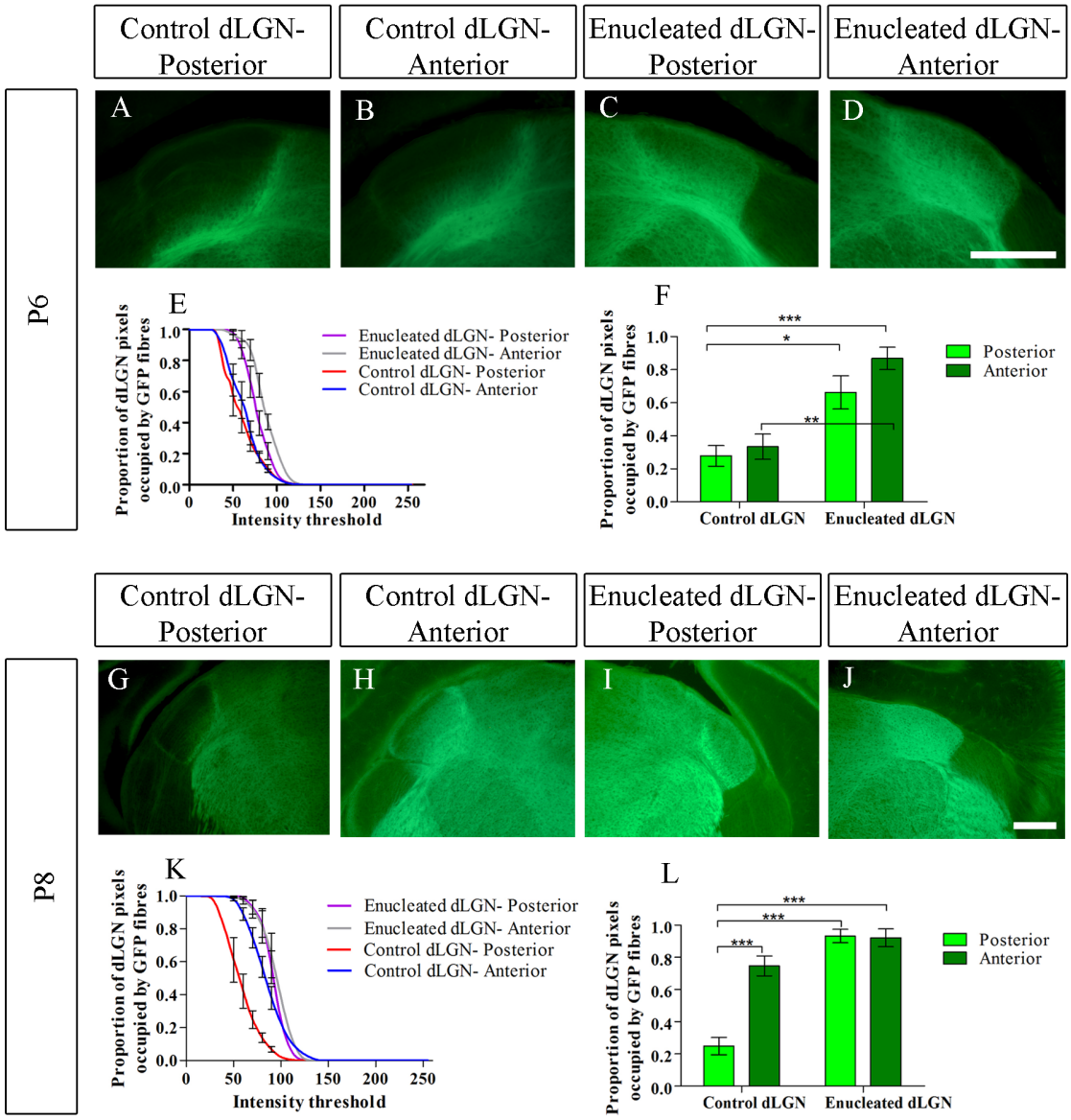

Figure 4.10. Ingrowth of Golli-τ-eGFP layer VI and VIb fibres to the dLGN from anterior to posterior with and without retinal input at P6 and P8. At P6 Golli-τ-eGFP fibres are not present in the posterior (A.) or anterior (B.) control dLGN but are present in both the posterior (C.) and anterior (D.) enucleated dLGN. E. Graph showing the proportion of pixels which are over a given intensity threshold for all 255 grey scale intensity values in anterior and posterior sections of control and enucleated dLGN. F. The proportion of pixels which are above the intensity threshold 70 in anterior and posterior sections of control and enucleated dLGN. At P8 Golli-τ-eGFP fibres are not present in the posterior control dLGN (G.) but are present in anterior control dLGN (H.) and the posterior (I.) and anterior (J.) enucleated dLGN. K. Graph showing the proportion of pixels which have an intensity value over a given intensity threshold for all 255 grey scale intensity values in anterior and posterior sections of control and enucleated dLGN. L. The proportion of pixels above the intensity threshold 70 in anterior and posterior sections of control and enucleated dLGN. Values shown are mean and standard error. Scale bars= 250μm (A-D and G- J).

four days prematurely following enucleation; at P2 compared to P6 (figure 4.9). Thus enucleation seems to abolish a "waiting period" of the ingrowing corticothalamic fibres outside the dLGN.

Following monocular enucleation the 'control' dLGN, ipsilateral to the removed eye, has also lost 5-10% of its normal input because of the ipsilateral contribution. The ipsilateral projection normally targets a patch in the dorsal/medial region of the dLGN (Godement et al., 1984). As such this 5-10% reduction in input might cause a subtler premature ingrowth phenotype. However at all ages studied the eGFP fibres have filled the control dLGN to the same extent as they fill the dLGN in animals which have had no intervention (chapter 3). This suggests that a reduction in retinal input to the dLGN of 5-10% is not severe enough to cause even slight premature entry of eGFP VI and VIb fibres to the normally ipsilateral region of dLGN. This result also confirms that the use of the intra-animal control is appropriate.

These results demonstrate that after enucleation the eGFP positive VI and VIb fibres enter the dLGN prematurely. Similar results have also been recently demonstrated by an independent laboratory using similar methods and the same transgenic line (Seabrook et al., 2013).

4.3.1.3. Anterior to posterior ingrowth of Golli-τ-eGFP VI and VIb fibres to the control and enucleated dLGN at P6 and P8

In chapter 3, I demonstrated that the Golli-τ-eGFP, VI and VIb fibres grow into the dLGN from anterior to posterior. I therefore chose to assess whether the fibres grow into the enucleated dLGN from anterior to posterior at P6 and P8.

At P6 in the control dLGN, in both anterior and posterior sections there is very little eGFP positive fibre ingrowth to the dLGN (figure 4.10 A and B). In the enucleated dLGN in both the posterior and anterior sections the eGFP positive VI and VIb fibres have filled the dLGN (figure 4.10 C- F). In enucleated dLGN eGFP fibres are densest in the anterior sections compared to posterior sections. At P8 in the control dLGN there is little eGFP positive fibre ingrowth into posterior sections of the dLGN (figure 4.10 G).

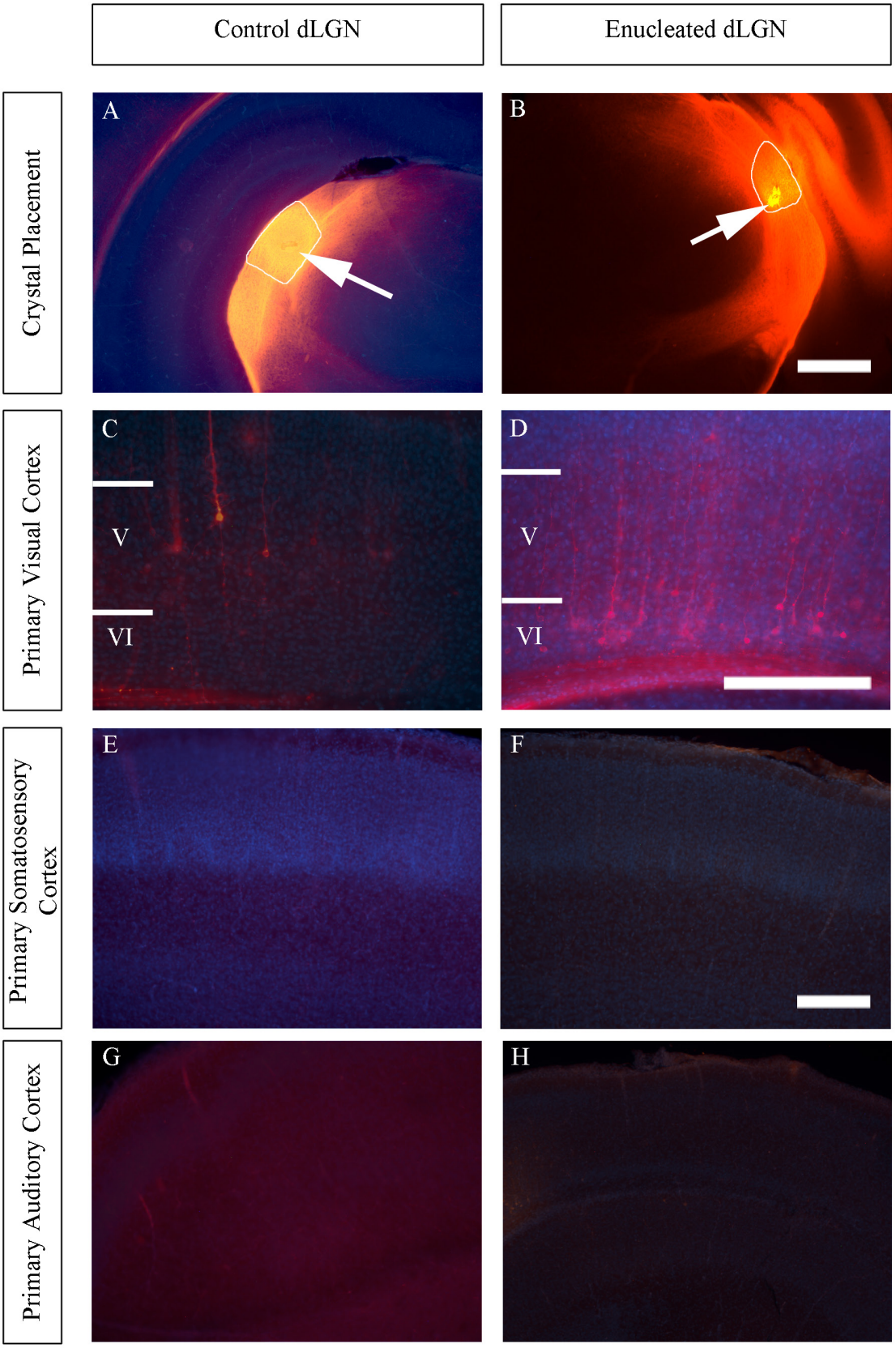

Figure 4.11. Retrograde DiI tracing from the dLGN labels cells in layer VI of the enucleated cortex and, rarely, layer V in the control cortex. A and B. Representative images of DiI crystal placements within the dLGN. C. In primary visual cortex sparse cells are retrogradely labelled in layer V of the control cortex however no cells are present in layer VI. D. In the enucleated primary visual cortex retrogradely labelled cells are present in layer VI. E and F. In control and enucleated primary

somatosensory cortex there are no cells retrogradely labelled from the dLGN. G and H. In control and enucleated primary auditory cortex there are no cells retrogradely labelled from the dLGN. Results based on 4 enucleated dLGN (P6- Golli-τ-eGFP) and 3 control dLGN (2 P6-Golli-τ-eGFP and 1 P7 Lpar1-eGFP) Scale bars= 500μm (A and B.) and 250μm (C-D, E-H.).

In the anterior sections, however, there is clear eGFP positive fibre ingrowth reaching far into the dLGN. These results confirm that the VI and VIb fibres follow the same anterior to posterior ingrowth pattern to the dLGN.

Age	Posterior/ Anterior dLGN	Intensity threshold used for bar graph	Proportion of pixels above intensity threshold in control dLGN± s.d.	Proportion of pixels above intensity threshold in enucleated dLGN± s.d.	p
P6	**Posterior**	70	0.2781 ± 0.1394	0.6618 ± 0.2247	*
	Anterior	70	0.3340 ± 0.1710	0.8680 ± 0.1515	**
P8	**Posterior**	70	0.2490 ± 0.1084	0.9318 ± 0.08354	***
	Anterior	70	0.7470 ± 0.1230	0.9212 ± 0.1109	No

Table 4.10. One-way ANOVA with Bonferroni Multiple Testing Correction showing the difference between the control and enucleated dLGN in posterior and anterior slices of the dLGN at P6 and P8. *= significant at p=0.05, **= significant at p=0.005, ***= significant at p=0.0005.

4.3.1.4. Primary visual cortex origin of eGFP positive corticothalamic fibres which enter the dLGN prematurely after enucleation

Due to early postnatal plasticity in the brain, the removal of peripheral input has been demonstrated to enable rewiring of the brain with other modalities taking over deprived areas (Sur et al., 1988; Angelucci et al., 1997; Sur and Leamey, 2001). One study demonstrated that rewired ferrets, in which visual input is transmitted to A1 via the MGN, there is novel thalamic input to A1 from the LP (visual higher order nucleus) (Pallas et al., 1990). Corticothalamic modality rewiring has not been previously reported, however the eGFP positive fibres that I observe invading the dLGN could be fibres from different cortical areas rewiring to innervate the dLGN, rather than premature ingrowth from the primary visual cortex. The fibres from S1 which innervate the VPM (which is adjacent to the dLGN) do so by P2 and are well positioned to innervate the dLGN. Therefore it is important to establish where the eGFP positive fibres that innervate the enucleated dLGN originate from.

My qualitative results suggest that the eGFP positive VI and VIb fibres innervating the

enucleated dLGN are from V1 as they have the same ingrowth patterns in the enucleated and control dLGN. Firstly the ingrowing fibres come from a dense band at the ventral edge of the dLGN. No eGFP fibres are visible crossing the external medullary laminar which sits between the VPM and dLGN and lacks eGFP labelling (figures 4.3-4.9). Furthermore the layer VI and VIb fibres continue to enter the dLGN from anterior to posterior (figure 4.10) whereas fibres from the somatosensory cortex may not follow this pattern if they were rewiring.

To confirm the cortical area from which the corticothalamic fibres innervate the enucleated dLGN, I performed retrograde carbocyanine dye crystal tracing from the dLGN. DiI was placed in the control and the enucleated dLGN of fixed brains. Brains were only assessed if the DiI crystal was placed within the dLGN. Brains were discarded if any crystals were present in other thalamic nuclei confirmed on serial sections (example crystal placements figure 4.11 A and B). Due to scarcity of brains with DiI crystals exclusively placed in the dLGN, one P7 Lpar1-eGFP hemisphere was included in the analysis (n=1 control hemisphere). All other brains were P6 Golli-τ-eGFP (n= 4 enucleated hemisphere, 2 control hemisphere). All cortical areas were assessed for retrograde labelling of neurons. In the enucleated hemisphere layer VI and VIb cells were visible in V1 (figure 4.11 D). In the control hemisphere layer VI and VIb cells were not visible in V1 and only very rare layer V cells were labelled (example shown in figure 4.11 C, these rare layer V cells were also sometimes seen in the enucleated V1, data not shown). In all other cortical areas including other primary sensory areas (S1 and A1 figure 4.11 E-H) and association areas (data not shown), there were no back-labelled cells in layer VI/ VIb in both the control and the enucleated hemisphere.

My retrograde tracing experiments from the dLGN confirm that the eGFP positive VI and VIb fibres which innervate the enucleated dLGN are primary visual cortex fibres which enter the dLGN prematurely.

4.3.1.5. The effect of abolishing spontaneous retinal waves on the area of the dLGN in the Golli-τ-eGFP

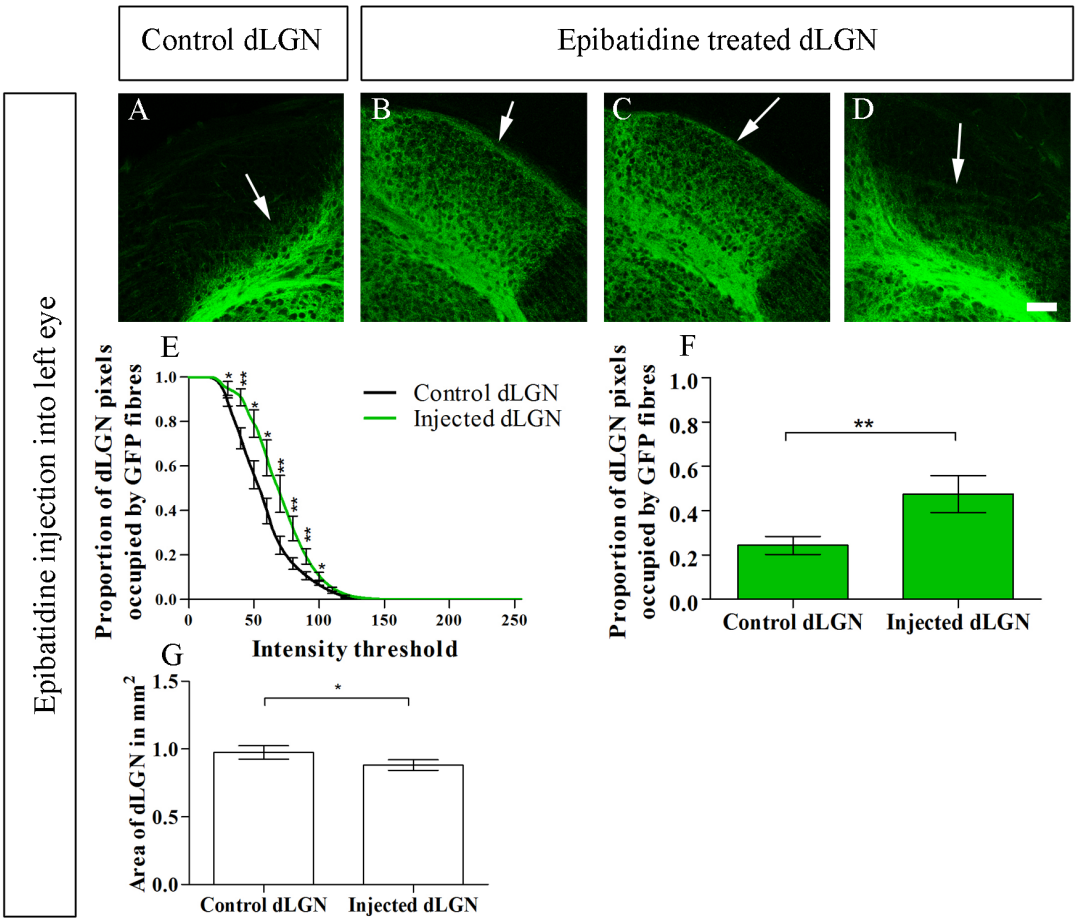
Control dLGN
Epibatidine treated dLGN
Epibatidine injection into left eye
A
B
C
D
E
Proportion of dLGN pixels occupied by GFP fibres
Control dLGN
Injected dLGN
Intensity threshold
F
Proportion of dLGN pixels occupied by GFP fibres
Control dLGN
Injected dLGN
G
Area of dLGN in mm2
Control dLGN
Injected dLGN

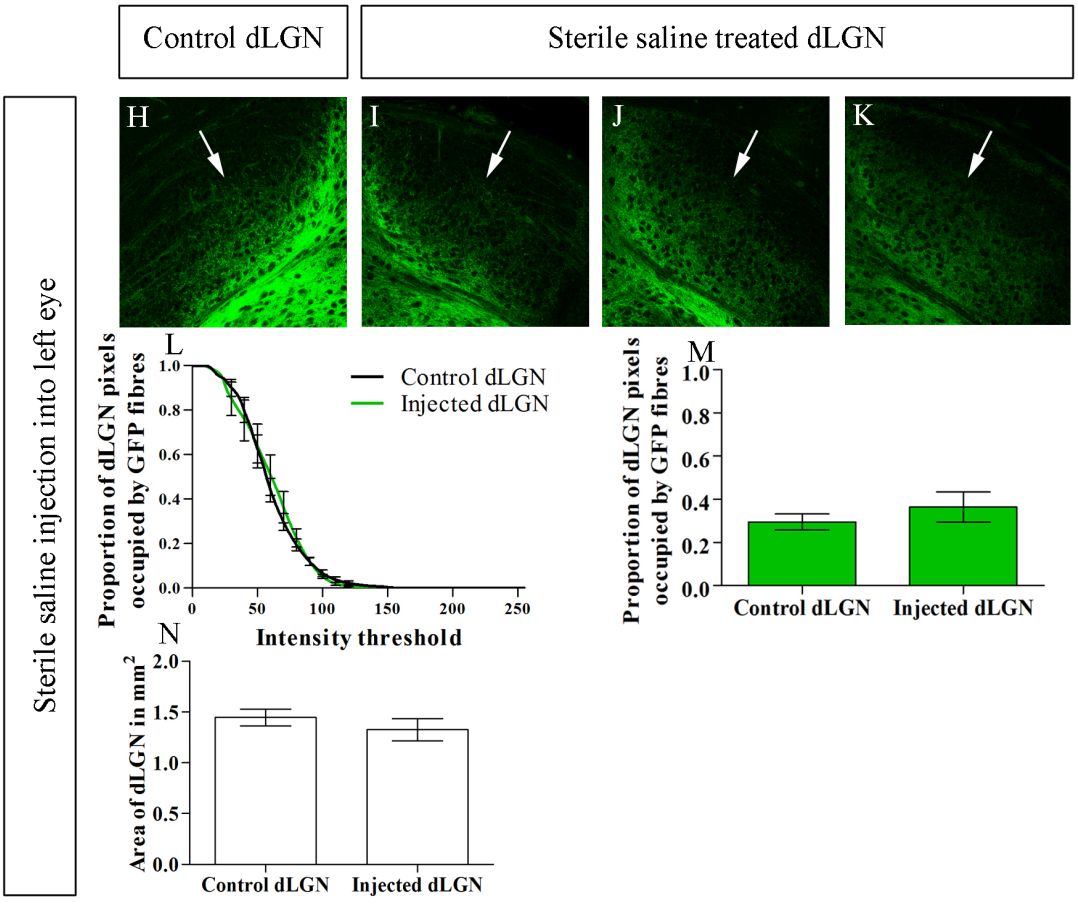
Control dLGN
Sterile saline treated dLGN
Sterile saline injection into left eye
H
I
J
K
L
Proportion of dLGN pixels occupied by GFP fibres
Control dLGN
Injected dLGN
Intensity threshold
M
Proportion of dLGN pixels occupied by GFP fibres
Control dLGN
Injected dLGN
N
Area of dLGN in mm2
Control dLGN
Injected dLGN

Figure 4.12. Ingrowth of Golli-τ-eGFP layer VI and VIb fibres to the dLGN after intraocular injections of epibatidine or sterile saline at P6. At P6 after intraocular injection into the left eye, Golli-τ-eGFP fibres were beginning to enter the control dLGN (A.). Golli-τ-eGFP fibres have entered and filled the epibatidine treated dLGN (B and C.) however in one animal the Golli-τ-eGFP fibres did not fill the dLGN only entering the ventral part (D.) similar to the control dLGN. E. The proportion of pixels in the dLGN with an intensity value over the intensity threshold for all 255 grey scale intensity values. F. The proportion of pixels which are above intensity threshold 70. G. Area of the control dLGN and the dLGN receiving input from the epibatidine injected eye ('Injected dLGN'). At P6 after injection of sterile saline into the left eye Golli-τ-eGFP fibres were beginning to enter the control dLGN (H.) and the saline treated dLGN (I, J and K.). L. The proportion of pixels in the dLGN with an intensity value over the intensity threshold for all 255 grey scale intensity values. M. The proportion of pixels which are above intensity threshold 70. N. Area of the control dLGN and the dLGN receiving input from the saline injected eye ('Injected dLGN'). Results based on 7 epibatidine injected animals and 6 sterile physiological saline injected animals. Values shown on graphs are mean and standard error. Scale bars= 25μm.

Monocular enucleation deprives the dLGN of retinal activity input. In addition to the loss of retinal activity, the retinal ganglion cell axons degenerate thus eliminating other neurotrophins and signals which retinal ganglion cells may provide. Furthermore axonal degeneration may cause damage and local inflammation in the dLGN (Heumann and Rabinowicz, 1980; Lam et al., 2009). To distinguish between the effects of the loss of retinal activity and the loss of the axons I decided to disrupt the early spontaneous retinal activity without removing the axons.

During the first postnatal week the eyes are not yet open in the mouse, however during this period patterned retinal activity exists in the form of spontaneous waves propagating across the retina (Meister et al., 1991; Wong et al., 1993). These waves of activity are transmitted to the dLGN via the retinal ganglion cells (Mooney et al., 1996). Between P0 and P10 these spontaneous waves are mediated by nicotinic cholinergic receptors (Feller et al., 1996; Penn et al., 1998; Bansal et al., 2000), which can be targeted pharmacologically. Epibatidine is a potent cholinergic agonist (Person and Wells, 2011) which reversibly blocks the propagation of spontaneous retinal waves across the retina by causing receptor desensitisation (Penn et al., 1998; Rebsam et al., 2009; Sun et al., 2008; Rebsam et al., 2012; Ackman et al., 2012). In addition to abolishing wave propagation, it also greatly reduces the activity of retinal ganglion cells although spontaneous activity is not eliminated (Penn et al., 1998; Sun et al., 2008).

To test whether disrupting retinal activity also caused premature ingrowth of

corticothalamic fibres to the dLGN I injected epibatidine into the left eye daily from P0-P5. The ingrowth of layer VI and VIb eGFP positive corticothalamic fibres to the dLGN was assessed at P6. The dLGN contralateral to the injected eye is compared to the control dLGN (ipsilateral to the injected eye). In addition, separate litters were injected with sterile saline in the left eye from P0-P5 as a control for the effects of the surgery and mechanical disruption to the retina which may be caused by increased pressure as a result of injecting fluid into the eye. Again the dLGN contralateral to the injected eye was compared to the control dLGN (ipsilateral to the injected eye). From now on I will use the following terms to refer to each dLGN: the control dLGN is the dLGN which receives input from the eye which has not been injected with epibatidine or saline, this is ipsilateral to the injected eye. The epibatidine treated dLGN will refer to the dLGN which receives input from the eye which has been injected with epibatidine, this dLGN is contralateral to the injected eye. The saline treated dLGN will refer to the dLGN which receives input from the eye which has been injected with saline.

In order to assess whether daily intraocular injections of epibatidine or saline caused damage to the retina (which might then impact on the retinal input to the dLGN) the area of the dLGN on coronal sections was analysed (figure 4.12 G, N and table 4.11). After intraocular epibatidine injections, the epibatidine treated dLGN was significantly smaller than the control eye (figure 4.12 G). There was no difference between the sizes of the dLGN after sterile saline injections into one eye (figure 4.12 N).

The reduction in the size of the epibatidine treated dLGN might suggest damage to the eye or retina which has caused partial degradation of the retinal ganglion cells. If the reduced area of the dLGN is symptomatic of partial degradation to the retinal axons this could alter the ingrowth of the corticothalamic fibres to the dLGN in a similar manner to the monocular enucleation thus any results must be considered in this light. None-the-less the reduction in area of the dLGN was less substantial than after monocular enucleation, suggesting that any impact of retinal intraocular injections on retinal degeneration is less severe.

The analysis of the dLGN area reveals that there is a difference in the size of dLGN between the pups from the epibatidine injected litters and the sterile saline injected litters. The size of the control dLGN was significantly smaller in the epibatidine injected pups compared to the sterile saline injected pups (one tailed, unpaired t-test p=0.0002).

	Area of control dLGN ± s.d.	Area of dLGN receiving input from injected eye ± s.d.	p	n
P6 epibatidine injection	0.9746 ± 0.1297	0.8817 ± 0.1052	0.0218	7
P6 sterile saline injection	1.445 ± 0.2322	1.325 ± 0.3119	0.1052	8

Table 4.11. Area of the dLGN on coronal sections in mm^2 in controls and dLGN receiving input from the eye receiving epibatidine injections or sterile saline injections.

4.3.1.6. The effect of abolishing spontaneous retinal waves on Golli-τ-eGFP layer VI and VIb corticogeniculate ingrowth

I set out to examine whether the ingrowth of layer VI and VIb corticothalamic fibres to the dLGN is affected by the injection of epibatidine to the eye that is innervating that dLGN. The ingrowth of eGFP positive VI and VIb fibres into the control dLGN was as previously described (figure 4.12, A). Following epibatidine injections eGFP positive VI and VIb fibres were visible throughout the ventral-dorsal extent of the epibatidine treated dLGN at P6 (figure 4.12, B and C). However, following epibatidine treatment there is greater variability in ingrowth than was seen following enucleation. One epibatidine treated animal had similar ingrowth into both dLGN (figure 4.12 D). Six out of seven animals demonstrated premature ingrowth of VI and VIb eGFP fibres to the epibatidine treated dLGN compared to the control dLGN. The outlier may be due to failed intraocular injections. If the initial hole in the sclera was made too large the epibatidine may leak out and as epibatidine is a reversible agonist this may enable recovery of retinal activity. The treated dLGN contained significantly more bright pixels than the control dLGN, confirming premature ingrowth of GFP-positive fibres (Figure 4.12 E and F, and table 4.12).

Injection of sterile saline into the eye did not cause premature entry of the VI and VIb Golli-τ-eGFP fibres (figure 4.12 H-M). There was no significant difference between the

proportion of bright pixels between hemispheres (figure 4.12 L and M). This confirms that any possible damage to the retina elicited by daily perforation with the needle or the injection of fluids to the eye is not sufficient to cause premature ingrowth of VI and VIb corticothalamic fibres to the dLGN and the effect I observed was therefore probably due to the altered wave activity pattern.

When comparing sham and epibatidine injected pups, the sham injected animals showed more advanced fibre ingrowth into both dLGN, which supports the idea of a general developmental delay in epibatidine treated animals. Whether this is because of the epibatidine directly, or the female neglecting the pups more is indeterminable. At this early developmental stage, the size of the mouse is correlated with developmental milestones; bigger animals can have more advanced cortical development by 2-4 days (judging from the appearance of the cytoarchitectonic barrels in S1) (Hoerder-Suabedissen et al., 2008). If the females neglect epibatidine injected pups, feeding them less, this could explain the difference between the size of the dLGN and the extent of corticothalamic ingrowth to the dLGN in sham and epibatidine injected litters.

The extent of the premature ingrowth is more pronounced following monocular enucleation than epibatidine injection. At intensity threshold 70 the difference between the epibatidine treated dLGN and the control dLGN is 23% (table 4.12). The difference between the enucleated dLGN and the control dLGN is 51% (table 4.9). Therefore the disruption of spontaneous retinal wave activity causes a less severe phenotype of premature corticothalamic ingrowth compared to the complete loss of retinal activity and axons.

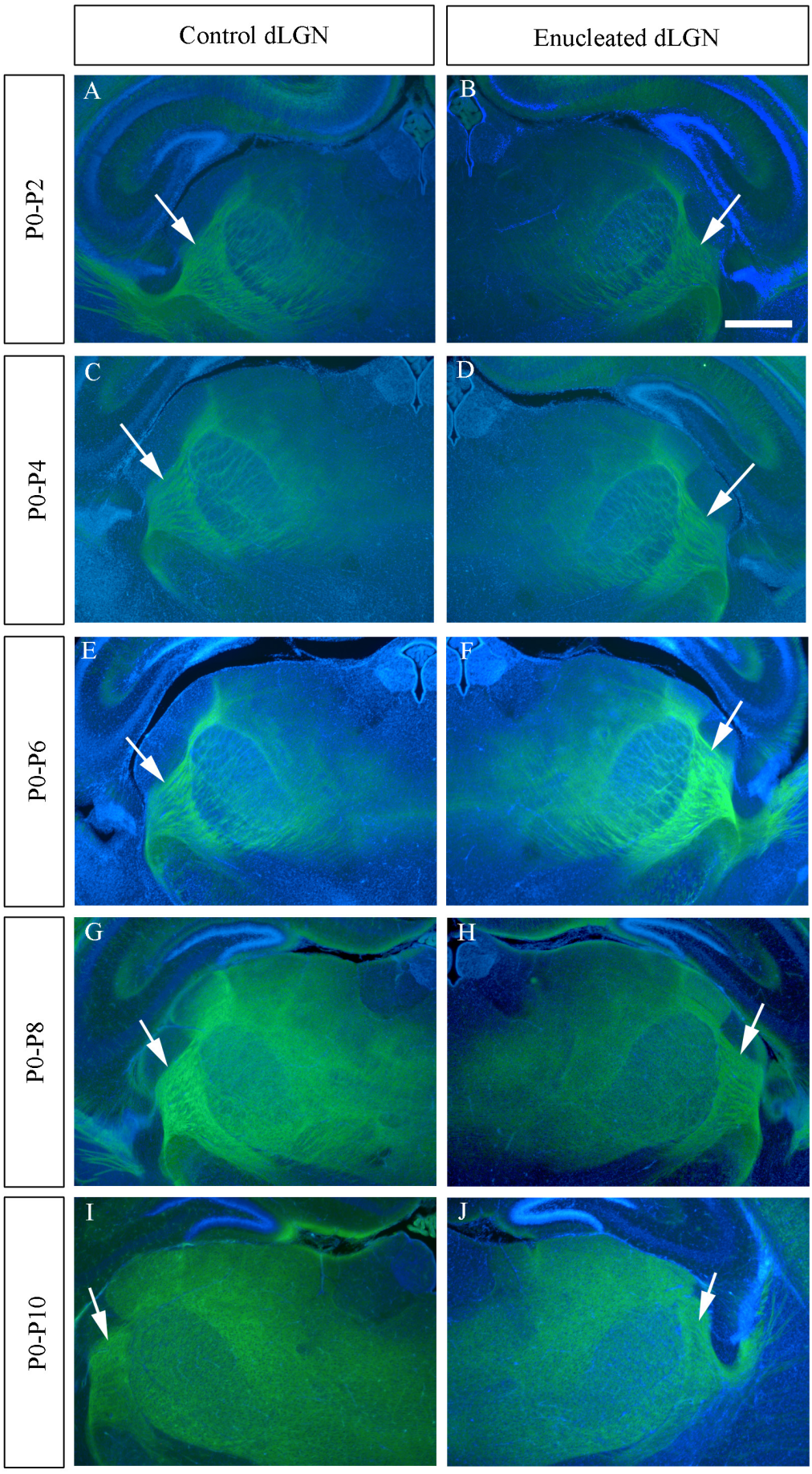
Control dLGN
Enucleated dLGN
P0-P2
P0-P4
P0-P6
P0-P8
P0-P10
A
B
C
D
E
F
G
H
I
J

Figure 4.13. Ingrowth of Golli-τ-eGFP layer VI and VIb fibres to the visual sector of the TRN in the control hemisphere and enucleated hemisphere. A-J. Golli-τ-eGFP fibres project to the visual sector of the TRN (white arrows). The Golli-τ-eGFP fibres project to the TRN in both the control hemisphere and the enucleated hemisphere by P2 and have the same pattern in both. The patterning of the Golli-τ-eGFP fibres within the TRN is not changed over development and is not different between the TRN in the control hemisphere and the enucleated hemisphere. Scale bar= 500μm.

	Intensity threshold used for bar graph	Proportion of pixels above intensity threshold in control dLGN± s.d.	Proportion of pixels above intensity threshold in dLGN receiving input from injected eye± s.d.	p	n
P6 epibatidine injection	70	0.2434 ± 0.1078	0.4747 ± 0.2199	0.0040	7
P6 sterile saline injection	70	0.2949 ± 0.1035	0.3639 ± 0.1980	0.1769	8

Table 4.12. The proportional pixel analysis in the dLGN receiving input from the control eye and the injected eye in animals injected with epibatidine or sterile physiological saline.

My results show that there is premature ingrowth of layer VI and VIb corticothalamic fibres to the epibatidine treated dLGN. This premature entry is not apparent after sterile saline injections thus suggesting that the loss of retinal activity causes layer VI and VIb fibres enter the dLGN prematurely.

However it is important to emphasise that the epibatidine treated dLGN is smaller than the control dLGN. This may suggest that the epibatidine itself damages the eye which then causes degeneration of the retinal ganglion axons. Degeneration of the retinal fibres could mimic monocular enucleation and thus it is possible that premature entry of the corticothalamic fibres to the epibatidine treated dLGN could be due to this, rather than due to the loss of retinal waves. To confirm my epibatidine results it would be valuable to perform retino-geniculate tracing from the injected eyes to confirm the presence of retinal ganglion cells fibres and to use alternative methods to silence the retina. It would be interesting to assess the ingrowth of Golli-τ-eGFP positive VI and VIb fibres when crossed with a mouse in which the retinal waves are abolished such as the nicotinic cholinergic receptor β2 subunit knockout mouse (Rossi et al., 2001; Bansal et al., 2000; Stafford et al., 2009).

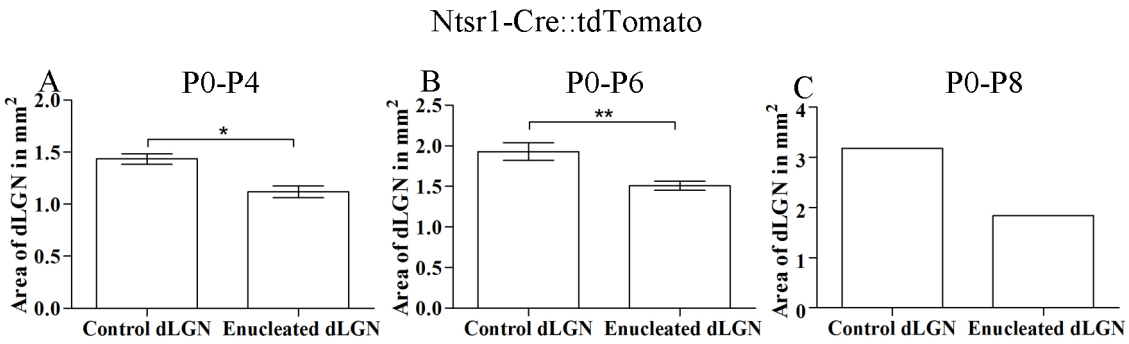

Figure 4.14. Graphs showing area in mm2 of control and enucleated dLGN on coronal slices in the Ntsr1-Cre::tdTomato line. A-C. The area in mm2 of the dLGN in coronal sections. The enucleated dLGN is reduced in size in the Ntsr1-Cre::tdTomato line at P4, P6 and P8. Based on 3 animals at P4, 4 animals at P6 and 1 animal at P8. Values shown on graphs are mean and standard error.

4.3.1.7. Ingrowth of VI and VIb corticothalamic fibres to the thalamic reticular nucleus after enucleation in the Golli-τ-eGFP mouse

In addition to direct connections between the thalamic relay cells and corticothalamic projection neurons, there is an indirect pathway via the GABAergic thalamic reticular nucleus (TRN figure 1.7 in introduction). Layer VI and VIb corticothalamic projection neurons and relay neurons from the thalamus, including the dLGN, innervate the TRN (which receives no direct input from the retina/ sensory periphery) (Molnár and Cordery, 1999; Mitrofanis and Baker, 1993; Molnár et al., 1998a; Jones, 2002b). The GABAergic neurons in the TRN then project to the thalamus and inhibit thalamic relay cells. TRN mediates both feed-forward and feedback inhibition (Lam and Sherman, 2010; Olsen et al., 2012). The TRN has loose modality specific sectors including a visual sector in the dorsal and caudal regions of the nucleus which both V1 and the dLGN project to (Coleman and Mitrofanis, 1996; Lozsadi et al., 1996). The loss of retinal input to the dLGN may alter the input from the dLGN to the visual sector of the TRN and in turn impact on the corticothalamic ingrowth to the visual sector of the TRN.

To assess this I analysed the ingrowth of VI and VIb Golli-τ-eGFP fibres to the visual sector of the TRN in the control hemisphere and enucleated hemisphere over development. The visual sector of the dLGN is the dorsal part of the nucleus in posterior sections (Coleman and Mitrofanis, 1996; Lozsadi et al., 1996). At all ages studied (P2, P4, P6, P8 and P10) the eGFP positive layer VI and VIb fibres enter the TRN in both the

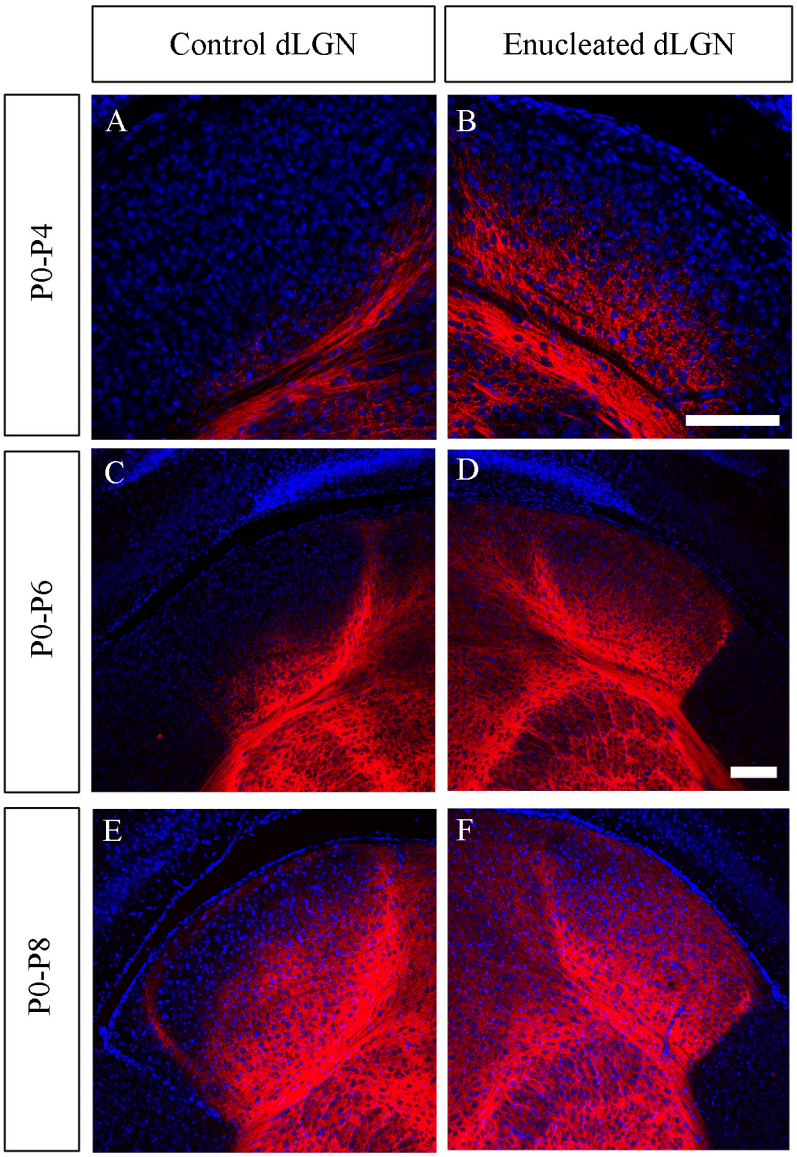

Figure 4.15. Ingrowth of Ntsr1-Cre::tdTomato layer VI fibres into the control and enucleated dLGN over P4, P6 and P8. A. At P4 tdTomato positive fibres have reached the ventral boarder of the control dLGN. B. The tdTomato fibres have entered the ventral part of the enucleated dLGN. C. At P6 the Ntsr1-Cre::tdTomato fibres have begun to enter the control dLGN. D. The fibres have extended throughout the ventral-dorsal extent of the enucleated dLGN however they are denser in the ventral part than the dorsal part. E. At P8 in the control dLGN the fibres have projected into the dorsal part of the dLGN but are not extended to the dorsal most part of the nucleus. F. The fibres are densely arborised throughout the enucleated dLGN, they are denser in the ventral area than the dorsal area. Scale bars= 50μm (A-B, C-F).

control and enucleated hemisphere with the same pattern (figure 4.13 A-J).

My results demonstrate that collateral branches from the layer VI and VIb corticothalamic projections grow into the TRN normally after enucleation. Thus the peripheral input to the dLGN is not important for the proper ingrowth of corticothalamic

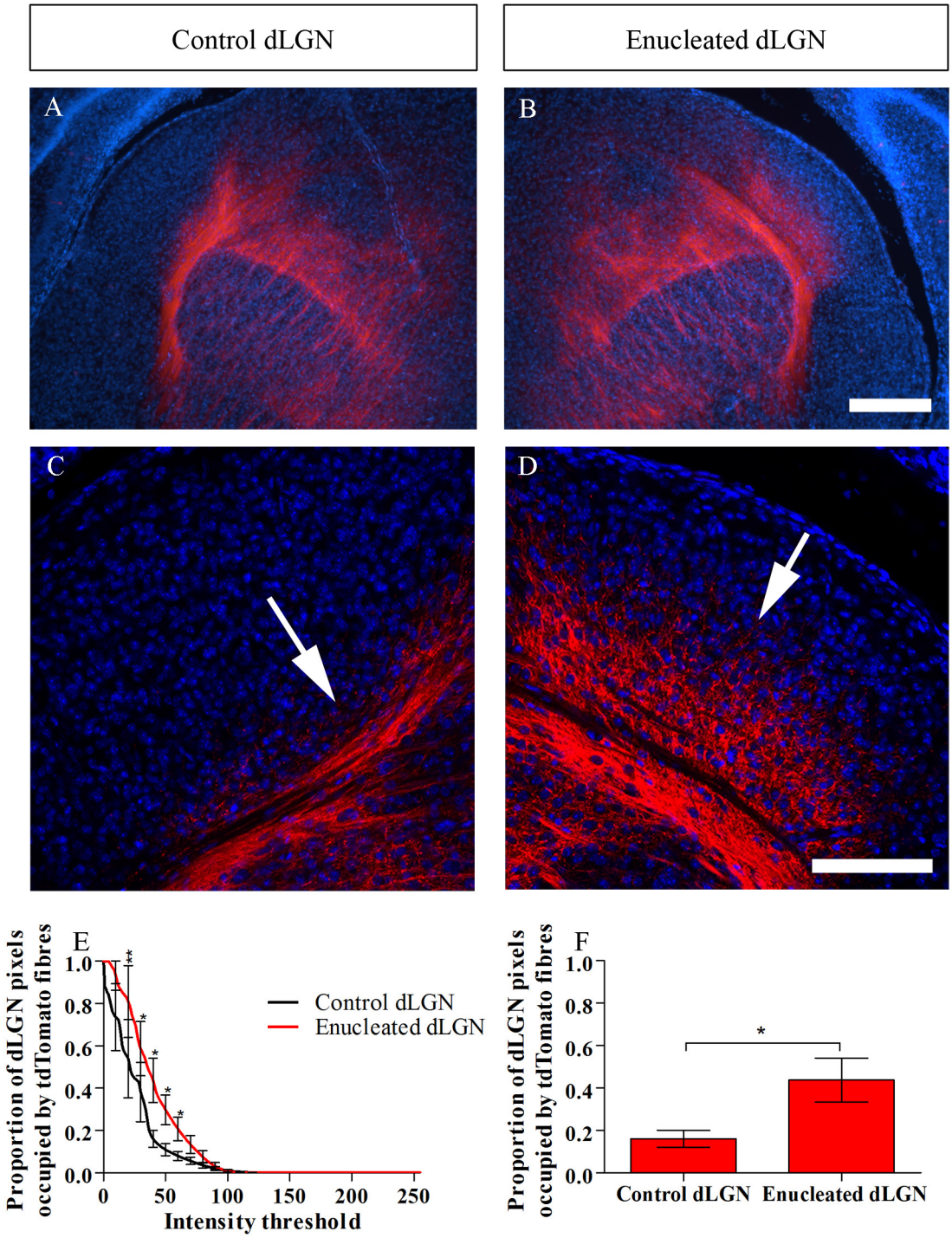

Figure 4.16. Ingrowth of Ntsr1-Cre::tdTomato layer VI fibres into the control and enucleated dLGN at P4. A and B. At P4 tdTomato positive fibres show the normal growth through the VPM and innervate the LP and Po normally. C. At the dLGN Ntrs1-Cre::tdTomato positive fibres form a band at the ventral boarder of the control dLGN (white arrow). D. The tdTomato fibres have entered the enucleated dLGN from the ventral edge and have extended to the middle of the dLGN (white arrow). E. The proportion of pixels in the dLGN with an intensity value over the intensity threshold for all 255 grey scale intensity values. F. The proportion of pixels which are above intensity threshold 40. Based on 3 animals. Values shown on graphs are mean and standard error. Scale bars= 250µm (A-B), 50µm (C-D).

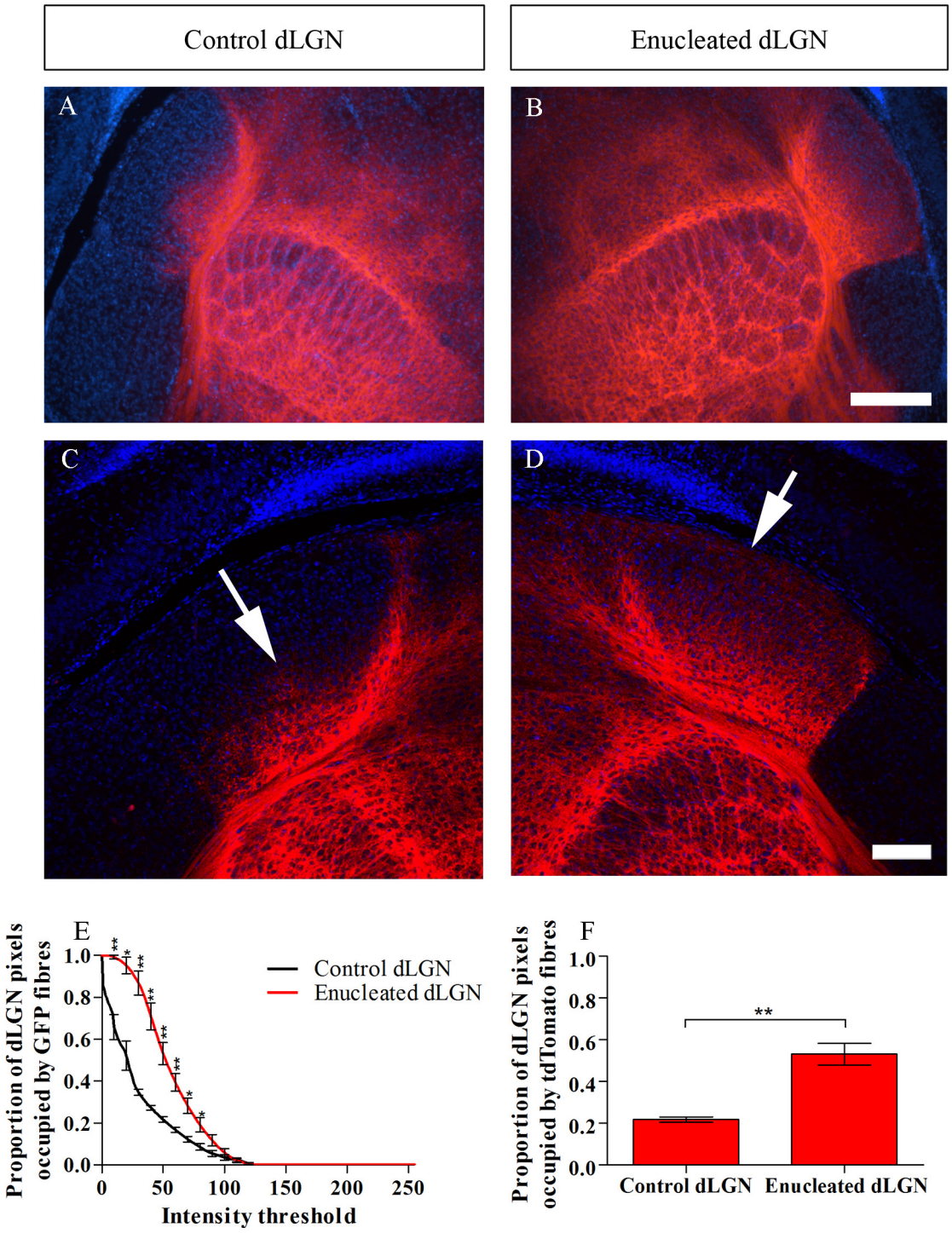

Figure 4.17. Ingrowth of Ntsr1-Cre::tdTomato layer VI fibres into the control and enucleated dLGN at P6. A and B. At P6 the Ntsr1-Cre::tdTomato fibres are patterned with distinct barreloid patterning in the VPM of both control and enucleated hemisphere. Fibres have densely innervated the LP and Po in the control and the enucleated hemisphere. C. At the dLGN Ntrs1-Cre::tdTomato positive fibres have entered the control dLGN from the ventral edge (white arrow). D. In the enucleated dLGN the tdTomato fibres are densely arborised throughout nucleus and have reached the dorsal edge (white arrow). The fibres are most dense in the ventral region of the enucleated dLGN. E. The proportion of pixels in the dLGN with an intensity value over the intensity threshold for all 255 grey scale intensity values. F. The proportion of pixels which are above intensity threshold 50. Based on 4 animals. Values shown on graphs are mean and standard error. Scale bars= 250μm (A-B), 50μm (C-D).

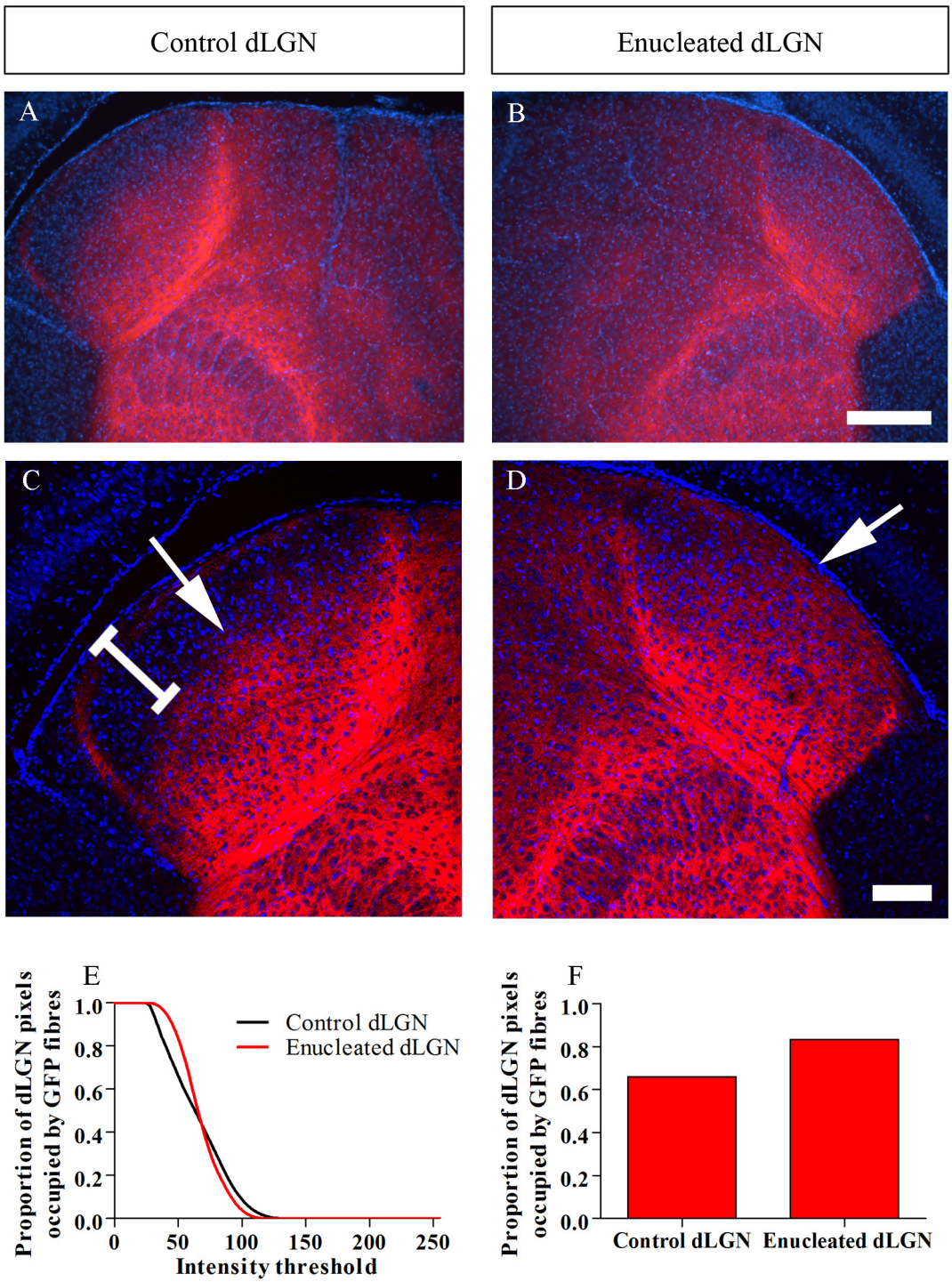

Figure 4.18. Ingrowth of Ntsr1-Cre::tdTomato layer VI fibres into the control and enucleated dLGN at P8. A and B. At P8 the distinctive barreloid patterning of the tdTomato fibres is visible in the VPM of both control and enucleated hemisphere. Fibres have densely innervated the LP and Po in both the control and the enucleated hemisphere. C. At the dLGN Ntrs1-Cre::tdTomato positive fibres have entered the control dLGN from the ventral edge and have extended into the dorsal region of the dLGN (white arrow) but have not yet filled the nucleus and there is a tdTomato fibre negative band in the dorsal area (white bracket). D. In the enucleated dLGN the tdTomato fibres are densely arborised throughout nucleus and have reached the dorsal edge (white arrow). The fibres are most dense in the ventral region of the enucleated dLGN. E. The proportion of pixels in the dLGN with an intensity value over the intensity threshold for all 255 grey scale intensity values. F. The proportion of pixels which are above intensity threshold 50. Based on 1 animal. Values shown on graphs are actual values as Scale bars= 250µm (A-B), 50µm (C-D).

fibres to the TRN.

4.3.1.8. The effect of monocular enucleation on the ingrowth of Ntsr1-Cre::tdTomato layer VI fibres to the dLGN

I have demonstrated that corticothalamic fibres from layer VI and VIb labelled in the Golli-τ-eGFP mouse enter the dLGN prematurely after the loss of retinal input. Ntsr1-Cre::tdTomato labels a subtly different subpopulation of layer VI corticothalamic fibres to the Golli-τ-eGFP VI and VIb line. I therefore chose to test whether monocular enucleation caused premature entry of this layer VI population of corticothalamic fibres.

I first demonstrate that in the Ntsr1-Cre::tdTomato, the area of the dLGN is significantly reduced in the enucleated dLGN compared to the control dLGN at P4, and P6 (figure 4.14, A, B table 4.13). At P8 only one animal in the litter was Cre positive and therefore expressed tdTomato. As such the difference between the sizes of the dLGN could not be statistically assessed but the enucleated dLGN is smaller than the control dLGN (figure 4.14 C, table 4.13).

	Area of control dLGN s.d.	Area of enucleated dLGN ± s.d.	p	n
P4	1.433 ± 0.08711	1.118 ± 0.09820	0.0124	3
P6	1.928 ± 0.2165	1.507 ± 0.1124	0.0040	4
P8	3.177	1.836	-	1

Table 4.13. The area of the dLGN in coronal sections in the control dLGN and enucleated dLGN in the Ntsr1-Cre::tdTomato mouse after monocular enucleation. P value for one tailed, paired t-test used to compare the means at P4 and P6.

My results show that the Ntsr1-Cre::tdTomato positive layer VI fibres enter the enucleated dLGN prematurely, similarly to the Golli-τ-eGFP VI and VIb fibres (figure 4.15).

At P4 Ntrs1-Cre::tdTomato positive fibres form a band at the ventral border of the control dLGN (figure 4.16 C). The tdTomato fibres have entered the enucleated dLGN as far as the middle of the dLGN (figure 4.16 D). The enucleated dLGN has a significantly higher proportion of bright pixels than the control dLGN (figure 4.16 E and F, table 4.13). The curves in figure 4.15 E are less smooth than the graphs for the Golli-τ-eGFP. This difference may be due to the difference between red tdTomato

fluorescence and green eGFP fluorescence.

Ntsr1-Cre:: tdTomato	Intensity threshold used for bar graph	Proportion of pixels above intensity threshold in control dLGN± s.d.	Proportion of pixels above intensity threshold in enucleated dLGN± s.d.	p	n
P4	40	0.1605 ± 0.07000	0.4373 ± 0.1802	0.0245	3
P6	50	0.2167 ± 0.02465	0.5310 ± 0.1046	0.0047	4
P8	50	0.6608	0.8344	-	1

Table 4.14. Mean and s.d. of pixels above the given intensity threshold in the Ntsr1-Cre::tdTomato dLGN with and without retinal input manipulated by monocular enucleation. P value for one tailed, paired t-test used to compare the means at P4 and P6.

At P6 the layer VI fibres have begun to enter the control dLGN from the ventral edge (figure 4.17 C). The tdTomato fibres have extended throughout the entire enucleated dLGN arborising most densely in the ventral region (figure 4.17 D). The enucleated dLGN has significantly more bright pixels than the control dLGN (figure 4.17 E and table 4.14).

At P8 the sole Ntsr1-Cre positive brain showed a clear difference between the ingrowth of layer VI Ntsr1-Cre::tdTomato fibres into the control and the enucleated dLGN. The tdTomato layer VI fibres arborise in the ventral region of the control dLGN (figure 4.18 C). In the enucleated dLGN the tdTomato positive fibres densely arborise throughout the nucleus although they are still densest in the ventral half of the dLGN (figure 4.18 D). The pixel analysis confirms the difference between the control and the enucleated dLGN. At lower thresholds the enucleated dLGN has a higher proportion of bright pixels (figure 4.18 E). However the enucleated dLGN has a steeper curve than the control dLGN and thus at threshold 69-70 the proportion of bright pixels in the enucleated dLGN drops below that of the control dLGN. Despite this the images demonstrate that the tdTomato positive fibres have extended further throughout the enucleated dLGN (to the dorsal edge; figure 4.18 C and D). Therefore, whilst at higher thresholds the control dLGN may have more intense pixels, the tdTomato fibres still appear to have progressed further in the enucleated dLGN. Increased n numbers may confirm this result.

I conclude from these experiments that at P4, P6 and P8 the layer VI fibres labelled by Ntsr1-Cre::tdTomato enter the enucleated dLGN prematurely. This mimics the results obtained in the Golli-τ-eGFP mouse where there is a stronger VIb component. These results confirm that losing retinal input affects distinct subpopulations of layer VI corticothalamic neurons as they grow into the dLGN.

4.3.1.9. Enucleation causes premature entry of layer VI and VIb fibres to the dLGN

In both the Golli-τ-eGFP and the Ntsr1-Cre::tdTomato lines the removal of retinal input causes premature entry of layer VI and VIb fibres to the dLGN. These analyses focus primarily on the dLGN however during my research I did not observe any differences between the control and enucleated hemisphere in other thalamic nuclei.

4.3.1.10. The effect of loss of retinal input by monocular enucleation on the Rbp4-Cre::tdTomato labelled layer V fibre projection through the dLGN

I have demonstrated that the loss of retinal input to the dLGN causes premature ingrowth of layer VI and VIb corticothalamic fibres to the dLGN. In chapter 3, I showed that Rbp4-Cre::tdTomato layer V does not innervate the first order dLGN, instead projecting to higher order nuclei including the LP and the Po. These layer V corticothalamic projections are driver inputs which means they drive activity in the postsynaptic neurons in the higher order nuclei (unlike modulator inputs which modulate the action of driver inputs) (Sherman and Guillery, 1998).

The loss of retinal input deprives the dLGN of its main driver input. Thus whilst enucleation has caused premature modulator ingrowth (from layer VI) to the dLGN, the dLGN may still lack driver input as it is unclear whether the layer VI modulatory inputs can drive dLGN neurons. The plastic nature of the developing brain means that various systems, including the visual system, show cross-modal plasticity after peripheral deprivation. This includes rewiring auditory input to visual cortex after visual deprivation (Izraeli et al., 2002; Chabot et al., 2008; Chabot et al., 2007; Charbonneau et al., 2012) and somatosensory input to the visual cortex after visual deprivation (Toldi et al., 1993; Toldi et al., 1996; Negyessy et al., 2000; Dye et al., 2012). Furthermore cross-modal plasticity has been demonstrated within the thalamus; peripheral deprivation can

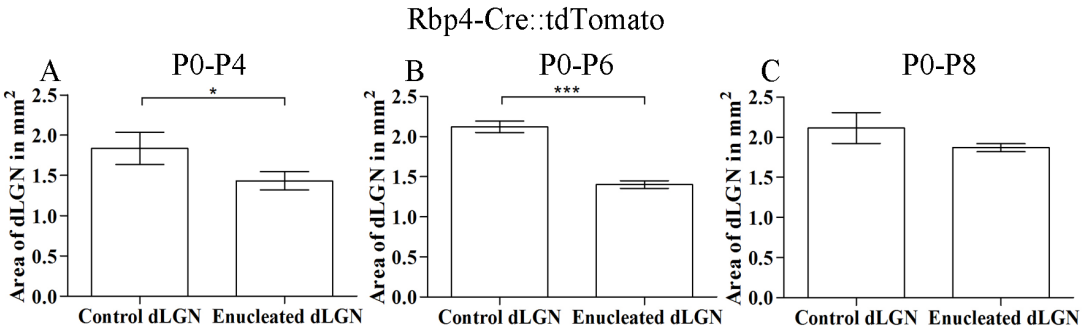

Figure 4.19. Graphs showing area in mm2 of control and enucleated dLGN on coronal slices in the Rbp4-Cre::tdTomato line. A-C. The area in mm2 of the dLGN in coronal sections. The enucleated dLGN is reduced in size in the Rbp4-Cre::tdTomato line at P4, P6 and P8. Results based on 3 animals at P4, 4 animals at P6 and 3 animals at P8. Values shown on graphs are mean and standard error.

alter the targeting of afferent axon populations from the sensory periphery to different thalamic nuclei, for example inducing retinal fibres to target the usually auditory thalamic nucleus the MGN (Sur et al., 1988; Asanuma and Stanfield, 1990; Angelucci et al., 1997).

Despite this focus on cross-modal plasticity little has been studied of cross-hierarchical plasticity (plasticity between first order and higher order thalamic nuclei and their targets). Recent work has demonstrated that the genetic ablation of the primarily first order VB (ventrobasal nucleus includes VPM and VPL) causes rewiring of the inputs from the Po into layer IV of the primary somatosensory cortex (Pouchelon et al., 2014b). The Po is a higher order thalamic nucleus which normally projects to layer IV of the association somatosensory cortex.

The Rbp4-Cre::tdTomato line which I have characterised offers me a unique opportunity to assess whether there is also cross-hierarchical plasticity of corticothalamic fibres following sensory deprivation. I therefore assessed whether the loss of retinal driver input onto dLGN neurons could induce the layer V fibres, which normally provide driver input exclusively to the higher order thalamic nuclei, to innervate the dLGN.

In the Rbp4-Cre::tdTomato positive mouse the area of the dLGN in coronal sections is significantly smaller after enucleation at P4 and P6 (figure 4.19 A and B, table 4.15). At P8 the area of the dLGN is smaller however the difference is not statistically significant.

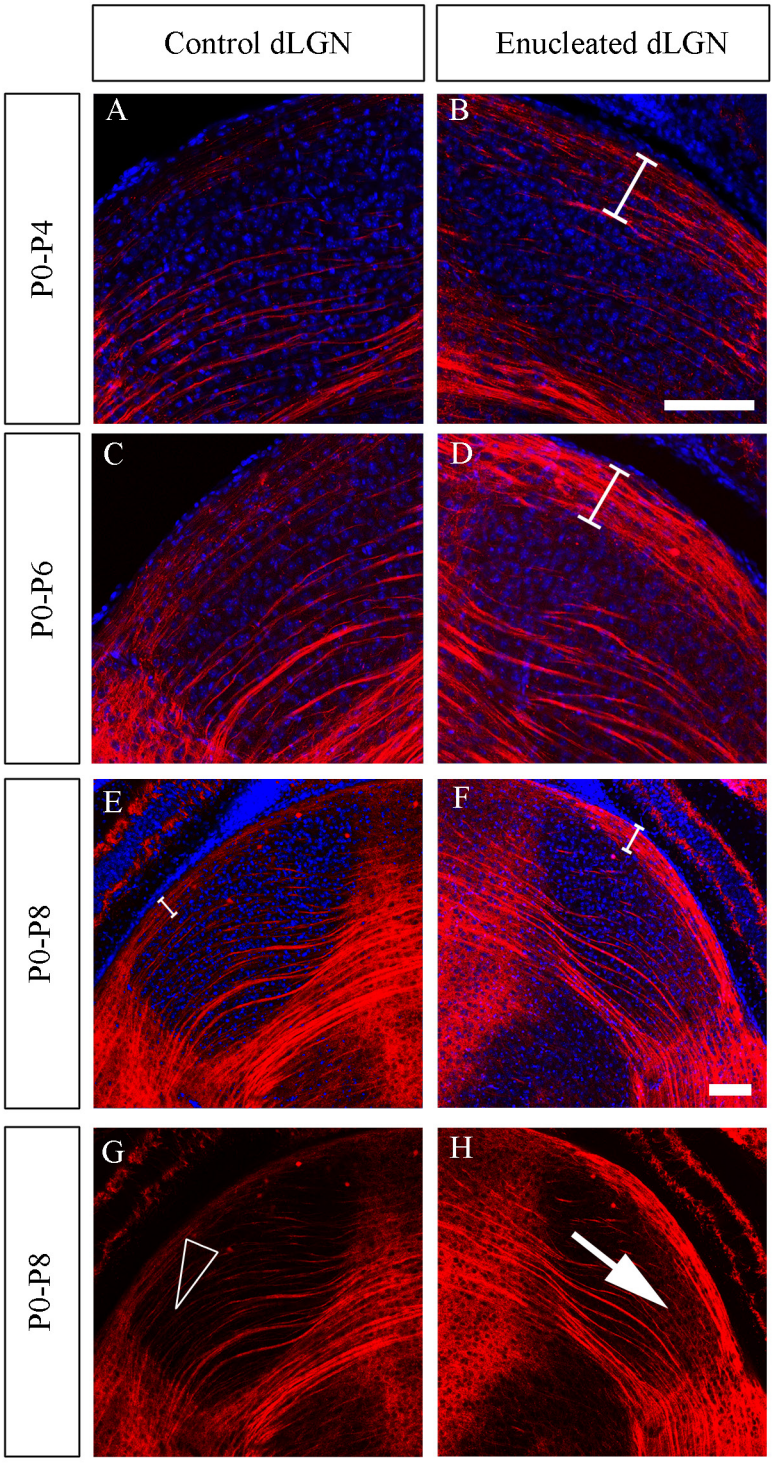

Figure 4.20. Ingrowth of Rbp4-Cre::tdTomato layer V fibres into the control and enucleated dLGN over P4, P6 and P8. A. At P4 layer V tdTomato positive fibres extended through the control dLGN. B. In the enucleated dLGN the layer V tdTomato fibres still projected through the dLGN however fewer fibres are visible in the ventral part compared to the control dLGN and they appear to be in smaller fascicles than in the control dLGN. There was increased density of fibres in a band across the dorsal part of the enucleated dLGN (white bracket). C. At P6 there are bundles of Rbp4-Cre::tdTomato fibres crossing the control dLGN. In more ventral regions the fibres are fasciculated in bundles. In the dorsal region the fibres are less fasciculated but do not have visible arborisations in the dLGN. D. In the enucleated dLGN the bundles traversing the ventral part of the dLGN are present. The band of fibres in the dorsal region is substantially denser in the enucleated dLGN compared to the control dLGN (white bracket) with fibres passing through the dLGN and an increased appearance of arborisations in the dorsal region. E.

At P8, fibres passing through the ventral control dLGN are still present and there appears to be a slightly denser band at the dorsal edge of the dLGN (white bracket) although no fibres are visible branching off or arborising. F. In the enucleated dLGN the ventral fibres are projecting through the dLGN and the dense band of fibres in the dorsal dLGN is still apparent (white bracket). In the lateral corner of the enucleated dLGN there appears to be increased density of fibre branches/ arborisations (seen clearly at P8 white arrow H.) which are not present in the control dLGN (hollow arrow head G). Scale bars= 50µm (A-D, E- H).

	Area of control dLGN s.d.	Area of enucleated dLGN ± s.d.	p	n
P4	1.836 ± 0.3461	1.434 ± 0.1965	0.0224	3
P6	2.122 ± 0.1406	1.402 ± 0.09496	0.0002	4
P8	2.114 ± 0.3322	1.870 ± 0.08951	0.1545	3

Table 4.15. The area of the dLGN in coronal sections is reduced in the enucleated dLGN.

4.3.1.11. Loss of retinal input causes cross-hierarchical re-wiring of layer V fibres to the first order dLGN

My results demonstrate that after monocular enucleation the layer V fibres rewire to innervate the enucleated dLGN (figure 4.20). This has not been observed in control conditions at any stages of development or adulthood.

At P4 in the control dLGN layer V fibres project through the nucleus in fasciculated bundles which do not branch into the dLGN. The bundles of fibres are more numerous in the ventral region of the dLGN (figure 4.21 C). In the enucleated dLGN the ventral bundles of fibres are still present however they appear less numerous. Additionally there is an increased density of tdTomato positive layer V fibres in a dorsal band (figure 4.21 D). Furthermore in the lateral corner of the enucleated dLGN there are branches arising from the tdTomato positive layer V fibres (figure 4.21 F). These branches are not present in the control dLGN.

I performed two types of pixel analysis on the layer V projections labelled in the Rbp4-Cre::tdTomato mice that innervate the enucleated and control dLGN. I first drew a line of up to 300µm across the dLGN from dorsal to ventral, midway through the nucleus (for placement of line see methods, figure 4.1 D). I then analysed the intensity of the pixels along this single line. This analysis demonstrates that in the dorsal region of the dLGN (the first 100µm of the line) the pixels are of a higher intensity value in the enucleated dLGN compared to the control dLGN (figure 4.21 G). The trace also shows

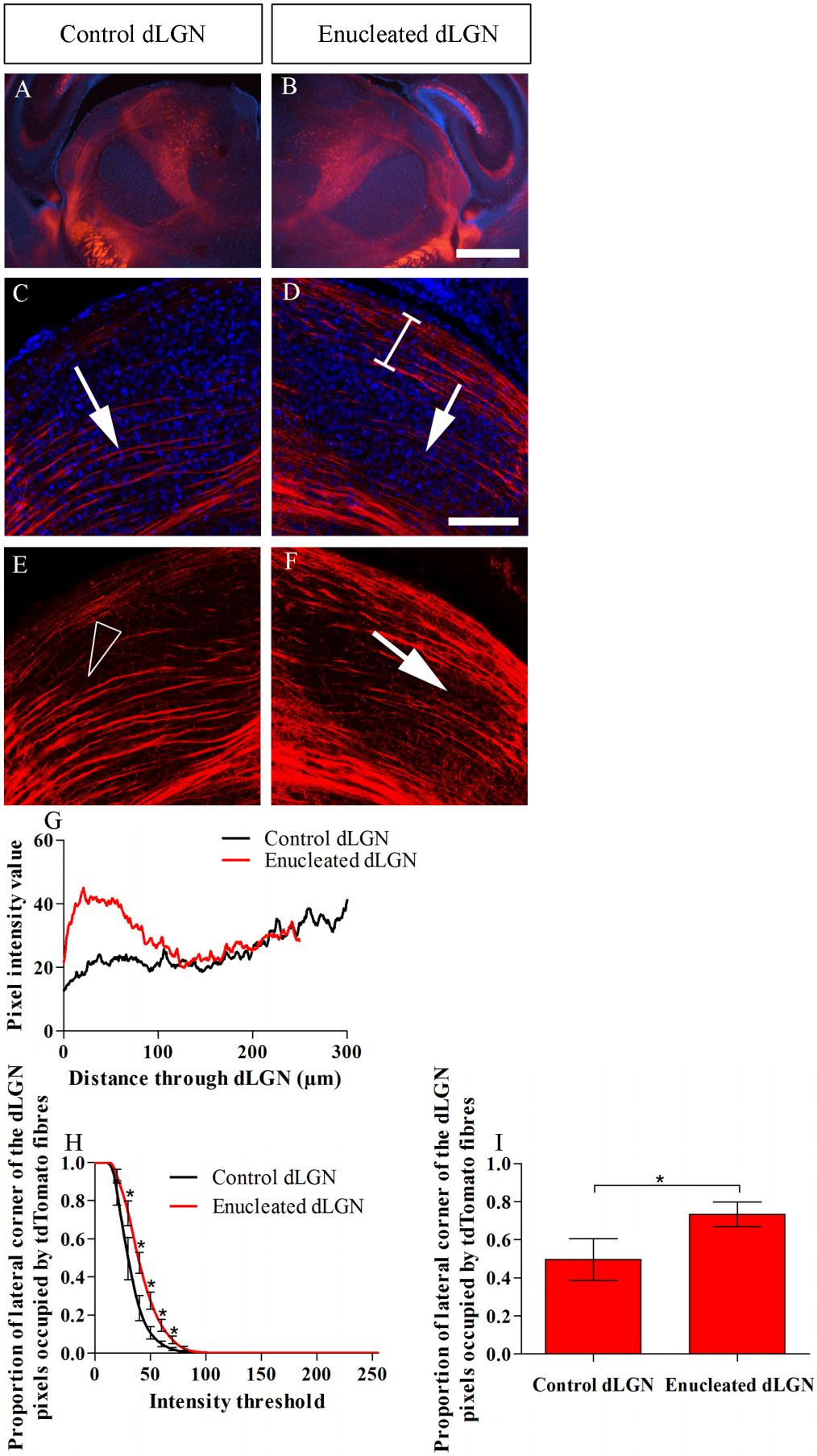
Control dLGN
Enucleated dLGN
A
B
C
D
E
F
G
Control dLGN
Enucleated dLGN
Pixel intensity value
Distance through dLGN (µm)
H
Control dLGN
Enucleated dLGN
Proportion of lateral corner of the dLGN pixels occupied by tdTomato fibres
Intensity threshold
I
Proportion of lateral corner of the dLGN pixels occupied by tdTomato fibres
Control dLGN
Enucleated dLGN

Figure 4.21. Ingrowth of layer V Rbp4-Cre::tdTomato fibres through the control and enucleated dLGN at P4. A and B. The layer V fibres grow through the thalamic nuclei in the control and enucleated hemisphere, there is no difference in pattern between the two hemispheres. C. Layer V tdTomato fibres project through the control dLGN in bundles which do not branch into the dLGN. The bundles of fibres are more numerous in the ventral part of the dLGN (white arrow). D. Layer V tdTomato fibres project through the enucleated dLGN however fibres are less numerous in the ventral region (white arrow) and in the dorsal region there is a denser band of fluorescent fibres (white bracket). E. In the control dLGN there is little branching of smaller fibres from the thicker bundles (hollow arrow head). F. In the enucleated dLGN thin fibres branch off from the thicker bundles and innervate the dLGN (white arrow). G. Pixel analysis along a 300μm line drawn from the dorsal edge of the dLGN demonstrates increased pixel intensity in the first 100μm of the enucleated dLGN compared to control dLGN. The enucleated dLGN is thinner than the control one and so intensity values were only taken along a line of 250μm. H. The proportion of pixels in the lateral corner of the dLGN with an intensity value over the intensity threshold for all 255 grey scale intensity values. I. The proportion of pixels which are above intensity threshold 30. Based on 3 animals. Values shown on graph G are the mean, values on H and I are mean ± SEM. Scale bars= 250μm (A and B.), 50μm (C-F.).

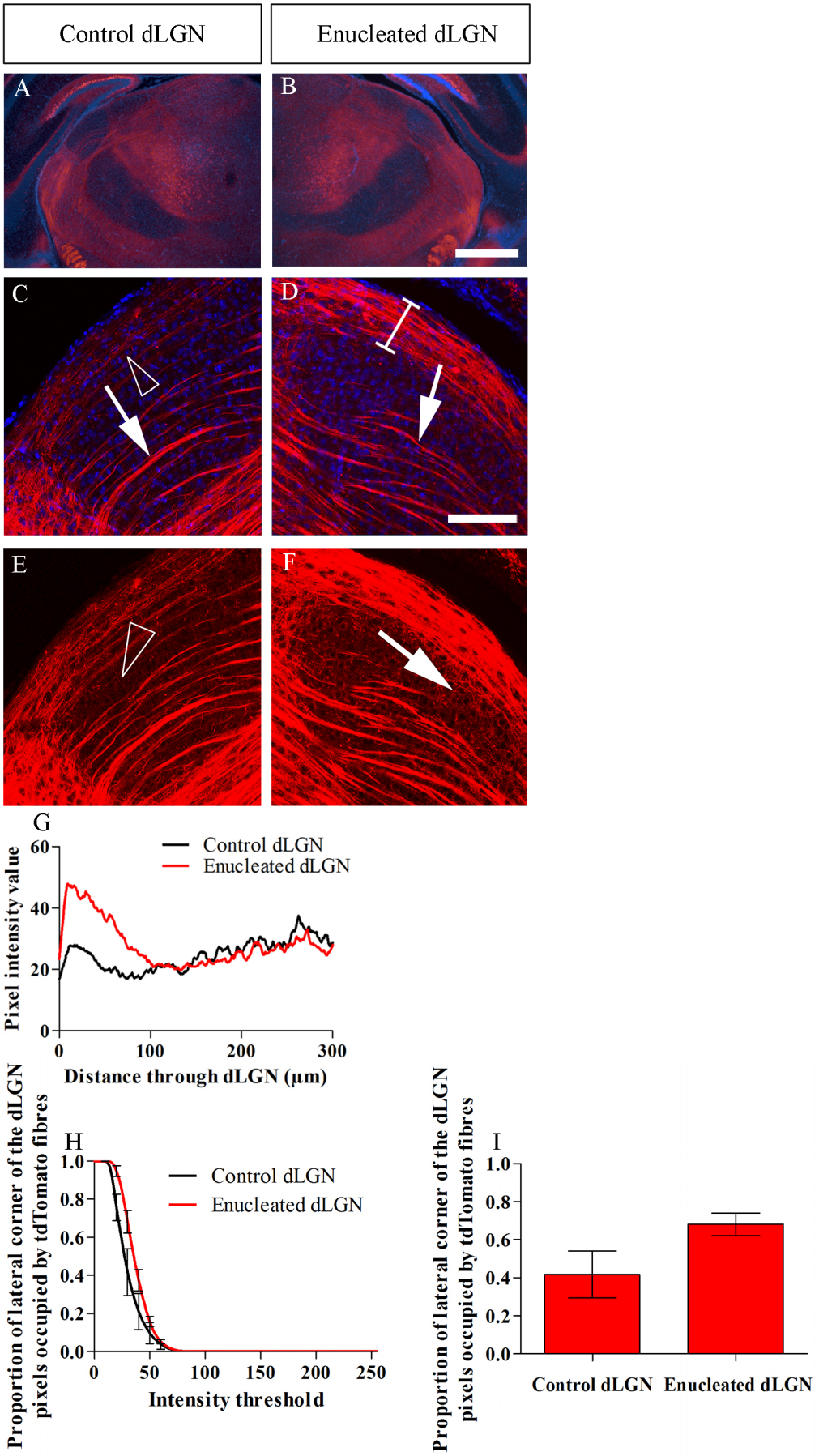
Control dLGN
Enucleated dLGN
A
B
C
D
E
F
G
Control dLGN
Enucleated dLGN
Pixel intensity value
60
40
20
0
0
100
200
300
Distance through dLGN (µm)
H
Control dLGN
Enucleated dLGN
Proportion of lateral corner of the dLGN pixels occupied by tdTomato fibres
1.0
0.8
0.6
0.4
0.2
0.0
0
50
100
150
200
250
Intensity threshold
I
Proportion of lateral corner of the dLGN pixels occupied by tdTomato fibres
1.0
0.8
0.6
0.4
0.2
0.0
Control dLGN
Enucleated dLGN

Figure 4.22. Ingrowth of layer V Rbp4-Cre::tdTomato fibres through the control and enucleated dLGN at P6. A and B. There is a similar pattern of fibre growth through the thalamic nuclei in the control and enucleated hemisphere. C. At P6 the layer V tdTomato fibres project through the control dLGN in fasciculated bundles which are more numerous in the ventral part of the dLGN (white arrow). In the dorsal region the fibres are less fasciculated but do not have visible arborisations in the dLGN (hollow arrow head). D. In the enucleated dLGN the bundles traversing the ventral part of the dLGN are present (white arrow). The band of fibres in the dorsal region is substantially denser in the enucleated dLGN compared to the control dLGN (white bracket) with fibres passing through the dLGN and an increased appearance of arborisations in the dorsal region. E. The tdTomato positive fibres project through the control dLGN without branching (hollow arrow head). F. The tdTomato positive fibres projecting through the enucleated dLGN generate small branches which innervate the dLGN (white arrow). G. Analysis of pixel intensity along a 300μm line drawn from the dorsal edge of the dLGN demonstrates increased pixel intensity in the first 100μm of the enucleated dLGN compared to control dLGN. H. The proportion of pixels in the lateral corner of the dLGN with an intensity value over the intensity threshold for all 255 grey scale intensity values. I. The proportion of pixels which are above intensity threshold 30. Based on 4 animals. Values shown on graph G are the mean, values on H and I are mean ± SEM. Scale bars= 250μm (A and B), 50μm (C-F.).

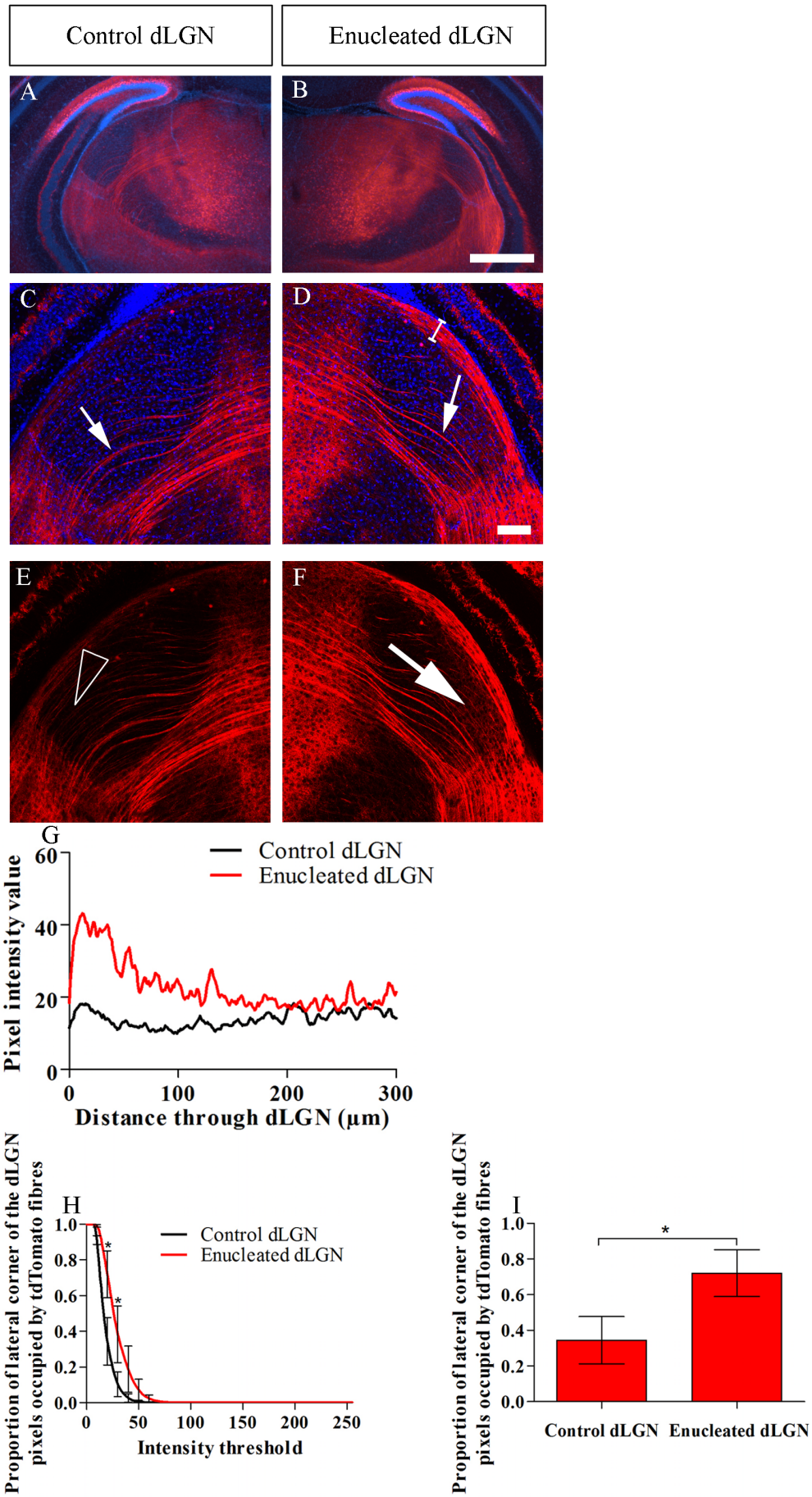
Control dLGN
Enucleated dLGN
A
B
C
D
E
F
G
Control dLGN
Enucleated dLGN
Pixel intensity value
60
40
20
0
0
100
200
300
Distance through dLGN (µm)
H
Proportion of lateral corner of the dLGN pixels occupied by tdTomato fibres
1.0
0.8
0.6
0.4
0.2
0.0
0
50
100
150
200
250
Intensity threshold
Control dLGN
Enucleated dLGN
*
*
I
Proportion of lateral corner of the dLGN pixels occupied by tdTomato fibres
1.0
0.8
0.6
0.4
0.2
0.0
*
Control dLGN
Enucleated dLGN

Figure 4.23. Ingrowth of layer V Rbp4-Cre::tdTomato fibres through the control and enucleated dLGN at P8. A and B. There is a similar pattern of fibre growth through the thalamic nuclei in the control and enucleated hemisphere. C. In the control dLGN at P8 the layer V tdTomato fibres which project in bundles through the ventral dLGN, are still present (white arrow). D. In the enucleated dLGN the bundles traversing the ventral part of the dLGN are present (white arrow). The band of fibres in the dorsal region is substantially denser in the enucleated dLGN compared to the control dLGN (white bracket) with fibres passing through the dLGN and an increased appearance of arborisations in this band in the dorsal region of the nucleus. E and F. At P8, in the lateral corner of the enucleated dLGN there appears to be increased density of fibre arborisations (white arrow E.) which are not present in the control dLGN (hollow arrow head F.). G. Analysis of pixel intensity along a 300μm line drawn from the dorsal edge of the dLGN demonstrates increased pixel intensity in the first 200μm of the enucleated dLGN compared to control dLGN. H. The proportion of pixels in the lateral corner of the dLGN with an intensity value over the intensity threshold for all 255 grey scale intensity values. I. The proportion of pixels which are above intensity threshold 20. Based on 3 animals. Values shown on graph G are the mean, values shown in graphs H and I are mean and standard error. Scale bars= 250μm (A and B.), 50μm (C.-F.).

that the intensity of pixels along the line from 100-300μm are no different between control and dLGN. These results confirm the presence of increased layer V tdTomato fibres in the dorsal side of the nucleus after enucleation. This may be due to abnormal arborisation and branching of the tdTomato positive fibres within the dorsal dLGN. They also indicate that this may not be simple re-arrangement of the fibres because there is no difference in intensity in more ventral regions of the dLGN.

I then performed proportional pixel intensity analysis of the lateral corner of the dLGN to quantify the difference in branching of the layer V fibres in the enucleated and control dLGN (for outline of lateral half of dLGN see methods, figure 4.1 E). The lateral corner of the dLGN was chosen rather than analysing the whole dLGN because the branched fibres are only visible in the lateral half of the dLGN. Analysing the whole dLGN may have hidden any difference between controls and enucleated. At P4 there is a significantly higher proportion of brighter pixels in the lateral corner of the enucleated dLGN compared to the control dLGN (figure 4.21 H).

Rbp4-Cre:: tdTomato	Intensity threshold used for bar graph	Proportion of pixels above intensity threshold in lateral half of control dLGN± s.d.	Proportion of pixels above intensity threshold in lateral half of enucleated dLGN± s.d.	p	n
P4	30	0.4958 ± 0.1902	0.7343 ± 0.1117	0.0262	3
P6	30	0.4172 ± 0.2466	0.6813 ± 0.1183	0.1074	4
P8	20	0.3442 ± 0.2301	0.7209 ± 0.2268	0.0212	3

Table 4.15. Proportion of pixels above the given intensity threshold in the lateral corner of the control and the enucleated dLGN. At P4 and P8 the difference was significant as tested by one tailed, paired t-test. At P6 the difference was not significant but was in the same direction as other results.

At P6 in the enucleated dLGN the band of tdTomato positive layer V fibres in dorsal area of the dLGN is substantially denser than the control dLGN (figure 4.22 C and D). Furthermore in the lateral corner of the enucleated dLGN there are branches/ arborisations arising from the tdTomato positive layer V fibres (figure 4.22 F). The pixels are of a higher intensity value in the dorsal region of the enucleated dLGN compared to the control dLGN (figure 4.22 G). In the lateral corner of the dLGN there was a higher proportion of bright pixels in the enucleated dLGN however the results were not significant (figure 4.22 H, I, table 4.15).

By P8 in the enucleated dLGN the band of Rbp4-Cre::tdTomato positive layer V fibres in dorsal area of the enucleated dLGN is substantially denser than the control dLGN (figure 4.23 C D). Furthermore in the lateral corner of the enucleated dLGN there are clear tdTomato positive branches arising from the layer V fibres and innervating the enucleated dLGN (figure 4.23 F). At this age they are patterned around the cell bodies within the dLGN thus suggesting they are arborising (figure 4.23 F). These branches are not present in the control dLGN (figure 4.23 E). Pixel analysis along the line demonstrated that in the dorsal region the pixels were of a higher intensity value in the enucleated dLGN compared to the control dLGN (figure 4.23 G). At P8 there was a significantly higher proportion of bright pixels in the lateral corner of the enucleated dLGN compared to the control dLGN (figure 4.23 H, I, table 4.15).

My results demonstrate that after enucleation the layer V fibres (labelled by Rbp4-Cre::tdTomato) display aberrant ingrowth into the dLGN. Firstly the layer V fibres form a dense band along the dorsal edge of the nucleus which may be due to arborisations from the layer V fibres which do not normally branch into the dLGN. Furthermore the layer V fibres extending through the enucleated dLGN generate branches which appear to arborise within the lateral dLGN. This is dramatically different to the control dLGN into which layer V fibres do not project. As the dLGN is a first order nucleus, layer V fibres do not normally innervate it. Therefore these results demonstrate that after the loss of retinal input to one dLGN the layer V fibres appear to rewire into the dLGN and

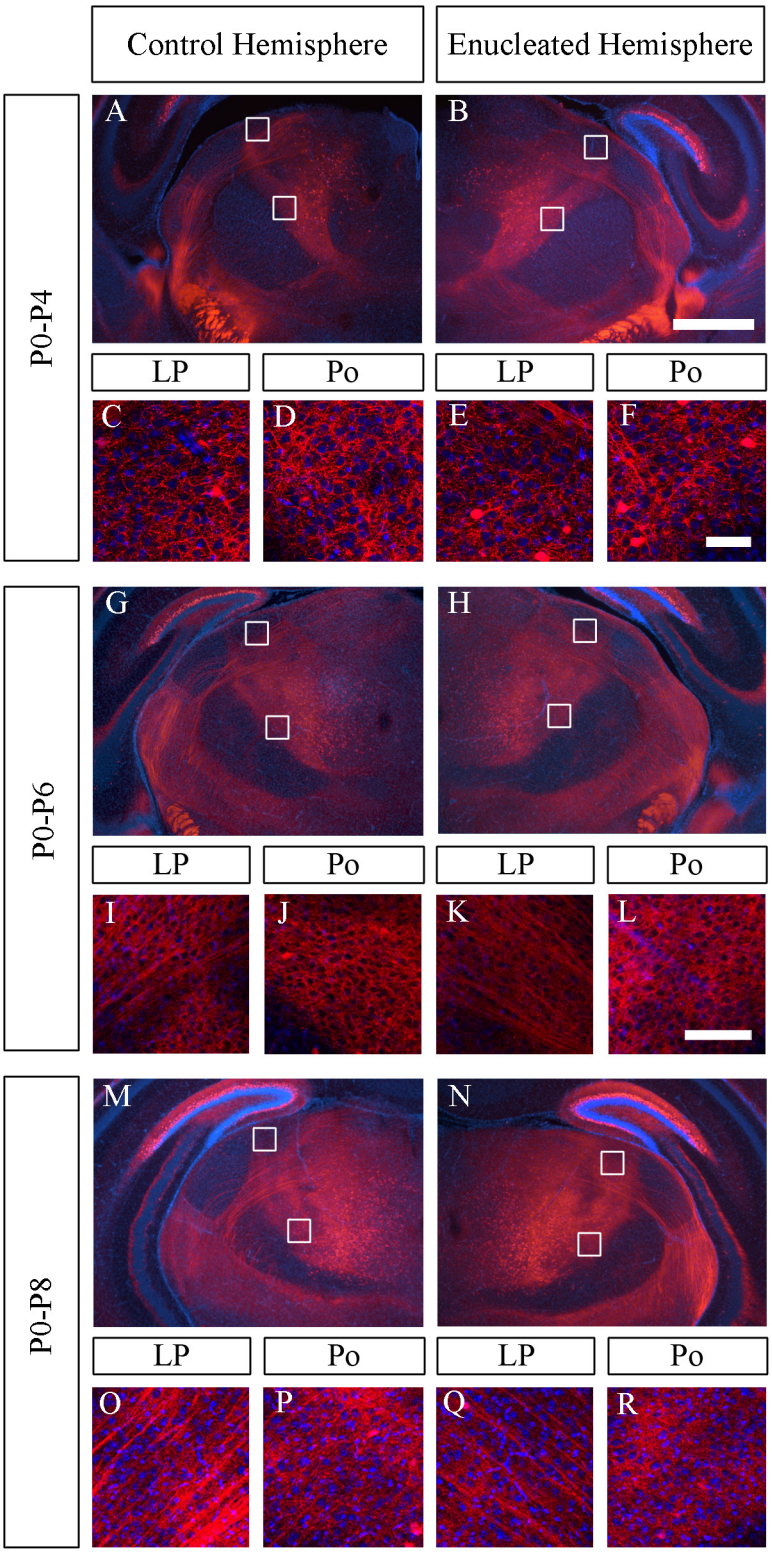

Figure 4.24. Patterning of layer V Rbp4-Cre::tdTomato positive corticothalamic fibres in the higher order posterior and lateral posterior thalamic nuclei of the control and enucleated hemisphere. At P4, P6 and P8 the patterning of tdTomato positive layer V fibres within the lateral posterior thalamic nucleus (LP) and the posterior thalamic nucleus (Po) was not altered in the hemisphere to which retinal input had been removed. White boxes represent area shown in higher magnification images. Abbreviations used: LP, lateral posterior thalamic nucleus; Po, posterior thalamic nucleus. Scale bars= 250μm (A, B, G, H, M, N.) and 25μm (C-F, I-R.).

begin to innervate it.

4.3.1.12. Monocular deprivation does not alter layer V corticothalamic ingrowth to higher thalamic nuclei LP and Po

I have demonstrated that following visual deprivation by monocular enucleation the layer V corticothalamic fibres labelled in Rbp4-Cre::td Tomato rewire to innervate the first order dLGN. Layer V fibres normally innervate exclusively higher thalamic nuclei including the LP and the Po. I next assessed whether the layer V corticothalamic ingrowth to the LP and Po is disrupted by loss of retinal input to one hemisphere. The higher order nuclei do not normally receive input from the retina and therefore any effect is likely to arise from rewiring or a systemic effect. The LP is a visual higher order nucleus (Kamishina et al., 2009; Reep et al., 1994) and the Po is the somatosensory higher order nucleus (Kichula and Huntley, 2008; Viaene et al., 2011a; Ohno et al., 2012).

My results demonstrate that there is no effect of loss of retinal input on the ingrowth of layer V, Rbp4-Cre::tdTomato, corticothalamic fibres to the higher order LP or Po at P4, P6 and P8 (figure 4.24). At all ages in both the control and the enucleated hemisphere Rbp4-Cre::tdTomato fibres are visible arbourising densely in the LP and Po. In addition there are some bundles of tdTomato positive fibres which can be seen traversing through the LP projecting to more medial nuclei.

My results suggest that ablation of major driver input from the retina induced the rewiring of layer V corticothalamic inputs to the first order dLGN. However, it does not affect the ingrowth of layer V corticothalamic fibres to the higher order LP and Po.

4.3.2. Early peripheral manipulation alters corticotectal ingrowth

4.3.2.1. The effect of visual deprivation by monocular enucleation on the ingrowth of layer V Rbp4-Cre::tdTomato positive fibres to the superficial grey layer of the superior colliculus

Above I have demonstrated that the loss of retinal input causes the premature ingrowth of layer VI and VIb modulator fibres to the deprived dLGN, and induces layer V driver inputs to rewire to innervate the deprived dLGN. I have also demonstrated that the

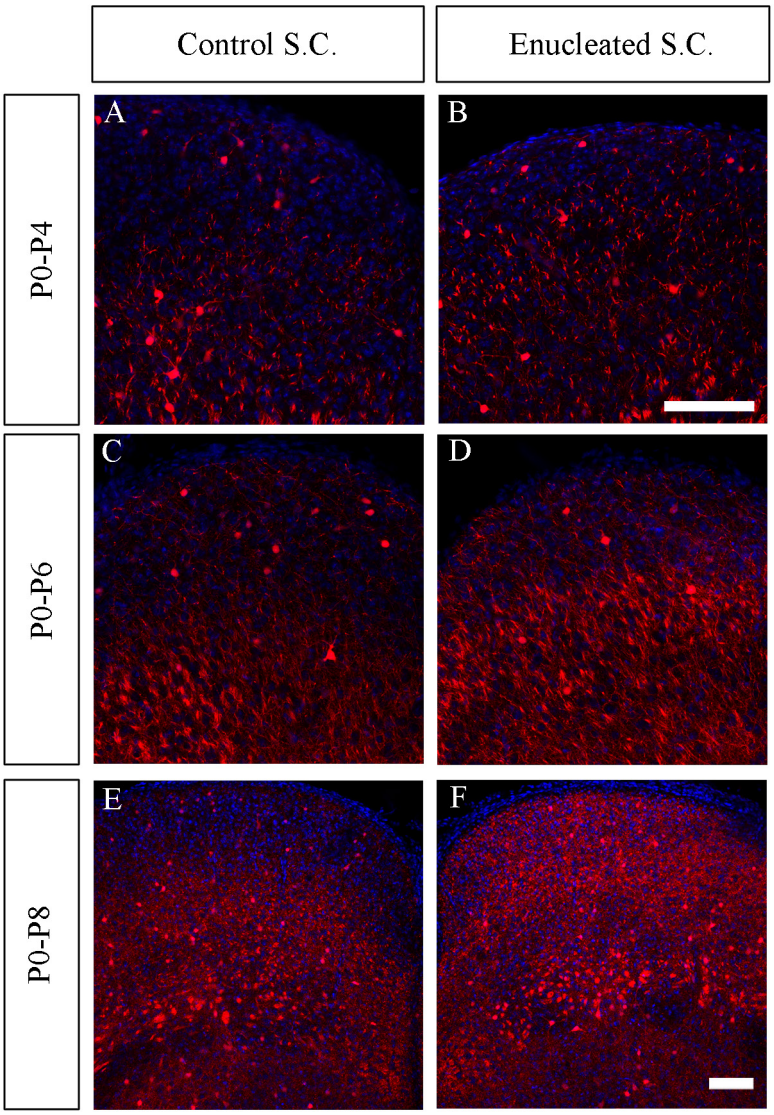

Figure 4.25. Layer V Rbp4-Cre::TdTomato fibre ingrowth to the control and enucleated superior colliculus over development. A-B. At P4 tdTomato positive layer V fibres are visible in the optic nerve layer of the superior colliculus. There are sparse fibres in the superficial grey layer of the control superior colliculus and more fibres are visible in the enucleated superior colliculus. C-D. By P6 the layer V tdTomato positive fibres are in the optic nerve layer of the superior colliculus. In the superficial grey layer of the superior colliculus, layer V fibres are visible in the control superior colliculus. In the enucleated superior colliculus the fibres are denser in the superficial grey, compared to the control superficial grey. E-F. At P8 the layer V tdTomato positive fibres are visible in dense bundles of fibres in the optic nerve layer of both control and enucleated superior colliculus. Layer V fibres are visible in the superficial grey layer in both control and enucleated superior colliculus however they are substantially denser in the superficial grey of the enucleated superior colliculus compared to the control superior colliculus. Scale bars= 50μm (A-D, E-F).

ingrowth of cortical fibres to corticothalamic targets which are not retino-recipient (the visual sector of the TRN and the higher order lateral posterior and posterior thalamic nuclei) is not disrupted after monocular enucleation (figure 4.13 and 4.24).

In the adult mouse dLGN, layer VI corticothalamic synapses outnumber the synapses from the retina. As such the premature entry of corticothalamic fibres after the loss of retinal input could be due to the loss of an inhibitory cue from the retina which prevents corticothalamic fibres from entering and synapsing until the appropriate time. In order to assess whether there is a general retinal mechanism which prevents early ingrowth of corticofugal fibres to their target I chose to look at another retino-recipient, cortico-recipient structure.

The superior colliculus receives driver input from the contralateral eye (Drager and Hubel, 1975; Lund, 1965; Godement et al., 1984; Godement et al., 1980). Furthermore layer V cortical fibres innervate the superior colliculus (De Carlos and O'Leary, 1992; Clascá et al., 1995). The corticofugal projections to the superior colliculus contribute to multimodal map registration and topography (King, 2004). This retina-colliculus-thalamus-cortex (extra-geniculocortical) system is another system where the retinal fibres have established their synapses and are transmitting spontaneous waves sometime before cortical fibres have grown in (Godement et al., 1984; Ackman et al., 2012; De Carlos and O'Leary, 1992; Clascá et al., 1995).

In chapter 3, I demonstrate that the layer V fibres labelled in the Rbp4-Cre::tdTomato line innervate the superficial grey layer of the superior colliculus. I therefore assessed the ingrowth of layer V Rbp4-Cre::tdTomato fibres into the control and enucleated superior colliculus. As the superior colliculus receives input from the 'crossed' retinal projection, the 'enucleated' superior colliculus is contralateral to the removed eye. As in the dLGN, the ipsilateral projection to the superior colliculus expands after enucleation to project into the superficial grey layer (ipsilateral projections to the superior colliculus normally target a very limited region on the anterior/ medial superior colliculus and not in the superficial grey layer) however the majority of input to the superficial grey layer

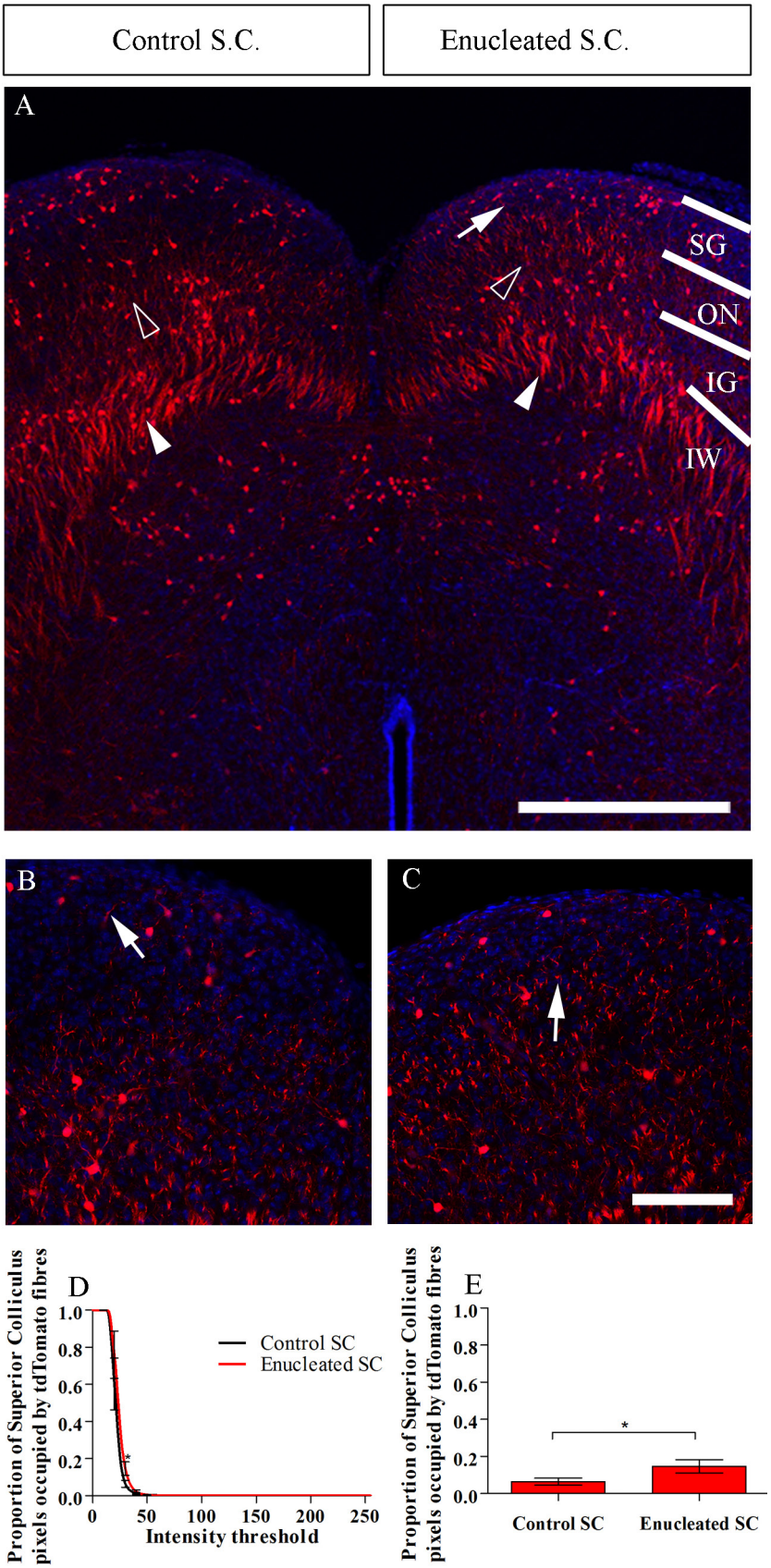
Control S.C.
Enucleated S.C.
A
SG
ON
IG
IW
B
C
D
Proportion of Superior Colliculus pixels occupied by tdTomato fibres
1.0
0.8
0.6
0.4
0.2
0.0
0
50
100
150
200
250
Intensity threshold
Control SC
Enucleated SC
E
Proportion of Superior Colliculus pixels occupied by tdTomato fibres
1.0
0.8
0.6
0.4
0.2
0.0
*
Control SC
Enucleated SC

Figure 4.26. Layer V Rbp4-Cre::TdTomato fibre ingrowth to the control and enucleated superior colliculus at P4. A. Rbp4-Cre::tdTomato positive layer V fibres are visible in thick fascicles in the intermediate white layer of the superior colliculus (filled arrow heads). The fibres then defasciculate and run in thinner bundles through the intermediate grey layer and the optic nerve layer of superior colliculus (hollow arrow heads). Fibres are visible in the superficial grey layer of the enucleated superior colliculus (filled arrow) B. There are sparse fibres in the control superficial grey (filled arrow). C. Layer V tdTomato fibres are more numerous in the enucleated superior colliculus (white arrow). D. Proportion of pixels in the superficial grey layer with an intensity value over the intensity threshold for all 255 grey scale intensity values. E. The proportion of pixels which are above intensity threshold 30. Abbreviations used: SG, superficial grey layer of the superior colliculus; ON, optic nerve layer of the superior colliculus; IG, intermediate grey layer of the superior colliculus; IW, intermediate white layer of the superior colliculus. Based on 3 animals. Values shown on graphs are mean and standard error. Scale bars= 200μm (A) 50μm (B- C).

has been lost (Godement et al., 1980).

The layer V corticotectal fibres innervate the superficial grey layer of the superior colliculus. The layers of the superior colliculus are hard to discern by DAPI staining and it is not possible to reliably assess the size of the superficial grey layer after monocular enucleation. However due to the patterning of the layer V corticothalamic fibres within the superior colliculus it was possible to discern the superficial grey layer to perform pixel analysis to assess the corticothalamic ingrowth after enucleation.

My results demonstrate that after monocular enucleation, the layer V Rbp4-Cre::tdTomato fibres enter the enucleated superficial grey layer of the superior colliculus prematurely (figure 4.25).

At P4 Rbp4-Cre::tdTomato positive layer V fibres are visible in thick fascicles in the intermediate white layer. The fibres defasciculate and run in thinner bundles through the intermediate grey layer and the optic nerve layer. In these layers there is no apparent difference between control and enucleated sides (figure 4.26 A). In the superficial grey layer few sparse tdTomato positive fibres are visible in the control superficial grey layer (figure 4.26 B). However in the enucleated superficial grey there are numerous clear tdTomato fibres (figure 4.26 C). Pixel analysis demonstrated that at most thresholds there was no difference between the control and the enucleated sides (figure 4.26 D). At threshold 30, however, there was a slight, statistically significant difference; the enucleated superficial grey layer had a higher proportion of bright pixels compared to control.

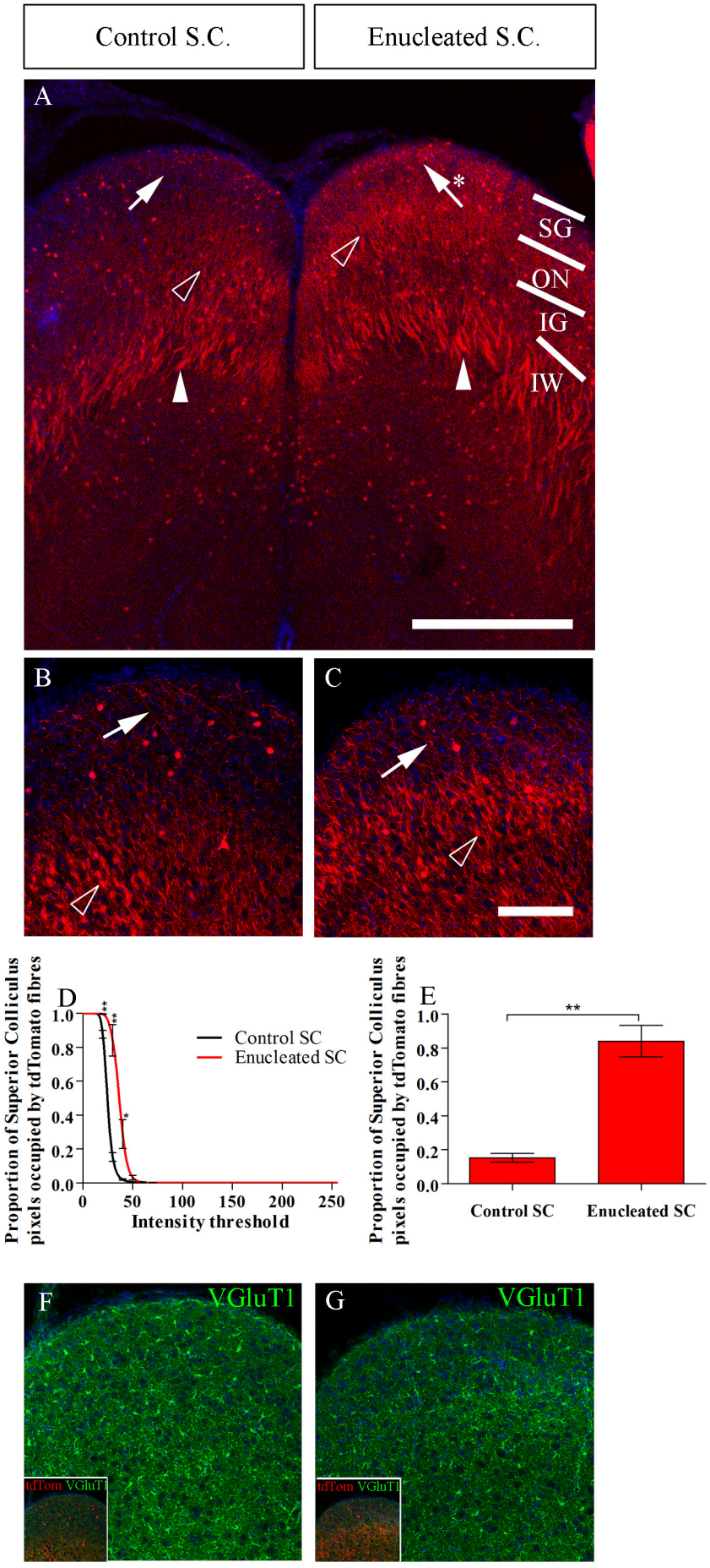
Control S.C.
Enucleated S.C.
A
SG
ON
IG
IW
B
C
D
Proportion of Superior Colliculus pixels occupied by tdTomato fibres
1.0
0.8
0.6
0.4
0.2
0.0
0
50
100
150
200
250
Intensity threshold
Control SC
Enucleated SC
E
**
Control SC
Enucleated SC
F
VGluT1
tdTom VGluT1
G
VGluT1
tdTom VGluT1

Figure 4.27. Layer V Rbp4-Cre::TdTomato fibre ingrowth to the control and enucleated superior colliculus at P6. A. Rbp4-Cre::tdTomato positive layer V fibres are visible in thick fascicles in the intermediate white layer of the superior colliculus (filled arrow heads). The tdTomato positive fibres run in thinner bundles in the intermediate grey layer and the optic nerve layer of superior colliculus (hollow arrow heads). Fibres are visible in the superficial grey layer of both the control and enucleated superficial grey layer (filled arrows) but are denser in the enucleated superficial grey (asterisk). B. There are fibres in the superficial grey layer of the control superior colliculus (filled arrow). Bundles of fibres in the optic nerve layer are also visible (hollow arrow head). C. The layer V fibres are visibly denser in the enucleated superior colliculus (white arrow). Bundles of fibres in the optic nerve layer are also visible (hollow arrow head). D. The proportion of pixels in the superficial grey layer with an intensity value over the intensity threshold for all 255 grey scale intensity values. E. The proportion of pixels which are above intensity threshold 30. F and G. VGluT1 immunohistochemistry shows sparse, punctate VGluT1 labelling in both the control and enucleated superficial grey layer of the superior colliculus. Abbreviations used: SG, superficial grey layer of the superior colliculus; ON, optic nerve layer of the superior colliculus; IG, intermediate grey layer of the superior colliculus; IW, intermediate white layer of the superior colliculus; VGluT1, Vesicular Glutamate Transporter 1. Based on 4 animals. Values shown on graphs are mean and standard error. Scale bars= 200μm (A.) 50μm (B-G.).

There are tdTomato positive cells in the superior colliculus which do not appear to give rise to thick long ranging projections and are thus unlikely to account for the thick bundles of fibres entering the superior colliculus. I therefore attribute the tdTomato fibres to layer V corticotectal projections. There does not appear to be a difference in the number of tdTomato positive cells in the control and enucleated superior colliculus.

Rbp4-Cre:: tdTomato	Intensity threshold used for bar graph	Proportion of pixels above intensity threshold in control superficial grey layer of the S.C. ± s.d.	Proportion of pixels above intensity threshold in enucleated superficial grey layer of the S.C. ± s.d.	p	n
P4	30	0.06515 ± 0.03321	0.1469 ± 0.06193	0.0239	3
P6	30	0.1531 ± 0.05162	0.8411 ± 0.1828	0.0011	4
P8	30	0.1444 ± 0.1617	0.6069 ± 0.1712	0.0007	3

Table 4.16. The proportions of pixels above intensity threshold 30 in the superficial grey layer of the control and enucleated superior colliculus, values shown are mean ± s.d. The p values from a one tailed, paired t-test comparing the control and enucleated superficial grey layer.

At P6 tdTomato layer V fibres have entered the superficial grey layer and are considerably denser in the enucleated superficial grey layer than in the control (figure 4.27 A and C). There is a higher proportion of bright pixels in the enucleated superficial grey layer compared to the control superficial grey (figure 4.27 D, E, table 4.16).

The layer V corticotectal fibres have prematurely entered the superficial grey layer of the superior colliculus however whether the fibres make early mature synapses with the tectal neurons is unclear. As such I performed immunohistochemistry against vesicular

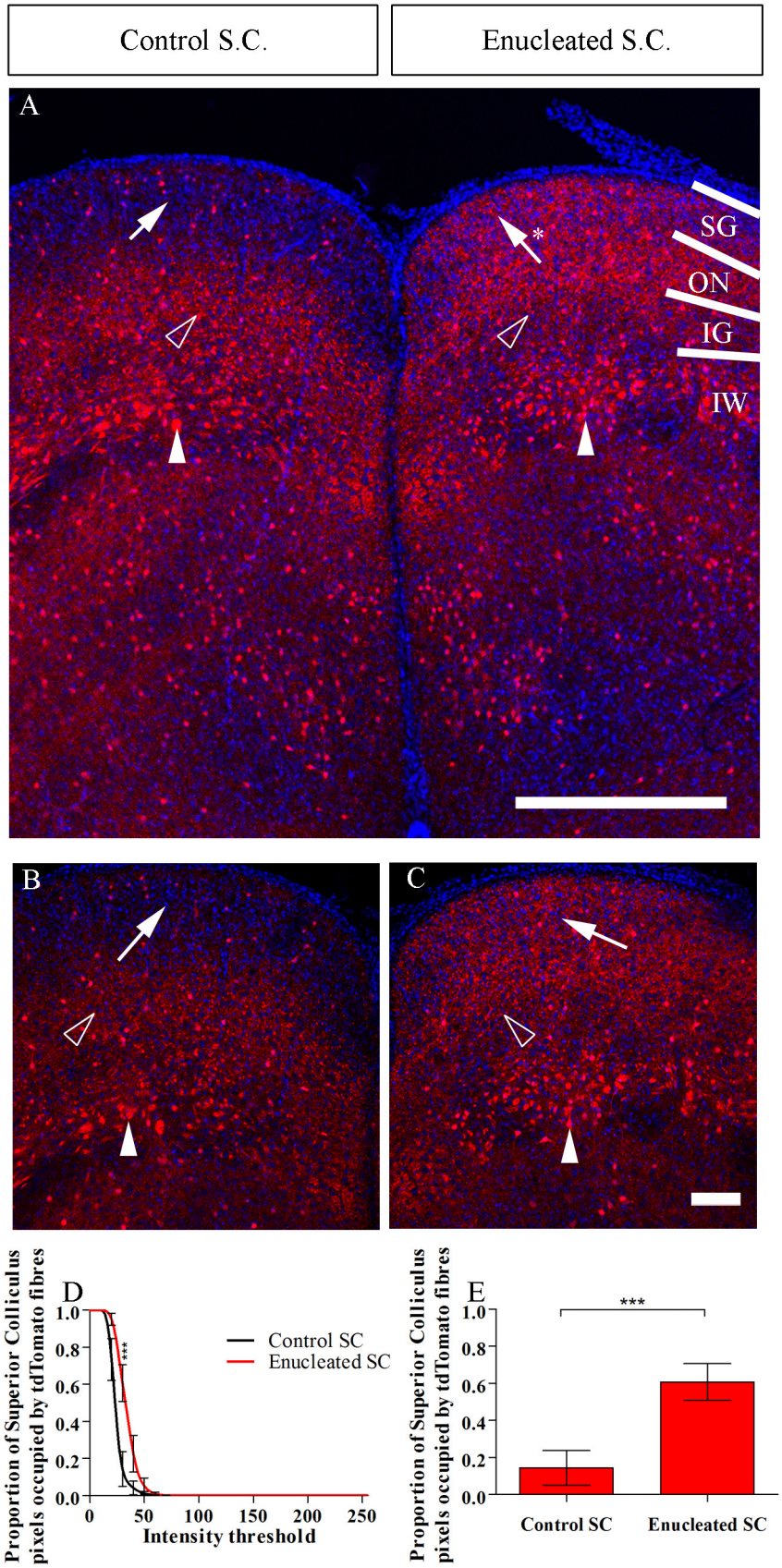
Control S.C.
Enucleated S.C.
A
SG
ON
IG
IW
B
C
D
Proportion of Superior Colliculus pixels occupied by tdTomato fibres
1.0
0.8
0.6
0.4
0.2
0.0
0
50
100
150
200
250
Intensity threshold
***
Control SC
Enucleated SC
E
***
Control SC
Enucleated SC

Figure 4.28. Layer V Rbp4-Cre::TdTomato fibre ingrowth to the control and enucleated superior colliculus at P8. A. Rbp4-Cre::tdTomato positive layer V fibres are visible in cross-sectioned fascicles in the intermediate white layer of the superior colliculus (filled arrow heads). The tdTomato positive fibres then appear to densely arborise in the intermediate grey layer and the optic nerve layer of superior colliculus (hollow arrow heads). Fibres are visible in the superficial grey layer of both the control and enucleated superficial grey layer (filled arrows) but are denser in the enucleated superficial grey (asterisk). B. Layer V fibres have reached the superficial grey layer of the control superior colliculus (filled arrow). Dense tdTomato positive labelling is visible in the optic nerve and intermediate grey layer which appears to be the arborisations of the layer V tdTomato positive fibres. The cut fascicles within the intermediate white layer are visible (hollow arrow head). C. The layer V fibres are visibly denser in the enucleated superficial grey of the superior colliculus (white arrow) compared to the control superficial grey layer. Dense tdTomato positive labelling in the optic nerve and intermediate grey layer appears to be the arborisations of the layer V tdTomato positive fibres. The cut fascicles within the intermediate white layer are visible (hollow arrow head). D. The proportion of pixels in the superficial grey layer with an intensity value over the given intensity threshold for all 255 grey scale intensity values. E. The proportion of pixels which are above intensity threshold 30. Abbreviations used: SG, superficial grey layer of the superior colliculus; ON, optic nerve layer of the superior colliculus; IG, intermediate grey layer of the superior colliculus; IW, intermediate white layer of the superior colliculus. Based on 3 animals. Values shown on graphs are mean and standard error. Scale bars= 200μm (A.) 50μm (B and C.).

glutamate transporter 1 (VGluT1) to assess the maturity of the layer V corticotectal synapses in the control and enucleated superficial grey layer. VGluT1 is a synaptic marker of mature cortical synapses (Nakamura et al., 2005; Wilson et al., 2005). VGluT1 immunohistochemistry shows sparse, punctate labelling in both the control and enucleated superficial grey layer (figure 4.27 F and G). There is no apparent difference between the control and enucleated side. This suggests the corticotectal fibres which have entered the enucleated superficial grey layer prematurely have not yet made mature synapses.

At P8 Rbp4-Cre::tdTomato positive layer V fibres have begun to arbourise within the intermediate grey layer and the optic nerve layer of superior colliculus (figure 4.28 A). Fibres are visible in both the control and enucleated superficial grey layer but are substantially denser in the enucleated superficial grey (fibre 4.28 A- C). There are significantly more bright pixels in the enucleated superficial grey layer than the control (figure 4.28 D).

My results on the study of layer V innervation of the enucleated superior colliculus demonstrate that after the loss of retinal input, layer V corticotectal fibres enter the superficial grey layer prematurely. This mimics my earlier results of premature entry of layer VI corticothalamic fibres into the dLGN after monocular enucleation.

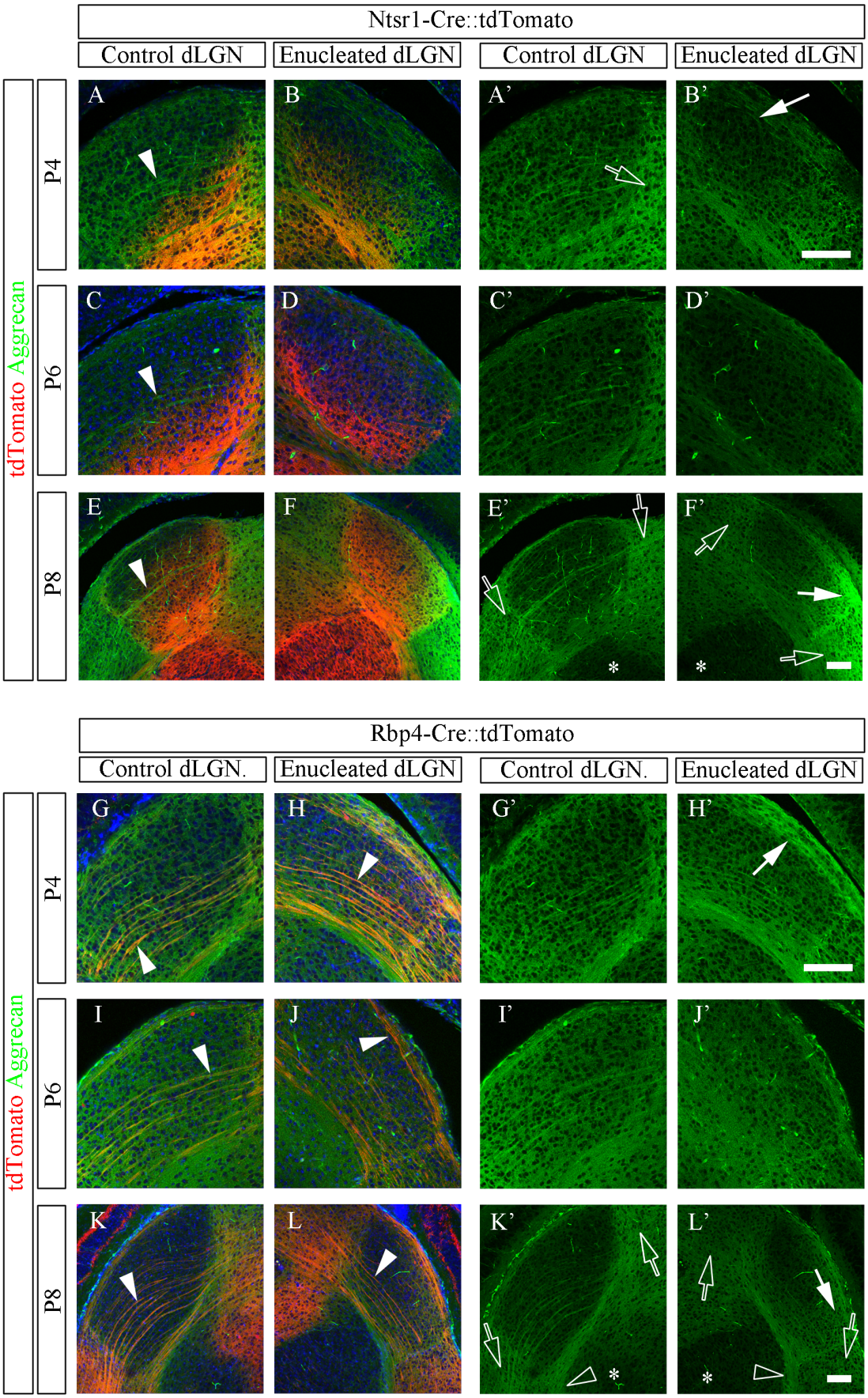
Ntsr1-Cre::tdTomato
Control dLGN
Enucleated dLGN
Control dLGN
Enucleated dLGN
tdTomato Aggrecan
P4
P6
P8
A
B
A'
B'
C
D
C'
D'
E
F
E'
F'
Rbp4-Cre::tdTomato
Control dLGN.
Enucleated dLGN
Control dLGN.
Enucleated dLGN
tdTomato Aggrecan
P4
P6
P8
G
H
G'
H'
I
J
I'
J'
K
L
K'
L'

Figure 4.29. Extracellular matrix molecule aggrecan immunohistochemistry in the control and enucleated dLGN over development in the Ntsr1-Cre::tdTomato and Rbp4-Cre::tdTomato line. Aggrecan protein is present in the extracellular matrix of the dLGN. A- B'. At P4 aggrecan is present in the control and enucleated dLGN in the Ntsr1-Cre::tdTomato mouse. Aggrecan shows an extracellular pattern and some labelled fibres crossing the dLGN (filled arrow head). The aggrecan expression is most dense around the dLGN (hollow arrows). B' There is reduced aggrecan labelling in the medial-dorsal corner of the enucleated dLGN (filled arrow). C-D'. At P6 the aggrecan labelling is less dense in the dLGN compared to P4. E-F'. At P8 the aggrecan labelling is less dense in the dLGN than at P4. Fibres crossing the dLGN are labelled (filled arrow head, E). At P8 the aggrecan labelling in the vLGN and LP is dense in the control and enucleated dLGN (hollow arrows, E' and F'). The VPM does not have aggrecan labelling (asterisk, E' and F'). In the enucleated dLGN there is dense aggrecan labelling in the lateral-dorsal corner (filled arrow F'). G- H'. At P4 aggrecan is present in the control and enucleated dLGN in the Rbp4-Cre::tdTomato mouse. Aggrecan shows an extracellular pattern and co-localises with Rbp4-Cre::tdTomato positive layer V fibres which project through the dLGN (filled arrow heads). In the enucleated dLGN there is denser staining in a band along the dorsal edge of the dLGN (filled arrow, H'). I- J'. At P6 aggrecan labels the Rbp4-Cre::tdTomato positive fibres which project through the dLGN (filled arrow head, I and J). At P8 the aggrecan labelling is less dense in the dLGN compared to P4 and P6. Rbp4-Cre::tdTomato positive fibres which project through the dLGN are also co-labelled by aggrecan (filled arrow head, K and L). The aggrecan labelling in the vLGN and LP is considerably denser than in the dLGN (hollow arrows, K' and L'). The VPM does not have aggrecan labelling (asterisk, K' and L'). In the enucleated dLGN there is denser aggrecan labelling in the lateral-dorsal corner (filled arrow) than the medial dorsal corner (L'). There is a dense band of aggrecan labelling running between the dLGN and the VPM (hollow arrow head, K' and L'). Based on 3 animals for all ages and lines except for P8 Ntsr1-Cre::tdTomato results which are based on one animal. Scale bars= 50μm (A-D', E-F', G-J', K-L').

4.3.3. The effect of retinal manipulation on aggrecan expression in the dLGN and the superior colliculus

4.3.3.1. Visual deprivation by monocular enucleation transiently alters aggrecan presence in the dLGN in Ntsr1-Cre::tdTomato and Rbp4-Cre::tdTomato

In this chapter I have demonstrated that following monocular enucleation, layer VI and VIb corticothalamic fibres enter the dLGN prematurely. Similar results to mine in the Golli-τ-eGFP mouse were recently published (Seabrook et al., 2013). Further research showed that extracellular matrix protein aggrecan (chondroitin sulfate proteoglycan 1) is responsible for the premature entry of Golli-τ-eGFP VI and VIb corticothalamic fibres to the dLGN after loss of retinal input (Brooks et al., 2013). Aggrecan has also been indicated in experience dependent changes in the visual cortex and somatosensory cortex after visual and somatosensory deprivation respectively (Kind et al., 2013; Matthews et al., 2002; McRae et al., 2007).

Inspired by these studies, I performed immunohistochemistry for aggrecan on the Ntsr1-Cre::tdTomato and Rbp4-Cre::tdTomato dLGN at P4, P6 and P8 after monocular enucleation at P0. I used anti-Chondroitin Sulfate Proteoglycan Antibody, Core Protein Epitope, clone Cat-315 which has been demonstrated to be specific for aggrecan in the

mouse (Matthews et al., 2002; Brooks et al., 2013).

In the Ntsr1-Cre::tdTomato, aggrecan protein displays the expected extracellular patterning within the dLGN at P4 (figure 4.29 A-B'). In addition to this extracellular matrix patterning, there were clear fibres crossing the dLGN with a layer V type trajectory (figure 4.29 A). There is stronger aggrecan labelling outlining the dLGN in the LP (figure 4.29 A'). There is less aggrecan labelling in the enucleated dLGN compared to the control dLGN (arrow in figure 4.29 B' compared to A').

By P6 the aggrecan labelling was absent from both control and enucleated dLGN (figure 4.29 C-D'). However there were still aggrecan positive fibres traversing the dLGN which may be layer V corticothalamic fibres (figure 4.29 C).

At P8 aggrecan labelling was strong in the regions surrounding the dLGN including the vLGN and LP (figure 4.29 E' and F'). Both control and enucleated dLGN have greatly reduced labelling however there is a labelled region in the lateral/dorsal corner of the enucleated dLGN which is not present in the control dLGN (figure 4.29 E' and F'). At this age the VPM also lacks aggrecan labelling (figure 4.29 E' and F').

In the Rbp4-Cre::tdTomato mouse, at P4 the aggrecan positive fibres which cross the dLGN are visible and co-express tdTomato thus confirming they are layer V corticothalamic fibres (figure 4.29 G and H). In this line the difference between the extracellular aggrecan labelling in the control and enucleated dLGN is not clear at P4 (figure 4.29 G' and H'). In the enucleated dLGN there is a thick band of aggrecan labelling at the dorsal edge of the dLGN which is not present in the control dLGN (figure 4.29 H'). This bundle is tdTomato positive (figure 4.29 H). This aberrant band of aggrecan labelling may be the layer V fibres that are differently patterned after enucleation (figure 4.26- 4.28).

At P6 the extracellular matrix aggrecan labelling is still present in the control dLGN but is reduced in the enucleated dLGN (figure 4.29 I-J'). This is different to the Ntsr1-Cre::tdTomato line in which the aggrecan labelling is reduced in both control and

enucleated dLGN by P6. This may be due to a difference between the two lines or due to slightly different levels of maturity between the litters. The aggrecan positive tdTomato positive layer V fibres which traverse the dLGN are still visible (figure 4.29 I) as is the thicker band of aggrecan labelling at the dorsal edge of the nucleus.

By P8 aggrecan is absent from both the control and the enucleated dLGN but it is still present in the vLGN and LP (figure 4.29 K- L'). In the enucleated dLGN there appears to be elevated aggrecan labelling in the lateral/dorsal region which is not present in the control dLGN (figure 4.29 L'). This aggrecan positive region is co-labelled by tdTomato (figure 4.29 L) and may be due to the rewiring of layer V corticothalamic fibres to the dLGN. This could also explain the dense labelling in this region on the Ntsr1-Cre::tdTomato enucleated dLGN at P8 (figure 4.29 F'). At P8 aggrecan labelling is absent from the first order VPM (figure 4.29 K' and L').

My results distinguish two patterns of aggrecan labelling within the dLGN. The two types I will discuss below are firstly the extracellular matrix patterned aggrecan labelling, and secondly the layer V corticothalamic fibre patterned aggrecan labelling.

My results demonstrate that there is reduced extracellular aggrecan expression in the enucleated dLGN at P4 in the Ntsr1-Cre::tdTomato and slightly later at P6 in the Rbp4-Cre::tdTomato. I further go on to show that by P6 (Ntsr1-Cre::tdTomato) and P8 (Rbp4-Cre::tdTomato) the extracellular aggrecan is reduced in the control dLGN and there is no difference between control and enucleated dLGN. This reiterates results of Brooks and colleagues who also demonstrate that the levels of aggrecan in the dLGN have reduced substantially by P4. My results also demonstrate that there is thalamic nuclei hierarchy specific aggrecan labelling and at later stages aggrecan is absent from first order nuclei, the dLGN and VPM, but is still present in the higher order nuclei, the LP and Po.

My results also identify aggrecan co-labelling of layer V fibres which cross the dLGN. This layer V associated aggrecan labelling appears to be also affected by enucleation.

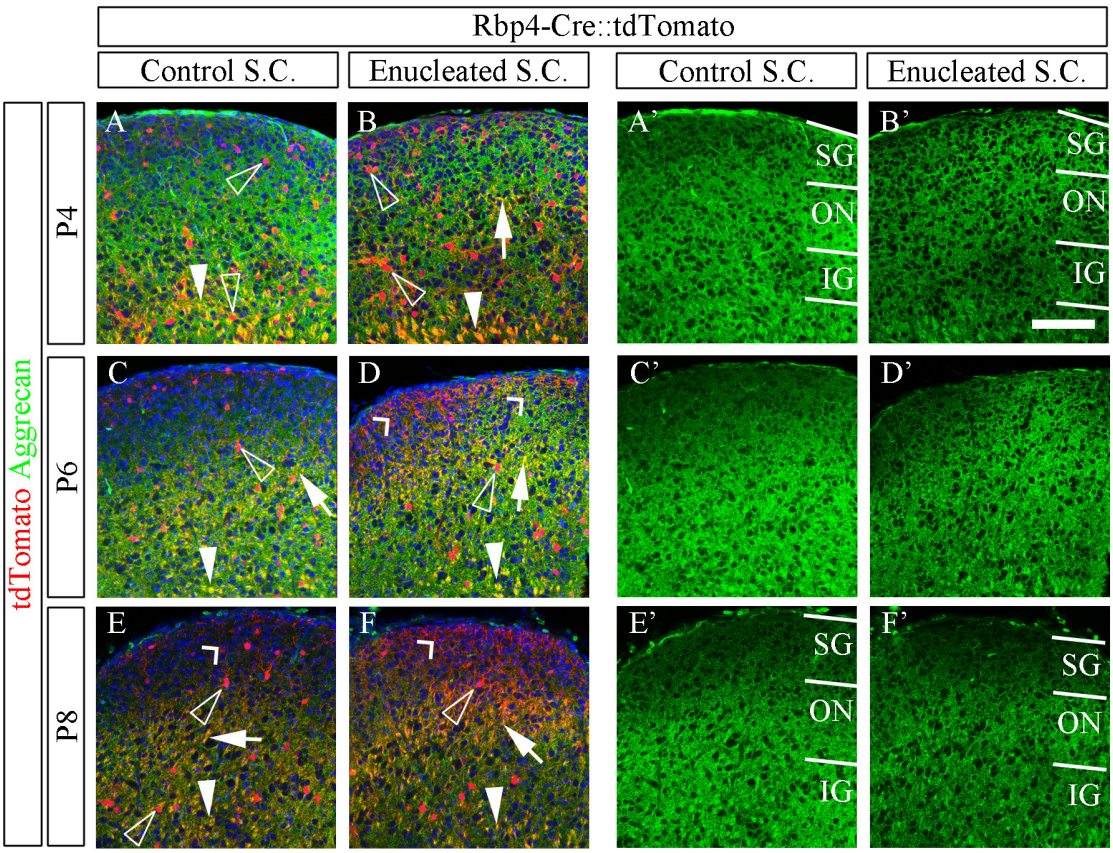

Figure 4.30. Extracellular matrix molecule aggrecan immunohistochemistry in the control and enucleated superior colliculus over development in the Rbp4-Cre::td-Tomato line. A and B. Aggrecan is present in the control and enucleated superior colliculus at P4. It co-localises with Rbp4-Cre::tdTomato positive layer V bundles in the intermediate white layer (filled arrow heads) and fibres in the optic nerve layer (filled arrow (B only)). It does not co-localise with tdTomato expressing cells which reside in the superior colliculus (hollow arrow heads). A' and B'. Aggrecan labelling is not different between the control and enucleated superior colliculus. C and D. At P6 aggrecan labelling is present in the control and enucleated superior colliculus. It co-localises with Rbp4-Cre::tdTomato positive layer V bundles in the intermediate white layer (filled arrow heads) and fibres in the optic nerve layer (filled arrow). TdTomato expressing cells which reside in the superior colliculus do not co-localise with aggrecan (hollow arrow heads). TdTomato expressing fibres in the superficial grey layer are present in the area with strong aggrecan labelling and the area with weaker aggrecan labelling (chevron arrows). C' and D'. Aggrecan labelling appears weaker in the superficial grey layer of the control superior colliculus but does not show this pattern in the enucleated superior colliculus. E and F. Aggrecan is present in the control and enucleated superior colliculus at P8. It co-localises with Rbp4-Cre::tdTomato positive layer V bundles in the intermediate white layer (filled arrow heads) and fibres in the optic nerve layer (filled arrow). It does not co-localise with the tdTomato positive cells which reside in the superior colliculus (hollow arrow heads). The Rbp4-Cre::tdTomato positive fibres in the superficial grey layer appear to have reduced aggrecan labelling (chevron arrow) E' and F'. Aggrecan labelling is weaker in the superficial grey layer of both the control and the enucleated superior colliculus. Images are in the correct orientation with regards to each other and as such the midline is between the control and the enucleated images (midline is on the right of control images and on the left of enucleated images). Based on 3 animals for all ages. Scale bar= 50μm.

However unlike the extracellular aggrecan, the layer V fibre associated aggrecan appears increased in the lateral/dorsal sector of the enucleated dLGN and along the dorsal edge of the enucleated dLGN.

4.3.3.2. Visual deprivation by monocular enucleation does not alter aggrecan protein levels in the superior colliculus from P4-P8 in the Rbp4-Cre::tdTomato

I have demonstrated that following monocular enucleation, layer V corticotectal fibres enter the superficial grey layer of the superior colliculus prematurely. As mentioned previously the retinal-colliculus-cortex system is similar to the retinal-geniculate-cortex system in which retinal fibres have established their synapses some time before cortical fibres can grow in. Furthermore in this chapter I have shown that the loss of retinal input causes or enables cortical fibres to enter each target prematurely (layer VI to the dLGN, layer V to the superficial grey layer of the superior colliculus).

Given these similarities in the coordinated ingrowth of retinal and cortical fibres and the dependence of cortical ingrowth on the presence of retinal input I suggest there may be a general mechanism by which retinal inputs regulate layer-specific corticofugal projection entrance to joint targets. Given the role aggrecan has been demonstrated to have in corticogeniculate guidance (Brooks et al., 2013). I then tested whether aggrecan may constitute the molecular mechanism by which retinal fibres regulate cortical entrance to the superficial grey layer. I therefore performed aggrecan immunohistochemistry on the superior colliculus at P4, P6 and P8 after monocular enucleation in the Rbp4-Cre::tdTomato line. If aggrecan is reduced in the enucleated superficial grey layer this would suggest that aggrecan may be a general mechanism by which retinal fibres prevent cortical fibres from entering their targets until after the retinal fibres have established their synapses.

In chapter 3, I demonstrate that layer V cortical ingrowth to the superior colliculus begins before P10 but increases between P10 and P15. I have shown previously in this chapter that the control superior colliculus remains relatively sparsely innervated by layer V fibres at P8. These results suggest that the ingrowth of layer V corticofugal

fibres to the superior colliculus is later than layer VI corticogeniculate ingrowth. By P6 there is no difference in aggrecan presence in the dLGN. However, if aggrecan also plays a role in preventing layer V corticotectal fibres from entering the superficial grey layer prematurely in the superior colliculus, then a difference should be still detected between control and enucleated superior colliculus between P4 and P8.

At P4 aggrecan is present in all layers of the control and enucleated superior colliculus (figure 4.30 A and B). It co-localises with Rbp4-Cre::tdTomato positive layer V bundles of fibres in the intermediate white and optic nerve layer (figure 4.30 A and B). It does not, however, co-localise with tdTomato expressing cells which reside in the superior colliculus (figure 4.30 A and B). This suggests that these cells are not expressing aggrecan (however without aggrecan *in situ* hybridisation we cannot confirm this). At P4 aggrecan labelling is not different between the control and enucleated superior colliculus (figure 4.30 A' and B').

At P6 aggrecan labelling is present in all layers of the superior colliculus except that it is reduced in the control superficial grey layer (figure 4.30 C'). In the enucleated superficial grey layer aggrecan expression is also reduced in the region of the superficial grey closest to the midline (midline is to the left of image D'). In the superficial grey layer the tdTomato positive layer V fibres are not less dense in the area with strong aggrecan labelling thus suggesting that the fibres are not repelled by aggrecan.

By P8 aggrecan immunoreactivity is still visible in the superior colliculus however it is reduced in both the control and enucleated superficial grey layer (figure 4.30 E- F').

Visualising aggrecan protein immunoreactivity from P4- P8 in the superior colliculus it is apparent that there is developmental regulation of aggrecan within the superficial grey layer and therefore activity dependent regulation of aggrecan is a promising mechanism for regulating ingrowth of corticotectal fibres to the superficial grey layer. This developmental regulation may contribute to controlling the ingrowth of layer V corticotectal fibres to the superficial grey layer by preventing their entry until aggrecan

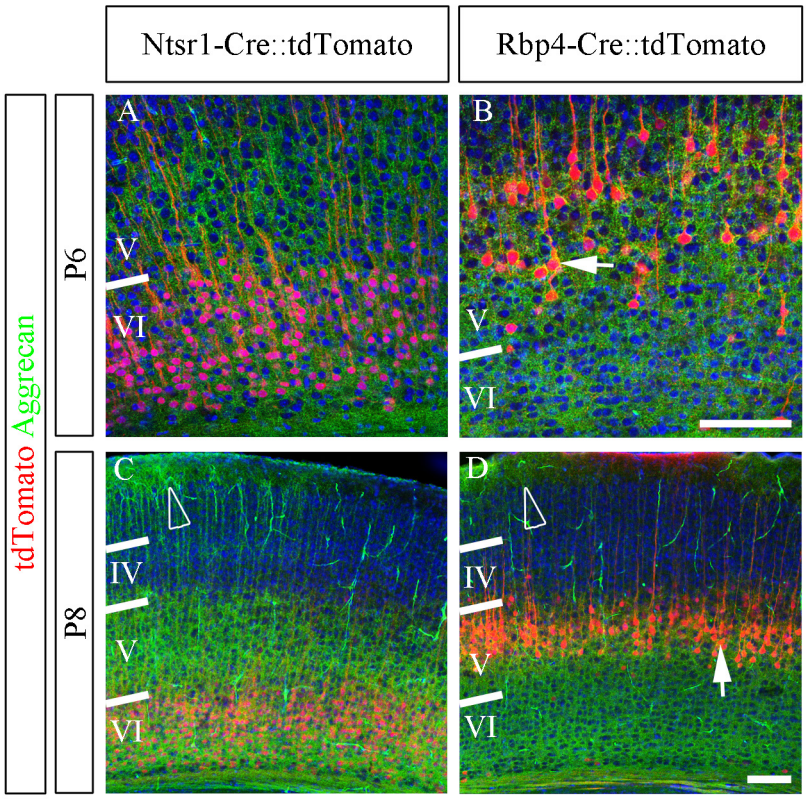

Figure 4.31. Cortical expression of extracellular matrix protein aggrecan in the Ntsr1-Cre::tdTomato and Rbp4-Cre::tdTomato mouse at P6 and P8. A-D. Aggrecan protein was diffusely present in layer V and VI of the posterior primary somatosensory cortex at P6 and P8 with an extracellular matrix patterning. At P8 there is diffuse aggrecan labelling in the marginal zone (hollow arrow heads, C and D). In the Rbp4-Cre::tdTomato cortex, aggrecan co-labels layer V tdTomato positive cells (white arrows, B and D.). Based on 3 animals at all ages and for all lines apart from P8 Ntsr1-Cre::tdTomato which is based on 1 animal. Scale bars= 50μm (A-B, C-D).

levels are reduced from P6. However there is not a clear difference in aggrecan labelling between the control and the enucleated superficial grey layer apart from at P6 where the enucleated superficial grey layer of the superior colliculus in fact appears to have stronger aggrecan labelling. Furthermore the tdTomato positive fibres in the superficial layer do not appear to avoid or be less dense in the area which has most aggrecan labelling at P6. This suggests that down-regulation of aggrecan in the superficial grey layer after enucleation is not responsible for the premature ingrowth of layer V corticotectal fibres.

4.3.3.3. Cortical expression of extracellular matrix protein aggrecan

Aggrecan is an extracellular matrix protein and therefore immunohistochemistry targeting it generates an extracellular pattern. However in addition to this extracellular pattern, in the two previous sections I have demonstrated that aggrecan labelling co-

localises with layer V, Rbp4-Cre::tdTomato positive fibres in both the dLGN and the superior colliculus (figures 4.29 and 4.30). This suggests that the layer V neurons may express aggrecan.

I chose to characterise cortical expression of aggrecan protein in the Ntsr1-Cre::tdTomato and Rbp4-Cre::tdTomato lines at P6 and P8 using immunohistochemistry on posterior primary somatosensory cortex.

At P6 aggrecan immunohistochemistry labelling is present in cortical layers V and VI of both lines. In the Ntsr1-Cre::tdTomato line aggrecan and tdTomato from the dendrites of layer VI neurons overlap but

there does not appear to be co-labelling of the tdTomato positive cells within layer VI (figure 4.31 A). In the Rbp4-Cre::tdTomato the aggrecan co-labels layer V tdTomato expressing cells. The aggrecan expression in layer V appears cytoplasmic. This suggests layer V neurons express aggrecan; *in situ* hybridisation has suggested aggrecan mRNA is expressed in layers IV-VI of somatosensory cortex (McRae et al., 2007).

At P8 aggrecan protein is limited to layer V and VI of the cortex (figure 4.31 C and D). At this lower magnification it is hard to discern cellular from extracellular labelling in the Ntsr1-Cre::tdTomato line however in the Rbp4-Cre::tdTomato line the aggrecan labelling can be seen to co-localise with tdTomato (figure 3.31 D). In both lines there was patchy labelling in the marginal zone (figure 4.31 C and D). The blood vessels were also clearly labelled, but it is not clear whether their labelling is true vascular aggrecan expression or due to nonspecific immunoreactivity on the vasculature due to incomplete or suboptimal perfusion of these particular brains.

4.4. Discussion

4.4.1. Retinal input to the dLGN and superior colliculus regulates cortical ingrowth to those structures

In chapter 3 I demonstrate the complementary patterns of ingrowth between corticothalamic fibres from layer V, VI and VIb. In this chapter I have shown that

manipulating retinal input to the dLGN by monocular enucleation or epibatidine injections alters corticothalamic ingrowth from all three populations.

4.4.1.1. Retinal input to the dLGN is important in regulating the ingrowth of layer VI and VIb corticothalamic fibres into the dLGN

In chapter 3 I demonstrated that the ingrowth of layer VI and VIb corticothalamic fibres to the dLGN is temporally regulated such that the fibres accumulate outside the dLGN before beginning to grow in four days postnatally. Whilst the cortical ingrowth to the dLGN is delayed the retinal innervation of the dLGN has developed perinatally and is mature enough to transmit spontaneous waves of activity from the retina to the dLGN (Godement et al., 1984; Ackman et al., 2012). Given the coincidence of the spontaneous retinal wave transmission and the delay to cortico-geniculate ingrowth, I chose to test whether retinal input was necessary for the regulation of corticothalamic ingrowth to the dLGN.

I first performed monocular enucleation. After monocular enucleation the hemisphere contralateral to the removed eye lacks the majority of its normal retinal input and only receives retinal input from the ipsilateral fibres (from the eye which is not removed). The ipsilateral input normally represents 5-15% of the usual retinal input to the dLGN (Godement et al., 1980; Jaubert-Miazza et al., 2005). The ipsilateral input expands after monocular enucleation, however it remains in under half of the dLGN and features such as topography are unaltered (Godement et al., 1980; Reese, 1986). Despite this expansion in ipsilateral input, the majority of the retinal input has been removed and thus monocular enucleation is a valuable model to study the role of peripheral input to the thalamus on the development of corticothalamic fibres.

My results show that following enucleation the layer VI and VIb primary visual cortex fibres enter the dLGN prematurely (in both Golli-τ-eGFP and Ntsr1-Cre::tdTomato). This suggests that retinal input to the dLGN is important for regulating the growth of layer VI and VIb corticothalamic fibres into the dLGN.

Monocular enucleation deprives the dLGN of retinal activity input. However, eye

removal also causes the retinal ganglion cell axons to degenerate thus removing neurotrophins and other signals, which retinal ganglion cells may provide. Furthermore retinal ganglion cell axon degeneration may cause local inflammation in the dLGN (Heumann and Rabinowicz, 1980; Lam et al., 2009). It is therefore important to discern whether the premature ingrowth might be due to the adverse effects of retinal ganglion cell degeneration.

Math5 is a transcription factor involved in retinal ganglion cell differentiation and the knockout mouse has a near complete loss of retinal ganglion cells (Seabrook et al., 2013). These animals lack retinal input to the dLGN without the mechanical damage which might be associated with monocular enucleation. Recent research using the math5$^{-/-}$ mutant mated with the Golli-τ-eGFP has shown similar results to those I report here. In this paper Seabrook and colleagues demonstrate that the Golli-τ-eGFP::math5$^{-/-}$ has premature ingrowth of the eGFP positive VI and VIb fibres to the dLGN. These results confirm my results and demonstrate that my results are unlikely to be due to the damaging effects of monocular enucleation.

4.4.1.2. Retinal activity is important for the ingrowth of corticothalamic layer VI and VIb fibres to the dLGN

My monocular enucleation results suggest that retinal input is important for regulating the growth of the layer VI and VIb fibres into the dLGN. However whether this regulation is in the form of retinal activity or molecular cues provided/ regulated by retinal axons is unclear.

In order to test this I performed intraocular injections of epibatidine to disrupt early spontaneous retinal activity. My results demonstrated that the loss of retinal activity (without losing the axons) also caused premature ingrowth of layer VI and VIb fibres to the dLGN, although it was less substantial after epibatidine injection than following monocular enucleation.

Previous research has demonstrated that aggrecan, a repulsive chondroitin sulfate proteoglycan, may be partially responsible for the specific temporal regulation of

corticothalamic ingrowth to the dLGN (Brooks et al., 2013). It is repulsive to primary visual corticothalamic axons from layers VI and VIb and is present in the dLGN at birth but down-regulated over the first 4 days postnatally. Furthermore enzymatic degradation of aggrecan or the knockout of aggrecan causes premature entry of layer VI and VIb corticothalamic fibres to the dLGN (Brooks et al., 2013). Furthermore aggrecan labelling is reduced in the dLGN of Golli-τ-eGFP::math5$^{-/-}$ mutants which lacks retinal ganglion cells (Brooks et al., 2013). As such retinal regulation of aggrecan expression appears to be responsible for the regulated ingrowth of VI and VIb corticothalamic fibres to the dLGN.

My epibatidine injection experiments in combination with Brooks and colleagues aggrecan results suggest that both neuronal activity and molecular mechanisms contribute to the proper temporal regulation of layer VI and VIb ingrowth into the dLGN.

Epibatidine injection did cause a decrease in the area of the dLGN and as such there may be some impact on corticothalamic ingrowth due to retinal damage however to address this it would be valuable to assess the ingrowth of Golli-τ-eGFP positive VI and VIb fibres when crossed with a mouse in which the retinal waves are abolished such as the nicotinic cholinergic receptor β2 subunit knockout mouse (Rossi et al., 2001; Bansal et al., 2000; Stafford et al., 2009).

4.4.1.3. Loss of retinal input causes cross-hierarchical plasticity in the visual corticothalamic system

My results demonstrate that after the removal of retinal input, layer V corticothalamic fibres, which normally only innervate higher order thalamic nuclei, can be induced to arborise within the first order dLGN. The layer V fibres densely innervate a dorsal band of the dLGN and the lateral corner of the dLGN. This area may represent the shell of the dLGN discussed as reciving mainly exclusively contralateral input as well as containing calbindin positive matrix relay cells (Grubb and Thomson, 2004; Reese, 1988). These two regions could be argued to experience the greatest loss of retinal fibres following

enucleation (Reese, 1988). The dorsal band is where the retina most densely innervates in the first few postnatal days (figure 1.10 introduction) (Godement et al., 1984; Jaubert-Miazza et al., 2005). Secondly the ipsilateral contribution to the dLGN is still present in the dorsomedial tip of the dLGN after monocular enucleation and as such thalamic relay cells in this region still receive some retinal input whereas the lateral corner is devoid of input (Godement et al., 1980; Godement et al., 1984). This could explain why at the ages studied the layer V fibres have not innervated all regions of the enucleated dLGN. To resolve this binocular enucleation experiments in which all retinal input is removed would help. It would also be interesting to assess whether the layer V fibres can be induced to enter the VPM after the loss of somatosensory input for example by infraorbital nerve transection.

My results showing layer V ingrowth to the dLGN are some of the first which suggest there is an order of cross-hierarchical plasticity after monocular enucleation. This cross-hierarchical rewiring may occur because the loss of retinal driver input to the dLGN causes the dLGN to appear more similar to a higher order thalamic nucleus. Alternatively the loss of retinal driver input may mean synaptic sites are available with reduced fibre competition. My results could therefore explain early electron microscopy results which demonstrate that after enucleation, the synaptic sites which normally receive retinal input become innervated by large terminals with round synaptic vesicles (characteristics of driver terminals) (Cullen and Kaiserman-Abramof, 1976). My results suggest these terminals may be layer V fibres aberrantly colonising dLGN synaptic sites. Whether this cross-hierarchical rewiring is functional is considered more in the general discussion.

My results demonstrate cross-hierarchical corticothalamic rewiring following sensory deprivation. Cross-hierarchical gene expression following sensory deprivation has also been recently demonstrated. Work by Pouchelon and colleagues has demonstrated that after sensory deprivation to the VPM by infraorbital nerve transection, the VPM (first order) shows gene expression changes which make it more similar to the higher order

Po (Pouchelon et al., 2014a). Thus sensory input to the first order thalamic nuclei may contribute to the determination of those nuclei as first order. The loss of this sensory input could then cause or permit these nuclei to follow a higher order type fate, thus encouraging layer V fibres to enter the normally first order nuclei. My results suggest that in addition to genetic shifts towards a higher order fate, there are connectivity and circuit changes such that layer V fibres begin to innervate the formerly first order nucleus. Whether the genetic changes then encourage the layer V fibres to grow in or whether the change in circuit connectivity encourages the genetic changes is unclear. In order to study this further it will be useful to determine whether the dLGN shows changes in gene expression to become more similar to the LP.

Previous work on plasticity within the developing brain has always focussed on cross-modal plasticity. This research has demonstrated that the loss of peripheral input such as visual input can cause other modalities to utilise cortical areas originally involved in visual processing. For example auditory and somatosensory input can invade visual cortex after visual deprivation (Izraeli et al., 2002; Chabot et al., 2008; Chabot et al., 2007; Charbonneau et al., 2012; Toldi et al., 1996; Toldi et al., 1993; Negyessy et al., 2000; Dye et al., 2012). Furthermore sensory input pathways are plastic such that afferent axon populations can colonise different thalamic nuclei, for example inducing retinal fibres to target the usually auditory thalamic nucleus the MGN (Sur et al., 1988; Asanuma and Stanfield, 1990; Angelucci et al., 1997).

My results are the earliest to show cross-hierarchical corticothalamic rewiring however cross-hierarchical thalamocortical rewiring has been demonstrated previously. Genetic ablation of the primarily first order VB (includes VPM and VPL), thus abolishing somatosensory input from the thalamus to the primary somatosensory cortex causes rewiring of inputs from the Po into layer IV of the primary somatosensory cortex (Pouchelon et al., 2014b). The Po is a higher order thalamic nucleus which normally projects to layer IV of the association somatosensory cortex.

My demonstration that following monocular enucleation layer V fibres innervate the

dLGN contributes to this early research into cross-hierarchical plasticity after peripheral input has been lost.

4.4.1.4. Retinal input is involved in the ingrowth of layer V corticotectal fibres to the superficial grey layer of the superior colliculus

The superior colliculus is another part of the visual system which receives direct input from decussated retinal ganglion cells and input from the cortex (layer V corticotectal projections). In the superior colliculus, as in the dLGN, retinal fibres innervate the superficial grey layer with mature, functional synapses capable of transmitting spontaneous waves, prior to cortical fibre ingrowth (Drager and Hubel, 1975; Lund, 1965; Godement et al., 1984; Godement et al., 1980; Ackman et al., 2012; De Carlos and O'Leary, 1992; Clascá et al., 1995).

Given these similarities with the retino-geniculo-cortical system I chose to assess whether the loss of retinal input to the superior colliculus also caused premature ingrowth of the layer V cortical fibres labelled by Rbp4-Cre::tdTomato to their target. My results demonstrated that indeed, after enucleation the layer V fibres can be seen entering the superficial grey layer of the superior colliculus prematurely by P6 and P8. My results also demonstrate that, despite the premature entry, the layer V fibres do not become synaptically mature early. This coincides with the published results showing the layer VI and VIb fibres which enter the dLGN prematurely are not mature (Seabrook et al., 2013).

These results confirm that in a second system in which retina and cortex innervate the same target, the loss of retinal input enables the cortical (layer V) projections to enter prematurely.

4.4.1.5. A common mechanism for cortical guidance preventing early ingrowth to target tissue

In this chapter I have discussed two systems which receive input from the retina and the cortex, the retino-geniculo-cortical system and the extrageniculo-cortical (retina-colliculus-LP-cortex) system. In both of these systems the retinal fibres innervate their target prior to cortical ingrowth. Furthermore I have shown that in both of these systems

the loss of retinal input causes premature ingrowth of cortical fibres to the target. This suggests there may be a common mechanism by which retinal fibres prevent cortical fibres from entering their joint target until it is appropriate.

Given the role of aggrecan in premature ingrowth of cortical fibres to the dLGN after the loss of retinal input (Brooks et al., 2013), I tested whether aggrecan could also be involved in the premature entry of layer V fibres to the superficial grey layer of the superior colliculus. My results demonstrate that aggrecan labelling in the superficial grey layer of the superior colliculus is not affected by monocular enucleation and that layer V Rbp4-Cre::tdTomato positive fibres densely innervate regions which express aggrecan.

These results suggest that there may be different molecular substrates by which retinal fibres prevent cortical fibres from entering the dLGN and the superior colliculus. This is consistent as layer V corticothalamic fibres are not repelled by aggrecan expression in the higher thalamic nuclei or in the superficial grey layer of the superior colliculus.

4.4.1.6. Layer V cortical neurons may be a source of aggrecan protein

My results also suggest that the layer V fibres may express aggrecan; there is co-labelling of layer V fibres within the thalamus and the superior colliculus with both Rbp4-Cre::tdTomato and aggrecan. Moreover in the cortex there is cytoplasmic labelling of layer V neurons with aggrecan. Without *in situ* hybridisation we cannot confirm whether layer V fibres express aggrecan mRNA however *in situ* results have suggested the deeper layers of the cortex do express aggrecan mRNA (Matthews et al., 2002; McRae et al., 2007). Aggrecan displays post-translational modifications such as oligosaccharides and glycosaminoglycans which are differentially targeted by different aggrecan antibodies (Matthews et al., 2002; Lander et al., 1997). Different cortical layers appear to differentially express the distinct aggrecan variants (Matthews et al., 2002; Lander et al., 1997). The functional relevance of layer V expressing the variant targeted by the antibody used here is unclear.

My results also demonstrate that after the first postnatal week aggrecan protein is

expressed exclusively in the higher order nuclei. Layer V fibres exclusively target higher order nuclei whereas layer VI fibres, which do not appear to express aggrecan, target both first order and higher order nuclei. This raises the question of whether layer V fibres are a source of aggrecan in the thalamus. If so, layer V fibre distribution in higher order nuclei may determine the continued presence of aggrecan in those nuclei. Alternatively if aggrecan is expressed by the thalamic neurons it may contribute to distinguishing higher order and first order nuclei molecularly thus contributing to layer V guidance into exclusively higher order nuclei. To distinguish these possibilities we could utilise genetic techniques to ablate layer V fibres and assess aggrecan distribution in the thalamus. Crossing the layer V specific Rbp4-Cre line presented here with a floxed diphtheria toxin fragment A line to ablate the layer V neurons would enable this analysis (Brockschnieder et al., 2004).

4.4.1.7. A role for delayed cortical fibre entry to target tissue

My results in this chapter have demonstrated that the loss of retinal input causes or enables premature ingrowth of corticothalamic (layer VI and VIb) and corticotectal (layer V) fibres to their target tissue (the dLGN and superficial grey layer of the superior colliculus respectively).

In the literature it has been demonstrated that retinal fibres enter the dLGN prior to corticogeniculate fibres and that corticogeniculate fibres are specifically delayed outside the dLGN in several species (Godement et al., 1980; Godement et al., 1984; Clascá et al., 1995; Shatz and Rakic, 1981; Anker, 1977). This suggests the ordering of ingrowth with retinal fibres entering and establishing functional synapses before cortical fibres can enter is important for the proper set up of the retino-geniculate system. Furthermore my results in the superior colliculus demonstrate this mechanism is conserved in an evolutionarily older system (the retino-tectal visual system).

This might suggest there is a mechanism by which retinal ganglion cells that project to the dLGN and the superior colliculus prevent cortical ingrowth thus ensuring the retinal fibres can make the appropriate number of synapses. This could be valuable as in adult

systems the synapses from cortical fibres outnumber those from retinal input (Guillery, 1969; Wilson et al., 1984; Mitrofanis and Guillery, 1993; Liu et al., 1995; Van Horn et al., 2000; Bickford et al., 2010).

Given this later dominance of cortical synapses, the enforced delay of corticothalamic fibres to the dLGN could be important for the proper set up of the corticothalamic circuit. It would therefore be interesting to see whether the circuit features of retinal input to dLGN and superior colliculus is disrupted after aberrant premature ingrowth of the cortical fibres. This could be tested by causing premature ingrowth of VI and VIb corticogeniculate fibres using enzymatic degradation of aggrecan in animals which still had retinal input (Brooks et al., 2013).

Furthermore whether other sensory modalities also have such a role in regulating cortical fibre ingrowth to 'joint' targets would be interesting to test. It is likely to be harder to assess as layer VI corticothalamic fibres have grown into the VPM (somatosensory) and MGN (auditory) thalamic nuclei prior to birth (Jacobs et al., 2007) and as such peripheral manipulations would need to be available *in utero*. Furthermore both somatosensory and auditory input is transmitted to midbrain nuclei before being relayed to the thalamus unlike visual input which is transmitted directly to the dLGN from the retina.

4.4.1.8. Conclusion

In conclusion I have demonstrated that the loss of retinal input alters corticothalamic and corticotectal ingrowth to central visual system structures, the dLGN and the superficial grey layer of the superior colliculus. My results demonstrate that retinal input regulates different features of all three corticothalamic populations; regulating the timing of layer VI and VIb ingrowth to the dLGN, regulating the timing of layer V ingrowth to the superficial grey layer of the superior colliculus and preventing layer V from entering the dLGN at all.

5 The effect of monocular enucleation on gene expression within the dLGN

5.1. Introduction

Early work on the development of the nervous system often placed theories of genetic programs and experience based mechanisms opposite one another, as mutually exclusive mechanisms (Sur and Rubenstein, 2005). Since then vast progress has been made confirming that these two mechanisms both contribute to neural circuit development and clarifying numerous interactions between experience based neural activity and the regulation of genetic programs (Cline, 2003; Sur and Leamey, 2001; Sur and Rubenstein, 2005).

To date there has been extensive research on the effect of peripheral deprivation on cortical gene expression. Within the visual system this has included establishing the effect of deprivation during the ocular dominance critical period, which is P19-32 in mice (Majdan and Shatz, 2006; Tagawa et al., 2005; Bozzi et al., 1995; Schoups et al., 1995; Kaczmarek et al., 1999; Lander et al., 1997) or the effect of deprivation in adulthood when the circuitry has been set up (Castren et al., 1992; Nys et al., 2014; Cheng et al., 2008).

The advent of high-throughput gene expression microarrays enabled a large-scale, systematic approach to determine genes that are regulated by peripheral input. Indeed gene networks can now be modelled by assessing correlated changes in gene expression across numerous microarray experiments (Langfelder and Horvath, 2008). In one important paper, microarray experiments were performed to establish changes in transcription in the mouse visual cortex, four days after monocular enucleation at different time points; P14- P18, P20- P24, P42- P46 and P100-P104 (Majdan and Shatz, 2006). They identified a common set of genes which were down-regulated at all ages studied and which included immediate early genes such as transcription factors Fos, Egr1 and 2 (early growth response), and neurotrophin BDNF (Majdan and Shatz, 2006).

The effect of monocular enucleation on gene expression within the dLGN

Many of the genes identified are regulated by MAP kinase/ MEK1/2 signalling pathway thus suggesting that the loss of visual input causes the differential activation of various signalling cascades which could underlie the changes in visual circuitry after monocular deprivation (Majdan and Shatz, 2006).

Despite this detailed research into sensory input dependent gene expression in the cortex, less has been done on input dependent gene expression within the thalamus. Microarray gene expression experiments have demonstrated that changing the modality of peripheral input to thalamic nuclei (rerouting retinal input to the normally auditory MGN) alters gene expression in the MGN (Horng et al., 2009). These results suggest that peripheral input to the thalamus contributes to gene expression profiles of different first order thalamic nuclei.

Whether retinal input contributes to gene expression in the dLGN has recently begun to be addressed. Using *in situ* hybridisation it has been demonstrated that ephrinA5 may have a reduced expression in the enucleated dLGN at P10 (Dye et al., 2012). Furthermore microarray results have demonstrated that at P3 in the dLGN of the math5$^{-/-}$ mutant (which lacks retinal ganglion cells) members of the adamts family of metalloproteases are differently expressed compared to control dLGN (Brooks et al., 2013).

In my previous chapters I have demonstrated that the loss of retinal input changes thalamocortical circuit development by enabling early ingrowth of layer VI and VIb corticothalamic fibres to the dLGN, and cross-hierarchical rewiring of layer V corticothalamic fibres into the dLGN. Given the considerable effect of the loss of retinal input on corticothalamic circuit development, and the scarcity of systematic research into early gene expression changes in the dLGN in response to visual deprivation, I have performed a microarray gene expression analysis comparing the control and enucleated dLGN at P6. Whilst we cannot determine whether retinal input regulates gene expression by neuronal activity or by neurotrophins and other signalling molecules we are able to speculate on the importance of retinal input to dLGN gene expression.

5.1.1. Aims of chapter 5

1. To analyse gene expression changes in the dLGN at P6 after enucleation at birth. This is in order to identify genes whose expression is regulated by retinal input, during the period that coincides with the premature ingrowth of the layer VI and VI projections to the dLGN.

    a. Using a microarray experiment and qPCR validation I compare control and enucleated dLGN to identify genes whose expression is changed after the loss of retinal input.

2. To analyse the functional properties of genes which are differentially expressed in the enucleated dLGN.

    a. Using DAVID (Database for Annotation, Visualisation and Integrated Discover) Gene Ontology analysis to investigate the functional groupings of genes which are differently expressed after enucleation and thus identify pathways of genes which retinal input may regulate (Huang da et al., 2009a; Huang da et al., 2009b).

3. Characterise the normal anatomical expression over development of the genes which are differentially expressed after enucleation.

    a. Using the Allen Developing Mouse Brain Atlas (Allen Institute for Brain Science, 2013) http://developingmouse.brain-map.org, I characterise the normal expression of genes that are differently expressed after enucleation, in the dLGN at E18.5, P4 and P14.

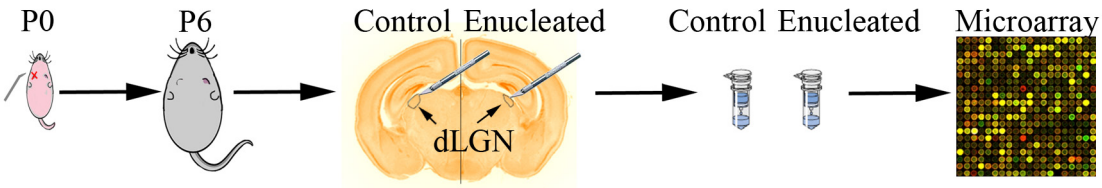

Figure 5.1. Schematic of microarray experiment. Pups were enucleated at P0. At P6 dLGN was dissected out. The mRNA was extracted and cDNA was synthesised. Control and enucleated dLGN were compared by microarray gene expression analysis.

4. Determine the developmental regulation of genes in the dLGN which are altered in the dLGN after enucleation.

    a. I will combine the results from two microarray experiments, the first discussed above comparing control and enucleated dLGN at P6, and the other analysing gene expression over development by comparing control dLGN at P0 and control dLGN at P10. Thus for each gene which is present in both lists we can establish their regulation after enucleation and over development.

5.2. Methods

In order to analyse the effect of monocular enucleation on gene expression within the dLGN I performed a microarray based gene expression experiment on P6 pups which were enucleated at P0 (figure 5.1).

5.2.1. Microarray sample preparation

Animals

C57/Bl6 females from Charles River (UK) were time mated for 12 hours overnight and 12.00pm the next day was designated E0.5. Day of birth was designated P0 and only litters born between E18.5 and E19.5 were used. Enucleation was performed at P0 as described previously. Pups were killed at P6 by cervical dislocation and processed immediately, keeping time between killing and protection of the micro-dissected dLGN pieces in RNALater (Sigma Aldrich, R0901-250ml) minimal. Four replicates were used. Eight pups were used per replicate from one or two litters per replicate. No litter was used in more than one replicate.

Condition	Replicate number	Number of pups per replicate	Number of litters to each replicate
Control and enucleated	5	8	2
Control and enucleated	6	8	2
Control and enucleated	7	8	1
Control and enucleated	8	8	2

Table 5.1. Table showing the number of animals (P6 pups) contributing to each replicate.

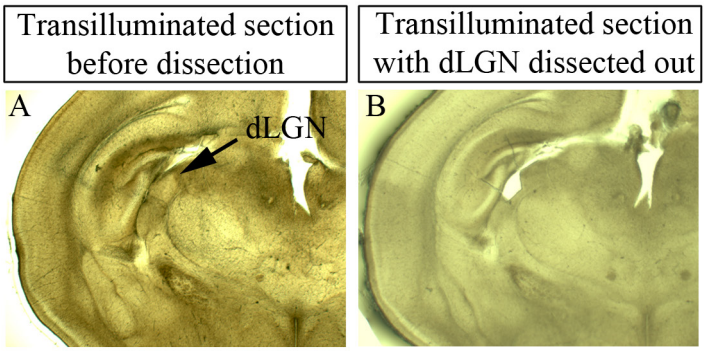

Figure 5.2. Micro-dissection of the dLGN. A. 200µm thick sections were cut from fresh brain tissue. The dLGN is visible by trans-illumination because of cytoarchitectonic boundaries. B. The dLGN was dissected out avoiding tissue in the vLGN, VPM or LP. The pia which is attached to the ventricular edge of the dLGN was removed.

Microarray tissue collection

The protocol was carried out in RNase free conditions. Glassware was baked at 200°C for four hours. Water was DEPC (Diethyl pyrocarbonate, Sigma Aldrich, D5758) treated for two hours at room temperature and autoclaved twice. Dissection tools were autoclaved twice, wiped with RNase Zap (Sigma Aldrich, R2020-250ml) and rinsed with DEPC treated water. Artificial Cerebro-Spinal Fluid (aCSF) stock solutions were made using DEPC treated water and autoclaved twice.

Fresh aCSF was made from chilled stock solutions on the day of collection and suction filtered. aCSF was kept on ice and bubbled through with 5% oxygen 95% carbon dioxide. 4% low melting point agarose was made with fresh aCSF.

Artificial Cerebro-Spinal Fluid (aCSF)

Stock I per litre: 2.94g CaCl2.2H2O, 4.93g MgSO4.7H2O, 2.24g KCl, 73.70g NaCl, 1.95g H2NaPO4.2H2O, added to DEPC nH20.

Stock II per litre: 20.16 NaHCO3, added to DEPC nH20.

Fresh aCSF per litre: 100ml stock I, 110ml stock II, 890ml DEPC nH2O, 1.8g glucose.

Pups were decapitated and the head was sprayed with RNase Zap. The brain was dissected out and rinsed with ice cold aCSF and placed in agarose on ice to set. 200µm slices were cut in fresh, chilled, bubbled aCSF and transferred to ice cold aCSF in Petri dishes. The dLGN was immediately micro-dissected out manually under visual

guidance through a transillium dissecting microscope (Leica MZFLIII, figure 5.2) and transferred using a sterile Pasteur pipette to an Eppendorf tube containing 500µl of RNALater. Three pieces of dLGN were collected per hemisphere per brain. After all pieces had been collected aCSF was removed and dLGN fragments were re-suspended in RNALater. Samples were stored at -20°C overnight to ensure full RNALater penetration of the tissue, before being stored at -80°C until RNA extraction.

RNA extraction

Samples were defrosted and those contributing to the same replicate were pooled. RNA extraction was performed using the Qiagen RNeasy Micro Kit (Qiagen Ltd, Manchester UK, 74004) according to the manufacturer's instructions. All samples were processed at the same time. An incubating step with DNaseI was performed to remove any contaminating genomic DNA. RNA was eluted in 12µl of RNase free water and stored at -80°C. RNA concentration was assessed by Nanodrop (Thermo Scientific, DE, USA) and quality was assessed by Agilent 2100 Bioanalyser Nano-Chip (Agilent Technologies Inc, CA, USA). Only replicates with RNA Integrity Numbers (RIN) of 8 or above were used for the microarray to maximise RNA integrity.

cDNA synthesis

40ng RNA starting material was reverse transcribed and linearly amplified using the NuGen Ovation Pico WTA System V2 (NuGen Technologies Inc, CA, USA, 3302-12). Linear amplification is considered more robust to biases (Van Gelder et al., 1990; Li et al., 2003a). Amplification starts at both the 3' end and sites throughout the transcript thus reducing 3' bias. Using reverse transcriptase and DNA/RNA chimeric primers the RNA was reverse transcribed to synthesise a cDNA/mRNA hybrid molecule with a SPIA RNA tag sequence at the 5' end of the cDNA. The mRNA strand is fragmented creating priming sites for DNA polymerase to synthesis the second cDNA strand which includes a DNA/RNA heteroduplex at one end. The cDNA is then amplified using the SPIA process. RNaseH removes the RNA portion from the remaining SPIA heteroduplex tag. DNA polymerase synthesises the new cDNA with DNA/RNA

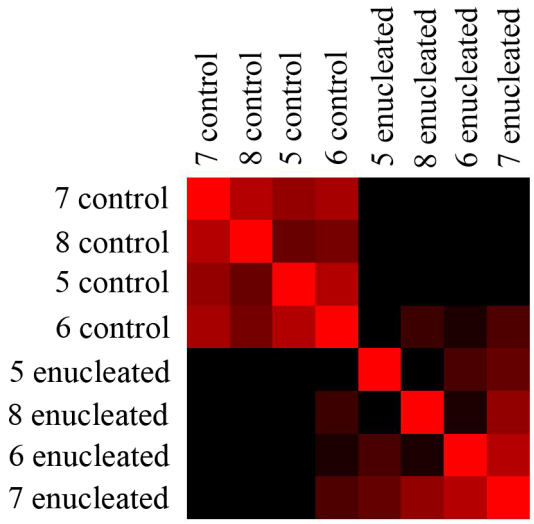

Figure 5.3. Pearson correlation analysis visualised as heat-map. Pearson correlation coefficient of 1= bright red squares. Pearson correlation coefficient of 0= black squares. Analysis shows that expression is strongly correlated between replicates of the same tissue condition (control or enucleated).

chimeric primers thus recapitulating the DNA/RNA heteroduplex tag providing another substrate for the RNaseH and allowing the process to be repeated leading to the rapid, linear amplification of the RNA. Negative controls lacking sample were included and no amplification was seen confirming lack of contamination.

The amplified, double-stranded cDNA was transformed into single strand sense cDNA which is then chemically and enzymatically fragmented to produce strands of 50-100bps in length. The sample was then run on an Agilent Bioanalyser NanoChip (Agilent) to confirm successful fragmentation. The strands were then labelled by biotin-labelled nucleotide to the 3-hydroxyl end. The fragmentation and biotin process was performed using the Encore Biotin Module (NuGen, 4200-12).

Sample hybridisation to the Affymetrix GeneChip Mouse 1.0 ST

Fragmented, labelled single strand sense cDNA was hybridised at 45°C overnight to the Affymetrix GeneChip Mouse 1.0 ST Array chip, according to the Affymetrix Manual (Affymetrix UK Ltd, High Wycombe, UK). The chips were washed and then stained with streptavidin-phycoerythrin using GeneChip Hybridization, Wash and Stain Kit (Affymetrix) which employs two rounds of biotin-streptavidin binding to amplify the fluorescent signal. The hybridised chips were scanned on the Affymetrix Gene Chip Scanner and GeneChip Operating System (Affymetrix) creating an image data file (.dat).

The Affymetrix GeneChip Mouse 1.0 ST chip has 25mer probes which recognise 28,853 annotated mouse transcripts. There are average 27 probes per gene. The probes target sequences along the length of the transcript ensuring that partially degraded, truncated or alternatively spliced transcripts are still detected.

All samples were processed at the same time. Quality control by the Expression Console™ 1.2.0.20 (Affymetrix) identified sample (5c) from the initial microarray run as faulty. That sample was run again and all measures of quality control confirmed that the separate run did not affect the results of the sample. The Pearson Correlation heat map demonstrates that ipsilateral samples are more similar to one another and contralateral samples are more similar to one another (figure 5.3).

The results from this microarray were later compared with results of a microarray comparing gene expression in the dLGN between P0 and P10, microarray performed in the laboratory of collaborator Professor Denis Jabaudon (University of Geneva, Switzerland). This microarray was performed on the Affymetrix GeneChip Mouse Genome 430 2.0 Array.

5.2.2. Microarray statistical analysis

Normalisation of gene expression values

Data processing was performed with Agilent GeneChip® Command Console® Software (AGCC) and GeneSpring GX 12.6.1 (Agilent Technologies, Germany). The data from the chip image was processed by AGCC and each probe was assigned an intensity value generating a .CEL file. The .CEL files were normalised in GeneSpring using Robust Multichip Average (RMA) normalisation which performs background subtraction, robust normalisation of intensity values across chips and probe set summarisation (Irizarry et al., 2003b; Irizarry et al., 2003a). Background correction is based on the distribution of positive signal intensities from perfect match (PM) probes on the array. Each PM value is made up of a signal and a noise component. The noise component of the PM value is assumed to be normally distributed and so the mean and variance of the error distribution can be estimated and the mean of the error subtracted from the PM

value. These background-subtracted intensity values are normalised across the chips using quantile normalisation. This generates normalised quantile values for each chip by scaling by the average of the quantile values across all chips thus reducing variability between chips in the distribution of the probe intensities. Each gene is targeted by 27 probes, as such the final normalisation step is to summarise the values from all probes targeting a gene to generate an intensity value per gene which is then used as the gene expression value for statistical comparisons.

Statistical analysis of control versus enucleated dLGN microarray- Linear Models for Microarray Data (Limma)

Gene expression values were compared between the control dLGN and the enucleated dLGN using GeneSpring GX 12.6.1 to perform Limma analysis (Linear Models for Microarray Data) (Smyth, 2004). The experiment is paired as each replicate provided both control and enucleated tissue. Asymptomatic p-value computation was used.

Limma uses a moderated t-statistic and empirical Bayes method to estimate the probability of differential expression of genes between samples and uses information across all genes to calculate the moderated t-statistic (Smyth, 2004). The Benjamini-Hochberg Multiple Testing Correction was used to correct the p values, taking into account the high number of statistical comparisons being performed and reducing the rate of false positives (Benjamini and Hochberg, 1995).

Statistical analysis of control versus enucleated dLGN microarray- ANOVA/t-test intercept method

Gene expression values were also compared using first a two way ANOVA test and then a paired t-test. The two separate gene lists generated by these methods are then combined and those genes which arise in both lists are used to generate a final list. This was performed on Partek Genomics Suite (Partek Inc. Saint Louis, MO).

This latter method was used to generate results which were comparable to results belonging to collaborator Professor Denis Jabaudon who has performed a microarray gene expression analysis comparing gene expression within the dLGN over early development between P0 and P10.

DAVID gene ontology analysis

In order to analyse functional enrichment in the list of genes which are differentially expressed I used DAVID (Database for Annotation, Visualization and Integrated Discovery) (Huang da et al., 2009a; Huang da et al., 2009b) on the genes differentially expressed according to Limma analysis (DAVID accessed latest 20.06.2014). Affymetrix gene identifiers were converted into biological annotations (which are then used to query the DAVID gene ontology analysis database) using the DAVID Gene ID Conversion Tool

The gene list of differentially expressed genes (with the identifiers assigned by the conversion tool) was uploaded to DAVID Analytical Module which returns gene ontology (GO) terms which are enriched/ overrepresented in the gene list (Huang da et al., 2009a; Huang da et al., 2009b).

5.2.3. Real-time quantitative PCR

To validate the genes identified as differentially expressed by Limma analysis, real-time quantitative PCR (qPCR) was performed.

Animals

Animals as in microarray experiment, enucleation at P0, tissue collected at P6. Four replicates were used. Sixteen pups from four litters were used per replicate. No litter was used in more than one replicate. Two replicates (1 and 2) were distinct from samples used for the microarray experiment and were processed as described below. Two replicates (3 and 4) were compiled from the four replicates which had previously been used for the microarray and were processed as described in the microarray section. RNase free conditions were as described previously.

Condition	Replicate number	Number of pups per replicate	Number of litters to each replicate
Control and enucleated	1	16	4
Control and enucleated	2	16	4
Control and enucleated	3	16	4
Control and enucleated	4	16	4

Table 5.2. Table showing the number of animals (P6 pups) per replicate.

Independent qPCR replicates tissue collection

Pups were killed at P6 by cervical dislocation. Initial processing was as described for the microarray tissue collection until cutting. 200µm slices were cut in chilled 50:50 RNALater: RNase free PBS and transferred to ice cold RNALater and stored as slices at -20°C until the dLGN was dissected out. The dLGN was micro-dissected out in RNALater and transferred using forceps to an eppendorf tube containing 500µl of RNALater. Three pieces of dLGN were collected per hemisphere per brain. After all three pieces had been collected the eppendorf was filled with RNALater. Samples were stored at -80°C until RNA extraction.

RNA extraction

Samples were defrosted and pooled into replicates. RNA was extracted and assessed for quantity and quality as described previously. Only replicates with RNA Integrity Numbers (RIN) of 5 or above were used for the qPCR as recommended (Fleige and Pfaffl, 2006).

cDNA synthesis

First strand cDNA was synthesized using the Qiagen Reverse Transcription kit (Qiagen 330401). 200ng of RNA starting material was used. RNA samples were incubated for 5 minutes at 42°C with DNase to remove any contaminating genomic DNA. A known concentration of exogenous RNA was spiked in to each sample for confirmation of reverse transcription efficiency after the qPCR run. Samples were then incubated at 42°C for 15 minutes with oligonucleotides which are extended by reverse transcriptase enzyme. The enzyme activity is arrested by 5 minutes at 95°C. Samples were the diluted and stored at -20°C until qPCR.

Real-time, quantitative PCR (qPCR)

Commercially available primers from Qiagen were used, but it is company policy not to disclose sequences. Qiagen primers are designed to meet the following criteria. Primer specificity was verified through BLAST to ensure homology to the mRNA of the mouse gene of interest and that there was no homology with other genomic mouse

DNA. Primers were designed to have uniform primer length, GC content and annealing temperature. This enables all primers to be run using the same cycling conditions and allows for the use of fewer housekeeping genes for normalisation (discussed below). Amplicon lengths of between 100-200bps to ensure extension of nascent DNA strand can be completed within the extension stage.

Primer specificity was confirmed experimentally by performing dissociation curve analysis on the PCR products after each qPCR run. The dissociation curve of our samples showed one thermal transition in fluorescence thus confirming that there were no none-specific targets of the primers.

qPCR was performed using Qiagen RT^2 SYBR Green ROX qPCR Master mix containing HotStart DNA *Taq* Polymerase, PCR buffer, dNTP mix, SYBR Green dye and ROX passive reference dye (Qiagen 330523).

Quality controls. Each biological replicate was run three times to provide technical replicates to control for pipetting error (Rieu and Powers, 2009). No technical replicates were deemed as outliers and as such all technical replicates for each biological sample were treated collectively. The exogenous RNA spike confirmed that reverse transcription was efficiently performed and was of uniform efficiency across all samples. A specific genomic DNA primer confirmed the lack of genomic DNA contamination in all samples. A spiked genomic DNA well confirmed the efficiency of the PCR amplification for each sample.

All genes were tested for on the same plate and each sample (one treatment condition of one biological replicate) was run on one 96 well plate to reduce experimenter pipetting error.

House-keeping genes were used as references to normalise the cycle number at which the threshold is crossed (Ct) values to control for variance in efficiency of RNA isolation or reverse transcription across samples or qPCR runs. Reference genes were chosen to be stably expressed in mouse brain tissue at early postnatal ages; Pgk1 and

Tfrc (Boda et al., 2009) and Hprt1 (Vandesompele et al., 2002).

The qPCR was run on the Stratagene Mx3005P (Agilent). The cycling conditions are described in table 5.3.

Cycles	Duration	Temperature	Notes
1	10 Minutes	95° C	Activating HotStart DNA Taq Polymerase.
40	15 Seconds	95° C	Double stranded DNA denaturation step.
	1 Minute	60° C	Joint annealing/extension step. Fluorescence data collected at end of this step.

Table 5.3. Cycling conditions for qPCR.

5.2.4. qPCR analysis

A shared threshold value for fold change in fluorescence intensity was set and Ct values were exported to Excel (Microsoft). All statistical analysis was performed in Excel (Microsoft). Ct values were normalised to reference genes to generate ΔCt using the following equation

$$\Delta Ct = Ct^{GOI} - Ct^{HKG}$$

Then the difference in ΔCt value was calculated to generate ΔΔCt using the following equation

$$\Delta\Delta Ct = \Delta Ct^{Enucleated} - \Delta Ct^{Control}$$

Then relative gene expression was calculated by

$$relative\ expression = 2^{-\Delta\Delta Ct}$$

Fold change for down regulated genes was calculated as

$$-\ \frac{1}{relative\ expression}$$

GOI= Gene of Interest. HKG= House Keeping Gene.

5.3. Results

5.3.1. Retinal input to the dLGN contributes to gene expression in the dLGN

Peripheral input dependent gene expression in the developing thalamus has not been systematically assessed following sensory deprivation. In order to identify genes expressed by the dLGN that are regulated by retinal input I performed a microarray on

the control and the enucleated dLGN at P6.

Monocular enucleation is a valuable tool to assess input dependent changes in gene expression. Due to the large number of comparisons made, microarray gene expression studies are vulnerable to inter-sample variation. Monocular enucleation (rather than binocular enucleation) allows inter-animal control thus preventing inter-litter variability from impacting on the results. Furthermore monocular enucleation has been previously demonstrated to provide a consistent level of gene expression changes unlike other methods of visual deprivation such as dark rearing and intraocular tetrodotoxin (TTX) injections (Majdan and Shatz, 2006).

5.3.1.1. Gene expression changes in the enucleated dLGN compared to the control dLGN

Following monocular enucleation at P0, gene expression in the control and the enucleated dLGN at P6 was assessed using a microarray gene expression experiment.

In order to limit false positives I chose a relative expression cut off value of >1.3 or <0.77 (equivalent to a fold change cut off of 1.3 and -1.3). 51 genes were differentially expressed between the control and the enucleated dLGN (table 5.4). 33 genes were down-regulated and 14 were up-regulated in the enucleated dLGN compared to the control dLGN. With a more stringent relative expression cut off of >1.5 or <0.66, 12 genes were differentially expressed between the enucleated and control dLGN. 9 were down-regulated after enucleation, 3 were up-regulated. All 51 genes identified with a relative gene expression of >1.3 or <0.77 were included for further analysis. This number of genes is similar to other microarray studies which have been based on monocular enucleation or rewired input to thalamic nuclei (Majdan and Shatz, 2006; Brooks et al., 2013; Horng et al., 2009).

Due to the stringency of Limma analysis I also looked at genes with relative expression of >1.25 or <0.8. With this cut off 81 genes were differentially expressed between the enucleated dLGN and the control dLGN (see appendix 1 for full list). 57 genes were down-regulated, 24 were up-regulated in the enucleated dLGN compared to the control

dLGN. Within the extra 30 genes I choose genes with relevant biological functions to include for further analysis: Adamts3, Timp4 and Egr2. Adamts3, a metalloprotease, was chosen because it is within a family of genes which regulate chondroitin sulfate proteoglycans (including aggrecan). Timp4 is within a family of metalloprotease inhibitors which regulate adamts metalloproteases (Kashiwagi et al., 2001). As such both were deemed biologically relevant given the previous evidence for the involvement of aggrecan in layer VI and VIb ingrowth to the dLGN and cortical plasticity after sensory deprivation (Brooks et al., 2013; Kind et al., 2013; Matthews et al., 2002; McRae et al., 2007; Lander et al., 1997). Egr2 is an immediate early gene which has been shown to be altered following monocular enucleation in the cortex (Kaczmarek and Chaudhuri, 1997; Majdan and Shatz, 2006; Van Brussel et al., 2011; Nys et al., 2014).

The greatest change in gene expression was of RIKEN cDNA E530001K10 which had a relative expression of 0.3031 (fold change of -3.2987) in the enucleated dLGN. The relative expression values are within the range of values shown in other peripheral manipulation studies (Majdan and Shatz, 2006; Brooks et al., 2013; Horng et al., 2009).

Individual genes which were identified in both mine and Majdan and colleagues cortical microarray were Visinin-like1, Fos, Egr2 all of which were down-regulated in both microarrays (Majdan and Shatz, 2006).

Gene symbol	Gene name	Relative gene expression	Moderated p value
	RIKEN cDNA E530001K10 gene	0.3031	2.71E-09
Hmcn1	hemicentin 1	0.5008	9.83E-08
Shc3	src homology 2 domain-containing transforming protein C3	0.5674	3.43E-08
Kcnk9	potassium channel, subfamily K, member 9	0.5724	3.88E-08
Dgkk	diacylglycerol kinase kappa	0.6111	8.10E-06
Hcrtr2	hypocretin (orexin) receptor 2	0.6584	5.09E-07
Fam19a4	family with sequence similarity 19, member A4	0.6584	1.14E-05
Osbpl3	oxysterol binding protein-like 3	0.6657	5.39E-07
Dusp4	dual specificity phosphatase 4	0.6730	1.48E-05
Gjd2	gap junction protein, delta 2	0.6808	4.58E-08

Vsnl1	visinin-like 1	0.6835	6.83E-06
Tacstd2	tumor-associated calcium signal transducer 2	0.6950	1.54E-05
Myot	myotilin	0.6967	1.74E-07
Sncg	synuclein, gamma	0.7039	3.19E-06
Spred2	sprouty-related, EVH1 domain containing 2	0.7046	1.23E-07
6530402D11Rik	RIKEN cDNA 6530402D11 gene	0.7049	5.99E-05
Moxd1	monooxygenase, DBH-like 1	0.7058	1.97E-05
Kcnn3	potassium intermediate/small conductance calcium-activated channel, subfamily N, member 3	0.7111	2.72E-05
Shisa6	shisa homologue 6 (Xenopus laevis)	0.7402	1.55E-06
Chrm2	cholinergic receptor, muscarinic 2, cardiac	0.7433	1.08E-04
Adra1d	adrenergic receptor, alpha 1d	0.7455	6.89E-06
Fos	FBJ osteosarcoma oncogene	0.7460	1.09E-05
Frem3	Fras1 related extracellular matrix protein 3	0.7472	3.22E-06
Ptgr1	prostaglandin reductase 1	0.7475	2.75E-04
Hmgn5	high-mobility group nucleosome binding domain 5	0.7544	4.39E-05
Gfra1	glial cell line derived neurotrophic factor family receptor alpha 1	0.7569	2.57E-05
Dgkg	diacylglycerol kinase, gamma	0.7575	2.78E-05
Igf1	insulin-like growth factor 1	0.7578	1.48E-06
Pdlim5	PDZ and LIM domain 5	0.7616	1.08E-04
Col6a5	collagen, type VI, alpha 5	0.7620	9.53E-05
Synm	synemin, intermediate filament protein	0.7636	1.31E-04
Chst2	carbohydrate sulfotransferase 2	0.7656	1.24E-06
Calb2	calbindin 2	0.7664	4.13E-05
Adamts3	a disintegrin-like and metallopeptidase (reprolysin type) with thrombospondin type 1 motif, 3	0.7744	5.87E-05
Timp4	tissue inhibitor of metalloproteinase 4	0.7747	1.82E-04
Egr2	early growth response 2	0.7786	5.79E-05
Mxd4	Max dimerization protein 4	1.3022	6.29E-05
Siah3	seven in absentia homologue 3 (Drosophila)	1.3049	2.14E-04
Rmnd5a	required for meiotic nuclear division 5 homologue A (S. cerevisiae)	1.3159	9.57E-05
Rnf114	ring finger protein 114	1.3192	3.23E-04
Krtap31-2	keratin associated protein 31-2	1.3197	4.52E-05
Gpr17	G protein-coupled receptor 17	1.3245	4.68E-04
Otx2	orthodenticle homologue 2 (Drosophila)	1.3394	4.28E-07
Ucp2	uncoupling protein 2 (mitochondrial, proton carrier)	1.3406	4.98E-06
Plp1	proteolipid protein (myelin) 1	1.3515	3.72E-04

Snord116	small nucleolar RNA, C/D box 116	1.3524	6.91E-05
Mir382	microRNA 382	1.3970	7.91E-05
CD24a	CD24a antigen	1.4007	2.26E-06
Cbln2	cerebellin 2 precursor protein	1.4123	2.82E-06
Taf1d	TATA box binding protein (Tbp)-associated factor, RNA polymerase I, D	1.4283	3.73E-04
Igf2	insulin-like growth factor 2	1.4513	1.84E-04
Txnip	thioredoxin interacting protein	1.5236	5.65E-05
Rny3	RNA, Y3 small cytoplasmic (associated with Ro protein)	1.5339	2.63E-04

Table 5.4. A list of the genes with differential expression in the enucleated dLGN compared to the control dLGN using Limma with a fold change cut off value of >1.3 or <0.77. Moderated p value is based on the moderated t-statistic generated by Limma analysis. Down-regulated genes are shaded blue. Up-regulated genes are shaded red.

5.3.1.2. Gene ontology analysis on differentially expressed genes

In order to assess whether specific gene ontologies were over-represented within the list of genes differentially expressed after enucleation I performed gene ontology (GO) analysis using DAVID (Huang da et al., 2009a; Huang da et al., 2009b). GO analysis includes the cellular component which genes are active in, the molecular function the gene performs or the broader biological process that a gene is within. Over-represented GOs may indicate how retinal input regulates dLGN function.

Twelve biological process GO terms were enriched in the differentially expressed genes (table 5.5). The majority of them are broad categories such as “cell surface receptor linked signal transduction”, “transmission of nerve impulses” and “regulation of kinase activity” which do not point at particular biological functions for further in depth analysis. Interestingly some of the functions highlighted are similar to functions enriched in the cortex after monocular enucleation in the critical period in mouse (Majdan and Shatz, 2006). These include kinase pathways, signalling molecules and synaptic proteins.

GO term from DAVID	**Number of genes**	**Percentage of microarray genes in GO term**	**p value**	**Genes**
cell surface receptor linked signal transduction	12	23.1%	2.90E-02	cd24a, gpr17, adamts3, adra1d, chrm2, dgkk, dgkg, gfra1, hcrt2, igf1, plp1, txnip

transmission of nerve impulses	5	9.6%	2.10E-03	cd24a, gjd2, plp1, shc3, timp4
lipoprotein	5	9.6%	5.60E-02	cd24a, adra1d, gfra1, plp1, vsnl1
regulation of transcription from RNA polymerase II promoter	5	9.6%	6.10E-02	fos, igf1, otx2, hmgn5, txnip
synaptic transmission	4	7.7%	9.00E-03	cd24a, gjd2, shc3, timp4
regulation of kinase activity	4	7.7%	1.00E-02	cd24a, dgkk, dgkg, spred2
regulation of transferase activity	4	7.7%	1.20E-02	cd24a, dgkk, dgkg, spred2
positive regulation of catalytic activity	4	7.7%	2.50E-02	cd24a, dgkk, dgkg, hcrt2
cell-cell signalling	4	7.7%	3.30E-02	cd24a, gjd2, shc3, timp4
regulation of phosphorylation activity	4	7.7%	3.30E-02	cd24a, dgkk, dgkg, spred2
positive regulation of molecular function	4	7.7%	3.80E-02	cd24a, dgkk, dgkg, hcrt2
chemical homeostasis	4	7.7%	5.80E-02	cd24a, gjd2, igf1, plp1

Table 5.5. Molecular function and biological process GO terms which were enriched within the genes differentially expressed between control and enucleated dLGN.

The cellular components which were identified also strengthen the role in cell signalling and nerve transmission pathways as many of the genes reside in the plasma membrane and extracellular regions (table 5.6).

DAVID: GO term Cellular component	Number of genes	Percentage of microarray genes in GO term	Genes
plasma membrane	15	28.8%	cd24a, gpr17, calb2, adra1d, chrm2, dgkk, gfra1, hmcn1, hcrt2, myot, kcnk9, spred2, syn, tacst2
extracellular region part	7	13.5%	frem3, adamts3, hmcn1, igf1, igf2, tgf-beta, timp4
proteinaceous extracellular matrix	5	9.6%	frem3, adamts3, hmcn1, tgf-beta, timp4
cell junction	5	9.6%	calb2, chrm2, gjd2, hmcn1, syn

Table 5.6. Cell component GO terms which were enriched within genes differentially expressed between control and enucleated dLGN.

As few pathways or specific biological functions were enriched in the list of genes differentially expressed after enucleation they do not suggest functions or pathways to further investigate. Despite this the function of various genes and how they fit into the

functional GO terms above is elaborated on in the discussion.

5.3.1.3. qPCR validation of differentially expressed genes

In order to validate the microarray results, 22 genes were chosen from the differentially expressed genes to perform real time, quantitative PCR (qPCR). 8 genes which were expressed at >1.5 or <0.66 after enucleation were included for qPCR validation. RIKEN cDNA E530001K10 and Rny3 were the only genes with a relative expression of >1.5 or <0.66 not included as commercially available primers were not available.

10 genes from those with a relative expression of >1.3 or <0.77 were chosen for qPCR verification. These were chosen from the larger list by biological relevance. They were Vsnl1, Myot, Moxd1, Kcnn3, Igf1, Calb2, Otx2, CD24a, Cbln2 Gjd2, Igf2 (see table 5.7 for biological relevance).

Additionally Adamts3, Timp4 and Egr2 were included to confirm that they were not false positives as they were outside the <0.77 threshold.

Gene symbol	Gene name	Relative expression in microarray	Function/ biological relevance
Hmcn1	hemicentin 1	0.5008	<0.667. Extracellular matrix protein involved in cell cell adhesion in epithelia.
Shc3	src homology 2 domain-containing transforming protein C3	0.5674	<0.667. A neuronal specific receptor tyrosine kinase adaptor protein involved in MAP-kinase signalling cascades.
Kcnk9	potassium channel, subfamily K, member 9	0.5724	<0.667. Potassium leak current channel, involved in establishing and maintaining resting membrane potential.
Dgkk	diacylglycerol kinase kappa	0.6111	<0.667. Phosphorylates DAG thus inhibiting downstream DAG/ PKC signalling.
Hcrtr2	hypocretin (orexin) receptor 2	0.6584	<0.667. GPCR which activates MAPkinase signalling cascade.
Fam19a4	family with sequence similarity 19, member A4	0.6584	<0.667. Uncharacterised chemokine like protein.
Osbpl3	oxysterol binding protein-like 3	0.6657	<0.667
Gjd2	gap junction protein, delta 2	0.6808	Member of connexion family (connexin36) important for electrical coupling of cells (Connors and Long, 2004). Visual deprivation lead to decreased connexin43 in the visual cortex (Majdan and Shatz, 2006).

Vsnl1	visinin-like 1	0.6835	Is a double-stranded mRNA binding protein which binds to and regulates the sub-cellular expression of TrkB mRNA (Mathisen et al., 1999; Tongiorgi et al., 1997). Is down-regulated in the cortex after visual deprivation (Majdan and Shatz, 2006).
Myot	myotilin	0.6967	Is up-regulated over development (section 5.3.1.6) and as such may represent a gene which is developmentally regulated or activity dependent and fails to be up-regulated after enucleation.
Moxd1	monooxygenase, DBH-like 1	0.7058	Is up-regulated over development (section 5.3.1.6) and as such may represent a gene which is developmentally regulated or activity dependent and fails to be up-regulated after enucleation.
Kcnn3	potassium intermediate/small conductance calcium-activated channel, subfamily N, member 3	0.7111	Small conductance potassium channel involved in after-hyperpolarisation (Sah, 1996; Lancaster and Adams, 1986) which may therefore regulate neuronal excitability.
Igf1	insulin-like growth factor 1	0.7578	Growth factor which activates receptor tyrosine kinases and therefore can alter downstream MAPK signalling (Werner and LeRoith, 2014). It is up-regulated in the magnocellular layers of the dLGN after visual deprivation in the rhesus monkey (Cheng et al., 2008). Furthermore it is normally up-regulated in the dLGN over development (see section 5.3.1.6).
Calb2	calbindin 2	0.7664	Calbindin2 (also known as calretinin) is a calcium sensitive protein which is normally up-regulated in the dLGN over development (see section 5.3.1.6). Is expressed by a subpopulation of interneurons distinct from Otx2+ interneurons (Rogers, 1992; Beurdeley et al., 2012).
Adamts3	a disintegrin-like and metallopeptidase (reprolysin type) with thrombospondin type 1 motif, 3	0.7744	<0.77. Adamts3, a metalloprotease, may be involved in the regulation of chondroitin sulfate proteoglycans (including aggrecan). Aggrecan has been shown to regulated corticothalamic ingrowth to the dLGN after enucleation (Brooks et al., 2013). Furthermore aggrecan appears to be affected by sensory deprivation in several systems (Brooks et al., 2013; Kind et al., 2013; Matthews et al., 2002; McRae et al., 2007).
Timp4	tissue inhibitor of metalloproteinase 4	0.7747	<0.77. Timp4 is within a family of metalloprotease inhibitors which can regulate the Adamts family of metalloproteases (Brooks et al., 2013).

Egr2	early growth response 2	0.7786	<0.77. An immediate early gene which may therefore be involved in other downstream changes in gene expression (Flavell and Greenberg, 2008; Kaczmarek and Chaudhuri, 1997). Egr2 has also been shown to be down-regulated in the visual cortex after visual deprivation (Majdan and Shatz, 2006).
Otx2	orthodenticle homologue 2 (Drosophila)	1.3394	Expressed by GABAergic interneurons which migrate into the dLGN from the vLGN. Interneuron migration and integration is affected after enucleation (Golding et al., 2013).
CD24a	CD24a antigen	1.4007	CD24a is a cell adhesion glycoprotein. Ligands include L1 and TAG1 which are expressed on thalamocortical and corticothalamic neurons respectively (Denaxa et al., 2001; Fukuda et al., 1997; Wiencken-Barger et al., 2004). L1 and TAG1 mediate CD24 induced regulation of neurite outgrowth (both attraction and repulsion depending on the cellular context) (Kleene et al., 2001; Lieberoth et al., 2009).
Cbln2	cerebellin 2 precursor protein	1.4123	Is a synaptic organiser which is down-regulated in the dLGN over development (section 5.3.1.6 and (Singh et al., 2012)) and therefore is one of the few genes which are unregulated after enucleation and down-regulated over development. As it plays a role in synaptic organisation it may alter synaptic targeting in normal development (Singh et al., 2012).
Igf2	insulin-like growth factor 2	1.4513	Growth factor which activates receptor tyrosine kinases and therefore can alter downstream MAPK signalling (Werner and LeRoith, 2014). Igf1 and 2 are similar and often perform similar cellular processes as such it is interesting that they appear differently expressed in the enucleated dLGN.
Txnip	thioredoxin interacting protein	1.5236	>1.5

Table 5.7. 22 genes were chosen from those identified as differentially expressed between control and enucleated dLGN including brief details of relevant biological functions.

The qPCR results showed that all genes were differentially expression in the same direction as shown by the microarray (figure 5.4A) thus validating my microarray results. To test significance a one tailed, paired t-test was performed. 21 out of 22 genes were significantly differently expressed in the enucleated dLGN compared to the control dLGN (figure 5.4B). Only Adamts3 was not significantly differentially expressed as

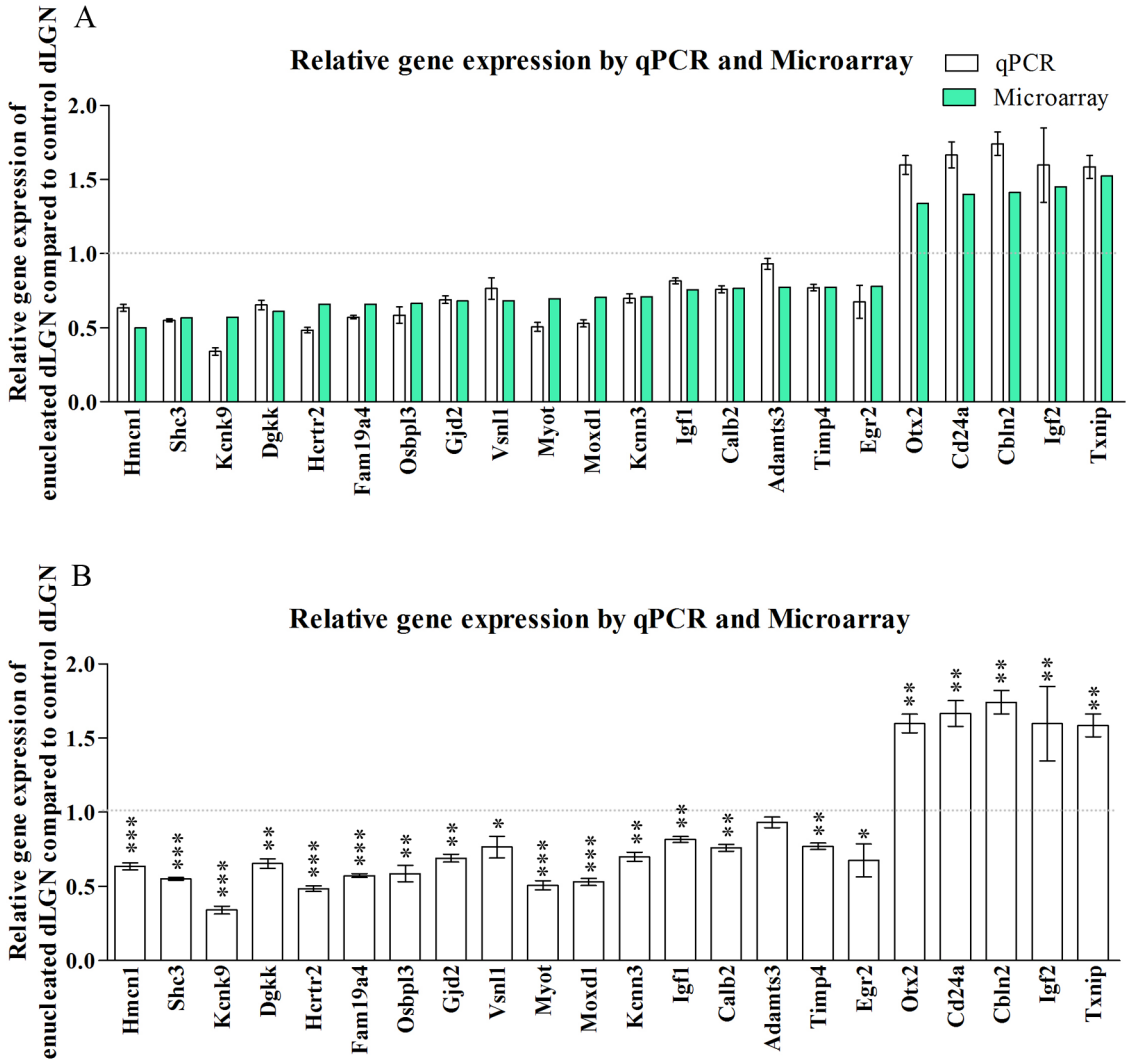

Figure 5.4. Graph showing relative expression levels of genes in enucleated dLGN compared to control dLGN as assessed by qPCR and microarray. A. The relative expression of 22 genes in the enucleated dLGN compared to the control dLGN. Relative expression of all genes, as assessed by qPCR, was in the same direction as relative expression assessed by the microarray. B. The significance of relative expression level of 22 genes in the enucleated dLGN compared to the control dLGN as assessed by qPCR. 21 out of 22 genes were significantly differently expressed in the enucleated dLGN compared to the control dLGN. Adamts3 was not significantly differentially expressed. Values shown are mean and standard error. One tailed, paired t-test was performed to assess statistical significance. *= significant at p=0.05, **= significant at p=0.005, ***= significant at p<0.0005

assessed by qPCR. Thus my microarray results were validate for 21/22 genes tested.

5.3.1.4. In situ hybridisation characterisation of differentially expressed genes over development using the resources of the Allan Developing Mouse Brain Atlas

In order to characterise the expression of the genes which are differentially expressed in the dLGN after enucleation I compiled *in situ* hybridisation images from the Allan Developing Mouse Brain Atlas (©2013 Allen Institute for Brain Science. Allen Developing Mouse Brain Atlas [Internet]. Available from: http://developingmouse.

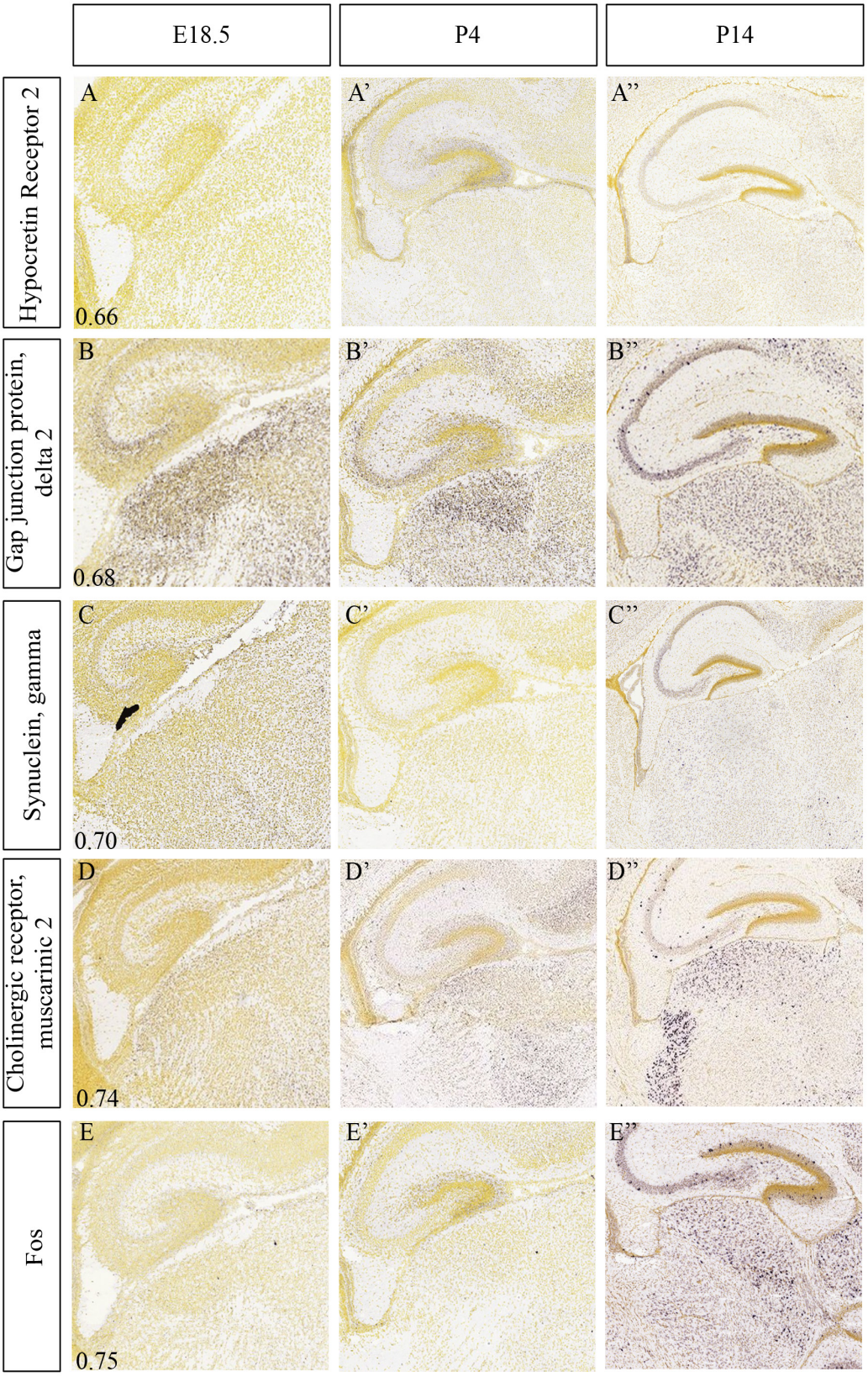

Figure 5.5. Developmental course of gene expression in the dLGN by in situ hybridisation from Allen Brain Atlas. Genes identified by microarray as differentially expressed in the enucleated dLGN compared to the control dLGN; hypocretin receptor 2, gap junction protein delta 2, synuclein gamma, cholinergic receptor- muscarinic 2, Fos. Ordered by relative expression. All images are sagittal sections. A-A". In situ hybridisation of hypocretin receptor 2 appears unsuccessful. B-B". Gap junction protein delta 2 shows clear labelling in the dLGN which is consistent over development from

E18.5-P14. C-C". In situ hybridisation of synuclein gamma appears unsuccessful. D-D". Cholinergic receptor muscarinic 2. In situ hybridisation at E18.5 is unclear. At P4 there is weak labelling in the anterior of the dLGN. At P14 it is expressed in the dLGN and the TRN. E-E" In situ hybridisation for Fos at E18.5 and P4 is unsuccessful. At P14 Fos expression is apparent throughout the thalamus and particularly in the dLGN. A-E includes the relative expression of the gene of interest in the enucleated dLGN compared to control dLGN. Abbreviations used: dLGN, dorsal Lateral Geniculate Nucleus; TRN, thalamic reticular nucleus. Scale bars unavailable as images are from publically available Allan Brain Atlas.

brain-map.org.). All 51 genes with a relative expression of >1.3 or <0.77 and Adamts3, Timp4 and Egr2 were searched for. Only 14 genes were present in the Allan Brain Development Mouse Brain Atlas. All 14 of these genes for which the Allan Developing Mouse Brain Atlas had *in situ* hybridisation experiments have been included in figures 5.5-5.7. Any genes which are absent from these figures were absent from the Allan Developing Mouse Brain Atlas at 20.06.2014. These figures show the genes in order of relative gene expression from most down-regulated to most up-regulated (for reference, panel A-E of each figure includes the relative expression value of the gene of interest).

First I discuss the genes which are down-regulated in the enucleated dLGN.

Gap junction protein delta 2 is expressed in the dLGN from E18.5- P10 (figure 5.5 B-B''). Its expression is not specific to the dLGN however it appears slightly denser in the dLGN than surrounding thalamic nuclei but this may be due to the increased cell density in the dLGN.

Cholinergic receptor muscarinic 2 is in the anterior dLGN at P4 (figure 5.5 D'). At P14 expression is strongest in the anterior region of the dLGN but is present throughout the dLGN and is up-regulated over development (figure 5.5D''). At P14 the only other labelling is in the TRN and thus within the thalamus is dLGN specific.

Fos expression is very low or absent in the thalamus at E18.5 and P4 (figure 5.5 E-E'). At P14 Fos expression is clearly present in the thalamus including the dLGN (figure 5.5 E'').

Glial cell line derived neurotrophic factor 1 is weakly expressed in the dLGN at E18.5 (figure 5.6 B). At P4 and P14 its expression has increased (figure 5.6 B'-B''). It appears enriched in the dLGN compared to the VPM. It is strongly expressed in the TRN at all

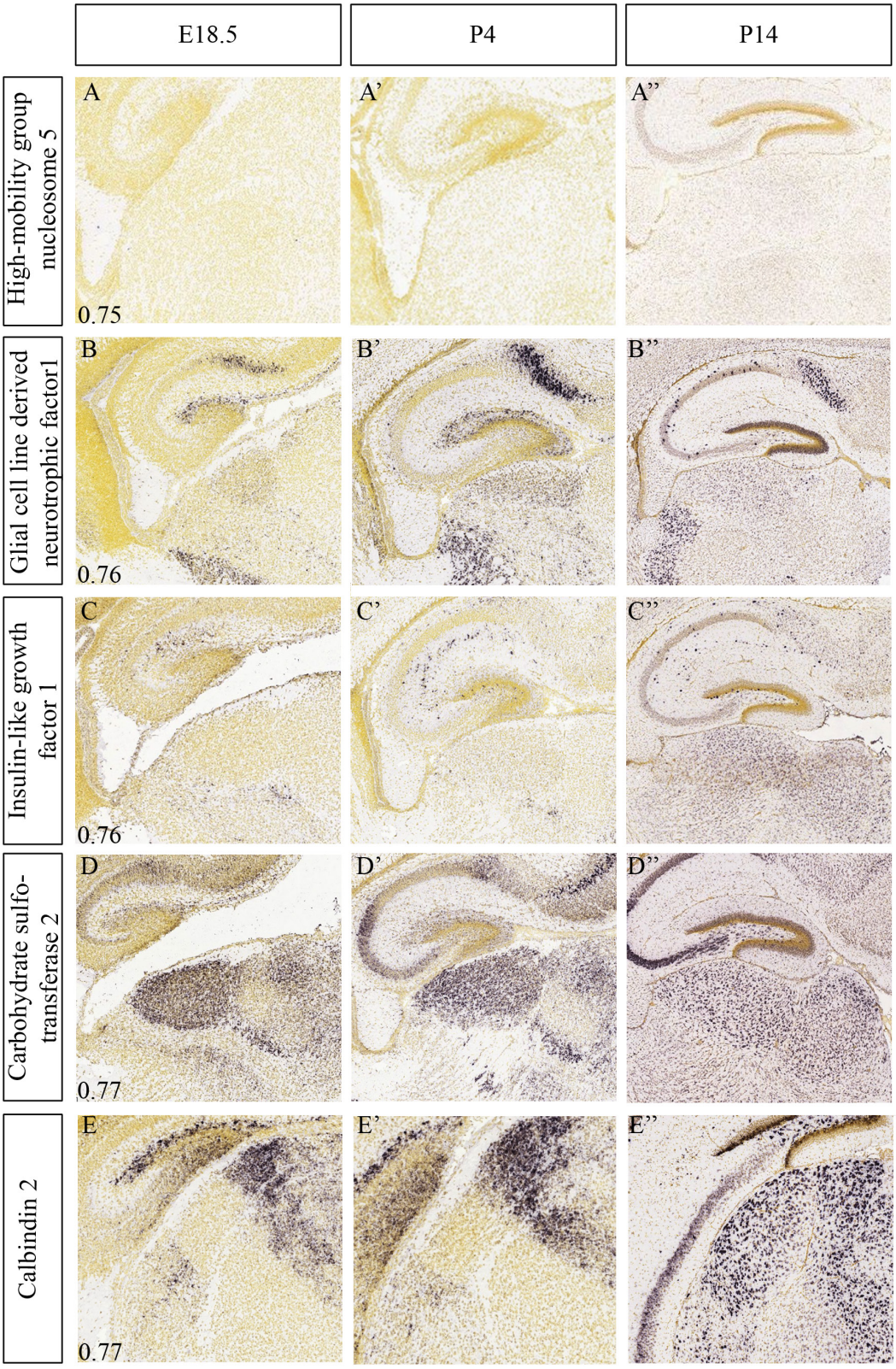

Figure 5.6. Developmental time course of gene expression in the dLGN by in situ hybridisation from Allen Brain Atlas. Genes identified by microarray as differentially expressed in the enucleated dLGN compared to the control dLGN: high mobility group nucleosome 5, glial cell line derived neurotrophic factor 1, insulin-like growth factor 1, carbohydrate sulfotransferase 2 and calbindin2. Ordered by relative expression. Images are sagittal sections apart from calbindin2 which is coronal. A-A". In situ hybridisation against high-mobility group nucleosome 5 appears unsuccessful. B-B". At E18.5 glial cell line derived neurotrophic factor is expressed in the dLGN and VPM and more densely in the

TRN. At P4 its expression appears denser in the dLGN than the VPM; it is most dense in the TRN. At P14 its expression remains slightly denser in the dLGN than the VPM and most dense in the TRN. C-C". Insulin-like growth factor 1 is expressed in the VPM but not dLGN at E18.5. At P4 there is weak expression in the VPM. At P14 it is expressed in the dLGN and surrounding thalamic nuclei. D-D". Carbohydrate sulfotransferase 2 is strongly expressed in the dLGN at E18.5 and P4 and is enriched in the dLGN compared to surrounding structures. At P14 it is still most densely expressed in the dLGN but it is also expressed in the other thalamic nuclei. E-E". Calbindin 2 is absent from the dLGN and VPM at E18.5 and P4 but is strongly present in the LP and Po. At P14 Calbindin is densely expressed in the dLGN, LP and Po and is expressed though less densely in the vLGN and VPM. A-E includes the relative expression of the gene of interest in the enucleated dLGN compared to control dLGN. Abbreviations used: dLGN, dorsal Lateral Geniculate Nucleus; VPM, ventrobasal thalamic nucleus; LP, lateral posterior nucleus; Po, posterior thalamic nucleus; TRN, thalamic reticular nucleus. Scale bars unavailable as images are from publically available Allan Brain Atlas.

three ages.

Insulin-like growth factor 1 is absent from the dLGN at E18.5 and P4 even though it is expressed in the external medullary laminar between the dLGN and the VPM (figure 5.6 C and C'). At P14 it is expressed in the dLGN (figure 5.6 C''). Thus Igf1 is developmentally regulated.

Carbohydrate sulfotransferase 2 is strongly expressed in the dLGN at E18.5 and P4 (figure 5.6 D-D'). At this age it is enriched in the dLGN and a band ventral to the MGN. At P14 it is also expressed in other thalamic nuclei including the MGN.

Calbindin 2 (calretinin) is absent from the dLGN at E18.5 and P4 although it is densely expressed in the higher order LP and Po nuclei and weakly expressed in the vLGN (figure 5.6 E and E'). By P14 it is expressed in the dLGN, the vLGN, the LP, the Po and weakly in the VPM (figure 5.6 E''). It appears highly specifically regulated over development.

Early growth response 2 is expressed throughout the thalamus at all ages however it is particularly dense at E18.5 (Figure 5.7 A- A'').

Of the genes which are down-regulated in the dLGN after enucleation, several of them are up-regulated in the dLGN over development as assessed by these *in situ* hybridisations. This includes Chrm2, Fos, Gfra1, Igf1 and Calb2.

I will now discuss the genes which are up-regulated in the enucleated dLGN.

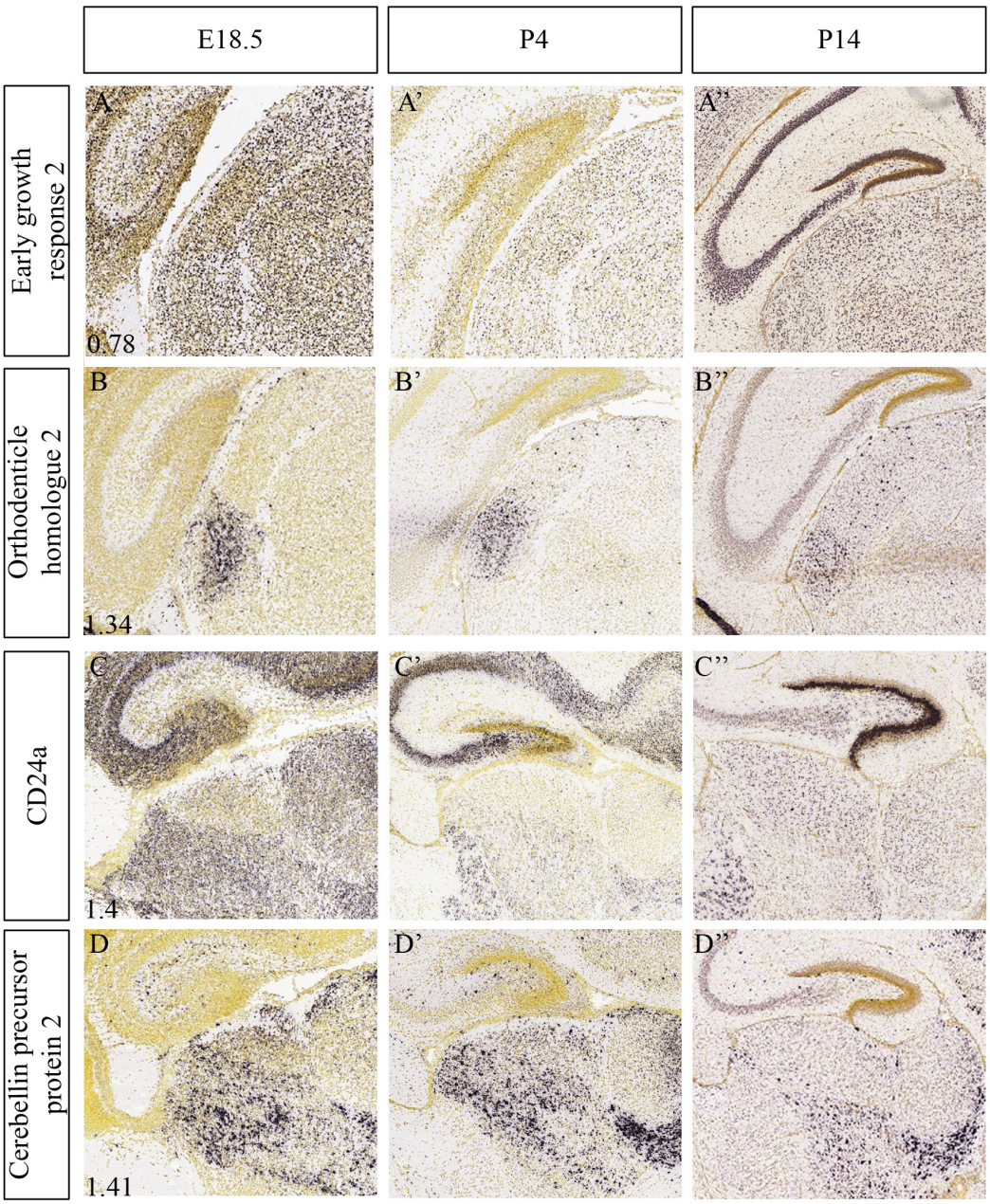

Figure 5.7. Developmental time course of gene expression in the dLGN by in situ hybridisation from Allen Brain Atlas. Genes identified by microarray as differentially expressed in the enucleated dLGN compared to the control dLGN: early growth response 2; orthodenticle homologue 2, CD24a, cerebellin precursor protein 2. Ordered by relative expression. Images are sagittal sections apart from early growth response 2 and orthodenticle homologue 2 which are coronal. A-A". Early growth response 2 is densely expressed in the dLGN, vLGN, VPM and LP at E18.5 At P4 its expression is reduced in these nuclei. At P14 its expression is increased again. B-B" Orthodenticle homologue 2 is expressed in the vLGN at E18.5. There is not clear orthodenticle homologue 2 labelling in the dLGN but there appears to be labelling at the ventral edge of the nucleus. At P4 the vLGN is labelled and a few spots of labelling are present in the dLGN. At P14 the vLGN is labelled and there are more numerous spots of labelling in the dLGN. C-C". At E18.5 CD24a is expressed in VPM, Po and MGN but is much less expressed in the dLGN. At P4 expression has greatly reduced in all thalamic nuclei. By P14 expression has increased again and is denser in the dLGN compared to surrounding nuclei. D-D". Cerebellin precursor protein 2 is expressed in the dLGN and the Po at E18.5 and P4. By P14 expression is reduced in the dLGN but is still present in Po. At all ages there is dense expression in a band beneath the MGN A-D includes the relative expression of the gene of interest in the enucleated dLGN compared to control dLGN. Abbreviations used: dLGN, dorsal Lateral Geniculate Nucleus; vLGN, ventral Lateral Geniculate Nucleus; VPM, ventrobasal thalamic nucleus; LP, lateral posterior thalamic nucleus; Po, posterior thalamic nucleus MGN, Medial Geniculate Nucleus. Scale

bars unavailable as images are from publically available Allan Brain Atlas.

Orthodenticle homologue 2 is expressed densely in the vLGN at E18.5, P4 and P14 (figure 5.7 B-B''). At E18.5 there is no clear labelling in the dLGN. At P4 a few spots of labelling are present in the dLGN. At P14 the vLGN is labelled and there are more numerous spots of labelling in the dLGN. This developmental pattern coheres with the migration of GABAergic interneurons into the dLGN from the vLGN (Golding et al., 2013). Otx2 is one of the few genes which increases in the enucleated dLGN and increases in the dLGN over development according to *in situ* hybridisation and the developmental microarray discussed in section 5.3.1.6. Otx2 protein is also transmitted throughout the visual system in an activity dependent manner, where it is important for visual cortex neuronal plasticity (Beurdeley et al., 2012; Sugiyama et al., 2008). However whether, and how, this is linked to the regulation of Otx2 mRNA expression in the dLGN GABAergic interneurons is unclear.

CD24a is expressed throughout the thalamus at E18.5 however it appears to have less expression in the dLGN compared to the VPM and MGN (figure 5.7 C). At P4 its expression has reduced considerably but it is still visible in the dLGN and VPM (figure 5.7 C'). At P14 CD24a remains expressed in the dLGN, VPM and MGN (Figure 5.7 C'').

Cerebellin precursor protein 2 is expressed in the dLGN and the Po at E18.5 and P4 (figure 5.7 D and D'). By P14 expression is reduced in the dLGN but is still present in the Po (figure 5.7 D'').

CD24a and Cbln2 are two genes which are up-regulated in the enucleated dLGN compared to the control dLGN however they appear in these *in situ* hybridisations to be down-regulated in the dLGN over development.

These results from the Allen Developing Mouse Brain Atlas show the developmental gene expression profile of genes which are differentially expressed in the dLGN after enucleation. 9 of these 14 genes showed some form of developmental regulation thus

suggesting the dLGN has dynamic gene expression over early postnatal development.

5.3.1.5. qPCR analysis of genes of interest in the enucleated compared to control dLGN

Microarray statistical analysis is purposefully stringent to reduce the number of false positives but this increases the chance of false negatives. I therefore chose to analyse the expression of a further 4 genes (chosen based on biological interest, table 5.8) by qPCR. These genes were aggrecan, ephrinA5, BDNF and early growth response 1.

Aggrecan was chosen because of the recent work suggesting it may have a role in ingrowth of corticothalamic fibres to the dLGN (Brooks et al., 2013). EphrinA5 was chosen because it was previously shown to have a reduced expression (as assessed by *in situ* hybridisation) in the dLGN after enucleation (Dye et al., 2012). Furthermore as a well-known guidance cue changes in its expression within the dLGN may cause changes in circuit formation (Castellani et al., 1998; Deschamps et al., 2010; Miao and Wang, 2012; O'Leary and McLaughlin, 2005; Pfeiffenberger et al., 2005; Pfeiffenberger et al., 2006). BDNF was chosen because it is well documented to be altered in the cortex after visual deprivation (Majdan and Shatz, 2006; Castren et al., 1992; Bozzi et al., 1995; Schoups et al., 1995). Egr1 was chosen as it is an immediate early gene which is related to Egr2 and is reduced in the cortex after visual deprivation (Majdan and Shatz, 2006; Kaczmarek and Chaudhuri, 1997; Van Brussel et al., 2011; Nys et al., 2014).

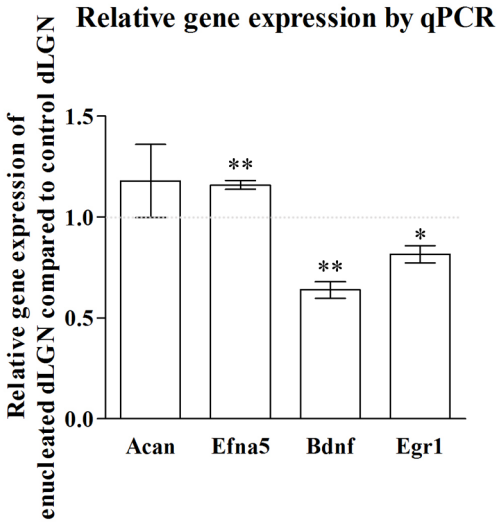

Figure 5.8. Graph showing relative expression by qPCR in enucleated dLGN compared to control dLGN of genes identified by biological interest. Aggrecan was not significantly differently expressed. EprhinA5 was significantly increased in the enucleated dLGN compared to control dLGN. BDNF was significantly decreased in enucleated dLGN compared to control dLGN. Early growth response 1 was significantly decreased in enucleated dLGN compared to control dLGN. Values shown are mean and standard error. *= significant at p=0.05, **= significant at p=0.005.

Gene symbol	Gene name	Function/ reason for biological interest
Acan	aggrecan	Functions include axon guidance; role in corticothalamic fibre ingrowth to the dLGN (Brooks et al., 2013).
Efna5	ephrinA5	Guidance cue, ligand for EphA receptors. Previously demonstrated to have reduced area of expression in the dLGN after enucleation (Dye et al., 2012).
BDNF	brain derived neurotrophic factor	Activity dependent gene which is down-regulated in visual system structures including the cortex after visual deprivation (Majdan and Shatz, 2006; Castren et al., 1992; Bozzi et al., 1995; Schoups et al., 1995).
Egr1	early growth response 1	Egr1 (also known as zif268) is one of the first immediate early genes (Kaczmarek et al., 1999; Flavell and Greenberg, 2008). It is related to Egr2 which was down-regulated in the enucleated dLGN according to my microarray. Egr1 is reduced in the other visual system structures such as cortex after visual deprivation (Majdan and Shatz, 2006; Kaczmarek and Chaudhuri, 1997; Nys et al., 2014). Immediate early genes often regulate downstream activity dependent changes in gene expression (Flavell and Greenberg, 2008).

Table 5.8. Genes which were chosen to perform qPCR analysis to compare expression between the control and the enucleated dLGN which were not differentially expressed according to the microarray. Details include biological reason for interest.

Aggrecan was not differentially expressed between the control and the enucleated dLGN (figure 5.8). This confirms my microarray results and microarray results comparing the dLGN in math5$^{-/-}$ mice (which lack retinal ganglion cells and therefore retinal input to the dLGN) with control mice (Brooks et al., 2013). These results support the hypothesis that the change in aggrecan protein within the dLGN after loss of retinal input is likely to be regulated at the protein level (e.g. degrading enzymes) rather than at a transcriptional level.

EphrinA5 was significantly up-regulated in the enucleated dLGN (figure 5.8). This contradicts recent results using *in situ* hybridisation which state that the area of ephrinA5 expression within the dLGN is reduced after enucleation (Dye et al., 2012). *In situ* hybridisation results are not quantitative and can be biased by inaccurate section matching especially for guidance molecules which are expressed in gradients. EphrinA5 has an anterior to posterior gradient in the dLGN (figure 5.9 A-A') and thus mismatched anterior to posterior sections could produce inaccurate results. In order to prevent anterior to posterior gradients affecting results I dissected out the entire dLGN from anterior to posterior (3 sections of 200µm thick). Furthermore the dLGN is smaller after enucleation thus an apparent reduction in expression could be due to fewer cells

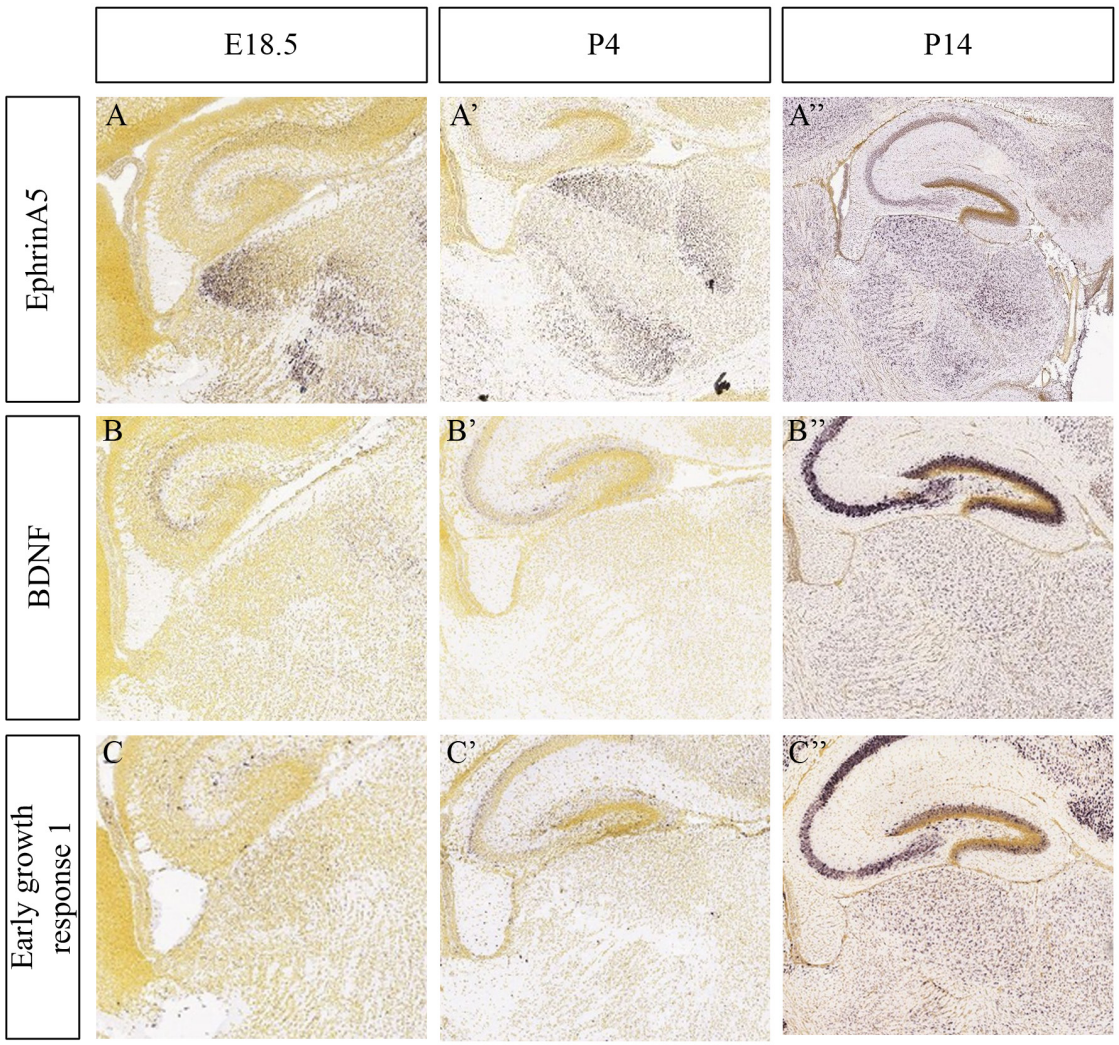

Figure 5.9. Developmental time course of expression of ephrinA5, BDNF and early growth response 1 in the dLGN by in situ hybridisation from Allan Brain Atlas. A-A". EphrinA5 is expressed in the dLGN from E18.5 to P14. At E18.5 and P4 it has a clear anterior to posterior gradient. B-B". BDNF in situ hybridisation is unclear at E18.5 and P4. At P14 BDNF is expressed in the dLGN and surrounding thalamic nuclei. C-C". Early growth response in situ hybridisation is unclear at E18.5 and P4. At P14 early growth response 1 is expressed in the dLGN and surrounding thalamic nuclei. Abbreviations used dLGN; dorsal Lateral Geniculate Nucleus, BDNF; brain derived neurotrophic factor. Scale bars unavailable as images are from publically available Allan Brain Atlas.

whereas qPCR adjusts for this by controlling the starting mRNA quantity.

BDNF was significantly down-regulated in the enucleated dLGN (figure 5.8). This result is consistent with previous results showing that BDNF is regulated in the cortex during the development of the visual system (Lein et al., 2000; Lein and Shatz, 2000) and is down-regulated in the cortex after visual deprivation (Majdan and Shatz, 2006; Cabelli et al., 1995; Tagawa et al., 2005; Castren et al., 1992). *In situ* hybridisation showed that BDNF is up-regulated over development with increased expressed in the

dLGN at P14 (figure 5.9 B''). Therefore the reduction in BDNF expression in the dLGN after enucleation may suggest the dLGN is less mature after enucleation.

Egr1 was significantly down-regulated in the enucleated dLGN (figure 5.8). Egr1 also has reduced expression in the cortex after visual deprivation (Majdan and Shatz, 2006; Kaczmarek and Chaudhuri, 1997; Van Brussel et al., 2011; Nys et al., 2014). *In situ* hybridisation showed that, like BDNF, Egr1 is expressed in the dLGN later in development (figure 5.9 C''). Therefore the reduction in Egr1 expression in the dLGN after enucleation further supports the suggestion that the dLGN is less mature after enucleation.

These qPCR results identify three more genes which are differentially expressed in the enucleated dLGN compared to the control dLGN. Two of them, BDNF and Egr1, overlap with genes which are differentially expressed in the cortex after enucleation (Majdan and Shatz, 2006).

5.3.1.6. Differential expression of genes after enucleation and over the first 10 postnatal days development

In the previous sections I have demonstrated that some of the genes which are differentially expressed after enucleation appear developmentally regulated. I therefore chose to systematically investigate whether genes whose expression is altered after enucleation are also developmentally regulated by comparing my microarray results with the results from a microarray comparing the dLGN at P0 and P10 (results kindly provided by Professor Denis Jabaudon).

There are four potential expression profiles that a gene could show after enucleation and over development:

1. Genes whose differential expression after enucleation is premature and would occur in the same direction over development. My tracing experiments in chapter 4 show that enucleation causes premature entry of the corticothalamic fibres to the dLGN. This precocious development could be underpinned by premature gene expression changes for example premature loss of inhibitory cues, or premature gain of attractive

cues.

2. Genes whose normal developmental regulation is delayed or disrupted by loss of input and as such would change in one direction after enucleation and change in the opposite direction over development. The loss of input could affect normal developmental regulation of gene expression in the nervous system.

3. Genes whose expression is altered after monocular enucleation but is not normally developmentally regulated.

4. Genes whose expression is developmentally regulated but are not affected by monocular enucleation.

To perform this comparison my control and enucleated .CEL files were analysed using the same statistical method as used to analyse the developmental array for compatibility (ANOVA and t-test intercept method). This analysis identified genes which were differentially expressed both between control and enucleated dLGN at P6, and between the P0 control dLGN and the P10 control dLGN (table 5.9). Direct microarray comparison could not be performed because different microarray chips were used.

With a fold change cut off of greater than 1.3 (or -1.3, equivalent to <.77 relative expressions) 69 genes were differentially expressed between the enucleated and the control dLGN. 42 were down-regulated and 26 were up-regulated in the enucleated dLGN.

43 genes which were differentially expressed after enucleation were also differentially expressed at P10 compared P0 (table 5.9). Fold change (rather than relative expression) was used to tabulate and graph these results to allow comparison with Professor Jabaudon's results. 19 genes were identified in the ANOVA/t-test intercept analysis method but were not identified by the Limma analysis method (* in table 5.9). These genes were discarded from further analysis because the Limma multiple testing correction is thought to be the most robust for microarray bioinformatics analysis thus reducing the chance of false positives (Smyth, 2004). Of the 43 genes which were

differentially expressed both after enucleation and over development, 30 were down-regulated in the enucleated dLGN, 13 were up-regulated in the enucleated dLGN (table 5.9).

Gene symbol	Gene name	Fold change after enucleation	Fold change over development from P0-P10
Shc3	src homology 2 domain-containing transforming protein C3	-1.8219	3.4082
Hcrtr2	hypocretin (orexin) receptor 2	-1.62088	1.2800
Osbpl3	oxysterol binding protein-like 3	-1.52345	-1.1790
Moxd1	monooxygenase, DBH-like 1	-1.51864	3.1421
Myot	myotilin	-1.51491	9.7488
Tacstd2	tumor-associated calcium signal transducer 2	-1.49733	1.5370
Spred2	sprouty-related, EVH1 domain containing 2	-1.48255	1.2718
Gjd2	gap junction protein, delta 2	-1.47835	1.3583
Fam19a4	family with sequence similarity 19, member A4	-1.4642	3.9706
Vsnl1	visinin-like 1	-1.46326	10.5566
Kcnn3	potassium intermediate/small conductance calcium-activated channel, subfamily N, member 3	-1.45767	-1.0089
Ecm2	extracellular matrix protein 2	-1.42854	1.0527
Ptgr1	prostaglandin reductase 1	-1.41455	2.3981
Sncg	synuclein, gamma	-1.40086	4.3147
Synm	synemin, intermediate filament protein	-1.39202	9.4875
Dgkg	diacylglycerol kinase, gamma	-1.38908	12.1429
Pdlim5	PDZ and LIM domain 5	-1.37741	5.3178
Egr2	early growth response 2	-1.35228	-1.1871
	2610318N02Rik *	-1.34751	-2.1116
Shisa6	shisa homologue 6 (Xenopus laevis)	-1.34632	3.5749
Fos	FBJ osteosarcoma oncogene	-1.34455	1.6558
Hmgb2	high mobility group box 2 *	-1.34431	-1.6807
Calb2	calbindin 2	-1.34087	4.7060
Lce1c	late cornified envelope 1C *	-1.33336	1.1469
Igf1	insulin-like growth factor 1	-1.33168	7.3543
Pvt1	plasmacytoma variant translocation 1 *	-1.3302	3.7026
Timp4	tissue inhibitor of metalloproteinase 4	-1.31561	5.5110
Hmgn5	high mobility group box 5	-1.30998	3.8549
Chst2	carbohydrate sulfotransferase 2	-1.3083	1.4138
Gfra1	glial cell line derived neurotrophic factor family receptor alpha 1	-1.30756	1.8884
Ucp2	uncoupling protein 2	1.31643	1.2418
Tac1	tachykinin 1 *	1.3246	1.9175
Rnf114	ring finger protein 114	1.32678	1.0594
Gpr17	G protein-coupled receptor 17	1.34438	8.1938
Hist1h4c	histone cluster 1 h4c *	1.36685	-3.9876

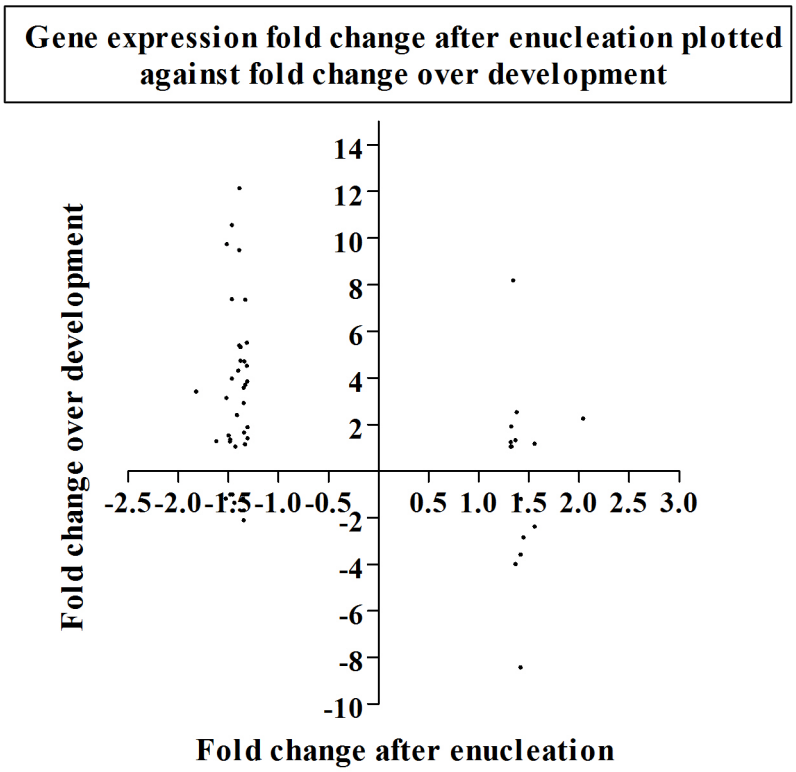

Figure 5.10. Graph showing genes which were differentially expressed after enucleation and over development. The fold change of genes differentially expressed in the enucleated dLGN compared to the control dLGN was plotted against their fold change value in the P10 dLGN compared to the P0 dLGN. The majority of genes are down-regulated in the enucleated dLGN. The majority of these down-regulated genes are up-regulated in the dLGN over development. Of the few genes which were up-regulated after enucleation, 8 were up-regulated over development and 6 were down-regulated over development.

Rmnd5a	required for meiotic nuclear division 5 homologue A	1.36687	1.3232
Otx2	orthodenticle homologue 2 (Drosophila)	1.37712	2.5278
Cd24a	CD24a antigen	1.41627	-8.4301
Taf1d	TATA box binding protein (Tbp)-associated factor, RNA polymerase I, D	1.4188	-1.2019
Cbln2	cerebellin 2 precursor protein	1.44633	-2.8478
Txnip	thioredoxin interacting protein	1.55786	-2.3892
Ptgds	prostaglandin synthase *	2.03973	2.2592

Table 5.9. A list of the genes with differential expression in the enucleated dLGN compared to the control dLGN and the P10 dLGN compared to the P0 dLGN. List generated using ANOVA/t-test intercept method using a fold change cut off value of >1.3 or <-1.3. Down-regulated genes are shaded blue. Up-regulated genes are shaded red. Genes not identified in Limma analysis denoted *.

These results demonstrate that, whilst the majority of genes are down-regulated in the enucleated dLGN compared to the control dLGN, the majority of those genes (25/30) are normally up-regulated between P0 and P10 (table 5.9 and figure 5.10).

The effect of monocular enucleation on gene expression within the dLGN

Of the genes which were up-regulated after enucleation there was not a trend in direction of changing expression over development: 7 were up-regulated over development, 6 were down-regulated over development (table 5.9 and figure 5.10).

Thus 12 genes were changed in the same direction after enucleation and over development whereas 31 genes were changed in the opposite direction after enucleation as over development. This suggests that loss of retinal input to the dLGN prevents the normal maturation of the transcriptome of the dLGN relay neurons.

These results suggest that the enucleated dLGN is transcriptionally delayed compared to the control dLGN. These results also indicate that this is mainly due to the failed or delayed up-regulation of genes. Whether the regulation is delayed or completely abolished could be assessed by performing enucleation at birth and examining the expression of these genes at a later age such as P21.

5.4. Discussion

5.4.1. Loss of retinal input alters gene expression in the dLGN

5.4.1.1. Differential gene expression in the enucleated dLGN compared to the control dLGN

In this chapter I have demonstrated that at P6, following monocular enucleation at P0, there are ~50 genes which are differentially expressed in the enucleated dLGN compared to the control dLGN. These results suggest that retinal input to the dLGN regulates the expression of genes within the dLGN although it is important to point out that there are several potential contributing factors to the changes in gene expression. Firstly, monocular enucleation removes both retinal activity and retinal axons and thus it is hard to distinguish the effect of these two losses. Secondly, in chapter 4 I demonstrate that layer VI and VIb fibres enter the enucleated dLGN prematurely. Therefore by P6 the control dLGN and the enucleated dLGN differ by two axon populations; the enucleated dLGN lacks retinal axons, but has premature corticothalamic VI and VIb fibres present whereas the P6 control dLGN maintains retinal input but does not yet have VI and VIb fibres present. Thus the premature gain of VI and VIb axons in the

dLGN may also contribute to the altered gene expression. These points will also be discussed in more detail presently in section 5.4.1.3.

My results are the first to provide systematic evidence of a clear change in transcription in the dLGN at P6 after the removal of retinal input at birth. Previous work addressing the question of early gene changes in the dLGN after visual deprivation included studies using *in situ* hybridisation on 4 genes chosen by biological relevance showed limited changes in ephrinA5 in the dLGN after monocular enucleation (Dye et al., 2012). However my own microarray and qPCR results demonstrate that ephrinA5 mRNA was significantly increased in the enucleated dLGN. A microarray comparing the dLGN at P3 in control mice and mice who lack retinal ganglion cells (math5$^{-/-}$ mutant) has demonstrated there are genes differentially expressed in dLGN lacking retinal input however the published genes includes only those within the adamts family (Brooks et al., 2013). Gene expression changes in thalamic nuclei after changes to peripheral input have also been clearly demonstrated. Modality specific input has been demonstrated to regulate gene expression in the ferret thalamic nuclei; when retinal input is rewired to the MGN, the MGN begins expressing genes which are normally expressed in the dLGN (Horng et al., 2009).

My results are among the first to examine visual system gene expression changes at an early time point, P6. For example many previous studies have addressed the gene expression changes in visual cortex after visual deprivation before or during the critical period, and assessing gene expression during the critical period (Majdan and Shatz, 2006; Bozzi et al., 1995; Schoups et al., 1995; Kaczmarek et al., 1999; Kind et al., 2013) or adulthood (Castren et al., 1992; Nys et al., 2014). One of the few papers which has addressed gene expression changes in the dLGN performed microarray analysis after long term visual deprivation (2 to 4 months) by reduced eye opening in the rhesus macaque monkey dLGN (Cheng et al., 2008). Thus previous research has focused on the molecular mechanisms behind processes such as ocular dominance or within the established circuits. My results on the other hand examine how retinal input to the

dLGN might affect molecular programs that are involved in the early development of the visual/ geniculate circuitry including the geniculocortical and corticogeniculate circuit.

My results reveal that the majority (65%) of the genes which were differentially expressed in the dLGN after enucleation were down-regulated. This is similar to results in the cortex which have shown that following visual deprivation in the critical period more genes are down-regulated rather than up-regulated (Majdan and Shatz, 2006). However after longer term deprivation in the rhesus monkey dLGN, slightly more genes were up-regulated (54%) than down-regulated (46%) (Cheng et al., 2008). My results reflect the gene changes which occur in the first week of development after enucleation and therefore in the immediate aftermath of the loss of retinal input (and the associated reduction in dLGN neuronal activity). After long term visual deprivation there is evidence that the visual system (including the dLGN and visual cortex) may undergo synaptic scaling and homeostatic plasticity and therefore have increased activity (Golding et al., 2013; Keck et al., 2013; Goel and Lee, 2007). These differences could suggest that the dynamics of gene expression changes are dependent on the length of visual deprivation and the age of the animal at the time of the study. The dominance of down-regulated genes present in my results leads me to speculate that this may be due to a failure/ delay to up-regulate important genes; this will be discussed in more detail presently in section 5.4.1.3.

5.4.1.2. Genes and functional groups (gene ontologies) of genes that are changed after monocular enucleation

In order to further investigate how monocular enucleation impacts on the molecular transcription programs within the developing dLGN I performed gene ontology analysis and extensive literature research on the genes which were differentially expressed.

The gene ontology analysis performed using DAVID brought up only a few gene ontology based biological processes. This is likely because the list of genes differentially expressed after enucleation was ~50, not in the hundreds- thousands

as recommended (Huang da et al., 2009b). Furthermore they suggest relative gene expression should be >2 <0.5 whereas in my microarray relative gene expression was >1.3 or <0.77. Therefore the list of genes which are differentially expressed in the P6 dLGN after enucleation is not ideal for DAVID (or other gene ontology/ pathway) analysis. Despite this my gene list is similar in number of genes and fold change values to published results which study gene expression changes using microarray experiments after visual deprivation (Majdan and Shatz, 2006; Brooks et al., 2013) or rewiring of input to thalamic nuclei (Horng et al., 2009).

The biological processes which were enriched in the GO terms included a variety of processes to do with cell cell signalling, nerve transmission and intracellular kinase cascades. Such cellular processes were represented in genes whose expression in the cortex changes after monocular enucleation at later ages (Majdan and Shatz, 2006). Furthermore there was overlap between the individual genes which changed in the cortex and in the dLGN in my study; Visinin-like1, Fos, Egr2, Egr1 and BDNF were all down-regulated in the enucleated dLGN and in the enucleated cortex (Majdan and Shatz, 2006).

Below I discuss in more detail some of the specific genes which were differentially expressed in the dLGN after enucleation, grouped by biological process.

Axon guidance cues:

There was a distinct lack of the well-established guidance molecules differentially expressed between the control and the enucleated dLGN. This is of interest because in chapter 4 I demonstrate that the loss of retinal input causes premature ingrowth of layer VI and VIb fibres to the dLGN and aberrant ingrowth of layer V fibres into the dLGN. How much these premature fibres or rerouting fibres might also alter gene expression is unclear.

Given this axon guidance phenotype one hypothesis was that loss of retinal input causes a change in guidance cues within the dLGN either by the up-regulation of an

attractive cue, or the premature down-regulation of a repulsive guidance cue. However no canonical guidance cues were differentially expressed in the dLGN following enucleation. This confirms recently published results which also showed that the lack of retinal input did not alter guidance cues within the dLGN (Brooks et al., 2013). The premature entry of layer VI and VIb fibres to the dLGN following enucleation is therefore unlikely to be the result of direct transcriptional regulation of traditional guidance cues. Despite this some genes linked to guidance were identified and are discussed below.

Aggrecan, a chondroitin sulfate proteoglycan which is repulsive to layer VI and VIb, V1 neurons and the protein is reduced in the enucleated dLGN (Brooks et al., 2013). However aggrecan is not differentially expressed between control and enucleated P6 dLGN or the dLGN of the P3 math5$^{-/-}$ mutant (Brooks et al., 2013). These results indicate that post-transcriptional/ protein level regulation of aggrecan expression underpins the premature entry, indeed enzymatic degradation mimicked the premature ingrowth of layer VI and VIb fibres (Brooks et al., 2013).

Given this, adamts3 and timp4, which were differentially expressed in the enucleated dLGN, were of interest. Adamts3 is a member of the adamts family of metalloproteases which can enzymatically cleave aggrecan (Gao et al., 2004; Tortorella and Malfait, 2008; Stanton et al., 2011) and was down-regulated in the enucleated dLGN. However using qPCR validation I demonstrated that this difference was not statistically significant ($p= 0.07$). This suggests adamts3 is unlikely to regulate aggrecan protein within the dLGN.

Timp4 was down-regulated in the enucleated dLGN compared to control (microarray and qPCR validated). Timp4 is a member of the tissue inhibitors of metalloproteases and has been shown to regulate members of the adamts family of metalloproteases, including adamts4 (aggrecanase1) (Gao et al., 2004; Murphy, 2011; Murphy et al., 2003; Kashiwagi et al., 2001). Adamts4 is one of the strongest aggrecanases (Brooks et al., 2013; Tortorella and Malfait, 2008). Given these results the reduced inhibition

of adamts4 by timp4 in the enucleated dLGN could lead to degradation of aggrecan by adamts4 thus altering corticothalamic ingrowth to the dLGN.

CD24a, a cell adhesion molecule, was up-regulated in the enucleated dLGN and is capable of both attractive and repulsive axon guidance via its interactions with L1 and TAG1 (Kleene et al., 2001; Lieberoth et al., 2009) which are expressed on thalamocortical and corticothalamic neurons respectively (Denaxa et al., 2001; Fukuda et al., 1997; Wiencken-Barger et al., 2004). Thus the up-regulation of CD24a in the dLGN after enucleation could alter neurite outgrowth. Indeed this could contribute to the premature entry of layer VI and VIb into the dLGN, or the aberrant ingrowth of layer V fibres into the dLGN.

No other axon guidance molecules were differentially expressed in the enucleated dLGN according to my microarray study however *in situ* hybridisation suggested ephrinA5 was reduced in the dLGN after enucleation (Dye et al., 2012). I therefore included ephrinA5 for qPCR analysis. My results demonstrated that ephrinA5 was significantly up-regulated in the enucleated dLGN. This contradicts Dye and colleagues results however *in situ* hybridisation is not quantitative and can be affected by exact section analysed (Dye et al., 2012). EphrinA5 is a well-known guidance cue which has been indicated in retinotopic mapping to the dLGN (Castellani et al., 1998; Deschamps et al., 2010; Miao and Wang, 2012; O'Leary and McLaughlin, 2005; Pfeiffenberger et al., 2005; Pfeiffenberger et al., 2006). Therefore up-regulation of ephrinA5 may alter retinotopic mapping and precise circuit formation within the dLGN after enucleation.

I have demonstrated that three genes which are differentially expressed in the dLGN after enucleation contribute to axon guidance. This differential expression may contribute to gross changes in circuit formation such as the premature or aberrant entry of corticothalamic fibres to the dLGN or changes in the topographic mapping.

Regulation of kinase signalling cascades:

Kinase signalling was enriched amongst differentially expressed genes according to

DAVID gene ontology analysis. Several of the genes identified by my microarray had regulatory roles in downstream kinase signalling particularly the mitogen activated protein kinase (MAPK) signalling cascades: shc3, dgkk, dgkg, dusp4, spred2, vsnl1 and BDNF.

Shc3 (src homology domain containing transforming protein c3- also n-shc, neuron specific shc) is an adaptor protein implicated in neurotrophin and growth factor signalling (Nakamura et al., 1998). Shc3 has high affinity for trkA and trkB, receptors for nerve growth factor (NGF) and brain-derived neurotrophic factor (BDNF) respectively (Nakamura et al., 1998). Downstream signalling pathways include the ras-dependent MAP kinase pathway (Liu and Meakin, 2002; Nakamura et al., 1998; Wills and Jones, 2012). The down-regulation of shc3 in the dLGN after enucleation could lead to further gene expression changes via the MAPK/CREB signalling cascades.

The transcripts for two diacyleglycerol kinases (kappa and gamma, dgkk and dgkg) were reduced in the enucleated dLGN. Both kinases phosphorylate diacyleglycerol (DAG) to generate the inactive phosphatidic acid (Topham, 2006; Topham and Prescott, 2002; van Blitterswijk and Houssa, 2000). DAG is involved in many signalling cascades including protein kinase-C (PKC) signalling. DAG phosphorylates PKC, which in turn phosphorylates growth factor receptors including EGFR thus reducing their expression and therefore limiting tyrosine kinase signalling pathways (Kanoh et al., 2002; Ron and Kazanietz, 1999).

Dusp4 (dual specificity phosphatase 4, also MAPK phosphatase 2- MKP2) dephosphorylates serine/ threonine and tyrosine residues on MAPK, erk1/2 and JNK thus inhibiting mitogen signal transduction as negative feedback. It also demonstrates nuclear localisation and could therefore regulate further gene transcription (Patterson et al., 2009). Dual specificity phosphatases are reduced expression in the visual cortex in both mouse and old world primates following visual deprivation in the critical period (Majdan and Shatz, 2006; Lachance and Chaudhuri, 2004). Furthermore another dusp, dusp1 has been indicated as an immediate early gene due to its increased expression in

the thalamus after sensory stimulation in songbirds (Horita et al., 2010).

Spred2 (sprout-related EVH1 domain containing 2) is in a family of membrane associated proteins which inhibit growth factor induced activation of the ERK/ ras/raf/ MAP kinase pathway (Wakioka et al., 2001; Sasaki et al., 2001; Sasaki et al., 2003; Garcia-Dominguez et al., 2011).

Visinin like 1(vsnl1- also neural visinin like calcium binding protein type 1) is a calcium sensitive double stranded RNA binding protein (Mathisen et al., 1999; Braunewell and Szanto, 2009). Vsnl1 binds the mRNA for trkB (BDNF receptor) which is localised to the dendrites following increased neuronal activity/ calcium influx (Mathisen et al., 1999; Tongiorgi et al., 1997) and thus regulates downstream tyrosine kinase- MAP kinase signalling (Yoshii and Constantine-Paton, 2010). Vsnl1 is down-regulated in the dLGN at P6 after enucleation and in the cortex after monocular enucleation at older ages (Majdan and Shatz, 2006). Furthermore vsnl1 is normally strongly up-regulated over development as shown by the microarray comparing P0-P10 dLGN.

My qPCR results show that BDNF is down-regulated in the enucleated dLGN. BDNF is a neurotrophic factor which has been implicated many times in molecular changes after sensory deprivation (Majdan and Shatz, 2006; Castren et al., 1992; Bozzi et al., 1995; Schoups et al., 1995). BDNF binds with high affinity to both pre and post-synaptic trkB (receptor tyrosine kinase) and signals via the MAP Kinase, PLC-DAG-PKC and PI3K signalling cascades ending in CREB-regulated gene transcription (Yoshii and Constantine-Paton, 2010) in both the geniculate relay cells and the corticothalamic fibres which are growing into it. Hence changes in BDNF may change circuit formation and synaptic plasticity for the circuits which form at the dLGN including cortical-geniculate relay cell synapses and GABAergic interneuron- geniculate relay cell synapses.

I have demonstrated that following enucleation there are several differentially expressed genes whose activity alters MAP kinase signalling cascade activities. Downstream

signalling from the MAPK cascades include ERK1/2 and CREB which can lead to changes in gene transcription via CREB responsive elements in their promoters (Naqvi and Arthur, 2013; Thomas and Huganir, 2004; Flavell and Greenberg, 2008). These kinase signalling pathways are important in regulating neuronal plasticity genes (McCoy et al., 2009). MAP kinase signalling is also affected by visual deprivation during the critical period (Majdan and Shatz, 2006; Lachance and Chaudhuri, 2004; Cheng et al., 2008). MAP kinase signalling cascades that are altered 6 days after monocular enucleation at birth could be involved in the overall program of genetic changes that are apparent after the loss of retinal input. Indeed inhibiting MEK kinase signalling has been shown to mimic the gene expression changes that are seen in the cortex after visual deprivation in the critical period (Majdan and Shatz, 2006).

Neural transmission and cell signalling:

Synaptic transmission and nerve signal transmission were biological processes which were enriched in the differentially expressed genes in the dLGN after enucleation.

Kcnk9 (potassium channel, subfamily K, member 9, also known as task3) is potassium leak channel which generates inward potassium currents responsible for the maintenance of resting membrane potential and therefore excitability (Goldstein et al., 2001). Kcnk9 is expressed in developing neurons and its expression in the mouse is regulated throughout development (Aller and Wisden, 2008). These results suggest that the expression of kcnk9 may be involved in establishing the normal excitability of geniculate relay neurons.

Kcnn3 (potassium small conductance calcium-activated channel, subfamily N, member 3, also known as SK3) is a member of the calcium dependent potassium channels (Kohler et al., 1996; Schumacher et al., 2001; Keen et al., 1999) which are involved in neuronal after-hyperpolarisation that limits neuronal spiking frequency (Sah, 1996; Lancaster and Adams, 1986).

The reduction of two important potassium channels after enucleation may alter

the dLGN relay neurons firing properties. Indeed monocular enucleation has been previously demonstrated to disrupt relay neuron firing properties in the dLGN at later ages after enucleation (Golding et al., 2013).

Immediate early genes:

Immediate early genes (IEGs) can be activated within hours by neural activity without de novo protein synthesis and can include transcription factors and other intracellular signals (Greenberg et al., 1986). IEGs whose transcription was altered in the P6 dLGN after neonatal enucleation; Fos, Egr2, Egr1.

Fos is a prototypical IEG that is expressed after neuronal activity. Its expression is linked to synaptic activity and it is a transcription factor (as part of the AP-1 complex) which has been demonstrated to be active in response to neural activity (by activation of CRE response elements) and reduced after visual deprivation (Greenberg et al., 1986; Kaczmarek and Chaudhuri, 1997; Kaczmarek et al., 1999; Flavell and Greenberg, 2008). Fos expression is down-regulated in the P6 enucleated dLGN which may alter transcription of other downstream genes.

Two further IEGs which are also transcription factors were differentially expressed after enucleation; Egr2 and Egr1 (also known as zif268). Both Egr1 and 2 are also down-regulated in the cortex after visual deprivation (Kaczmarek and Chaudhuri, 1997; Kaczmarek et al., 1999; Majdan and Shatz, 2006).

Despite the early identification of Fos and Egr1, which genes these two transcription factors regulate after activation is as yet un-determined (Flavell and Greenberg, 2008; Kaczmarek and Chaudhuri, 1997) it is therefore difficult to speculate the exact nature that their down-regulation will have on the dLGN.

5.4.1.3. Factors regulating the differential expression- which fibres and the role of activity

In section above I have discussed the functions of genes whose expression is altered in the P6 enucleated dLGN. The genes which are differentially expressed include both

genes which go on to regulate the expression of other genes (the immediate early genes) and genes contributing to neurite guidance and neural activity and will regulate the development and maintenance of circuit connectivity and activity directly.

The genes identified are regulated by the loss of retinal input. Whether this regulation is via neuronal activity or neurotrophic/ signalling molecule release from the retinal ganglion cell axons, or perhaps even from the axons of the premature corticofugal projections from layers VI and VIb, is unclear. To role of retinal activity versus secretion could be investigated by comparing gene expression in dLGN which have retinal axons present but without the spontaneous waves of activity, for example the nicotinic cholinergic β-2 subunit knock out mouse (Rossi et al., 2001; Bansal et al., 2000; Stafford et al., 2009). Furthermore the influence of cortical axons from layers VI and VIb could be tested by crossing the Ntsr1-Cre mouse characterised in my earlier chapters with a floxed Snap25 conditional KO (to abolish their activity) or the floxed diphtheria toxin fragment A (to kill the neurons and their axons) (Brockschnieder et al., 2004).

Included in the list are immediate early genes (Fos, Egr2) that have been shown to be regulated by NMDA receptor activation and intracellular calcium signalling thus this list includes some activity dependent genes. One way to assess which genes are specifically regulated by neuronal activity would be to assess whether their promoters include known activity dependent promoter sequences. Two such sequences include the CRE (cAMP response elements) and the calcium responsive sequence 1. BDNF which is down-regulated in the enucleated dLGN has both CRE and calcium responsive sequence 1 in its promoter sequence (Shieh et al., 1998; Tao et al., 1998; Tao et al., 2002). Analysing the genes for the presence of such sequences in their promoter regions could identify which genes are regulated by retinal (or corticothalamic) activity.

Whilst we can assess the expression of activity regulated genes, we currently know little about the early changes in the neuronal activity in the dLGN following enucleation. Clarifying this by using *in vivo* recording techniques will be important to further

understand activity dependent gene expression in the dLGN.

5.4.1.4. Discussion of differential expression of genes after enucleation compared to differential expression of genes over development

In this chapter I have demonstrated that monocular enucleation at P0 alters the transcriptome of dLGN relay neurons by P6. The differentially expressed genes underlie a range of biological processes which can contribute to neuronal maturation and circuit development. The period over which retinal input was removed is one at which retinal input is progressively increasing and providing important activity based instructions within the dLGN such as those involved in retinotopic mapping (Shatz and Stryker, 1988; O'Leary and McLaughlin, 2005; Huberman, 2007; Huberman et al., 2008). I therefore speculated as to whether the retinal input is important for the normal transcriptomic development of dLGN relay neurons and so whether the gene expression changes after enucleation are indicative of a delay in the normal maturation of the transcriptome.

When characterising the thalamic expression of some of the genes by *in situ* hybridisation from publically available resources it became clear that many were developmentally regulated; 9 out of 14 between E18.5 and P10. The majority of the genes which were regulated over development were regulated in the opposite direction to their differential expression after enucleation.

I then performed a secondary comparison between my enucleated/control dLGN microarray and a developmental microarray comparing the P10 dLGN to the P0 dLGN. Examining the pattern of regulation by both traits, it is apparent that many of the genes that are differently expressed after enucleation are regulated in the opposite direction over development. The majority of differentially expressed genes are down-regulated in the enucleated dLGN and the majority of these genes are up-regulated between P0 and P10. The transcription of these genes during normal development may be positively regulated by retinal input.

Interestingly the genes which were up-regulated after enucleation were evenly up-, and

down-regulated over development. This is different to the genes which were down-regulated after enucleation which were primarily up-regulated over development. One explanation could be that the loss of retinal input is sufficient to cause normal up-regulation of gene expression to fail, whilst the normal developmental down-regulation of gene expression might succeed even without retinal input. If this were the case those genes which are normally down-regulated continue to be so and as such are not identified as up-regulated in the enucleated dLGN. Instead only genes which are up-regulated due to other reasons are identified.

My results emphasise that the loss of retinal input to the dLGN causes a delay in the development of the dLGN transcriptome. This indicates that retinal input is important for the normal development and maturation of the dLGN relay neurons.

5.4.1.5. Cross-hierarchical gene expression changes after enucleation

During chapter 4 I demonstrate that the loss of retinal input to the dLGN causes cross-hierarchical rewiring; specifically layer V, which normally innervates exclusively higher order nuclei, enters the enucleated first order dLGN. In this chapter I have demonstrated that following enucleation the maturation of the dLGN appears delayed. One explanation of this result is that retinal input is crucial for the normal developmental regulation of the dLGN transcriptome. A second possibility is that retinal input confers some first order transcriptome identity on the dLGN, which may be lost with the loss of the retinal input. Previous work has demonstrated that the loss of somatosensory information by infraorbital nerve transection causes the transcriptome of the first order VPM to become more similar to that of the higher order Po (Pouchelon et al., 2014a). Thus it would be interesting to compare the transcriptome of the control and enucleated dLGN with that of the control LP (the higher order visual nucleus). If the enucleated dLGN transcriptome becomes more similar to that of the LP, it would suggest that the retinal input to the dLGN contributes to the first order identity on the dLGN neurons.

5.4.1.6. Conclusion

In this chapter I have demonstrated that the loss of retinal activity causes gene

expression changes in the enucleated dLGN at P6. Genes which were differentially expressed included those involved in neuronal activity Kcnk9 and Kcnn3, kinase pathways Shc3 and Dgkk, and immediate early genes Fos, BDNF, Egr1 and Egr2. Many of the genes which were differentially expressed after enucleated are normally developmentally regulated in the early postnatal weeks. This suggests that the loss of retinal input causes the delay/ stalling of the development of the dLGN transcriptome.

6 Discussion

My aim in this thesis was to contribute to our understanding of the development of corticothalamic and corticotectal circuits in the normal and sensory deprived brain with a particular focus on the visual system.

In the introduction I set out three questions regarding the development of corticofugal fibres which I have answered in this thesis. Firstly, what order do the layer V, VI and VIb fibres enter the thalamus and are they already patterned according to the hierarchy of thalamic nuclei? Secondly, does peripheral input regulate corticothalamic ingrowth; does retinal input to the dLGN regulate corticothalamic ingrowth, does retinal input to the superior colliculus regulate corticocollicular ingrowth? Finally, can peripheral input from the retina regulate gene expression within the dLGN?

6.1. Summary of my major findings

6.1.1. What order do layer V, VI and VIb fibres enter thalamus and are they already patterned according to the hierarchy of thalamic nuclei?

I first characterised the timing and pattern of ingrowth of corticothalamic and corticotectal projections into their targets in the first two postnatal weeks in the mouse. I did this by using recently developed transgenic mouse lines which express fluorescent labels in the three cortical subpopulations which project sub-cortically; Rbp4-Cre::tdTomato labels layer V, Ntsr1-Cre::tdTomato labels layer VI, and Golli-τ-eGFP labels layer VI and VIb (the subplate). Despite the selective labelling of the corticothalamic populations by these transgenic lines they are unable to answer the question of what order the three subpopulations reach the thalamus in because Cre mediated recombination in the Rbp4-Cre and Ntsr1-Cre lines occurs after E16.5/E17.5. Consequently the fibres are not labelled early enough to characterise the progression of the corticothalamic fibres until they have reached the thalamus.

Using these lines to analyse the ingrowing corticothalamic fibre patterns within the thalamus my results showed that during normal development layer V corticothalamic

projections avoid first order thalamic nuclei and immediately target the more medial higher order thalamic nuclei. The layer VI and VIb fibres on the other hand project to all thalamic nuclei in a temporal pattern that is approximately ventral/lateral nuclei earlier which includes first order nuclei such as VPM, before entering dorsal/medial nuclei later including higher order nuclei such as LP and Po. The one nucleus which did not fit this pattern is the dLGN which is a first order nucleus and is in a lateral position and thus is one which the corticothalamic fibres come across early. Despite this the layer VI and VIb corticothalamic fibres accumulate at the ventral edge of the dLGN and do not begin to enter it until several days after birth thus suggesting there is specific regulation of the corticothalamic fibres to the dLGN.

6.1.2. Does retinal input to the dLGN and superior colliculus regulate corticothalamic and corticocollicular ingrowth, respectively?

I next studied whether retinal input regulates the waiting period prior to layer VI and VIb corticothalamic fibre entry to the dLGN. To test the hypothesis of whether early sensory input regulates corticothalamic fibre ingrowth, I removed retinal input from one eye at birth by performing monocular enucleation and analysed the ingrowth of layer V, VI and VIb fibres into the dLGN. My results demonstrated that following the loss of retinal input shortly after birth, layer VI and VIb fibres entered the dLGN prematurely, from P2 instead of P6. I confirmed with tracing experiments from the dLGN that these early corticothalamic projections originated from layer VI and VIb of the primary visual cortex. This premature entry appears to be retinal activity dependent because the use of epibatidine to abolish early spontaneous retinal waves without removing retinal ganglion cell axons from the dLGN also caused premature ingrowth of VI and VIb fibres to the dLGN.

Additionally my results demonstrate that at P6 and P8 layer V fibres, which normally only innervate higher order thalamic nuclei, entered the first order dLGN aberrantly after enucleation, a form of cross-hierarchical rewiring. To investigate which cortical area these fibres originate from we could deliver AAV viruses with a floxed fluorescent reporter (tdTomato, eGFP) into different cortical areas of the Rbp4-Cre mouse following

monocular enucleation.

I then studied the effect of enucleation on corticotectal ingrowth; layer V fibres entered the superficial grey layer of the superior colliculus prematurely after enucleation. We could use the above viral tracing method to discern the cortical origin of these fibres too. Thus in my thesis I have described two instances of retinal fibres preventing cortical entry to joint targets. As such I tested whether they might share the same molecular mechanism. My result showed that the premature ingrowth of layer V to the superficial grey layer is not caused by reduced aggrecan expression, unlike the premature ingrowth of layer VI and VIb fibres to the dLGN (Brooks et al., 2013). This result indicates that different mechanisms are employed by the retinal fibres at the dLGN and the superior colliculus. This is coherent given that the two subpopulations of cortical fibres are likely to be responsive to distinct guidance cues. Indeed layer V is not repelled from aggrecan expressing higher order thalamic nuclei and thus it is consistent that they are not repelled by aggrecan in the superior colliculus.

6.1.3. Can peripheral input from the retina regulate gene expression within the dLGN?

Given the considerable effect of the loss of retinal input on the development of corticothalamic and corticotectal circuitry I chose to assess whether the loss of retinal input can direct transcriptional changes in the dLGN using microarray gene expression analysis. My results demonstrated that approximately 50 genes were differentially expressed in the dLGN after enucleation, many of them down-regulated. Differentially expressed genes included those involved in axon guidance (timp4, CD24a and ephrinA5), intracellular kinase signalling (shc3, dgkk, dgkg, dusp4, spred2, vsnl1 and BDNF), neuronal signalling and activity (kcnk9, kcnn3, hcrtr2, chrm2 and adra1d) and immediate early genes which orchestrate cellular responses to neural activity (fos, egr2 and egr1). I then further analysed these genes by their developmental regulation and the majority of those down-regulated after enucleation are normally up-regulated over the first two weeks of postnatal development (developmental data kindly provided by Professor Denis Jabaudon). As such the loss of retinal input appears to cause a delay in

the transcriptional development of the dLGN.

In each results chapter I have discussed in detail how the experimental results presented within that chapter contribute to that area of literature. In this final general discussion I consider the results from all three experimental chapters and discuss where they may advance our understanding of specific features of the development of the corticothalamic system.

6.2. General Discussion

6.2.1. Waiting periods in the development of the corticothalamic system

6.2.1.1. Corticothalamic waiting period outside the dLGN

In chapter 3 I characterise the ingrowth patterns of layer V, VI and VIb corticothalamic fibres to specific thalamic nuclei. Using these results I demonstrated that the layer VI and VIb fibres which are destined to innervate the dLGN, reach the ventral edge of the nucleus by P2. However before entering the nucleus proper the fibres accumulate here for several days. My results are among the first to conclusively demonstrate this accumulation period because of the ability to label the corticothalamic fibre subpopulations specifically (Jacobs et al., 2007; Grant et al., 2012; Seabrook et al., 2013). However this corticothalamic fibre waiting period has been previously described using indirect tracing methods in the cat and rhesus monkey (Anker, 1977; Shatz and Rakic, 1981). The results in the rhesus monkey emphasised that the accumulation of corticothalamic fibres outside of the dLGN had the effect of synchronising the ingrowth of thalamocortical and corticothalamic fibres to their targets (Rakic, 1976; Rakic, 1977; Shatz and Rakic, 1981).

This corticothalamic fibre waiting period outside the dLGN mirrors an earlier described waiting period which thalamocortical fibres undergo before invading the cortical plate. Thalamocortical fibres reach the cortex and remain in layer VIb for several days before invading the cortical plate to target layer IV (E15-E18 in mouse) (Rakic, 1976; Lund and Mustari, 1977; Rakic, 1977; Shatz and Luskin, 1986; López-Bendito and Molnar,

2003; Molnár et al., 2003a). Thus it appears both corticothalamic and thalamocortical fibres progress towards their target tissue early when the distances are minimal, but then undergo a waiting period before entering their target tissue.

Despite the similarity between these waiting periods, work on the role of the thalamocortical waiting period and the results I present in this thesis suggest the two waiting periods have different roles in cortical development.

6.2.1.2. Distinct roles for the thalamocortical and corticothalamic waiting period

During the thalamocortical waiting period, thalamocortical axons integrate into an early transient circuit involving layer VIb and layer IV. Initially thalamocortical axons robustly innervate layer VIb (the subplate) and at this stage there is only disynaptic activation of layer IV (Friauf and Shatz, 1991; Higashi et al., 2002; Molnár et al., 2003b; Zhao et al., 2009). After several days the thalamocortical fibres innervate layer IV directly (Friauf and Shatz, 1991; Higashi et al., 2002; Molnár et al., 2003b; Zhao et al., 2009). Before the thalamic inputs withdraw from innervating layer VIb there is a feed-forward circuit whereby thalamic input is relayed to layer IV both indirectly via layer VIb and by direct connections. This feed-forward circuit is proposed to strengthen and stabilise the developing thalamus to layer IV synapses. Functional properties of the cortical circuits which are disrupted when this feed-forward circuit is lost include ocular dominance and orientation column formation in visual cortex (Ghosh et al., 1990; Ghosh and Shatz, 1994; Kanold et al., 2003; Kanold and Shatz, 2006), and barrel organisation in somatosensory cortex (Tolner et al., 2012). Furthermore the maturation of cortical inhibition is disrupted if the transient circuit in the subplate is abolished; cortical neurons fail to up-regulate KCC2 channel expression and thus maintain high intracellular chloride concentrations so GABAergic activity remains depolarising (Kanold et al., 2003). As such the thalamocortical waiting period in which fibres accumulate at the subplate before entering the cortex appears to be to enable to thalamic fibres to integrate into a transient circuit with the subplate neurons which contributes to the proper development of adult circuit properties. The thalamocortical fibres also

undergo rearrangements deep to the cortical plate which are vital for the transformation of topographic representations between the thalamus and the cortex (Connolly and Van Essen, 1984; Nelson and LeVay, 1985; Grant et al., 2012).

The accumulation period which corticothalamic fibres undergo at the ventral edge of the dLGN does not appear to play an analogous role. Firstly the corticothalamic fibres do not accumulate in a compartment which is similar to layer VIb. The subplate (layer VIb) is a layer deep to cortical layer VI which is early born, synaptically mature prior to other cortical layers, and partially transient (Price et al., 1997; Higashi et al., 2002; Hoerder-Suabedissen and Molnár, 2012; Hoerder-Suabedissen and Molnár, 2013). The ventral band where the corticothalamic fibres accumulate outside the dLGN does not share anatomical or functional features with the subplate; it is not especially early born (thalamic neurons including those in the dLGN and VPM are born E11-E12 (Angevine, 1970)) and there does not appear to be the early integration of mature corticothalamic synapses into a transient circuit at this region (Seabrook et al., 2013; Grant et al., 2012).

Corticothalamic fibres also undergo another waiting period at the thalamic reticular nucleus (TRN), prior to reaching the thalamus (Mitrofanis and Baker, 1993; Molnár and Cordery, 1999). This waiting period appears more similar to the waiting period of thalamic fibres at the subplate as the cortical fibres display early mature, functional innervation of the TRN (Grant et al., 2012) and corticothalamic fibres appear to undergo crucial rearrangements at the TRN which contribute to pathway topography (Lozsádi et al., 1996; Adams et al., 1997).

Thus whilst the respective fibre waiting periods at the subplate and the TRN appear to provide substrates for early, transient circuits and compartments in which topographic rearrangements occur, my results suggest a different role which the corticothalamic waiting period outside the dLGN could be fulfilling.

In chapter 4 I discuss the evidence which demonstrates that, at targets which receive input from both the retina and the cortex, there is a specific order of ingrowth of the

two inputs. Retinal input to both the dLGN and the superficial grey layer of the superior colliculus enters and matures prior to cortical ingrowth to the same structures (Drager and Hubel, 1975; Lund, 1965; Anker, 1977; Godement et al., 1980; Shatz and Rakic, 1981; Godement et al., 1984; De Carlos and O'Leary, 1992; Clascá et al., 1995; Mooney et al., 1996; Ackman et al., 2012; Grant et al., 2012; Seabrook et al., 2013). Thus there is a conserved order of ingrowth- retinal fibres enter before cortical fibres in several species and in two central visual structures, the thalamus and the evolutionarily older tectal system.

My results in chapter 4 demonstrate that this order is likely to arise from retinal fibres regulating the ingrowth of cortical fibres, thus coordinating the entry of two distinct fibre populations to two different 'joint' targets. The removal of retinal input in my experimental paradigm enables the cortical fibres to enter the 'joint' target prematurely (layer VI and VIb to the dLGN, layer V to the superficial grey layer of the superior colliculus). From this we can infer that retinal input normally delays layer VI/VIb and V ingrowth to their respective targets until an appropriate time point.

I hypothesise that by preventing cortical fibre entry to joint targets, the retinal fibres ensure they are able to make sufficient synapses, thus employing a form of fibre competition. This could be crucial as in the adult mouse synapses from cortical fibres onto dLGN relay neurons outnumber retinal synapses 10:1 (Guillery, 1969; Wilson et al., 1984; Mitrofanis and Guillery, 1993; Liu et al., 1995; Van Horn et al., 2000; Bickford et al., 2010).

Despite the potential competition between the retinal and layer VI and VIb fibres during development, in the adult dLGN, the retinal and layer VI/VIb corticothalamic fibres provide distinct forms of input to the thalamic relay cells. The VI and VIb inputs to the dLGN are modulators unlike retinal inputs which are drivers. As such one might suggest that the two inputs are not truly in competition for synaptic sites; modulator inputs target distal regions of the dendrites whereas driver inputs target regions proximal to the cell soma (Sherman and Guillery, 1998).

However, it has been demonstrated that at P7-P9 retinal input to the mouse geniculate can occupy as much as 50% of the cell surface area of dLGN relay neurons, including both proximal and distal regions of the dendrites (Ziburkus and Guido, 2006; Guido, 2008). This early extensive input is then refined firstly by eye specific segregation such that retinal input from only one eye innervates each geniculate relay cell, and eventually by synaptic pruning leaving each thalamic relay cell to be innervated by between one and three retinal ganglion cells, from around two weeks after birth (Godement et al., 1984; Chen and Regehr, 2000; Jaubert-Miazza et al., 2005). Therefore these results indicate that during the earliest postnatal weeks the layer VI and VIb fibres and the retinal fibres are directly competing for contact surface area on the dLGN relay neurons.

The early extensive input from the retina on to each dLGN relay neuron has been suggested to contribute to Hebbian synaptic plasticity mechanisms whereby the transient extensive and convergent synapses from the retina to the dLGN relay neurons helps to refine the connections between the dLGN and the cortex (Chen and Regehr, 2000; Tavazoie and Reid, 2000). This suggests that, despite the fact that at later ages synapses from retinal and corticothalamic fibres do not spatially coincide on the dLGN relay neurons, in early development it is important for retinal fibres to synapse diffusely upon the dLGN relay neurons for the proper development of the geniculocortical circuits. Therefore, it is important for retinal fibres to prevent corticothalamic fibres from prematurely colonising these synapse spaces.

To summarise, the combined results in chapter 3 and chapter 4 allow us to speculate on the role of the timing of corticothalamic fibre entry to distinct thalamic nuclei. Firstly they confirm that layer VI and VIb fibres experience a waiting period outside the dLGN. Secondly they allow us to speculate that the corticothalamic waiting period outside of the dLGN is not to provide time to integrate into a transient circuit but instead may function to provide time for retinal fibres to establish synapses with thalamic relay neurons in the dLGN before the cortical fibres invade. These results indicate that this early diffuse retinal input may be crucial for thalamocortical circuit development. Thus

whilst both thalamocortical and corticothalamic fibres experience numerous waiting periods en route to their targets, different waiting periods serve different functions.

6.2.1.3. Does premature corticothalamic layer VI and VIb fibre entry disrupt the retinogeniculate circuit?

From these results I hypothesise that the corticothalamic waiting period immediately outside the dLGN is important to enable incoming retinal fibres to generate synapses before corticothalamic fibres enter. My hypothesis predicts that without this waiting period the corticothalamic fibres would colonise synaptic sites that retinal fibres normally use and would thus disrupt the retinal geniculate connection. Below I discuss some experiments which could be used to test this hypothesis.

To explore the hypothesis that retinal fibres prevent cortical fibres from entering in order to ensure the correct developmental mechanisms contributing to the visual circuitry, we would need to demonstrate that the retinal-geniculate circuit is disrupted by premature corticothalamic ingrowth.

Initially it will be important to investigate whether retinal synapses are disrupted or reduced if corticothalamic fibres enter the dLGN prematurely. Brooks and colleagues showed that enzymatic degradation of aggrecan in the dLGN can mimic the premature entry of VI and VIb corticothalamic fibres to the dLGN produced by the loss of visual input (Brooks et al., 2013). As such in this experimental model the retinal input is still present but the corticothalamic fibres enter prematurely. Using this paradigm we could assess the quantity of retinal synapses on the geniculate relay cells during development and at later stages. First one would quantify retinal input onto the dLGN relay neurons at P8 and P15. At P8 up to 50% of the dLGN cell surface area occupied by retinal synapses and by P15 this has reduced to closer reflect the adult numbers (5-10%) (Ziburkus and Guido, 2006; Guido, 2008). If these experiments demonstrate that the early retinal input is disrupted then one would want to establish whether the normal situation is recovered at later ages or whether the disruption is maintained into adulthood. In the adult approximately 5-10% of synapses on to thalamic relay cells in

the dLGN originate from the retina (Van Horn et al., 2000; Ziburkus and Guido, 2006; Guido, 2008; Bickford et al., 2010). If this was reduced/ disrupted after experimentally premature ingrowth of corticothalamic fibres into the dLGN this would suggest the normal adult circuit cannot be recovered.

6.2.1.4. Is the geniculo-cortical circuit maintained or also disrupted?

It would then be interesting to expand this to question assess whether the geniculo-cortical circuit is heavily disrupted by the inappropriate corticothalamic circuitry and disrupted retinal input and, if so, whether compensatory cortical plasticity allows a relatively normal functional circuit. Firstly we could test the basic electrophysiological properties of the geniculate input to the visual cortex such as the strength of post-synaptic potentials in V1 after geniculocortical activation using the visual thalamocortical slices (MacLean et al., 2006). Then to assess the broader functional features of the visual cortex we could test whether there is the normal feature selectivity in connected visual cortex neurons. In carnivores and primates this can be seen in the form of ocular dominance columns and orientation columns (Drager, 1975; Metin et al., 1988; Hubener, 2003; Niell and Stryker, 2008). There are similar features in the mouse visual cortex although the neurons which respond to the same features (and are connected to one another) are not organised into patches that can be seen as orientation pin-wheels (Ko et al., 2013; Ko et al., 2011).

6.2.1.5. Behavioural effects

It would be interesting to assess the performance of these mice in in complex visual behaviour tasks following aggrecan degradation to manipulate the visual system development. Paradigms which test both the ‘first order’ relay of visual information to the cortex by testing visual acuity and which test the ‘higher order’ relays such as visuo-motor integration would be interesting. Visual acuity could be tested by a water maze in which the ability to discriminate gratings on a computer screen alerts the animals to the hidden platform (Prusky et al., 2000). The visual higher order nucleus, the LP, mediates directed attention and visuo-motor integration (Sukekawa, 1988; Kamishina et al., 2009; Reep et al., 1994; Reep and Corwin, 1999). Visuo-motor integration could be

tested by complex grasping tasks for example reaching for food that can be seen through a clear barrier although it would be important to take into account the basic effects that the manipulation is likely to have had on visual capabilities (Whishaw, 1996; Klein and Dunnett, 2012).

6.2.1.6. Summary

Here I have proposed that the corticothalamic waiting period outside the dLGN serves to ensure the retinal fibres need not compete for synaptic places within the dLGN and that this could contribute to the development of the adult circuitry. My results support this hypothesis by demonstrating that the loss of retinal input causes premature entry of corticothalamic fibres. I go on to suggest functional experiments to determine whether this premature entry disrupts the proper development and function of the retina-geniculate-cortex system.

6.2.2. Corticothalamic subpopulations and the first order and higher order hierarchy of the thalamus

6.2.2.1. Early corticothalamic ingrowth integrates into the thalamic hierarchy

In chapter 3 I demonstrate that as early as two days after birth the layer V and layer VI/VIb fibres are differently patterned within the thalamus, based on thalamic nucleus hierarchy. The thalamic hierarchy organisation is distinct from sensory modality. The first order group of thalamic nuclei includes the dLGN (visual modality) the VPM (somatosensory modality) and the MGN-ventral (auditory modality). The higher order nuclei include the LP (visual modality), the Po (somatosensory modality) and the MGN-dorsal (auditory modality). Whilst the first order nuclei relay peripheral sensory information to the relevant, modality specific primary cortical area, the higher order nuclei provide a trans-thalamic relay for cortico-cortical input (figure 1.7 from introduction) (Sherman and Guillery, 1996; Sherman and Guillery, 2002).

That layer V innervates the higher order nuclei and VI innervates the first order nuclei in adult is well established however the innervation patterns over development have been harder to confirm due to the inherent problems with previous tracing techniques. My results confirm that even throughout early development (from P2) layer V fibres

exclusively innervate higher order thalamic nuclei whereas the layer VI and VIb fibres innervate both higher order and first order nuclei. This result suggests that the first order and higher order nuclei may have molecular identities that guide the corticothalamic fibres to the relevant nuclei. For example there may be guidance cues which differentiate between first order and higher order nuclei that the different cortical subpopulations are selectively responsive to. Thus it could be speculated that the distinction between the first order and higher order thalamic nuclei is determined early before the corticothalamic fibres enter and that the hierarchical identity of the thalamic nuclei determines which corticothalamic fibres will innervate it.

Despite this suggestion, however, my results in chapter 4 go on to suggest that the sharp distinction between corticothalamic fibre guidance to the first order and higher order nuclei can be blurred once peripheral input is removed. After the loss of retinal input, layer V corticothalamic fibres which normally only innervate higher order thalamic nuclei enter and arborise within the first order dLGN. I will term this rewiring cross-hierarchical rewiring/ plasticity. As such whilst the boundaries between first order and higher order may be established early, a lack of retinal input appears to enable higher order circuitry to take over the first order dLGN. As discussed in chapter 4 evidence for cross-hierarchical rewiring is relatively recent and includes cross-hierarchical rewiring of thalamic inputs from the higher order Po to layer IV of the primary somatosensory cortex (Pouchelon et al., 2014b). As such mine are some of the earliest results to demonstrated cross-hierarchical rewiring in the corticothalamic system.

6.2.2.2. Do layer V fibres drive dLGN neurons?

My results show anatomically that following monocular enucleation layer V fibres innervate a normally first order thalamic nucleus; however, whether this new input to the dLGN is functional is unknown. It would be interesting to determine whether cross-hierarchical layer V projections begin to drive the thalamic relay neurons within the dLGN. This could firstly be assessed by electron-microscopy to confirm that the synapses of the layer V fibres in the dLGN exhibit the usual driver properties including

large terminal bouton morphology and targeting proximal dendritic regions (Sherman and Guillery, 1998). Previous evidence has shown non-retinal 'driver' type synapses in the enucleated dLGN (Cullen and Kaiserman-Abramof, 1976).

To show whether layer V fibres drive dLGN relay neurons it would be ideal to record activity in the dLGN receiving layer V input. First to confirm from which cortical area the layer V fibres innervating the dLGN arise retrograde tracing is necessary. My results in chapter 4 did demonstrate very sparse retrograde labelling of layer V cells in the visual cortex thus suggesting visual cortex is an appropriate region to start. If the visual cortex is confirmed as the origin of the layer V fibres one could use optogenetic stimulation to exclusively activate layer V corticothalamic terminals onto thalamic relay neurons the dLGN (Jurgens et al., 2012). Using a slice preparation with the optic tract removed after transfecting layer V with channel rhodopsin one could record from the dLGN whilst stimulating layer V terminals *in vitro* (Boyden et al., 2005; Fenno et al., 2011; Yizhar et al., 2011). This would allow us to determine whether there are driver like responses in the dLGN despite the lack of retinal input.

6.2.2.3. Changes to geniculocortical innervation

If layer V can drive dLGN neurons it would be interesting to investigate whether this activity is propagated to the primary visual cortex and if so, whether the primary visual cortex acquires association cortex activity profiles. Association visual cortex demonstrates some activity which is distinct from primary visual cortex such as a preference for higher velocity stimuli in un-manipulated animals (Tohmi et al., 2009; Tohmi et al., 2014; Marshel et al., 2011; Andermann et al., 2011). The properties of activity within the association visual cortex after enucleation is less well established, however, and would need to be characterised to enable these analyses to go ahead.

One difficulty in assessing whether layer V fibres can drive dLGN activity is that the role of the higher order thalamic nuclei and the layer V driver fibres is not as well characterised as drivers from the peripheral nervous system. The lateral posterior nucleus mediates directed attention and visuo-motor integration (Sukekawa, 1988;

Kamishina et al., 2009; Reep et al., 1994; Reep and Corwin, 1999). However whether it still plays this role after monocular enucleation (via ipsilateral connections perhaps) and how one would test it is unclear.

Next I will focus on a question which these results raise of how the hierarchy of the thalamic nuclei is established and whether peripheral inputs contribute to the determination of thalamic nuclei order.

6.2.2.4. Cross-hierarchical rewiring of layer V fibres into the VPM

My results demonstrate that the loss of peripheral input in the visual system causes normally higher order corticothalamic fibres (layer V) to invade the visual first order thalamic nucleus the dLGN. Whether this corticothalamic cross-hierarchical rewiring can occur in other modalities can be tested by performing manipulations of other sensory organs.

This could first be addressed by assessing whether the layer V fibres enter the VPM following somatosensory deprivation by infraorbital nerve transection. Whilst this is not in the scope of my thesis I am performing these experiments on the Rbp4-Cre::tdTomato mouse and will be testing whether labelled layer V fibres aberrantly grow into the VPM following infraorbital nerve transection. If these results demonstrate that layer V does enter the VPM following loss of peripheral input, this will confirm that in a second modality specific system layer V fibres can be induced to enter a normally first order nucleus. This, in turn, would support the hypothesis that peripheral input may prevent the first order nuclei from taking on a higher order circuit identity.

6.2.3. The role of peripheral input in determining the hierarchy of thalamic nuclei

6.2.3.1. Peripheral input contributes to thalamic nucleus gene expression

For some time there has been interest in the contribution of peripheral input to the identity and function of the receiving neuron, with particular interest in the balance between extrinsic activity and intrinsic genetic programs.

Sensory modality specific activity, through thalamic afferents, can trigger changes in the

developing cortical circuits and function. Sur and colleagues rewired visual modality input to the auditory cortex (via rewiring of retinal input to the MGN instead of the dLGN) (Sur et al., 1988; Angelucci et al., 1997; Angelucci et al., 1998; Sharma et al., 2000). They demonstrated that the rewired visual input directs the auditory cortex to exhibit functional visual properties including orientation columns, and to mediate visually evoked behaviour (Angelucci et al., 1997; Sharma et al., 2000; von Melchner et al., 2000).

Furthermore input from specific thalamic nuclei can contribute to the genetic identity of the cortical neurons. The ventrobasal thalamic complex (VB- includes the first order somatosensory thalamic nucleus the VPM) projects to layer IV of the primary somatosensory cortex (S1). The higher order somatosensory thalamic nucleus the Po does not project to layer IV of S1; Po projects to layer I and Va in S1, and layer IV in secondary somatosensory cortex (S2) (Wimmer et al., 2010; Ohno et al., 2012; Kichula and Huntley, 2008; Viaene et al., 2011a). The genetic ablation of VB allows the Po fibres to aberrantly target S1 layer IV neurons. The aberrant Po to layer IV driver input alters the transcriptional, electrophysiological and functional identity of the S1layer IV neurons (Pouchelon et al., 2014b). Functionally the layer IV fibres become responsive to nociceptive stimuli and behaviourally this wiring mediates a reduction in pain tolerance in the mice (Pouchelon et al., 2014b). In addition to these functional changes the rewiring causes molecular changes too. As assessed by microarray gene expression the transcriptional identity of the S1layer IV neurons shifts to be more similar to an S2 layer IV neuron (Pouchelon et al., 2014b). These results establish that the precise identity of the thalamic input to the cortex can contribute to the transcriptional identity of cortical neurons.

A similar mechanism of input dependent transcriptional identity has also been indicated in the thalamus. In ferret, removing the cochlear and ablating the dLGN encourages retinal input to rewire to innervate the normally auditory first order thalamic nucleus the MGN (Sur et al., 1988; Angelucci et al., 1997; Angelucci et al., 1998). Not only

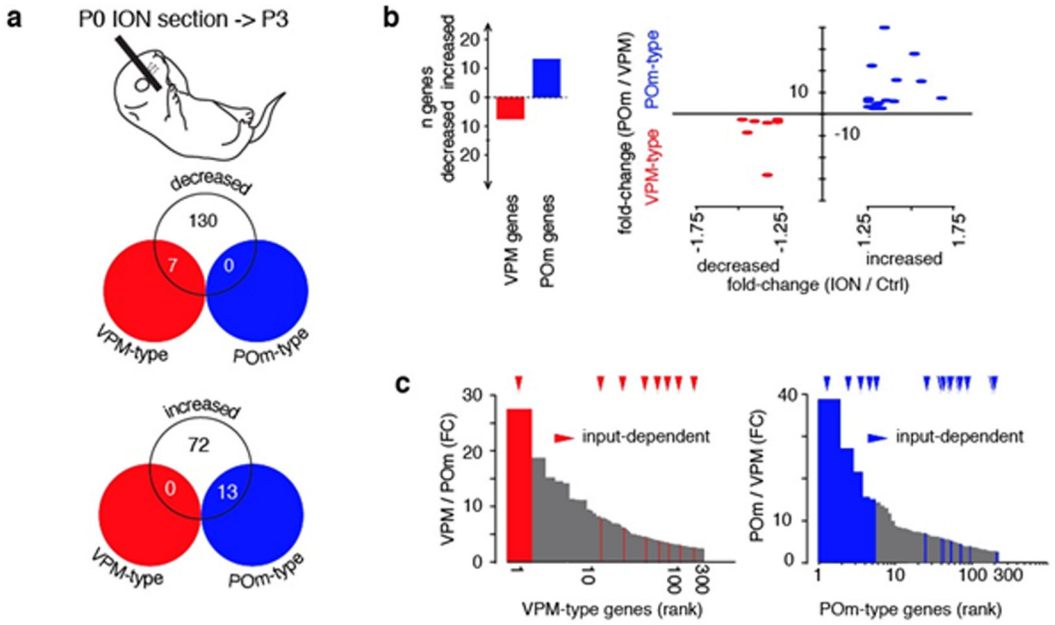

Figure 6.1. Gene expression changes in the VPM following infraorbital nerve transection. A. Infraorbital nerve transection (ION) was performed at P0 and VPM tissue samples were taken at P3 from microarray gene expression analysis. Of 130 genes down-regulated in the VPM following ION, 7 were categorised as VPM type genes, 0 were categorised as POm (Po) type genes. Of 72 genes up-regulated in the VPM, 0 were VPM type genes, 13 were POm type genes. B. VPM type genes were exclusively down-regulated after ION, POm type genes were exclusively up-regulated after ION. C. Genes which were ranked very strongly as typical of VPM tissue or POm tissue, many of the highest ranked were input dependent (altered following ION). Abbreviations used: ION, infraorbital nerve transection; VPM, ventral posterior (medial) nucleus; POm, posterior (medial) nucleus, also referred to as posterior nucleus/ Po. Figure kindly provided by Professor Denis Jabaudon.

does the rewiring of retinal input to the MGN then enable the auditory cortex to display visual cortex like functions but the transcriptional identity of the MGN becomes more similar to the dLGN (Horng et al., 2009). Ten genes up-regulated in the rewired MGN are dLGN enriched genes, this includes *Zic4*, a transcription factor which is important in dLGN development. This suggests that the rewired retinal input to the MGN contributes to determining gene expression in the receiving thalamic nucleus.

6.2.3.2. Can the sensory periphery alter hierarchy specific transcriptional identity of thalamic nuclei?

Above I have discussed how cortical cross-hierarchical rewiring can alter transcription in layer IV neurons and how peripheral input to the thalamus can contribute to the transcriptional profile of specific thalamic nuclei. It has recently been demonstrated that peripheral input may in fact contribute to the hierarchy specific transcriptional identity of thalamic nuclei.

Recent work within the laboratory of collaborator Professor Jabaudon (University of Geneva, Switzerland) on the transcriptome of first order and higher order thalamic nuclei has demonstrated that thalamic nuclei are clustered by hierarchy. That is a nucleus is more similar to another nucleus of the same hierarchical level rather than to another nucleus which attends to the same sensory modality (Pouchelon et al., 2014a). This extends earlier work identifying several genes which are expressed in one order of nuclei (Nakagawa and O'Leary, 2001; Nakagawa and O'Leary, 2003; Vue et al., 2009; Yuge et al., 2011; Suzuki-Hirano et al., 2011).

The first order VPM (which represents somatosensory information) is more similar to the first order dLGN (which represents visual information) than it is to the higher order Po (which is somatosensory) (Pouchelon et al., 2014a). In this unpublished work Pouchelon and colleagues then demonstrated that the loss of somatosensory input to the VPM by infraorbital nerve transection shifts the VPM transcriptome to be more similar to that of the Po (figure 6.1). They show that 7 VPM specific genes are down-regulated and 13 Po specific genes are up-regulated in the VPM after infraorbital nerve transection (Pouchelon et al., 2014a).

My layer V tracing results suggest that not only might the transcriptional identity of the first order nuclei change after loss of peripheral input, but that the corticothalamic circuitry also changes. Visual deprivation by monocular enucleation causes or enables layer V input to invade the originally first order dLGN. Thus layer V projects to a former first order nucleus; the dLGN becomes part of a 'higher order' thalamic relay. Whether it plays a functional role in the higher order relay is discussed previously in 6.2.2.2.

As such these results identify some features of first order/ higher order nucleus identity which can be determined by peripheral input. The loss of somatosensory input causes first order VPM to acquire some higher order Po transcriptional features. The loss of retinal input causes the dLGN to receive input from layer V which normally only projects to higher order nuclei.

6.2.3.3. Cross-hierarchical gene expression in the dLGN

I have shown cross-hierarchical rewiring of layer V to the first order dLGN. Pouchelon and colleagues demonstrate that in the somatosensory system the VPM expresses more higher order Po genes after infraorbital nerve transection (Pouchelon et al., 2014a). Thus in combination our results show a shift of thalamic nucleus identity to a higher order profile after peripheral manipulation in two different sensory modalities but using different read outs (circuit connectivity vs gene expression). As such we were interested in whether these results can be extended into the other modality; whether layer V can be induced to enter the VPM after infraorbital nerve transection (which I have discussed in section 6.2.2.4) and whether the differential gene expression in the dLGN after enucleation shifts it towards higher order expression. My microarray gene expression analysis comparing control and enucleated dLGN at P6 can contribute to answering the question regarding the specification of the higher order thalamic nucleus transcriptome.

My microarray results identify genes which are differentially expressed in the enucleated dLGN. If the enucleated dLGN shifts towards a higher order gene expression profile it is likely to become more similar to the LP, the visual higher order thalamic nucleus. As such we could compare the gene expression in the enucleated dLGN with gene expression in the LP. Firstly using microarray gene expression analysis one would need to identify genes which are dLGN specific and genes which are LP specific by. Once this has been performed we can then see whether dLGN specific genes are down-regulated in the dLGN after enucleation and whether LP specific genes are up-regulated in the dLGN after enucleation.

The LP microarray gene expression microarray is currently being performed in Professor Jabaudon's laboratory, to compare to their previous dLGN gene expression experiments. Once complete the gene expression of the LP will be compared to gene expression in the control and enucleated dLGN results from my microarray. If these results confirm that the enucleated dLGN becomes transcriptionally more similar to the LP they will support the hypothesis that peripheral input determines the expression of

some hierarchy-specific genes.

It would also be interested to then see whether the de-innervated dLGN and the de-innervated VPM cluster together and whether they cluster midway between the control dLGN and VPM and the control LP and Po.

Thus my cross-hierarchical rewiring results support the hypothesis that peripheral input to the first order thalamic nuclei may direct thalamic relay cell transcriptome and circuitry towards a first order fate. This would explain why the loss of peripheral input allows first order nuclei to revert to a higher order identity. To further test this hypothesis we are performing several experiments to determine whether layer V can be induced to enter the VPM after infraorbital nerve transection and whether the enucleated dLGN transcriptome becomes more similar to the higher order LP transcriptome following enucleation.

6.2.3.4. The role of retinal fibres and layer V and VI and VIb corticothalamic fibres

One question which warrants further investigation is the causal relationship between these changes in first order thalamic nuclei features (transcriptional read out or layer V ingrowth read out). Does the loss of peripheral input cause a shift in genetic identity, and therefore alter corticothalamic ingrowth patterns? Alternatively does the loss of peripheral input generate free ‘synapse spaces’ which the layer V, VI and VIb fibres colonise due to lack of competition? This aberrant ingrowth of layer V or premature ingrowth of layer VI and VIb fibres may consequently alter the gene expression in the thalamic nucleus.

To distinguish these possibilities we could perform peripheral manipulations (monocular enucleation or infraorbital nerve transection) in a mouse which lacks layer V or layer VI corticothalamic neurons. This could be performed through genetic ablation using the layer specific Cre lines, such as Rbp4-Cre and Ntsr1-Cre that I present in this thesis, and crossing them with a line expressing floxed diphtheria toxin fragment A which causes cell death of Cre positive cells (Brockschnieder et al., 2004).

If peripheral manipulation in these lines continues to cause the changes in gene expression in the thalamic nuclei we could conclude that thalamic nuclei transcription changes as a result of the loss of peripheral input. Alternatively if the transcriptional changes no longer occur we could conclude that the aberrant layer V ingrowth or premature layer VI ingrowth contributes to the transcriptional changes within the nucleus. The most likely outcome is that both peripheral input and corticothalamic input contribute to gene expression and therefore such an experiment could resolve which genes are differentially expressed due to the loss of peripheral input and which are differentially expressed due to the aberrant ingrowth of layer V and premature ingrowth of VI.

It may also be that the activity of the layer V or layer VI neurons is important in the changing gene expression. This could be tested by crossing the Rbp4-Cre and Ntrs-Cre lines with a floxed-Snap25 conditional mutant (thus silencing layer V and layer VI fibres, respectively). This could distinguish whether the activity of these neurons is important in gene expression changes. Furthermore silencing layer V and layer VI would demonstrate whether these corticothalamic fibres need to be synaptically active in order to rewire or prematurely project to the dLGN.

6.2.3.5. Can retinal fibres colonise former higher order nuclei and confer first order identity there?

My results, in combination with results from our collaborators, strongly suggest that peripheral input to thalamic nuclei is important for the identity and connections of the thalamic nuclei especially with regards to the position of the thalamic nuclei within the hierarchy of first order and second order nuclei. These results have led to the hypothesis that fibres from the periphery may ‘divert’ thalamic nucleus fate to become first order whilst without peripheral input they continue along a high order fate. However so far we only have evidence that the loss of peripheral inputs causes normally first order nuclei to take some features of higher order nuclei (the VPM expresses some higher order genes, the dLGN receives input from layer V).

The next step would be to assess whether peripheral input can establish first order features in normally higher order nuclei. As layer V fibres are able to invade the dLGN following enucleation, it would be interesting to see whether retinal fibres can invade higher order nuclei such as the LP. This could be performed by injecting tracers into the eye after layer V fibres are abolished in experiments such as those described above where layer V cells are removed by crossing Rbp4-Cre with floxed diphtheria toxin (Brockschnieder et al., 2004). This would demonstrate if there is cross-hierarchical wiring in the other direction. Following this it would be interesting to assess whether the LP begins to display a transcriptome more similar to that of the dLGN.

6.2.3.6. What is the extent of the re-specification of thalamic relay neurons?

The results discussed regarding cross-hierarchical 're-specification' of first order thalamic relay neurons show that there are some features of first order/ higher order nucleus identity which can be determined by peripheral input. The loss of somatosensory input causes first order VPM to acquire some higher order Po transcriptional features and we are further testing this in the visual system. The loss of retinal input causes the dLGN to receive input from layer V which normally only projects to higher order nuclei and we are assessing whether this is replicated in the somatosensory system.

However these features do not represent full re-specification of the first order thalamic relay neurons to 'higher order' relay fates. Cross-modal plasticity in the cortex is not 'complete'. Rewiring visual information via the MGN to the primary auditory cortex generates visual functional features in A1 such as orientation columns and can mediate visually evoked behaviour. However the rewired A1 is not identical to the normal V1; the orientation columns in rewired A1 are less ordered than in the normal V1 and the horizontal connections between visual neurons are not recapitulated in A1 (Sharma et al., 2000) and the visual acuity is less good (von Melchner et al., 2000). Thus whether re-specification of the first order neurons really recapitulates higher order thalamic relay neuron identity should be tested.

Considerable re-specification of post-mitotic neurons has been achieved; over-expressing Fezf2 in layer IV neurons causes layer V identity as assessed by the transcriptome, morphology, physiology and connectivity of the reprogrammed neurons (De la Rossa et al., 2013). Further functional features of the thalamic relay neurons need to be assessed in order to assess the extent of the re-specification. Functional features to assess would include the projections of 're-specified' relay neurons to the cortex; for example higher order nuclei project to layers I, II/III and V or primary cortex whereas first order nuclei project to layer IV. This could be assessed by establishing the pattern of VGluT2 in the primary cortex of peripherally manipulated animals. VGluT2 is expressed by mature thalamocortical synapses (Nakamura et al., 2005; Jabaudon et al., 2012). In normal primary cortex VGluT2 is strong in layer IV but not other cortical layers. If VGluT2 is expressed more strongly in layers I, II/III and V of primary visual cortex after monocular enucleation, or primary sensory cortex after infraorbital nerve transection this would suggest the 're-specified' thalamic relay neurons are taking on higher order projection patterns.

Following thorough characterisation of the re-specified neurons, unsupervised cluster analysis on the combined features such as that done for distinct layer V projection neuron populations (Oswald et al., 2013) would suggest how similar the re-specified first order neurons are to normal first order and higher order neurons.

6.3. Conclusion

In this thesis I have presented three distinct contributions to our understanding of the development of the corticothalamic system and the role of retinal input on this development. In chapter 3 I conclusively characterise the ingrowth of corticothalamic fibres from layer V, VI and VIb into the thalamus, demonstrating distinct hierarchical patterning which is present from P2. In chapter 4 I demonstrate that the loss of retinal input to cortical targets disrupts the ingrowth pattern of all three subpopulations of corticothalamic fibres, causing premature entry of layer VI and VIb into the dLGN, the premature entry of layer V into the superficial grey layer of the superior colliculus and

the abnormal entry of layer V into the normally first order dLGN (cross-hierarchical rewiring). In chapter 5 I demonstrate that retinal input to the dLGN is important for the transcriptome of dLGN neurons and that the loss of retinal input appears to cause a delay in the development of the dLGN transcriptome.

My results emphasise that peripheral input is crucial in the development of corticothalamic circuitry and regulates transcription in maturing thalamic nuclei. This supports theories that peripheral inputs can instruct functional neural development and contributes to evidence of functional plasticity in non-cortical structures. My results also demonstrate that the hierarchy of thalamic relays and corticothalamic projections is specified early in development but can be moderated by peripheral input. These results allow us to hypothesise that early peripheral input to the thalamus contributes to the transcriptional and circuit hierarchy identity of thalamic nuclei.

7 References

ABE, K. 2008. Neural activity-dependent regulation of gene expression in developing and mature neurons. *Development, Growth & Differentiation,* 50**,** 261-271.

ABRAMSON, B. P. & CHALUPA, L. M. 1985. The laminar distribution of cortical connections with the tecto- and cortico-recipient zones in the cat's lateral posterior nucleus. *Neuroscience,* 15**,** 81-95.

ACKMAN, J. B., BURBRIDGE, T. J. & CRAIR, M. C. 2012. Retinal waves coordinate patterned activity throughout the developing visual system. *Nature,* 490**,** 219-225.

ADAMS, N. C., LOZSÁDI, D. A. & GUILLERY, R. W. 1997. Complexities in the thalamocortical and corticothalamic pathways. *European Journal of Neuroscience,* 9**,** 204-209.

ALLEN INSTITUTE FOR BRAIN SCIENCE. 2013. ©2013 Allen Institute for Brain Science. Allen Developing Mouse Brain Atlas.

[Online]. Available: http://developingmouse.brain-map.org [Accessed 20 June 2014].

ALLENDOERFER, K. L. & SHATZ, C. J. 1994. The subplate, a transient neocortical structure: its role in the development of connections between thalamus and cortex. *Annu Rev Neurosci,* 17**,** 185-218.

ALLER, M. I. & WISDEN, W. 2008. Changes in expression of some two-pore domain potassium channel genes (KCNK) in selected brain regions of developing mice. *Neuroscience,* 151**,** 1154-1172.

ALTMAN, J. & BAYER, S. A. 1979. Development of the diencephalon in the rat. VI. Re-evaluation of the embryonic development of the thalamus on the basis of thymidine-radiographic datings. *J Comp Neurol,* 188**,** 501-24.

ALTMAN, J. & BAYER, S. A. 1989. Development of the rat thalamus: VI. The posterior lobule of the thalamic neuroepithelium and the time and site of origin and settling pattern of neurons of the lateral geniculate and lateral posterior nuclei. *J Comp Neurol,* 284**,** 581-601.

ANDERMANN, M. L., KERLIN, A. M., ROUMIS, D. K., GLICKFELD, L. L. & REID, R. C. 2011. Functional specialization of mouse higher visual cortical areas. *Neuron,* 72**,** 1025-39.

ANDERSON, G. & PRICE, D. J. 2002. Layer-specific thalamocortical innervation in organotypic cultures is prevented by substances that alter neural activity. *European Journal of Neuroscience,* 16**,** 345-349.

ANDERSON, S. A., EISENSTAT, D. D., SHI, L. & RUBENSTEIN, J. L. 1997. Interneuron migration from basal forebrain to neocortex: dependence on Dlx genes. *Science,* 278**,** 474-6.

ANGELUCCI, A., CLASCA, F., BRICOLO, E., CRAMER, K. S. & SUR, M. 1997. Experimentally induced retinal projections to the ferret auditory thalamus:

development of clustered eye-specific patterns in a novel target. *J Neurosci,* 17**,** 2040-55.

ANGELUCCI, A., CLASCÁ, F. & SUR, M. 1998. Brainstem inputs to the ferret medial geniculate nucleus and the effect of early deafferentation on novel retinal projections to the auditory thalamus. *The Journal of Comparative Neurology,* 400**,** 417-439.

ANGEVINE, J. B. 1970. Time of neuron origin in the diencephalon of the mouse. An autoradiographic study. *The Journal of Comparative Neurology,* 139**,** 129-187.

ANGEVINE, J. B. & SIDMAN, R. L. 1961. Autoradiographic study of cell migration during histogenesis of cerebral cortex in the mouse. *Nature,* 192**,** 766-768.

ANKER, R. L. 1977. The prenatal development of some of the visual pathways in the cat. *J Comp Neurol,* 173**,** 185-204.

ANTHONY, T. E., KLEIN, C., FISHELL, G. & HEINTZ, N. 2004. Radial glia serve as neuronal progenitors in all regions of the central nervous system. *Neuron,* 41**,** 881-90.

ARCELLI, P., FRASSONI, C., REGONDI, M. C., DE BIASI, S. & SPREAFICO, R. 1997. GABAergic neurons in mammalian thalamus: a marker of thalamic complexity? *Brain Res Bull,* 42**,** 27-37.

ARIMATSU, Y. & ISHIDA, M. 2002. Distinct neuronal populations specified to form corticocortical and corticothalamic projections from layer VI of developing cerebral cortex. *Neuroscience,* 114**,** 1033-45.

ARIMATSU, Y., ISHIDA, M., SATO, M. & KOJIMA, M. 1999a. Corticocortical associative neurons expressing latexin: specific cortical connectivity formed in vivo and in vitro. *Cereb Cortex,* 9**,** 569-76.

ARIMATSU, Y., KOJIMA, M. & ISHIDA, M. 1999b. Area- and lamina-specific organization of a neuronal subpopulation defined by expression of latexin in the rat cerebral cortex. *Neuroscience,* 88**,** 93-105.

ASANUMA, C. & STANFIELD, B. B. 1990. Induction of somatic sensory inputs to the lateral geniculate nucleus in congenitally blind mice and in phenotypically normal mice. *Neuroscience,* 39**,** 533-45.

ASANUMA, C., THACH, W. T. & JONES, E. G. 1983. Distribution of cerebellar terminations and their relation to other afferent terminations in the ventral lateral thalamic region of the monkey. *Brain Res,* 286**,** 237-65.

AULADELL, C., PEREZ-SUST, P., SUPER, H. & SORIANO, E. 2000. The early development of thalamocortical and corticothalamic projections in the mouse. *Anat Embryol (Berl),* 201**,** 169-79.

BANSAL, A., SINGER, J. H., HWANG, B. J., XU, W., BEAUDET, A. & FELLER, M. B. 2000. Mice lacking specific nicotinic acetylcholine receptor subunits exhibit dramatically altered spontaneous activity patterns and reveal a limited role for

retinal waves in forming ON and OFF circuits in the inner retina. *The Journal of Neuroscience,* 20**,** 7672-7681.

BEN-ARI, Y. & SPITZER, N. C. 2010. Phenotypic checkpoints regulate neuronal development. *Trends Neurosci,* 33**,** 485-92.

BENJAMINI, Y. & HOCHBERG, Y. 1995. Controlling the false discovery rate: a practical and powerful approach to multiple testing. *Journal of the Royal Statistical Society, Series B,* 57**,** 289-300.

BERRY, M. & ROGERS, A. W. 1965. The migration of neuroblasts in the developing cerebral cortex. *J Anat,* 99**,** 691-709.

BEURDELEY, M., SPATAZZA, J., LEE, H. H. C., SUGIYAMA, S., BERNARD, C., DI NARDO, A. A., HENSCH, T. K. & PROCHIANTZ, A. 2012. Otx2 Binding to Perineuronal Nets Persistently Regulates Plasticity in the Mature Visual Cortex. *The Journal of Neuroscience,* 32**,** 9429-9437.

BICKFORD, M. E., SLUSARCZYK, A., DILGER, E. K., KRAHE, T. E., KUCUK, C. & GUIDO, W. 2010. Synaptic development of the mouse dorsal lateral geniculate nucleus. *J Comp Neurol,* 518**,** 622-35.

BICKNESE, A., SHEPPARD, A., O'LEARY, D. & PEARLMAN, A. 1994. Thalamocortical axons extend along a chondroitin sulfate proteoglycan-enriched pathway coincident with the neocortical subplate and distinct from the efferent path. *The Journal of Neuroscience,* 14**,** 3500-3510.

BISHOP, K. M., GOUDREAU, G. & O'LEARY, D. D. 2000. Regulation of area identity in the mammalian neocortex by Emx2 and Pax6. *Science,* 288**,** 344-9.

BLAKEY, D., WILSON, M. C. & MOLNAR, Z. 2012. Termination and initial branch formation of SNAP-25-deficient thalamocortical fibres in heterochronic organotypic co-cultures. *Eur J Neurosci,* 35**,** 1586-94.

BODA, E., PINI, A., HOXHA, E., PAROLISI, R. & TEMPIA, F. 2009. Selection of reference genes for quantitative real-time RT-PCR studies in mouse brain. *J Mol Neurosci,* 37**,** 238-53.

BORTONE, D. S., OLSEN, S. R. & SCANZIANI, M. 2014. Translaminar inhibitory cells recruited by layer 6 corticothalamic neurons suppress visual cortex. *Neuron,* 82**,** 474-85.

BOURASSA, J. & DESCHENES, M. 1995. Corticothalamic projections from the primary visual cortex in rats: a single fiber study using biocytin as an anterograde tracer. *Neuroscience,* 66**,** 253-63.

BOURASSA, J., PINAULT, D. & DESCHENES, M. 1995. Corticothalamic projections from the cortical barrel field to the somatosensory thalamus in rats: a single-fibre study using biocytin as an anterograde tracer. *Eur J Neurosci,* 7**,** 19-30.

BOYDEN, E. S., ZHANG, F., BAMBERG, E., NAGEL, G. & DEISSEROTH, K. 2005. Millisecond-timescale, genetically targeted optical control of neural activity. *Nat*

Neurosci, 8**,** 1263-8.

BOZZI, Y., PIZZORUSSO, T., CREMISI, F., ROSSI, F. M., BARSACCHI, G. & MAFFEI, L. 1995. Monocular deprivation decreases the expression of messenger RNA for brain-derived neurotrophic factor in the rat visual cortex. *Neuroscience,* 69**,** 1133-44.

BRACKEN, B. K. & TURRIGIANO, G. G. 2009. Experience-dependent regulation of TrkB isoforms in rodent visual cortex. *Developmental Neurobiology,* 69**,** 267-278.

BRAISTED, J. E., CATALANO, S. M., STIMAC, R., KENNEDY, T. E., TESSIER-LAVIGNE, M., SHATZ, C. J. & O'LEARY, D. D. M. 2000. Netrin-1 promotes thalamic axon growth and is required for proper development of the thalamocortical projection. *The Journal of Neuroscience,* 20**,** 5792-5801.

BRAISTED, J. E., TUTTLE, R. & O'LEARY, D. D. M. 1999. Thalamocortical Axons Are Influenced by Chemorepellent and Chemoattractant Activities Localized to Decision Points along Their Path. *Developmental Biology,* 208**,** 430-440.

BRAUNEWELL, K.-H. & SZANTO, A. K. 2009. Visinin-like proteins (VSNLs): interaction partners and emerging functions in signal transduction of a subfamily of neuronal Ca2+-sensor proteins. *Cell and Tissue Research,* 335**,** 301-316.

BROCKSCHNIEDER, D., LAPPE-SIEFKE, C., GOEBBELS, S., BOESL, M. R., NAVE, K. A. & RIETHMACHER, D. 2004. Cell depletion due to diphtheria toxin fragment A after Cre-mediated recombination. *Mol Cell Biol,* 24**,** 7636-42.

BRODMANN, K. 1909. *Vergleichende Lokalisationslehre der Gro hirnrinde; in ihren Prinzipien dargestellt auf Grund des Zellenbaues,* Leipzig, JA Barth.

BROOKS, JUSTIN M., SU, J., LEVY, C., WANG, JESSICA S., SEABROOK, TANIA A., GUIDO, W. & FOX, MICHAEL A. 2013. A molecular mechanism regulating the timing of corticogeniculate innervation. *Cell Reports,* 5**,** 573-581.

CABELLI, R. J., HOHN, A. & SHATZ, C. J. 1995. Inhibition of ocular dominance column formation by infusion of NT-4/5 or BDNF. *Science,* 267**,** 1662-6.

CASTELLANI, V., YUE, Y., GAO, P.-P., ZHOU, R. & BOLZ, J. 1998. Dual Action of a Ligand for Eph Receptor Tyrosine Kinases on Specific Populations of Axons during the Development of Cortical Circuits. *The Journal of Neuroscience,* 18**,** 4663-4672.

CASTREN, E., ZAFRA, F., THOENEN, H. & LINDHOLM, D. 1992. Light regulates expression of brain-derived neurotrophic factor mRNA in rat visual cortex. *Proc Natl Acad Sci U S A,* 89**,** 9444-8.

CATALANO, S. M., ROBERTSON, R. T. & KILLACKEY, H. P. 1991. Early ingrowth of thalamocortical afferents to the neocortex of the prenatal rat. *Proceedings of the National Academy of Sciences,* 88**,** 2999-3003.

CATALANO, S. M. & SHATZ, C. J. 1998. Activity-dependent cortical target selection

by thalamic axons. *Science,* 281**,** 559-562.

CAVINESS, V. S., JR. & FROST, D. O. 1980. Tangential organization of thalamic projections to the neocortex in the mouse. *J Comp Neurol,* 194**,** 335-67.

CHABOT, N., CHARBONNEAU, V., LARAMEE, M. E., TREMBLAY, R., BOIRE, D. & BRONCHTI, G. 2008. Subcortical auditory input to the primary visual cortex in anophthalmic mice. *Neurosci Lett,* 433**,** 129-34.

CHABOT, N., ROBERT, S., TREMBLAY, R., MICELI, D., BOIRE, D. & BRONCHTI, G. 2007. Audition differently activates the visual system in neonatally enucleated mice compared with anophthalmic mutants. *Eur J Neurosci,* 26**,** 2334-48.

CHARBONNEAU, V., LARAMEE, M. E., BOUCHER, V., BRONCHTI, G. & BOIRE, D. 2012. Cortical and subcortical projections to primary visual cortex in anophthalmic, enucleated and sighted mice. *Eur J Neurosci,* 36**,** 2949-63.

CHEN, C. & REGEHR, W. G. 2000. Developmental remodeling of the retinogeniculate synapse. *Neuron,* 28**,** 955-66.

CHENG, G., KAMINSKI, H. J., GONG, B., ZHOU, L., HATALA, D., HOWELL, S. J., ZHOU, X. & MUSTARI, M. J. 2008. Monocular visual deprivation in macaque monkeys: a profile in the gene expression of lateral geniculate nucleus by laser capture microdissection. *Mol Vis,* 14**,** 1401-13.

CHOU, S. J., BABOT, Z., LEINGARTNER, A., STUDER, M., NAKAGAWA, Y. & O'LEARY, D. D. 2013. Geniculocortical input drives genetic distinctions between primary and higher-order visual areas. *Science,* 340**,** 1239-42.

CLASCÁ, F., ANGELUCCI, A. & SUR, M. 1995. Layer-specific programs of development in neocortical projection neurons. *Proceedings of the National Academy of Sciences,* 92**,** 11145-11149.

CLINE, H. 2003. Sperry and Hebb: oil and vinegar? *Trends Neurosci,* 26**,** 655-61.

COLEMAN, K. A. & MITROFANIS, J. 1996. Organization of the visual reticular thalamic nucleus of the rat. *Eur J Neurosci,* 8**,** 388-404.

CONLEY, M. & RACZKOWSKI, D. 1990. Sublaminar organization within layer VI of the striate cortex in Galago. *J Comp Neurol,* 302**,** 425-36.

CONNOLLY, M. & VAN ESSEN, D. 1984. The representation of the visual field in parvicellular and magnocellular layers of the lateral geniculate nucleus in the macaque monkey. *J Comp Neurol,* 226**,** 544-64.

CONNORS, B. W. & LONG, M. A. 2004. Electrical synapses in the mammalian brain. *Annu Rev Neurosci,* 27**,** 393-418.

CRANDALL, J. E. & CAVINESS, V. S., JR. 1984. Thalamocortical connections in newborn mice. *J Comp Neurol,* 228**,** 542-56.

CRUIKSHANK, S. J., URABE, H., NURMIKKO, A. V. & CONNORS, B. W. 2010.

Pathway-specific feedforward circuits between thalamus and neocortex revealed by selective optical stimulation of axons. *Neuron,* 65**,** 230-245.

CULLEN, M. J. & KAISERMAN-ABRAMOF, I. R. 1976. Cytological organization of the dorsal lateral geniculate nuclei in mutant anophthalmic and postnatally enucleated mice. *J Neurocytol,* 5**,** 407-24.

DE CAMILLI, P., MILLER, P. E., LEVITT, P., WALTER, U. & GREENGARD, P. 1984. Anatomy of cerebellar Purkinje cells in the rat determined by a specific immunohistochemical marker. *Neuroscience,* 11**,** 761-817.

DE CARLOS, J. & O'LEARY, D. 1992. Growth and targeting of subplate axons and establishment of major cortical pathways [published erratum appears in J Neurosci 1993 Mar;13(3):following table of contents]. *The Journal of Neuroscience,* 12**,** 1194-1211.

DE LA ROSSA, A., BELLONE, C., GOLDING, B., VITALI, I., MOSS, J., TONI, N., LUSCHER, C. & JABAUDON, D. 2013. In vivo reprogramming of circuit connectivity in postmitotic neocortical neurons. *Nat Neurosci,* 16**,** 193-200.

DECK, M., LOKMANE, L., CHAUVET, S., MAILHES, C., KEITA, M., NIQUILLE, M., YOSHIDA, M., YOSHIDA, Y., LEBRAND, C., MANN, F., GROVE, ELIZABETH A. & GAREL, S. 2013. Pathfinding of corticothalamic axons relies on a rendezvous with thalamic projections. *Neuron,* 77**,** 472-484.

DEL RIO, J. A., MARTINEZ, A., AULADELL, C. & SORIANO, E. 2000. Developmental history of the subplate and developing white matter in the murine neocortex. Neuronal organization and relationship with the main afferent systems at embryonic and perinatal stages. *Cereb Cortex,* 10**,** 784-801.

DENAXA, M., CHAN, C. H., SCHACHNER, M., PARNAVELAS, J. G. & KARAGOGEOS, D. 2001. The adhesion molecule TAG-1 mediates the migration of cortical interneurons from the ganglionic eminence along the corticofugal fiber system. *Development,* 128**,** 4635-44.

DESCHAMPS, C., MOREL, M., JANET, T., PAGE, G., JABER, M., GAILLARD, A. & PRESTOZ, L. 2010. EphrinA5 protein distribution in the developing mouse brain. *BMC Neuroscience,* 11**,** 105.

DESCHÊNES, M., BOURASSA, J. & PINAULT, D. 1994. Corticothalamic projections from layer V cells in rat are collaterals of long-range corticofugal axons. *Brain Research,* 664**,** 215-219.

DIAMOND, I. T., JONES, E. G. & POWELL, T. P. 1969. The projection of the auditory cortex upon the diencephalon and brain stem in the cat. *Brain Res,* 15**,** 305-40.

DIAMOND, M. E., ARMSTRONG-JAMES, M., BUDWAY, M. J. & EBNER, F. F. 1992. Somatic sensory responses in the rostral sector of the posterior group (POm) and in the ventral posterior medial nucleus (VPM) of the rat thalamus: dependence on the barrel field cortex. *J Comp Neurol,* 319**,** 66-84.

DOUGLAS, R. J. & MARTIN, K. A. 2004. Neuronal circuits of the neocortex. *Annu*

Rev Neurosci, 27**,** 419-51.

DRAGER, U. C. 1975. Receptive fields of single cells and topography in mouse visual cortex. *J Comp Neurol,* 160**,** 269-90.

DRAGER, U. C. & HUBEL, D. H. 1975. Responses to visual stimulation and relationship between visual, auditory, and somatosensory inputs in mouse superior colliculus. *J Neurophysiol,* 38**,** 690-713.

DUM, R. P. & STRICK, P. L. 2003. An unfolded map of the cerebellar dentate nucleus and its projections to the cerebral cortex. *J Neurophysiol,* 89**,** 634-9.

DURHAM, D. & WOOLSEY, T. A. 1984. Effects of neonatal whisker lesions on mouse central trigeminal pathways. *J Comp Neurol,* 223**,** 424-47.

DYE, C. A., ABBOTT, C. W. & HUFFMAN, K. J. 2012. Bilateral enucleation alters gene expression and intraneocortical connections in the mouse. *Neural Dev,* 7**,** 5.

ERZURUMLU, R. S. & GASPAR, P. 2012. Development and critical period plasticity of the barrel cortex. *Eur J Neurosci,* 35**,** 1540-53.

ERZURUMLU, R. S. & JHAVERI, S. 1992. Emergence of Connectivity in the Embryonic Rat Parietal Cortex. *Cerebral Cortex,* 2**,** 336-352.

EVRARD, A. & ROPERT, N. 2009. Early development of the thalamic inhibitory feedback loop in the primary somatosensory system of the newborn mice. *The Journal of Neuroscience,* 29**,** 9930-9940.

FELDHEIM, D. A. & O'LEARY, D. D. 2010. Visual map development: bidirectional signaling, bifunctional guidance molecules, and competition. *Cold Spring Harb Perspect Biol,* 2**,** a001768.

FELDMEYER, D. 2012. Excitatory neuronal connectivity in the barrel cortex. *Front Neuroanat,* 6**,** 24.

FELLER, M. B., WELLIS, D. P., STELLWAGEN, D., WERBLIN, F. S. & SHATZ, C. J. 1996. Requirement for cholinergic synaptic transmission in the propagation of spontaneous retinal waves. *Science,* 272**,** 1182-7.

FENNO, L., YIZHAR, O. & DEISSEROTH, K. 2011. The development and application of optogenetics. *Annu Rev Neurosci,* 34**,** 389-412.

FISHELL, G. & HANASHIMA, C. 2008. Pyramidal neurons grow up and change their mind. *Neuron,* 57**,** 333-338.

FLAVELL, S. W. & GREENBERG, M. E. 2008. Signaling mechanisms linking neuronal activity to gene expression and plasticity of the nervous system. *Annu Rev Neurosci,* 31**,** 563-90.

FLEIGE, S. & PFAFFL, M. W. 2006. RNA integrity and the effect on the real-time qRT-PCR performance. *Mol Aspects Med,* 27**,** 126-39.

FRANKIN, K. B. J. & PAXINOS, G. 1996. *The mouse brain in stereotaxic coordinates*,

Academic Press.

FRIAUF, E. & SHATZ, C. J. 1991. Changing patterns of synaptic input to subplate and cortical plate during development of visual cortex. *J Neurophysiol,* 66**,** 2059-71.

FROST, D. O., BOIRE, D., GINGRAS, G. & PTITO, M. 2000. Surgically created neural pathways mediate visual pattern discrimination. *Proc Natl Acad Sci U S A,* 97**,** 11068-73.

FROST, D. O. & CAVINESS, V. S., JR. 1980. Radial organization of thalamic projections to the neocortex in the mouse. *J Comp Neurol,* 194**,** 369-93.

FROST, D. O. & METIN, C. 1985. Induction of functional retinal projections to the somatosensory system. *Nature,* 317**,** 162-4.

FUKUDA, T., KAWANO, H., OHYAMA, K., LI, H. P., TAKEDA, Y., OOHIRA, A. & KAWAMURA, K. 1997. Immunohistochemical localization of neurocan and L1 in the formation of thalamocortical pathway of developing rats. *J Comp Neurol,* 382**,** 141-52.

GALLI, L. & MAFFEI, L. 1988. Spontaneous impulse activity of rat retinal ganglion cells in prenatal life. *Science,* 242**,** 90-91.

GAO, G., PLAAS, A., THOMPSON, V. P., JIN, S., ZUO, F. & SANDY, J. D. 2004. ADAMTS4 (aggrecanase-1) activation on the cell surface involves C-terminal cleavage by glycosylphosphatidyl inositol-anchored membrane type 4-matrix metalloproteinase and binding of the activated proteinase to chondroitin sulfate and heparan sulfate on syndecan-1. *J Biol Chem,* 279**,** 10042-51.

GAO, P., SULTAN, K. T., ZHANG, X.-J. & SHI, S.-H. 2013. Lineage-dependent circuit assembly in the neocortex. *Development,* 140**,** 2645-2655.

GARCIA-DOMINGUEZ, C. A., MARTINEZ, N., GRAGERA, T., PEREZ-RODRIGUEZ, A., RETANA, D., LEON, G., SANCHEZ, A., OLIVA, J. L., PEREZ-SALA, D. & ROJAS, J. M. 2011. Sprouty2 and Spred1-2 proteins inhibit the activation of the ERK pathway elicited by cyclopentenone prostanoids. *PLoS One,* 6**,** e16787.

GAREL, S. & RUBENSTEIN, J. L. R. 2004. Intermediate targets in formation of topographic projections: inputs from the thalamocortical system. *Trends in Neurosciences,* 27**,** 533-539.

GENSAT. Available: http://www.gensat.org/cre.jsp 2013].

GERFEN, C. R., PALETZKI, R. & HEINTZ, N. 2013. GENSAT BAC Cre-recombinase driver lines to study the functional organization of cerebral cortical and basal ganglia circuits. *Neuron,* 80**,** 1368-83.

GHOSH, A., ANTONINI, A., MCCONNELL, S. K. & SHATZ, C. J. 1990. Requirement for subplate neurons in the formation of thalamocortical connections. *Nature,* 347**,** 179-81.

GHOSH, A. & SHATZ, C. J. 1994. Segregation of geniculocortical afferents during the critical period: a role for subplate neurons. *J Neurosci,* 14**,** 3862-80.

GILBERT, C. D. 1983. Microcircuitry of the visual cortex. *Annu Rev Neurosci,* 6**,** 217-47.

GILBERT, C. D. & KELLY, J. P. 1975. The projections of cells in different layers of the cat's visual cortex. *J Comp Neurol,* 163**,** 81-105.

GODEMENT, P., SAILLOUR, P. & IMBERT, M. 1980. The ipsilateral optic pathway to the dorsal lateral geniculate nucleus and superior colliculus in mice with prenatal or postnatal loss of one eye. *J Comp Neurol,* 190**,** 611-26.

GODEMENT, P., SALAUN, J. & IMBERT, M. 1984. Prenatal and postnatal development of retinogeniculate and retinocollicular projections in the mouse. *J Comp Neurol,* 230**,** 552-75.

GODEMENT, P., VANSELOW, J., THANOS, S. & BONHOEFFER, F. 1987. A study in developing visual systems with a new method of staining neurones and their processes in fixed tissue. *Development,* 101**,** 697-713.

GOEL, A. & LEE, H. K. 2007. Persistence of experience-induced homeostatic synaptic plasticity through adulthood in superficial layers of mouse visual cortex. *J Neurosci,* 27**,** 6692-700.

GOLDING, B., POUCHELON, G., BELLONE, C., MURTHY, S., DI NARDO, ARIEL A., GOVINDAN, S., OGAWA, M., SHIMOGORI, T., LÜSCHER, C., DAYER, A. & JABAUDON, D. 2013. Retinal input directs the recruitment of inhibitory interneurons into thalamic visual circuits. *Neuron,* 81**,** 1057-1069.

GOLDSTEIN, S. A. N., BOCKENHAUER, D., O'KELLY, I. & ZILBERBERG, N. 2001. Potassium leak channels and the KCNK family of two-p-domain subunits. *Nat Rev Neurosci,* 2**,** 175-184.

GOMEZ, T. M., ROBLES, E., POO, M. & SPITZER, N. C. 2001. Filopodial calcium transients promote substrate-dependent growth cone turning. *Science,* 291**,** 1983-7.

GOMEZ, T. M., SNOW, D. M. & LETOURNEAU, P. C. 1995. Characterization of spontaneous calcium transients in nerve growth cones and their effect on growth cone migration. *Neuron,* 14**,** 1233-46.

GOMEZ, T. M. & SPITZER, N. C. 1999. In vivo regulation of axon extension and pathfinding by growth-cone calcium transients. *Nature,* 397**,** 350-5.

GONG, S., DOUGHTY, M., HARBAUGH, C. R., CUMMINS, A., HATTEN, M. E., HEINTZ, N. & GERFEN, C. R. 2007. Targeting Cre recombinase to specific neuron populations with bacterial artificial chromosome constructs. *The Journal of Neuroscience,* 27**,** 9817-9823.

GONG, S., ZHENG, C., DOUGHTY, M. L., LOSOS, K., DIDKOVSKY, N., SCHAMBRA, U. B., NOWAK, N. J., JOYNER, A., LEBLANC, G., HATTEN,

M. E. & HEINTZ, N. 2003. A gene expression atlas of the central nervous system based on bacterial artificial chromosomes. *Nature,* 425**,** 917-925.

GRANT, E. L., HOERDER-SUABEDISSEN, A. & MOLNAR, Z. 2012. Development of the corticothalamic projections. *Frontiers in Neuroscience,* 6.

GREENBERG, M. E., HERMANOWSKI, A. L. & ZIFF, E. B. 1986. Effect of protein synthesis inhibitors on growth factor activation of c-fos, c-myc, and actin gene transcription. *Mol Cell Biol,* 6**,** 1050-7.

GREIG, L. C., WOODWORTH, M. B., GALAZO, M. J., PADMANABHAN, H. & MACKLIS, J. D. 2013. Molecular logic of neocortical projection neuron specification, development and diversity. *Nat Rev Neurosci,* 14**,** 755-769.

GROH, A., BOKOR, H., MEASE, R. A., PLATTNER, V. M., HANGYA, B., STROH, A., DESCHENES, M. & ACSÁDY, L. 2013. Convergence of Cortical and Sensory Driver Inputs on Single Thalamocortical Cells. *Cerebral Cortex*.

GROH, A., DE KOCK, C. P., WIMMER, V. C., SAKMANN, B. & KUNER, T. 2008. Driver or coincidence detector: modal switch of a corticothalamic giant synapse controlled by spontaneous activity and short-term depression. *J Neurosci,* 28**,** 9652-63.

GRUBB, M. S. & THOMPSON, I. D. 2004. Biochemical and anatomical subdivision of the dorsal lateral geniculate nucleus in normal mice and in mice lacking the beta2 subunit of the nicotinic acetylcholine receptor. Vision Res, 44, 3365-76.

GUIDO, W. 2008. Refinement of the retinogeniculate pathway. *J Physiol,* 586**,** 4357-62.

GUILLERY, R. W. 1967. Patterns of fiber degeneration in the dorsal lateral geniculate nucleus of the cat following lesions in the visual cortex. *J Comp Neurol,* 130**,** 197-221.

GUILLERY, R. W. 1969. A quantitative study of synaptic interconnections in the dorsal lateral geniculate nucleus of the cat. *Cell and Tissue Research,* 96**,** 39-48.

GUILLERY, R. W. 1995. Anatomical evidence concerning the role of the thalamus in corticocortical communication: a brief review. *J Anat,* 187 (Pt 3)**,** 583-92.

GUILLERY, R. W. & SHERMAN, S. M. 2002. Thalamic relay functions and their role in corticocortical communication: generalizations from the visual system. *Neuron,* 33**,** 163-175.

HADA, Y., YAMADA, Y., IMAMURA, K., MATAGA, N., WATANABE, Y. & YAMAMOTO, M. 1999. Effects of monocular enucleation on parvalbumin in rat visual system during postnatal development. *Invest Ophthalmol Vis Sci,* 40**,** 2535-45.

HATANAKA, Y. & MURAKAMI, F. 2002. In vitro analysis of the origin, migratory behavior, and maturation of cortical pyramidal cells. *J Comp Neurol,* 454**,** 1-14.

HATTOX, A. M. & NELSON, S. B. 2007. Layer V neurons in mouse cortex projecting

to different targets have distinct physiological properties. 98**,** 3330-3340.

HAYANO, Y. & YAMAMOTO, N. 2008. Activity-dependent thalamocortical axon branching. *Neuroscientist,* 14**,** 359-68.

HAYES, S. G., MURRAY, K. D. & JONES, E. G. 2003. Two epochs in the development of γ-aminobutyric acidergic neurons in the ferret thalamus. *The Journal of Comparative Neurology,* 463**,** 45-65.

HENDRY, S. H., SCHWARK, H. D., JONES, E. G. & YAN, J. 1987. Numbers and proportions of GABA-immunoreactive neurons in different areas of monkey cerebral cortex. *J Neurosci,* 7**,** 1503-19.

HERRMANN, K. & SHATZ, C. J. 1995. Blockade of action potential activity alters initial arborization of thalamic axons within cortical layer 4. *Proc Natl Acad Sci U S A,* 92**,** 11244-8.

HEUMANN, D. & RABINOWICZ, T. 1980. Postnatal development of the dorsal lateral geniculate nucleus in the normal and enucleated albino mouse. *Exp Brain Res,* 38**,** 75-85.

HEVNER, R. F., MIYASHITA-LIN, E. & RUBENSTEIN, J. L. R. 2002. Cortical and thalamic axon pathfinding defects in Tbr1, Gbx2, and Pax6 mutant mice: Evidence that cortical and thalamic axons interact and guide each other. *The Journal of Comparative Neurology,* 447**,** 8-17.

HIGASHI, S., MOLNÁR, Z., KUROTANI, T. & TOYAMA, K. 2002. Prenatal development of neural excitation in rat thalamocortical projections studied by optical recording. *Neuroscience,* 115**,** 1231-1246.

HOERDER-SUABEDISSEN, A. & MOLNÁR, Z. 2012. Morphology of mouse subplate cells with identified projection targets changes with age. *The Journal of Comparative Neurology,* 520**,** 174-185.

HOERDER-SUABEDISSEN, A. & MOLNÁR, Z. 2013. Molecular diversity of early-born subplate neurons. *Cerebral Cortex,* 23**,** 1473-1483.

HOERDER-SUABEDISSEN, A., PAULSEN, O. & MOLNÁR, Z. 2008. Thalamocortical maturation in mice is influenced by body weight. *The Journal of Comparative Neurology,* 511**,** 415-420.

HOERDER-SUABEDISSEN, A., WANG, W. Z., LEE, S., DAVIES, K. E., GOFFINET, A. M., RAKIC, S., PARNAVELAS, J., REIM, K., NICOLIC, M., PAULSEN, O. & MOLNAR, Z. 2009. Novel markers reveal subpopulations of subplate neurons in the murine cerebral cortex. *Cereb Cortex,* 19**,** 1738-50.

HOHL-ABRAHAO, J. C. & CREUTZFELDT, O. D. 1991. Topographical mapping of the thalamocortical projections in rodents and comparison with that in primates. *Exp Brain Res,* 87**,** 283-94.

HONG, K., NISHIYAMA, M., HENLEY, J., TESSIER-LAVIGNE, M. & POO, M. 2000. Calcium signalling in the guidance of nerve growth by netrin-1. *Nature,*

403**,** 93-8.

HONIG, M. G. & HUME, R. I. 1989. Dil and DiO: versatile fluorescent dyes for neuronal labelling and pathway tracing. *Trends Neurosci,* 12**,** 333-5, 340-1.

HOOGLAND, P. V., WELKER, E. & VAN DER LOOS, H. 1987. Organization of the projections from barrel cortex to thalamus in mice studied with Phaseolus vulgaris-leucoagglutinin and HRP. *Exp Brain Res,* 68**,** 73-87.

HOOKS, B. M. & CHEN, C. 2006. Distinct Roles for Spontaneous and Visual Activity in Remodeling of the Retinogeniculate Synapse. *Neuron,* 52**,** 281-291.

HORITA, H., WADA, K., RIVAS, M. V., HARA, E. & JARVIS, E. D. 2010. The dusp1 immediate early gene is regulated by natural stimuli predominantly in sensory input neurons. *The Journal of Comparative Neurology,* 518**,** 2873-2901.

HORNG, S., KREIMAN, G., ELLSWORTH, C., PAGE, D., BLANK, M., MILLEN, K. & SUR, M. 2009. Differential gene expression in the developing lateral geniculate nucleus and medial geniculate nucleus reveals novel roles for Zic4 and Foxp2 in visual and auditory pathway development. *The Journal of Neuroscience,* 29**,** 13672-13683.

HORTON, J. C. & ADAMS, D. L. 2005. The cortical column: a structure without a function. *Philos Trans R Soc Lond B Biol Sci,* 360**,** 837-62.

HUANG DA, W., SHERMAN, B. T. & LEMPICKI, R. A. 2009a. Bioinformatics enrichment tools: paths toward the comprehensive functional analysis of large gene lists. *Nucleic Acids Res,* 37**,** 1-13.

HUANG DA, W., SHERMAN, B. T. & LEMPICKI, R. A. 2009b. Systematic and integrative analysis of large gene lists using DAVID bioinformatics resources. *Nat Protoc,* 4**,** 44-57.

HUBEL, D. H. & WIESEL, T. N. 1962. Receptive fields, binocular interaction and functional architecture in the cat's visual cortex. *J Physiol,* 160**,** 106-54.

HUBEL, D. H. & WIESEL, T. N. 1963. Shape and arrangement of columns in cat's striate cortex. *J Physiol,* 165**,** 559-68.

HUBEL, D. H. & WIESEL, T. N. 1968. Receptive fields and functional architecture of monkey striate cortex. *J Physiol,* 195**,** 215-43.

HUBEL, D. H. & WIESEL, T. N. 1977. Ferrier Lecture: functional architecture of macaque monkey visual cortex. *Proceedings of the Royal Society of London. Series B. Biological Sciences,* 198**,** 1-59.

HUBEL, D. H., WIESEL, T. N. & STRYKER, M. P. 1977. Orientation columns in macaque monkey visual cortex demonstrated by the 2-deoxyglucose autoradiographic technique. *Nature,* 269**,** 328-30.

HUBENER, M. 2003. Mouse visual cortex. *Curr Opin Neurobiol,* 13**,** 413-20.

HUBERMAN, A. D. 2007. Mechanisms of eye-specific visual circuit development.

Current Opinion in Neurobiology, 17**,** 73-80.

HUBERMAN, A. D., FELLER, M. B. & CHAPMAN, B. 2008. Mechanisms underlying development of visual maps and receptive fields. *Annual Review of Neuroscience,* 31**,** 479-509.

HUBERMAN, A. D., SPEER, C. M. & CHAPMAN, B. 2006. Spontaneous Retinal Activity Mediates Development of Ocular Dominance Columns and Binocular Receptive Fields in V1. *Neuron,* 52**,** 247-254.

INNOCENTI, G. M. & PRICE, D. J. 2005. Exuberance in the development of cortical networks. *Nat Rev Neurosci,* 6**,** 955-65.

IRIZARRY, R. A., BOLSTAD, B. M., COLLIN, F., COPE, L. M., HOBBS, B. & SPEED, T. P. 2003a. Summaries of Affymetrix GeneChip probe level data. *Nucleic Acids Res,* 31**,** e15.

IRIZARRY, R. A., HOBBS, B., COLLIN, F., BEAZER-BARCLAY, Y. D., ANTONELLIS, K. J., SCHERF, U. & SPEED, T. P. 2003b. Exploration, normalization, and summaries of high density oligonucleotide array probe level data. *Biostatistics,* 4**,** 249-64.

IZRAELI, R., KOAY, G., LAMISH, M., HEICKLEN-KLEIN, A. J., HEFFNER, H. E., HEFFNER, R. S. & WOLLBERG, Z. 2002. Cross-modal neuroplasticity in neonatally enucleated hamsters: structure, electrophysiology and behaviour. *Eur J Neurosci,* 15**,** 693-712.

JABAUDON, D., SHNIDER, S. J., TISCHFIELD, D. J., GALAZO, M. J. & MACKLIS, J. D. 2012. RORbeta induces barrel-like neuronal clusters in the developing neocortex. *Cereb Cortex,* 22**,** 996-1006.

JACOBS, E. C., CAMPAGNONI, C., KAMPF, K., REYES, S. D., KALRA, V., HANDLEY, V., XIE, Y. Y., HONG-HU, Y., SPREUR, V., FISHER, R. S. & CAMPAGNONI, A. T. 2007. Visualization of corticofugal projections during early cortical development in a tau-GFP-transgenic mouse. *Eur J Neurosci,* 25**,** 17-30.

JAUBERT-MIAZZA, L., GREEN, E., LO, F. S., BUI, K., MILLS, J. & GUIDO, W. 2005. Structural and functional composition of the developing retinogeniculate pathway in the mouse. *Vis Neurosci,* 22**,** 661-76.

JONES, E. G. 1985. *The Thalamus,* New York, Plenum Press.

JONES, E. G. 2001. The thalamic matrix and thalamocortical synchrony. *Trends in Neurosciences,* 24**,** 595-601.

JONES, E. G. 2002a. Dichronous appearance and unusual origins of GABA neurons during development of the mammalian thalamus. *Thalamus & Related Systems,* 1**,** 283-288.

JONES, E. G. 2002b. Thalamic circuitry and thalamocortical synchrony. *Philosophical Transactions of the Royal Society of London Series B-Biological Sciences,* 357**,**

1659-1673.

JONES, E. G. & POWELL, T. P. 1968. The projection of the somatic sensory cortex upon the thalamus in the cat. *Brain Res,* 10**,** 369-91.

JONES, E. G. & POWELL, T. P. 1970. An anatomical study of converging sensory pathways within the cerebral cortex of the monkey. *Brain,* 93**,** 793-820.

JONES, E. G. & RAKIC, P. 2010. Radial columns in cortical architecture: it is the composition that counts. *Cereb Cortex,* 20**,** 2261-4.

JONES, E. G. & ROCKEL, A. J. 1971. The synaptic organization in the medial geniculate body of afferent fibres ascending from the inferior colliculus. *Z Zellforsch Mikrosk Anat,* 113**,** 44-66.

JONES, E. G. & RUBENSTEIN, J. L. R. 2004. Expression of regulatory genes during differentiation of thalamic nuclei in mouse and monkey. *The Journal of Comparative Neurology,* 477**,** 55-80.

JONES, L., LÓPEZ-BENDITO, G., GRUSS, P., STOYKOVA, A. & MOLNÁR, Z. 2002. Pax6 is required for the normal development of the forebrain axonal connections. *Development,* 129**,** 5041-5052.

JURGENS, C. W., BELL, K. A., MCQUISTON, A. R. & GUIDO, W. 2012. Optogenetic stimulation of the corticothalamic pathway affects relay cells and GABAergic neurons differently in the mouse visual thalamus. *PLoS One,* 7**,** e45717.

KAAS, J. H. 1997. Topographic maps are fundamental to sensory processing. *Brain Res Bull,* 44**,** 107-12.

KAAS, J. H. 2012. Evolution of columns, modules, and domains in the neocortex of primates. *Proc Natl Acad Sci U S A,* 109 Suppl 1**,** 10655-60.

KACZMAREK, L. & CHAUDHURI, A. 1997. Sensory regulation of immediate-early gene expression in mammalian visual cortex: implications for functional mapping and neural plasticity. *Brain Res Brain Res Rev,* 23**,** 237-56.

KACZMAREK, L., ZANGENEHPOUR, S. & CHAUDHURI, A. 1999. Sensory regulation of immediate-early genes c-fos and zif268 in monkey visual cortex at birth and throughout the critical period. *Cereb Cortex,* 9**,** 179-87.

KAGEYAMA, G. H. & ROBERTSON, R. T. 1993. Development of geniculocortical projections to visual cortex in rat: evidence early ingrowth and synaptogenesis. *J Comp Neurol,* 335**,** 123-48.

KAKEI, S., NA, J. & SHINODA, Y. 2001. Thalamic terminal morphology and distribution of single corticothalamic axons originating from layers 5 and 6 of the cat motor cortex. *J Comp Neurol,* 437**,** 170-85.

KAMISHINA, H., CONTE, W. L., PATEL, S. S., TAI, R. J., CORWIN, J. V. & REEP, R. L. 2009. Cortical connections of the rat lateral posterior thalamic nucleus.

Brain Res, 1264**,** 39-56.

KANOH, H., YAMADA, K. & SAKANE, F. 2002. Diacylglycerol kinases: emerging downstream regulators in cell signaling systems. *J Biochem,* 131**,** 629-33.

KANOLD, P. O., KARA, P., REID, R. C. & SHATZ, C. J. 2003. Role of subplate neurons in functional maturation of visual cortical columns. *Science,* 301**,** 521-525.

KANOLD, P. O. & LUHMANN, H. J. 2010. The subplate and early cortical circuits. *Annual Review of Neuroscience,* 33**,** 23-48.

KANOLD, P. O. & SHATZ, C. J. 2006. Subplate neurons regulate maturation of cortical inhibition and outcome of ocular dominance plasticity. *Neuron,* 51**,** 627-638.

KARLEN, S. J., KAHN, D. M. & KRUBITZER, L. 2006. Early blindness results in abnormal corticocortical and thalamocortical connections. *Neuroscience,* 142**,** 843-58.

KASHIWAGI, M., TORTORELLA, M., NAGASE, H. & BREW, K. 2001. TIMP-3 is a potent inhibitor of aggrecanase 1 (ADAM-TS4) and aggrecanase 2 (ADAM-TS5). *J Biol Chem,* 276**,** 12501-4.

KATAOKA, A. & SHIMOGORI, T. 2008. Fgf8 controls regional identity in the developing thalamus. *Development,* 135**,** 2873-2881.

KATZ, L. C. & SHATZ, C. J. 1996. Synaptic activity and the construction of cortical circuits. *Science,* 274**,** 1133-8.

KECK, T., KELLER, GEORG B., JACOBSEN, R. I., EYSEL, ULF T., BONHOEFFER, T. & HÜBENER, M. 2013. Synaptic scaling and homeostatic plasticity in the mouse visual cortex in vivo. *Neuron,* 80**,** 327-334.

KEEN, J. E., KHAWALED, R., FARRENS, D. L., NEELANDS, T., RIVARD, A., BOND, C. T., JANOWSKY, A., FAKLER, B., ADELMAN, J. P. & MAYLIE, J. 1999. Domains responsible for constitutive and Ca2+-dependent interactions between calmodulin and small conductance Ca2+-activated potassium channels. *The Journal of Neuroscience,* 19**,** 8830-8838.

KELLER, A., WHITE, E. L. & CIPOLLONI, P. B. 1985. The identification of thalamocortical axon terminals in barrels of mouse Sml cortex using immunohistochemistry of anterogradely transported lectin (Phaseolus vulgaris-leucoagglutinin). *Brain Research,* 343**,** 159-165.

KELLY, L. R., LI, J., CARDEN, W. B. & BICKFORD, M. E. 2003. Ultrastructure and synaptic targets of tectothalamic terminals in the cat lateral posterior nucleus. *The Journal of Comparative Neurology,* 464**,** 472-486.

KICHULA, E. A. & HUNTLEY, G. W. 2008. Developmental and comparative aspects of posterior medial thalamocortical innervation of the barrel cortex in mice and rats. *J Comp Neurol,* 509**,** 239-58.

KIM, G. J., SHATZ, C. J. & MCCONNELL, S. K. 1991. Morphology of pioneer and follower growth cones in the developing cerebral cortex. *J Neurobiology,* 22**,** 629-42.

KIM, J., MATNEY, C. J., BLANKENSHIP, A., HESTRIN, S. & BROWN, S. P. 2014. Layer 6 corticothalamic neurons activate a cortical output layer, layer 5a. *The Journal of Neuroscience,* 34**,** 9656-9664.

KIND, P. C., SENGPIEL, F., BEAVER, C. J., CROCKER-BUQUE, A., KELLY, G. M., MATTHEWS, R. T. & MITCHELL, D. E. 2013. The Development and Activity-Dependent Expression of Aggrecan in the Cat Visual Cortex. *Cerebral Cortex,* 23**,** 349-360.

KING, A. J. 2004. The superior colliculus. *Curr Biol,* 14**,** R335-8.

KLEENE, R., YANG, H., KUTSCHE, M. & SCHACHNER, M. 2001. The neural recognition molecule L1 is a sialic acid-binding Lectin for CD24, which induces promotion and inhibition of neurite outgrowth. *Journal of Biological Chemistry,* 276**,** 21656-21663.

KLEIN, A. & DUNNETT, S. B. 2012. Analysis of skilled forelimb movement in rats: the single pellet reaching test and staircase test. *Curr Protoc Neurosci,* Chapter 8**,** Unit8 28.

KO, H., COSSELL, L., BARAGLI, C., ANTOLIK, J., CLOPATH, C., HOFER, S. B. & MRSIC-FLOGEL, T. D. 2013. The emergence of functional microcircuits in visual cortex. *Nature,* 496**,** 96-100.

KO, H., HOFER, S. B., PICHLER, B., BUCHANAN, K. A., SJOSTROM, P. J. & MRSIC-FLOGEL, T. D. 2011. Functional specificity of local synaptic connections in neocortical networks. *Nature,* 473**,** 87-91.

KOESTER, S. E. & O'LEARY, D. D. 1992. Functional classes of cortical projection neurons develop dendritic distinctions by class-specific sculpting of an early common pattern. *J Neurosci,* 12**,** 1382-93.

KOHLER, M., HIRSCHBERG, B., BOND, C. T., KINZIE, J. M., MARRION, N. V., MAYLIE, J. & ADELMAN, J. P. 1996. Small-conductance, calcium-activated potassium channels from mammalian brain. *Science,* 273**,** 1709-14.

KOSTOVIC, I. & RAKIC, P. 1980. Cytology and time of origin of interstitial neurons in the white matter in infant and adult human and monkey telencephalon. *J Neurocytol,* 9**,** 219-42.

KRIEGSTEIN, A. R. & NOCTOR, S. C. 2004. Patterns of neuronal migration in the embryonic cortex. *Trends in Neurosciences,* 27**,** 392-399.

LACHANCE, P. E. & CHAUDHURI, A. 2004. Microarray analysis of developmental plasticity in monkey primary visual cortex. *J Neurochem,* 88**,** 1455-69.

LAM, D., JIM, J., TO, E., RASMUSSEN, C., KAUFMAN, P. L. & MATSUBARA, J. 2009. Astrocyte and microglial activation in the lateral geniculate nucleus and

visual cortex of glaucomatous and optic nerve transected primates. *Mol Vis,* 15**,** 2217-29.

LAM, Y. W. & SHERMAN, S. M. 2010. Functional organization of the somatosensory cortical layer 6 feedback to the thalamus. *Cereb Cortex,* 20**,** 13-24.

LANCASTER, B. & ADAMS, P. R. 1986. *Calcium-dependent current generating the afterhyperpolarization of hippocampal neurons*.

LANDER, C., KIND, P., MALESKI, M. & HOCKFIELD, S. 1997. A family of activity-dependent neuronal cell-surface chondroitin sulfate proteoglycans in cat visual cortex. *J Neurosci,* 17**,** 1928-39.

LANGFELDER, P. & HORVATH, S. 2008. WGCNA: an R package for weighted correlation network analysis. *BMC Bioinformatics,* 9**,** 559.

LE GROS CLARK, W. E. 1932. The structure and connections of the thalamus. *Brain,* 55**,** 406-470.

LEBRAND, C., CASES, O., WEHRLÉ, R., BLAKELY, R. D., EDWARDS, R. H. & GASPAR, P. 1998. Transient developmental expression of monoamine transporters in the rodent forebrain. *The Journal of Comparative Neurology,* 401**,** 506-524.

LEE, C. C. & SHERMAN, S. M. 2008. Synaptic Properties of Thalamic and Intracortical Inputs to Layer 4 of the First- and Higher-Order Cortical Areas in the Auditory and Somatosensory Systems. *Journal of Neurophysiology,* 100**,** 317-326.

LEE, C. C. & SHERMAN, S. M. 2010. Topography and physiology of ascending streams in the auditory tectothalamic pathway. *Proc Natl Acad Sci U S A,* 107**,** 372-7.

LEE, L. J., IWASATO, T., ITOHARA, S. & ERZURUMLU, R. S. 2005a. Exuberant thalamocortical axon arborization in cortex-specific NMDAR1 knockout mice. *J Comp Neurol,* 485**,** 280-92.

LEE, L. J., LO, F. S. & ERZURUMLU, R. S. 2005b. NMDA receptor-dependent regulation of axonal and dendritic branching. *J Neurosci,* 25**,** 2304-11.

LEHIGH, K. M., LEONARD, C. E., BARANOSKI, J. & DONOGHUE, M. J. 2013. Parcellation of the thalamus into distinct nuclei reflects EphA expression and function. *Gene Expression Patterns,* 13**,** 454-463.

LEIN, E. S., HOHN, A. & SHATZ, C. J. 2000. Dynamic regulation of BDNF and NT-3 expression during visual system development. *J Comp Neurol,* 420**,** 1-18.

LEIN, E. S. & SHATZ, C. J. 2000. Rapid regulation of brain-derived neurotrophic factor mRNA within eye-specific circuits during ocular dominance column formation. *J Neurosci,* 20**,** 1470-83.

LI, J., ADAMS, L., SCHWARTZ, S. M. & BUMGARNER, R. E. 2003a. RNA

amplification, fidelity and reproducibility of expression profiling. *Comptes Rendus Biologies,* 326**,** 1021-1030.

LI, J., GUIDO, W. & BICKFORD, M. E. 2003b. Two distinct types of corticothalamic EPSPs and their contribution to short-term synaptic plasticity. *J Neurophysiol,* 90**,** 3429-40.

LICKISS, T., CHEUNG, A. F., HUTCHINSON, C. E., TAYLOR, J. S. & MOLNAR, Z. 2012. Examining the relationship between early axon growth and transcription factor expression in the developing cerebral cortex. *J Anat,* 220**,** 201-11.

LIEBEROTH, A., SPLITTSTOESSER, F., KATAGIHALLIMATH, N., JAKOVCEVSKI, I., LOERS, G., RANSCHT, B., KARAGOGEOS, D., SCHACHNER, M. & KLEENE, R. 2009. Lewisx and α2,3-Sialyl Glycans and their receptors TAG-1, Contactin, and L1 mediate CD24-dependent neurite outgrowth. *The Journal of Neuroscience,* 29**,** 6677-6690.

LIU, H. Y. & MEAKIN, S. O. 2002. ShcB and ShcC activation by the Trk family of receptor tyrosine kinases. *J Biol Chem,* 277**,** 26046-56.

LIU, X. B., HONDA, C. N. & JONES, E. G. 1995. Distribution of four types of synapse on physiologically identified relay neurons in the ventral posterior thalamic nucleus of the cat. *The Journal of Comparative Neurology,* 352**,** 69-91.

LÓPEZ-BENDITO, G., CAUTINAT, A., SÁNCHEZ, J. A., BIELLE, F., FLAMES, N., GARRATT, A. N., TALMAGE, D. A., ROLE, L. W., CHARNAY, P., MARÍN, O. & GAREL, S. 2006. Tangential neuronal migration controls axon guidance: a role for neuregulin-1 in thalamocortical axon navigation. *Cell,* 125**,** 127-142.

LÓPEZ-BENDITO, G. & MOLNAR, Z. 2003. Thalamocortical development: how are we going to get there? *Nat Rev Neurosci,* 4**,** 276-289.

LOZSADI, D. A., GONZALEZ-SORIANO, J. & GUILLERY, R. W. 1996. The course and termination of corticothalamic fibres arising in the visual cortex of the rat. *Eur J Neurosci,* 8**,** 2416-27.

LOZSÁDI, D. A., GONZALEZ-SORIANO, J. & GUILLERY, R. W. 1996. The course and termination of corticothalamic fibres arising in the visual cortex of the rat. *European Journal of Neuroscience,* 8**,** 2416-2427.

LUBKE, J. & FELDMEYER, D. 2007. Excitatory signal flow and connectivity in a cortical column: focus on barrel cortex. *Brain Struct Funct,* 212**,** 3-17.

LUND, R. D. 1965. Uncrossed Visual Pathways of Hooded and Albino Rats. *Science,* 149**,** 1506-7.

LUND, R. D. & MUSTARI, M. J. 1977. Development of the geniculocortical pathway in rats. *J Comp Neurol,* 173**,** 289-306.

LUSKIN, M. B. & SHATZ, C. J. 1985. Studies of the earliest generated cells of the cat's visual cortex: cogeneration of subplate and marginal zones. *J Neurosci,* 5**,** 1062-75.

LYCKMAN, A. W., HORNG, S., LEAMEY, C. A., TROPEA, D., WATAKABE, A., VAN WART, A., MCCURRY, C., YAMAMORI, T. & SUR, M. 2008. Gene expression patterns in visual cortex during the critical period: synaptic stabilization and reversal by visual deprivation. *Proc Natl Acad Sci U S A,* 105**,** 9409-14.

MACCIONE, A., HENNIG, M. H., GANDOLFO, M., MUTHMANN, O., VAN COPPENHAGEN, J., EGLEN, S. J., BERDONDINI, L. & SERNAGOR, E. 2014. Following the ontogeny of retinal waves: pan-retinal recordings of population dynamics in the neonatal mouse. *J Physiol,* 592**,** 1545-63.

MACLEAN, J. N., FENSTERMAKER, V., WATSON, B. O. & YUSTE, R. 2006. A visual thalamocortical slice. *Nat Methods,* 3**,** 129-34.

MADISEN, L., ZWINGMAN, T. A., SUNKIN, S. M., OH, S. W., ZARIWALA, H. A., GU, H., NG, L. L., PALMITER, R. D., HAWRYLYCZ, M. J., JONES, A. R., LEIN, E. S. & ZENG, H. 2010. A robust and high-throughput Cre reporting and characterization system for the whole mouse brain. *Nat Neurosci,* 13**,** 133-40.

MAEDA, N., KAWAKAMI, S., OHMOTO, M., LE COUTRE, J., VINYES-PARES, G., ARIGONI, F., OKADA, S., ABE, K., AIZAWA, H. & MISAKA, T. 2013. Differential expression analysis throughout the weaning period in the mouse cerebral cortex. *Biochemical and Biophysical Research Communications,* 431**,** 437-443.

MAJDAN, M. & SHATZ, C. J. 2006. Effects of visual experience on activity-dependent gene regulation in cortex. *Nat Neurosci,* 9**,** 650-659.

MALATESTA, P., HACK, M. A., HARTFUSS, E., KETTENMANN, H., KLINKERT, W., KIRCHHOFF, F. & GOTZ, M. 2003. Neuronal or glial progeny: regional differences in radial glia fate. *Neuron,* 37**,** 751-64.

MALATESTA, P., HARTFUSS, E. & GOTZ, M. 2000. Isolation of radial glial cells by fluorescent-activated cell sorting reveals a neuronal lineage. *Development,* 127**,** 5253-63.

MALLAMACI, A., IANNONE, R., BRIATA, P., PINTONELLO, L., MERCURIO, S., BONCINELLI, E. & CORTE, G. 1998. EMX2 protein in the developing mouse brain and olfactory area. *Mech Dev,* 77**,** 165-72.

MALLAMACI, A., MUZIO, L., CHAN, C. H., PARNAVELAS, J. & BONCINELLI, E. 2000. Area identity shifts in the early cerebral cortex of Emx2-/- mutant mice. *Nat Neurosci,* 3**,** 679-86.

MALLAMACI, A. & STOYKOVA, A. 2006. Gene networks controlling early cerebral cortex arealization. *European Journal of Neuroscience,* 23**,** 847-856.

MARIN-PADILLA, M. 1971. Early prenatal ontogenesis of the cerebral cortex (neocortex) of the cat (Felis domestica). A Golgi study. I. The primordial neocortical organization. *Z Anat Entwicklungsgesch,* 134**,** 117-45.

MARKRAM, H., TOLEDO-RODRIGUEZ, M., WANG, Y., GUPTA, A.,

SILBERBERG, G. & WU, C. 2004. Interneurons of the neocortical inhibitory system. *Nat Rev Neurosci,* 5**,** 793-807.

MARSHEL, J. H., GARRETT, M. E., NAUHAUS, I. & CALLAWAY, E. M. 2011. Functional specialization of seven mouse visual cortical areas. *Neuron,* 72**,** 1040-54.

MATHISEN, P. M., JOHNSON, J. M., KAWCZAK, J. A. & TUOHY, V. K. 1999. Visinin-like protein (VILIP) is a neuron-specific calcium-dependent double-stranded RNA-binding protein. *J Biol Chem,* 274**,** 31571-6.

MATTHEWS, R. T., KELLY, G. M., ZERILLO, C. A., GRAY, G., TIEMEYER, M. & HOCKFIELD, S. 2002. Aggrecan glycoforms contribute to the molecular heterogeneity of perineuronal nets. *The Journal of Neuroscience,* 22**,** 7536-7547.

MCALLISTER, J. P., II & DAS, G. D. 1977. Neurogenesis in the epithalamus, dorsal thalamus and ventral thalamus of the rat: an autoradiographic and cytological study. *J Comp Neurol,* 172**,** 647-86.

MCCONNELL, S., GHOSH, A. & SHATZ, C. 1994. Subplate pioneers and the formation of descending connections from cerebral cortex. *The Journal of Neuroscience,* 14**,** 1892-1907.

MCCONNELL, S. K., GHOSH, A. & SHATZ, C. J. 1989. Subplate neurons pioneer the first axon pathway from the cerebral cortex. *Science,* 245**,** 978-82.

MCCOY, P. A., HUANG, H.-S. & PHILPOT, B. D. 2009. Advances in understanding visual cortex plasticity. *Current Opinion in Neurobiology,* 19**,** 298-304.

MCRAE, P. A., ROCCO, M. M., KELLY, G., BRUMBERG, J. C. & MATTHEWS, R. T. 2007. Sensory deprivation alters aggrecan and perineuronal net expression in the mouse barrel cortex. *The Journal of Neuroscience,* 27**,** 5405-5413.

MEISTER, M., WONG, R. O., BAYLOR, D. A. & SHATZ, C. J. 1991. Synchronous bursts of action potentials in ganglion cells of the developing mammalian retina. *Science,* 252**,** 939-43.

MÉTIN, C., DELEGLISE, D., SERAFINI, T., KENNEDY, T. E. & TESSIER-LAVIGNE, M. 1997. A role for netrin-1 in the guidance of cortical efferents. *Development,* 124**,** 5063-5074.

METIN, C. & FROST, D. O. 1989. Visual responses of neurons in somatosensory cortex of hamsters with experimentally induced retinal projections to somatosensory thalamus. *Proc Natl Acad Sci U S A,* 86**,** 357-61.

METIN, C., GODEMENT, P. & IMBERT, M. 1988. The primary visual cortex in the mouse: receptive field properties and functional organization. *Exp Brain Res,* 69**,** 594-612.

MIAO, H. & WANG, B. 2012. EphA receptor signaling—Complexity and emerging themes. *Seminars in Cell & Developmental Biology,* 23**,** 16-25.

MILLER, B., CHOU, L. & FINLAY, B. L. 1993. The early development of thalamocortical and corticothalamic projections. *J Comp Neurol,* 335**,** 16-41.

MISSON, J. P., AUSTIN, C. P., TAKAHASHI, T., CEPKO, C. L. & CAVINESS, V. S., JR. 1991. The alignment of migrating neural cells in relation to the murine neopallial radial glial fiber system. *Cereb Cortex,* 1**,** 221-9.

MITROFANIS, J. & BAKER, G. E. 1993. Development of the thalamic reticular and perireticular nuclei in rats and their relationship to the course of growing corticofugal and corticopetal axons. *The Journal of Comparative Neurology,* 338**,** 575-587.

MITROFANIS, J. & GUILLERY, R. W. 1993. New views of the thalamic reticular nucleus in the adult and the developing brain. *Trends in Neurosciences,* 16**,** 240-245.

MIYATA, T., KAWAGUCHI, A., OKANO, H. & OGAWA, M. 2001. Asymmetric inheritance of radial glial fibers by cortical neurons. *Neuron,* 31**,** 727-41.

MOLNÁR, Z., ADAMS, R. & BLAKEMORE, C. 1998a. Mechanisms underlying the early establishment of thalamocortical connections in the rat. *The Journal of Neuroscience,* 18**,** 5723-5745.

MOLNÁR, Z., ADAMS, R., GOFFINET, A. & BLAKEMORE, C. 1998b. The Role of the first postmitotic cortical cells in the development of thalamocortical innervation in the reeler mouse. *The Journal of Neuroscience,* 18**,** 5746-5765.

MOLNÁR, Z. & BLAKEMORE, C. 1995. How do thalamic axons find their way to the cortex? *Trends in Neurosciences,* 18**,** 389-397.

MOLNÁR, Z. & CHEUNG, A. F. P. 2006. Towards the classification of subpopulations of layer V pyramidal projection neurons. *Neuroscience Research,* 55**,** 105-115.

MOLNÁR, Z. & CORDERY, P. 1999. Connections between cells of the internal capsule, thalamus, and cerebral cortex in embryonic rat. *The Journal of Comparative Neurology,* 413**,** 1-25.

MOLNÁR, Z., HIGASHI, S. & LÓPEZ-BENDITO, G. 2003a. Choreography of Early Thalamocortical Development. *Cerebral Cortex,* 13**,** 661-669.

MOLNÁR, Z., KUROTANI, T., HIGASHI, S., YAMAMOTO, N. & TOYAMA, K. 2003b. Development of functional thalamocortical synapses studied with current source-density analysis in whole forebrain slices in the rat. *Brain Research Bulletin,* 60**,** 355-371.

MOLNÁR, Z., LOPEZ-BENDITO, G., SMALL, J., PARTRIDGE, L. D., BLAKEMORE, C. & WILSON, M. C. 2002. Normal development of embryonic thalamocortical connectivity in the absence of evoked synaptic activity. *J Neurosci,* 22**,** 10313-23.

MOLYNEAUX, B. J., ARLOTTA, P., MENEZES, J. R. & MACKLIS, J. D. 2007. Neuronal subtype specification in the cerebral cortex. *Nat Rev Neurosci,* 8**,** 427-

37.

MOONEY, R., PENN, A. A., GALLEGO, R. & SHATZ, C. J. 1996. Thalamic relay of spontaneous retinal activity prior to vision. *Neuron,* 17**,** 863-74.

MOUNTCASTLE, V. B. 1957. Modality and topographic properties of single neurons of cat's somatic sensory cortex. *J Neurophysiol,* 20**,** 408-34.

MOUNTCASTLE, V. B. 1997. The columnar organization of the neocortex. *Brain,* 120 (Pt 4)**,** 701-22.

MURPHY, G. 2011. Tissue inhibitors of metalloproteinases. *Genome Biol,* 12**,** 233.

MURPHY, G., KNAUPER, V., LEE, M. H., AMOUR, A., WORLEY, J. R., HUTTON, M., ATKINSON, S., RAPTI, M. & WILLIAMSON, R. 2003. Role of TIMPs (tissue inhibitors of metalloproteinases) in pericellular proteolysis: the specificity is in the detail. *Biochem Soc Symp***,** 65-80.

NAEGELE, J. R. & BARNSTABLE, C. J. 1989. Molecular determinants of GABAergic local-circuit neurons in the visual cortex. *Trends in Neurosciences,* 12**,** 28-34.

NAKAGAWA, Y. & O'LEARY, D. D. 2001. Combinatorial expression patterns of LIM-homeodomain and other regulatory genes parcellate developing thalamus. *J Neurosci,* 21**,** 2711-25.

NAKAGAWA, Y. & O'LEARY, D. D. 2003. Dynamic patterned expression of orphan nuclear receptor genes RORalpha and RORbeta in developing mouse forebrain. *Dev Neurosci,* 25**,** 234-44.

NAKAMURA, K., HIOKI, H., FUJIYAMA, F. & KANEKO, T. 2005. Postnatal changes of vesicular glutamate transporter (VGluT)1 and VGluT2 immunoreactivities and their colocalization in the mouse forebrain. *J Comp Neurol,* 492**,** 263-88.

NAKAMURA, T., MURAOKA, S., SANOKAWA, R. & MORI, N. 1998. N-Shc and Sck, two neuronally expressed Shc adapter homologs: their differential regional expression in the brain and roles in neurotrophin and Src signalling. *Journal of Biological Chemistry,* 273**,** 6960-6967.

NAQVI, S. & ARTHUR, J. S. C. 2013. The Activation of CREB Downstream of Mitogen−Activated Protein Kinase (MAPK) Signaling. *In:* ARTHUR, J. S. C. (ed.) *MSKs.* Lands Bioscience.

NEGYESSY, L., GAL, V., FARKAS, T. & TOLDI, J. 2000. Cross-modal plasticity of the corticothalamic circuits in rats enucleated on the first postnatal day. *Eur J Neurosci,* 12**,** 1654-68.

NELSON, S. B. & LEVAY, S. 1985. Topographic organization of the optic radiation of the cat. *J Comp Neurol,* 240**,** 322-30.

NICOL, X., VOYATZIS, S., MUZERELLE, A., NARBOUX-NEME, N., SUDHOF, T. C., MILES, R. & GASPAR, P. 2007. cAMP oscillations and retinal activity are permissive for ephrin signaling during the establishment of the retinotopic map.

Nat Neurosci, 10**,** 340-7.

NIELL, C. M. & STRYKER, M. P. 2008. Highly selective receptive fields in mouse visual cortex. *J Neurosci,* 28**,** 7520-36.

NOCTOR, S. C., FLINT, A. C., WEISSMAN, T. A., DAMMERMAN, R. S. & KRIEGSTEIN, A. R. 2001. Neurons derived from radial glial cells establish radial units in neocortex. *Nature,* 409**,** 714-20.

NOCTOR, S. C., FLINT, A. C., WEISSMAN, T. A., WONG, W. S., CLINTON, B. K. & KRIEGSTEIN, A. R. 2002. Dividing precursor cells of the embryonic cortical ventricular zone have morphological and molecular characteristics of radial glia. *J Neurosci,* 22**,** 3161-73.

NOCTOR, S. C., MARTINEZ-CERDENO, V., IVIC, L. & KRIEGSTEIN, A. R. 2004. Cortical neurons arise in symmetric and asymmetric division zones and migrate through specific phases. *Nat Neurosci,* 7**,** 136-144.

NYS, J., AERTS, J., YTEBROUCK, E., VREYSEN, S., LAEREMANS, A. & ARCKENS, L. 2014. The cross-modal aspect of mouse visual cortex plasticity induced by monocular enucleation is age dependent. *Journal of Comparative Neurology,* 522**,** 950-970.

O'LEARY, D. D. M. 1989. Do cortical areas emerge from a protocortex? *Trends in Neurosciences,* 12**,** 400-406.

O'LEARY, D. D. M. & MCLAUGHLIN, T. 2005. Mechanisms of retinotopic map development: Ephs, ephrins, and spontaneous correlated retinal activity. *In:* J. VAN PELT, M. K. C. N. L. A. V. O. G. J. A. R. & ROELFSEMA, P. R. (eds.) *Progress in Brain Research.* Elsevier.

O'LEARY, D. D. M. & SAHARA, S. 2008. Genetic regulation of arealization of the neocortex. *Current Opinion in Neurobiology,* 18**,** 90-100.

OHNO, S., KURAMOTO, E., FURUTA, T., HIOKI, H., TANAKA, Y. R., FUJIYAMA, F., SONOMURA, T., UEMURA, M., SUGIYAMA, K. & KANEKO, T. 2012. A morphological analysis of thalamocortical axon fibers of rat posterior thalamic nuclei: a single neuron tracing study with viral vectors. *Cerebral Cortex,* 22**,** 2840-2857.

OLSEN, S. R., BORTONE, D. S., ADESNIK, H. & SCANZIANI, M. 2012. Gain control by layer six in cortical circuits of vision. *Nature,* 483**,** 47-52.

OSWALD, M. J., TANTIRIGAMA, M. L., SONNTAG, I., HUGHES, S. M. & EMPSON, R. M. 2013. Diversity of layer 5 projection neurons in the mouse motor cortex. *Front Cell Neurosci,* 7**,** 174.

PALLAS, S. L., ROE, A. W. & SUR, M. 1990. Visual projections induced into the auditory pathway of ferrets. I. Novel inputs to primary auditory cortex (AI) from the LP/pulvinar complex and the topography of the MGN-AI projection. *J Comp Neurol,* 298**,** 50-68.

PARNAVELAS, J. G. 2000. The origin and migration of cortical neurones: new vistas. *Trends in Neurosciences,* 23**,** 126-131.

PATTERSON, K. I., BRUMMER, T., O'BRIEN, P. M. & DALY, R. J. 2009. Dual-specificity phosphatases: critical regulators with diverse cellular targets. *Biochem J,* 418**,** 475-89.

PENN, A. A., RIQUELME, P. A., FELLER, M. B. & SHATZ, C. J. 1998. Competition in retinogeniculate patterning driven by spontaneous activity. *Science,* 279**,** 2108-12.

PERSON, A. M. & WELLS, G. B. 2011. Characterizing low affinity epibatidine binding to alpha4beta2 nicotinic acetylcholine receptors with ligand depletion and nonspecific binding. *BMC Biophys,* 4**,** 19.

PFEIFFENBERGER, C., CUTFORTH, T., WOODS, G., YAMADA, J., RENTERIA, R. C., COPENHAGEN, D. R., FLANAGAN, J. G. & FELDHEIM, D. A. 2005. Ephrin-As and neural activity are required for eye-specific patterning during retinogeniculate mapping. *Nat Neurosci,* 8**,** 1022-1027.

PFEIFFENBERGER, C., YAMADA, J. & FELDHEIM, D. A. 2006. Ephrin-As and patterned retinal activity act together in the development of topographic maps in the primary visual system. *J Neurosci,* 26**,** 12873-84.

PIÑON, M. C., JETHWA, A., JACOBS, E., CAMPAGNONI, A. & MOLNÁR, Z. 2009. Dynamic integration of subplate neurons into the cortical barrel field circuitry during postnatal development in the Golli-tau-eGFP (GTE) mouse. *The Journal of Physiology,* 587**,** 1903-1915.

POUCHELON, G., FRANGEUL, L. & JABAUDON, D. 2014a. Circuit-specific molecular identity of thalamocortical neurons. Poster- Cortical Development Meeting, Chania, Crete.

POUCHELON, G., GAMBINO, F., BELLONE, C., TELLEY, L., VITALI, I., LUSCHER, C., HOLTMAAT, A. & JABAUDON, D. 2014b. Modality-specific thalamocortical inputs instruct the identity of postsynaptic L4 neurons. *Nature*.

PRICE, D. J., ASLAM, S., TASKER, L. & GILLIES, K. 1997. Fates of the earliest generated cells in the developing murine neocortex. *The Journal of Comparative Neurology,* 377**,** 414-422.

PRICE, D. J., CLEGG, J. M., OLIVER DUOCASTELLA, X., WILLSHAW, D. J. & PRATT, T. 2012. The importance of combinatorial gene expression in early mammalian thalamic patterning and thalamocortical axonal guidance. *Frontiers in Neuroscience,* 6.

PRUSKY, G. T., WEST, P. W. R. & DOUGLAS, R. M. 2000. Behavioral assessment of visual acuity in mice and rats. *Vision Research,* 40**,** 2201-2209.

RAKIC, P. 1976. Prenatal genesis of connections subserving ocular dominance in the rhesus monkey. *Nature,* 261**,** 467-471.

RAKIC, P. 1977. Prenatal development of the visual system in rhesus monkey. *Philos Trans R Soc Lond B Biol Sci,* 278**,** 245-60.

RAKIC, P. 1988. Specification of cerebral cortical areas. *Science,* 241**,** 170-6.

RAKIC, P. 1990. Principles of neural cell migration. *Experientia,* 46**,** 882-891.

RAKIC, P. 2008. Confusing cortical columns. *Proc Natl Acad Sci U S A,* 105**,** 12099-100.

RALSTON III, H. J. 1969. The synaptic organization of lemniscal projections to the ventrobasal thalamus of the cat. *Brain Research,* 14**,** 99-115.

RASH, B. G. & GROVE, E. A. 2006. Area and layer patterning in the developing cerebral cortex. *Current Opinion in Neurobiology,* 16**,** 25-34.

RASHID, T., UPTON, A. L., BLENTIC, A., CIOSSEK, T., KNOLL, B., THOMPSON, I. D. & DRESCHER, U. 2005. Opposing gradients of ephrin-As and EphA7 in the superior colliculus are essential for topographic mapping in the mammalian visual system. *Neuron,* 47**,** 57-69.

REBSAM, A., BHANSALI, P. & MASON, C. A. 2012. Eye-specific projections of retinogeniculate axons are altered in albino mice. *J Neurosci,* 32**,** 4821-6.

REBSAM, A., PETROS, T. J. & MASON, C. A. 2009. Switching retinogeniculate axon laterality leads to normal targeting but abnormal eye-specific segregation that is activity dependent. *J Neurosci,* 29**,** 14855-63.

REEP, R. L., CHANDLER, H. C., KING, V. & CORWIN, J. V. 1994. Rat posterior parietal cortex: topography of corticocortical and thalamic connections. *Exp Brain Res,* 100**,** 67-84.

REEP, R. L. & CORWIN, J. V. 1999. Topographic organization of the striatal and thalamic connections of rat medial agranular cortex. *Brain Res,* 841**,** 43-52.

REESE, B. E. 1986. The topography of expanded uncrossed retinal projections following neonatal enucleation of one eye: differing effects in dorsal lateral geniculate nucleus and superior colliculus. *J Comp Neurol,* 250**,** 8-32.

REESE, B. E. 1988. 'Hidden lamination' in the dorsal lateral geniculate nucleus: the functional organization of this thalamic region in the rat. Brain Research Reviews, 13, 119-137.

REICHOVA, I. & SHERMAN, S. M. 2004. Somatosensory Corticothalamic Projections: Distinguishing Drivers From Modulators. *Journal of Neurophysiology,* 92**,** 2185-2197.

RICHARDS, L. J., KOESTER, S. E., TUTTLE, R. & O'LEARY, D. D. M. 1997. Directed growth of early cortical axons is influenced by a chemoattractant released from an intermediate target. *The Journal of Neuroscience,* 17**,** 2445-2458.

RIEU, I. & POWERS, S. J. 2009. Real-time quantitative RT-PCR: design, calculations,

and statistics. *Plant Cell,* 21**,** 1031-3.

ROE, A. W., GARRAGHTY, P. E., ESGUERRA, M. & SUR, M. 1993. Experimentally induced visual projections to the auditory thalamus in ferrets: Evidence for a W cell pathway. *The Journal of Comparative Neurology,* 334**,** 263-280.

ROE, A. W., PALLAS, S. L., HAHM, J. O. & SUR, M. 1990. A map of visual space induced in primary auditory cortex. *Science,* 250**,** 818-20.

ROE, A. W., PALLAS, S. L., KWON, Y. H. & SUR, M. 1992. Visual projections routed to the auditory pathway in ferrets: receptive fields of visual neurons in primary auditory cortex. *J Neurosci,* 12**,** 3651-64.

ROGERS, J. H. 1992. Immunohistochemical markers in rat cortex: co-localization of calretinin and calbindin-D28k with neuropeptides and GABA. *Brain Res,* 587**,** 147-57.

RON, D. & KAZANIETZ, M. G. 1999. New insights into the regulation of protein kinase C and novel phorbol ester receptors. *FASEB J,* 13**,** 1658-76.

ROSSI, F. M., PIZZORUSSO, T., PORCIATTI, V., MARUBIO, L. M., MAFFEI, L. & CHANGEUX, J. P. 2001. Requirement of the nicotinic acetylcholine receptor beta 2 subunit for the anatomical and functional development of the visual system. *Proc Natl Acad Sci U S A,* 98**,** 6453-8.

ROUILLER, E. M., TANNÉ, J., MORET, V., KERMADI, I., BOUSSAOUD, D. & WELKER, E. 1998. Dual morphology and topography of the corticothalamic terminals originating from the primary, supplementary motor, and dorsal premotor cortical areas in Macaque monkeys. *The Journal of Comparative Neurology,* 396**,** 169-185.

ROUILLER, E. M. & WELKER, E. 2000. A comparative analysis of the morphology of corticothalamic projections in mammals. *Brain Res Bull,* 53**,** 727-41.

RUBENSTEIN, J. L. & RAKIC, P. 1999. Genetic control of cortical development. *Cereb Cortex,* 9**,** 521-3.

SAH, P. 1996. Ca2+-activated K+ currents in neurones: types, physiological roles and modulation. *Trends in Neurosciences,* 19**,** 150-154.

SAHARA, S., YANAGAWA, Y., O'LEARY, D. D. & STEVENS, C. F. 2012. The fraction of cortical GABAergic neurons is constant from near the start of cortical neurogenesis to adulthood. *J Neurosci,* 32**,** 4755-61.

SASAKI, A., TAKETOMI, T., KATO, R., SAEKI, K., NONAMI, A., SASAKI, M., KURIYAMA, M., SAITO, N., SHIBUYA, M. & YOSHIMURA, A. 2003. Mammalian Sprouty4 suppresses Ras-independent ERK activation by binding to Raf1. *Nat Cell Biol,* 5**,** 427-32.

SASAKI, A., TAKETOMI, T., WAKIOKA, T., KATO, R. & YOSHIMURA, A. 2001. Identification of a dominant negative mutant of sprouty that potentiates Fibroblast Growth Factor- but not Epidermal Growth Factor-induced ERK

Activation. *Journal of Biological Chemistry,* 276**,** 36804-36808.

SCHNEIDER, C. A., RASBAND, W. S. & ELICEIRI, K. W. 2012. NIH Image to ImageJ: 25 years of image analysis. *Nat Meth,* 9**,** 671-675.

SCHOUPS, A. A., ELLIOTT, R. C., FRIEDMAN, W. J. & BLACK, I. B. 1995. NGF and BDNF are differentially modulated by visual experience in the developing geniculocortical pathway. *Brain Res Dev Brain Res,* 86**,** 326-34.

SCHUMACHER, M. A., RIVARD, A. F., BACHINGER, H. P. & ADELMAN, J. P. 2001. Structure of the gating domain of a Ca2+-activated K+ channel complexed with Ca2+/calmodulin. *Nature,* 410**,** 1120-1124.

SEABROOK, T. A., EL-DANAF, R. N., KRAHE, T. E., FOX, M. A. & GUIDO, W. 2013. Retinal input regulates the timing of corticogeniculate innervation. *J Neurosci,* 33**,** 10085-97.

SHARMA, J., ANGELUCCI, A. & SUR, M. 2000. Induction of visual orientation modules in auditory cortex. *Nature,* 404**,** 841-847.

SHATZ, C. J. & LUSKIN, M. B. 1986. The relationship between the geniculocortical afferents and their cortical target cells during development of the cat's primary visual cortex. *J Neurosci,* 6**,** 3655-68.

SHATZ, C. J. & RAKIC, P. 1981. The genesis of efferent connections from the visual cortex of the fetal rhesus monkey. *J Comp Neurol,* 196**,** 287-307.

SHATZ, C. J. & STRYKER, M. P. 1988. Prenatal tetrodotoxin infusion blocks segregation of retinogeniculate afferents. *Science,* 242**,** 87-9.

SHERMAN, S. M. & GUILLERY, R. W. 1996. Functional organization of thalamocortical relays. *J Neurophysiol,* 76**,** 1367-95.

SHERMAN, S. M. & GUILLERY, R. W. 1998. On the actions that one nerve cell can have on another: Distinguishing "drivers" from "modulators". *Proceedings of the National Academy of Sciences,* 95**,** 7121-7126.

SHERMAN, S. M. & GUILLERY, R. W. 2002. The role of the thalamus in the flow of information to the cortex. *Philos Trans R Soc Lond B Biol Sci,* 357**,** 1695-708.

SHERMAN, S. M. & GUILLERY, R. W. 2006. *Exploring the thalamus and its role in cortical function,* Cambridge, Massachusetts; London, England, The MIT Press.

SHERMAN, S. M. & GUILLERY, R. W. 2013. *Functional connections of cortical areas; a new view from the thalamus,* Cambridge, Massachusetts.

London, England., MIT Press.

SHIEH, P. B., HU, S. C., BOBB, K., TIMMUSK, T. & GHOSH, A. 1998. Identification of a signaling pathway involved in calcium regulation of BDNF expression. *Neuron,* 20**,** 727-40.

SINGH, R., SU, J., BROOKS, J. M., TERAUCHI, A., UMEMORI, H. & FOX, M.

A. 2012. Fibroblast growth factor 22 (FGF22) contributes to the development of retinal nerve terminals in the dorsal lateral geniculate nucleus. *Frontiers in Molecular Neuroscience,* 4.

SMITH, R. L. 1973. The ascending fiber projections from the principal sensory trigeminal nucleus in the rat. *The Journal of Comparative Neurology,* 148**,** 423-445.

SMYTH, G. K. 2004. Linear models and empirical bayes methods for assessing differential expression in microarray experiments. *Stat Appl Genet Mol Biol,* 3**,** Article3.

STAFFORD, B. K., SHER, A., LITKE, A. M. & FELDHEIM, D. A. 2009. Spatial-temporal patterns of retinal waves underlying activity-dependent refinement of retinofugal projections. *Neuron,* 64**,** 200-212.

STANTON, H., MELROSE, J., LITTLE, C. B. & FOSANG, A. J. 2011. Proteoglycan degradation by the ADAMTS family of proteinases. *Biochim Biophys Acta,* 1812**,** 1616-29.

STRATFORD, K. J., TARCZY-HORNOCH, K., MARTIN, K. A., BANNISTER, N. J. & JACK, J. J. 1996. Excitatory synaptic inputs to spiny stellate cells in cat visual cortex. *Nature,* 382**,** 258-61.

SUGIYAMA, S., DI NARDO, A. A., AIZAWA, S., MATSUO, I., VOLOVITCH, M., PROCHIANTZ, A. & HENSCH, T. K. 2008. Experience-dependent transfer of Otx2 homeoprotein into the visual cortex activates postnatal plasticity. *Cell,* 134**,** 508-20.

SUKEKAWA, K. 1988. Reciprocal connections between medial prefrontal cortex and lateral posterior nucleus in rats. *Brain Behav Evol,* 32**,** 246-51.

SUN, C., SPEER, C. M., WANG, G. Y., CHAPMAN, B. & CHALUPA, L. M. 2008. Epibatidine application in vitro blocks retinal waves without silencing all retinal ganglion cell action potentials in developing retina of the mouse and ferret. *Journal of neurophysiology,* 100**,** 3253-3263.

SUR, M., GARRAGHTY, P. E. & ROE, A. W. 1988. Experimentally induced visual projections into auditory thalamus and cortex. *Science,* 242**,** 1437-41.

SUR, M. & LEAMEY, C. A. 2001. Development and plasticity of cortical areas and networks. *Nature Reviews Neuroscience,* 2**,** 251-262.

SUR, M. & RUBENSTEIN, J. L. 2005. Patterning and plasticity of the cerebral cortex. *Science,* 310**,** 805-10.

SUZUKI-HIRANO, A., OGAWA, M., KATAOKA, A., YOSHIDA, A. C., ITOH, D., UENO, M., BLACKSHAW, S. & SHIMOGORI, T. 2011. Dynamic spatiotemporal gene expression in embryonic mouse thalamus. *The Journal of Comparative Neurology,* 519**,** 528-543.

SYED, M. M., LEE, S., HE, S. & ZHOU, Z. J. 2004a. *Spontaneous waves in the*

ventricular zone of developing mammalian retina.

SYED, M. M., LEE, S., ZHENG, J. & ZHOU, Z. J. 2004b. Stage-dependent dynamics and modulation of spontaneous waves in the developing rabbit retina. *The Journal of Physiology,* 560**,** 533-549.

TAGAWA, Y., KANOLD, P. O., MAJDAN, M. & SHATZ, C. J. 2005. Multiple periods of functional ocular dominance plasticity in mouse visual cortex. *Nat Neurosci,* 8**,** 380-8.

TAKEUCHI, Y., YAMASAKI, M., NAGUMO, Y., IMOTO, K., WATANABE, M. & MIYATA, M. 2012. Rewiring of Afferent Fibers in the Somatosensory Thalamus of Mice Caused by Peripheral Sensory Nerve Transection. *The Journal of Neuroscience,* 32**,** 6917-6930.

TAN, X. & SHI, S.-H. 2013. Neocortical neurogenesis and neuronal migration. *Wiley Interdisciplinary Reviews: Developmental Biology,* 2**,** 443-459.

TAO, X., FINKBEINER, S., ARNOLD, D. B., SHAYWITZ, A. J. & GREENBERG, M. E. 1998. Ca2+ influx regulates BDNF transcription by a CREB family transcription factor-dependent mechanism. *Neuron,* 20**,** 709-26.

TAO, X., WEST, A. E., CHEN, W. G., CORFAS, G. & GREENBERG, M. E. 2002. A calcium-responsive transcription factor, CaRF, that regulates neuronal activity-dependent expression of BDNF. *Neuron,* 33**,** 383-95.

TAVAZOIE, S. F. & REID, R. C. 2000. Diverse receptive fields in the lateral geniculate nucleus during thalamocortical development. *Nat Neurosci,* 3**,** 608-16.

THEYEL, B. B., LLANO, D. A. & SHERMAN, S. M. 2010. The corticothalamocortical circuit drives higher-order cortex in the mouse. *Nat Neurosci,* 13**,** 84-88.

THOMAS, G. M. & HUGANIR, R. L. 2004. MAPK cascade signalling and synaptic plasticity. *Nat Rev Neurosci,* 5**,** 173-183.

THOMSON, A. M. & BANNISTER, A. P. 2003. Interlaminar Connections in the Neocortex. *Cerebral Cortex,* 13**,** 5-14.

THOMSON, A. M. & LAMY, C. 2007. Functional maps of neocortical local circuitry. *Front Neurosci,* 1**,** 19-42.

TIAN, N. M., PRATT, T. & PRICE, D. J. 2008. Foxg1 regulates retinal axon pathfinding by repressing an ipsilateral program in nasal retina and by causing optic chiasm cells to exert a net axonal growth-promoting activity. *Development,* 135**,** 4081-9.

TOHMI, M., MEGURO, R., TSUKANO, H., HISHIDA, R. & SHIBUKI, K. 2014. The Extrageniculate Visual Pathway Generates Distinct Response Properties in the Higher Visual Areas of Mice. *Current Biology,* 24**,** 587-597.

TOHMI, M., TAKAHASHI, K., KUBOTA, Y., HISHIDA, R. & SHIBUKI, K. 2009. Transcranial flavoprotein fluorescence imaging of mouse cortical activity and plasticity. *J Neurochem,* 109 Suppl 1**,** 3-9.

TOLDI, J., FEHER, O. & WOLFF, J. R. 1996. Neuronal plasticity induced by neonatal monocular (and binocular) enucleation. *Prog Neurobiol,* 48**,** 191-218.

TOLDI, J., ROJIK, I. & FEHER, O. 1993. Modification in primary visual cortical activity of rat induced by neonatal monocular enucleation, an electrophysiological and autoradiographic study. *Acta Physiol Hung,* 81**,** 175-81.

TOLNER, E. A., SHEIKH, A., YUKIN, A. Y., KAILA, K. & KANOLD, P. O. 2012. Subplate neurons promote spindle bursts and thalamocortical patterning in the neonatal rat somatosensory cortex. *The Journal of Neuroscience,* 32**,** 692-702.

TONGIORGI, E., RIGHI, M. & CATTANEO, A. 1997. Activity-dependent dendritic targeting of BDNF and TrkB mRNAs in hippocampal neurons. *The Journal of Neuroscience,* 17**,** 9492-9505.

TOPHAM, M. K. 2006. Signaling roles of diacylglycerol kinases. *J Cell Biochem,* 97**,** 474-84.

TOPHAM, M. K. & PRESCOTT, S. M. 2002. Diacylglycerol kinases: regulation and signaling roles. *Thromb Haemost,* 88**,** 912-8.

TORII, M. & LEVITT, P. 2005. Dissociation of corticothalamic and thalamocortical axon targeting by an EphA7-mediated mechanism. *Neuron,* 48**,** 563-75.

TORTORELLA, M. D. & MALFAIT, A. M. 2008. Will the real aggrecanase(s) step up: evaluating the criteria that define aggrecanase activity in osteoarthritis. *Curr Pharm Biotechnol,* 9**,** 16-23.

TREVELYAN, A. J., UPTON, A. L., CORDERY, P. M. & THOMPSON, I. D. 2007. An experimentally induced duplication of retinotopic mapping within the hamster primary visual cortex. *European Journal of Neuroscience,* 26**,** 3277-3290.

TROPEA, D., VAN WART, A. & SUR, M. 2009. Molecular mechanisms of experience-dependent plasticity in visual cortex. *Philosophical Transactions of the Royal Society B: Biological Sciences,* 364**,** 341-355.

UDIN, S. B. & FAWCETT, J. W. 1988. Formation of topographic maps. *Annu Rev Neurosci,* 11**,** 289-327.

UESAKA, N., HAYANO, Y., YAMADA, A. & YAMAMOTO, N. 2007. Interplay between laminar specificity and activity-dependent mechanisms of thalamocortical axon branching. *J Neurosci,* 27**,** 5215-23.

UPTON, A. L., RAVARY, A., SALICHON, N., MOESSNER, R., LESCH, K. P., HEN, R., SEIF, I. & GASPAR, P. 2002. Lack of 5-HT(1B) receptor and of serotonin transporter have different effects on the segregation of retinal axons in the lateral geniculate nucleus compared to the superior colliculus. *Neuroscience,* 111**,** 597-610.

UPTON, A. L., SALICHON, N., LEBRAND, C., RAVARY, A., BLAKELY, R., SEIF, I. & GASPAR, P. 1999. Excess of serotonin (5-HT) alters the segregation of ispilateral and contralateral retinal projections in monoamine oxidase A

knock-out mice: possible role of 5-HT uptake in retinal ganglion cells during development. *J Neurosci,* 19**,** 7007-24.

VALVERDE, F. 1968. Structural changes in the area striata of the mouse after enucleation. *Exp Brain Res,* 5**,** 274-92.

VAN BLITTERSWIJK, W. J. & HOUSSA, B. 2000. Properties and functions of diacylglycerol kinases. *Cell Signal,* 12**,** 595-605.

VAN BRUSSEL, L., GERITS, A. & ARCKENS, L. 2011. Evidence for cross-modal plasticity in adult mouse visual cortex following monocular enucleation. *Cerebral Cortex,* 21**,** 2133-2146.

VAN DER LOOS, H. 1976. Barreloids in mouse somatosensory thalamus. *Neurosci Lett,* 2**,** 1-6.

VAN DER LOOS, H. & WOOLSEY, T. A. 1973. Somatosensory cortex: structural alterations following early injury to sense organs. *Science,* 179**,** 395-8.

VAN GELDER, R. N., VON ZASTROW, M. E., YOOL, A., DEMENT, W. C., BARCHAS, J. D. & EBERWINE, J. H. 1990. Amplified RNA synthesized from limited quantities of heterogeneous cDNA. *Proc Natl Acad Sci U S A,* 87**,** 1663-7.

VAN HORN, S. C., ERIŞIR, A. & SHERMAN, S. M. 2000. Relative distribution of synapses in the A-laminae of the lateral geniculate nucleus of the cat. *The Journal of Comparative Neurology,* 416**,** 509-520.

VANDESOMPELE, J., DE PRETER, K., PATTYN, F., POPPE, B., VAN ROY, N., DE PAEPE, A. & SPELEMAN, F. 2002. Accurate normalization of real-time quantitative RT-PCR data by geometric averaging of multiple internal control genes. *Genome Biol,* 3**,** RESEARCH0034.

VIAENE, A. N., PETROF, I. & SHERMAN, S. M. 2011a. Properties of the thalamic projection from the posterior medial nucleus to primary and secondary somatosensory cortices in the mouse. *Proc Natl Acad Sci U S A,* 108**,** 18156-61.

VIAENE, A. N., PETROF, I. & SHERMAN, S. M. 2011b. Synaptic properties of thalamic input to layers 2/3 and 4 of primary somatosensory and auditory cortices. *J Neurophysiol,* 105**,** 279-92.

VIAENE, A. N., PETROF, I. & SHERMAN, S. M. 2011c. Synaptic properties of thalamic input to the subgranular layers of primary somatosensory and auditory cortices in the mouse. *J Neurosci,* 31**,** 12738-47.

VON ECONOMO, C. & KOSKINAS, G. N. 1925. *Die Cytoarchitektonik der Hirnrinde des erwachsenen Menschen. Textband und Atlas.*, Springer.

VON MELCHNER, L., PALLAS, S. L. & SUR, M. 2000. Visual behaviour mediated by retinal projections directed to the auditory pathway. *Nature,* 404**,** 871-876.

VUE, T. Y., AAKER, J., TANIGUCHI, A., KAZEMZADEH, C., SKIDMORE, J. M.,

MARTIN, D. M., MARTIN, J. F., TREIER, M. & NAKAGAWA, Y. 2007. Characterization of progenitor domains in the developing mouse thalamus. *The Journal of Comparative Neurology,* 505**,** 73-91.

VUE, T. Y., BLUSKE, K., ALISHAHI, A., YANG, L. L., KOYANO-NAKAGAWA, N., NOVITCH, B. & NAKAGAWA, Y. 2009. Sonic Hedgehog Signaling Controls Thalamic Progenitor Identity and Nuclei Specification in Mice. *The Journal of Neuroscience,* 29**,** 4484-4497.

VUE, T. Y., LEE, M., TAN, Y. E., WERKHOVEN, Z., WANG, L. & NAKAGAWA, Y. 2013. Thalamic control of neocortical area formation in mice. *J Neurosci,* 33**,** 8442-53.

WAKIOKA, T., SASAKI, A., KATO, R., SHOUDA, T., MATSUMOTO, A., MIYOSHI, K., TSUNEOKA, M., KOMIYA, S., BARON, R. & YOSHIMURA, A. 2001. Spred is a Sprouty-related suppressor of Ras signalling. *Nature,* 412**,** 647-51.

WARREN, R. A., GOLSHANI, P. & JONES, E. G. 1997. GABAB-Receptor-Mediated Inhibition in Developing Mouse Ventral Posterior Thalamic Nucleus. *Journal of Neurophysiology,* 78**,** 550-553.

WASHBOURNE, P., THOMPSON, P. M., CARTA, M., COSTA, E. T., MATHEWS, J. R., LOPEZ-BENDITO, G., MOLNÁR, Z., BECHER, M. W., VALENZUELA, C. F., PARTRIDGE, L. D. & WILSON, M. C. 2002. Genetic ablation of the t-SNARE SNAP-25 distinguishes mechanisms of neuroexocytosis. *Nat Neurosci,* 5**,** 19-26.

WELIKY, M. & KATZ, L. C. 1999. Correlational structure of spontaneous neuronal activity in the developing lateral geniculate nucleus in vivo. *Science,* 285**,** 599-604.

WERNER, H. & LEROITH, D. 2014. Insulin and insulin-like growth factor receptors in the brain: Physiological and pathological aspects. *European Neuropsychopharmacology*.

WHISHAW, I. Q. 1996. An endpoint, descriptive, and kinematic comparison of skilled reaching in mice (Mus musculus) with rats (Rattus norvegicus). *Behav Brain Res,* 78**,** 101-11.

WHITE, E. L. 1978. Identified neurons in mouse smi cortex which are postsynaptic to thalamocortical axon terminals: A combined golgi-electron microscopic and degeneration study. *The Journal of Comparative Neurology,* 181**,** 627-661.

WIENCKEN-BARGER, A. E., MAVITY-HUDSON, J., BARTSCH, U., SCHACHNER, M. & CASAGRANDE, V. A. 2004. The role of L1 in axon pathfinding and fasciculation. *Cereb Cortex,* 14**,** 121-31.

WILLS, M. K. & JONES, N. 2012. Teaching an old dogma new tricks: twenty years of Shc adaptor signalling. *Biochem J,* 447**,** 1-16.

WILSON, J. R., FRIEDLANDER, M. J. & SHERMAN, S. M. 1984. Fine structural morphology of identified X- and Y-cells in the cat's lateral geniculate nucleus.

Proceedings of the Royal Society of London. Series B, Biological Sciences, 221**,** 411-436.

WILSON, N. R., KANG, J., HUESKE, E. V., LEUNG, T., VAROQUI, H., MURNICK, J. G., ERICKSON, J. D. & LIU, G. 2005. Presynaptic regulation of quantal size by the vesicular glutamate transporter VGLUT1. *J Neurosci,* 25**,** 6221-34.

WIMMER, V. C., BRUNO, R. M., DE KOCK, C. P., KUNER, T. & SAKMANN, B. 2010. Dimensions of a projection column and architecture of VPM and POm axons in rat vibrissal cortex. *Cereb Cortex,* 20**,** 2265-76.

WONG, R. O., MEISTER, M. & SHATZ, C. J. 1993. Transient period of correlated bursting activity during development of the mammalian retina. *Neuron,* 11**,** 923-38.

WOOLSEY, T. A. & VAN DER LOOS, H. 1970. The structural organization of layer IV in the somatosensory region (SI) of mouse cerebral cortex. The description of a cortical field composed of discrete cytoarchitectonic units. *Brain Res,* 17**,** 205-42.

YAMAMOTO, N. & LÓPEZ-BENDITO, G. 2012. Shaping brain connections through spontaneous neural activity. *European Journal of Neuroscience,* 35**,** 1595-1604.

YANG, L., PAN, Z., ZHOU, L., LIN, S. & WU, K. 2009. Continuously changed genes during postnatal periods in rat visual cortex. *Neuroscience Letters,* 462**,** 162-165.

YIZHAR, O., FENNO, L. E., DAVIDSON, T. J., MOGRI, M. & DEISSEROTH, K. 2011. Optogenetics in neural systems. *Neuron,* 71**,** 9-34.

YOSHII, A. & CONSTANTINE-PATON, M. 2010. Postsynaptic BDNF-TrkB signaling in synapse maturation, plasticity, and disease. *Dev Neurobiol,* 70**,** 304-22.

YUGE, K., KATAOKA, A., YOSHIDA, A. C., ITOH, D., AGGARWAL, M., MORI, S., BLACKSHAW, S. & SHIMOGORI, T. 2011. Region-specific gene expression in early postnatal mouse thalamus. *The Journal of Comparative Neurology,* 519**,** 544-561.

ZHAO, C., KAO, J. P. Y. & KANOLD, P. O. 2009. Functional excitatory microcircuits in neonatal cortex connect thalamus and layer 4. *The Journal of Neuroscience,* 29**,** 15479-15488.

ZIBURKUS, J. & GUIDO, W. 2006. Loss of binocular responses and reduced retinal convergence during the period of retinogeniculate axon segregation. *J Neurophysiol,* 96**,** 2775-84.

ZIKOPOULOS, B. & BARBAS, H. 2006. Prefrontal Projections to the Thalamic Reticular Nucleus form a Unique Circuit for Attentional Mechanisms. *The Journal of Neuroscience,* 26**,** 7348-7361.

ZOU, D. J. & CLINE, H. T. 1996. Expression of constitutively active CaMKII in target tissue modifies presynaptic axon arbor growth. *Neuron,* 16**,** 529-39.

8 Appendix

Appendix 1. Table with all genes which were differentially expressed in the enucleated dLGN compared to the control dLGN using Limma analysis with fold change cut off of >1.25, < -1.25, ordered by fold change.

Fold change value	Gene name	Gene symbol	moderated p value
-3.298758	RIKEN cDNA E530001K10 gene		2.71E-09
-1.996662	hemicentin 1	Hmcn1	9.83E-08
-1.7623256	src homology 2 domain-containing transforming protein C3	Shc3	3.43E-08
-1.7469152	potassium channel, subfamily K, member 9	Kcnk9	3.88E-08
-1.6364568	diacylglycerol kinase kappa	Dgkk	8.10E-06
-1.5188475	hypocretin (orexin) receptor 2	Hcrtr2	5.09E-07
-1.5187187	family with sequence similarity 19, member A4	Fam19a4	1.14E-05
-1.5021893	oxysterol binding protein-like 3	Osbpl3	5.39E-07
-1.4858443	dual specificity phosphatase 4	Dusp4	1.48E-05
-1.4687761	gap junction protein, delta 2	Gjd2	4.58E-08
-1.4629729	visinin-like 1	Vsnl1	6.83E-06
-1.4388474	tumor-associated calcium signal transducer 2	Tacstd2	1.54E-05
-1.4353602	myotilin	Myot	1.74E-07
-1.4207125	synuclein, gamma	Sncg	3.19E-06
-1.4192011	sprouty-related, EVH1 domain containing 2	Spred2	1.23E-07
-1.4186974	RIKEN cDNA 6530402D11 gene	6530402D11Rik	5.99E-05
-1.4169043	monooxygenase, DBH-like 1	Moxd1	1.97E-05
-1.4062924	potassium intermediate/small conductance calcium-activated channel, subfamily N, member 3	Kcnn3	2.72E-05
-1.3509669	shisa homolog 6 (Xenopus laevis)	Shisa6	1.55E-06
-1.3452755	cholinergic receptor, muscarinic 2, cardiac	Chrm2	1.08E-04
-1.3413906	adrenergic receptor, alpha 1d	Adra1d	6.89E-06
-1.3404461	FBJ osteosarcoma oncogene	Fos	1.09E-05
-1.3382416	Fras1 related extracellular matrix protein 3	Frem3	3.22E-06

-1.3378423	prostaglandin reductase 1	Ptgr1	2.75E-04
-1.3254905	high-mobility group nucleosome binding domain 5	Hmgn5	4.39E-05
-1.3211801	glial cell line derived neurotrophic factor family receptor alpha 1	Gfra1	2.57E-05
-1.3201692	diacylglycerol kinase, gamma	Dgkg	2.78E-05
-1.3195268	insulin-like growth factor 1	Igf1	1.48E-06
-1.3129569	PDZ and LIM domain 5	Pdlim5	1.08E-04
-1.3123636	collagen, type VI, alpha 5	Col6a5	9.53E-05
-1.3096302	synemin, intermediate filament protein	Synm	1.31E-04
-1.3060958	carbohydrate sulfotransferase 2	Chst2	1.24E-06
-1.3047525	calbindin 2	Calb2	4.13E-05
-1.2953379	transforming growth factor, beta 2	Tgfb2	2.64E-05
-1.2912956	a disintegrin-like and metallopeptidase (reprolysin type) with thrombospondin type 1 motif, 3	Adamts3	5.87E-05
-1.2907695	tissue inhibitor of metalloproteinase 4	Timp4	1.82E-04
-1.2851033	olfactomedin 3	Olfm3	2.56E-06
-1.2844355	early growth response 2	Egr2	5.79E-05
-1.2835208	potassium voltage gated channel, Shab-related subfamily, member 2	Kcnb2	1.12E-04
-1.2813138	cholinergic receptor, nicotinic, alpha polypeptide 3	Chrna3	9.89E-06
-1.2798768	RIKEN cDNA 5730455O13 gene	5730455O13Rik	1.24E-04
-1.2790416	transient receptor potential cation channel, subfamily C, member 5	Trpc5	8.26E-05
-1.2701505	Purkinje cell protein 4-like 1	Pcp4l1	9.55E-05
-1.2673393	choroideremia-like	Chml	3.22E-04
-1.2673117	Ly6/neurotoxin 1	Lynx1	1.06E-05
-1.267008	predicted gene 9909	Gm9909	1.37E-04
-1.26426	plasmacytoma variant translocation 1	Pvt1	1.67E-05
-1.2631869	MACRO domain containing 2	Macrod2	7.86E-05
-1.2628143	nexilin	Nexn	2.25E-05
-1.260123	opsin 3	Opn3	7.47E-05
-1.259473	stearoyl-Coenzyme A desaturase 1	Scd1	8.20E-06
-1.259159	VPS10 domain receptor protein SORCS 1	Sorcs1	1.02E-04
-1.2555207	proline rich 16	Prr16	1.59E-04
-1.2544047	cyclin B1 /// predicted gene 5593	Ccnb1 /// Gm5593	9.19E-05
-1.2537282	potassium inwardly-rectifying channel, subfamily J, member 6	Kcnj6	1.15E-05
-1.2532419	fibroblast growth factor 15	Fgf15	3.15E-06
-1.250215	protein tyrosine phosphatase, non-receptor type 3	Ptpn3	1.67E-04
1.2560561	histone cluster 1, H4m /// histone cluster 1, H4j	Hist1h4m /// Hist1h4j	4.41E-04
1.2571056	histone cluster 4, H4	Hist4h4	1.54E-04
1.2579546	RIKEN cDNA 9430021M05 gene	9430021M05Rik	1.25E-04

1.263999	solute carrier family 44, member 5	Slc44a5	1.52E-05
1.2787403	S100 calcium binding protein A6 (calcyclin)	S100a6	6.01E-05
1.2806529	reelin	Reln	1.07E-04
1.2965746	predicted gene 12618	Gm12618	3.42E-04
1.3021678	Max dimerization protein 4	Mxd4	6.29E-05
1.3048782	seven in absentia homolog 3 (Drosophila)	Siah3	2.14E-04
1.3158649	required for meiotic nuclear division 5 homolog A (S. cerevisiae)	Rmnd5a	9.57E-05
1.3191636	ring finger protein 114	Rnf114	3.23E-04
1.3196843	keratin associated protein 31-2	Krtap31-2	4.52E-05
1.3245299	G protein-coupled receptor 17	Gpr17	4.68E-04
1.3393537	orthodenticle homolog 2 (Drosophila)	Otx2	4.28E-07
1.3406079	uncoupling protein 2 (mitochondrial, proton carrier)	Ucp2	4.98E-06
1.3514786	proteolipid protein (myelin) 1	Plp1	3.72E-04
1.3523811	small nucleolar RNA, C/D box 116	Snord116	6.91E-05
1.3970422	microRNA 382	Mir382	7.91E-05
1.4006735	CD24a antigen	Cd24a	2.26E-06
1.4122561	cerebellin 2 precursor protein	Cbln2	2.82E-06
1.4282686	TATA box binding protein (Tbp)-associated factor, RNA polymerase I, D	Taf1d	3.73E-04
1.451349	insulin-like growth factor 2	Igf2	1.84E-04
1.5235516	thioredoxin interacting protein	Txnip	5.65E-05
1.5339487	RNA, Y3 small cytoplasmic (associated with Ro protein)	Rny3	2.63E-04